

# Prospect of gastroenterology and hepatology in the next century \*

Rudi Schmid

**Subject headings** gastroenterology; hepatology; next century

The task of predicting what Gastroenterology and Hepatology may look like in the coming century is a great personal challenge and at the same time an awe-inspiring assignment. Not only have these two medical specialties become very large and diversified but there are so many new discoveries and ideas that it is a capricious undertaking to attempt fore-telling which of them may become part of the next century's medical practice. I therefore will take the personal privilege of being highly selective, choosing only topics for discussion which I believe have a distinct potential of generating novel scientific concepts, fresh approaches or new therapeutic modalities.

Over the past few decades, the biological sciences which form the basis of contemporary medicine have evolved enormously, producing an ever-increasing volume of new information and technology that is keeping Gastroenterology and Hepatology changing and advancing at an accelerating pace. Looking back half a century to the end of WWII and China's liberation, it may seem astounding how elementary gastroenterology had been at that time. Modern science hardly had touched it and most of the diagnostic and therapeutic dogmas were still those of the 19th century. But over the past 50 years, Gastroenterology and Hepatology have profoundly been remade. We have witnessed a dramatic increase of insight into the causes and mechanisms of disease and our diagnostic and therapeutic capabilities have vastly expanded and improved, for example, the discovery of the viruses causing infectious hepatitis, of transplantation of the liver, pancreas and small bowel, or of the introduction of fiberoptic endoscopy. And to top it all, recall the recent revolution in peptic ulcer disease which

unceremoniously has toppled old dogmas about gastric acid and made it instead a readily curable infectious disease.

I believe with confidence that this dynamic evolution will continue and probably accelerate in the coming century. And there is no question that it will bring much novel and unanticipated clarification about currently obscure diseases. It will also greatly refine diagnostic procedures and expand therapeutic choices. What seems more difficult to predict though, is what directions this evolution will take, and how we are going to make use of the new opportunities and how we will pay for them.

## *Human Genome Project*

The Human Genome Project is a joint enterprise that undoubtedly will have an enormous and irreversible impact on the future of Gastroenterology and Hepatology. It probably is the largest international scientific project ever undertaken. Once its ultimate goals are reached, presumably early in the next century, the entire human genome will have been sequenced and mapped and it will be possible and perhaps become routine to screen an individual's genome from a simple blood sample. Genetic mutations which result in hereditary diseases of the gastrointestinal tract or the liver will readily be identifiable. Individuals or families at risk for a hereditary disease may be screened for the genetic defect. And eventually, such screening may become available even for prenatal use. It is likely, of course, that the function of many of the new genes identified by the sequencing initially will not be known and will have to be determined stepwise, one by one. This will be a huge task which may well take several decades of painstaking investigations. But once this has been accomplished, gastroenterologists of the future will look at intestinal and liver diseases from a vastly different perspective, and they will use treatments which are far beyond today's imagination.

The sequencing of the full human genome will have far-reaching consequences in many other ways. Many genetic diseases are polygenic, i.e., there is more than one allele in the same location or the phenotypic expression of a primary gene defect is modified by one or several additional as yet unidentified genes. This probably accounts for the

Rudi Schmid, M.D., Ph.D., F.R.C.P., M.A.C.P.  
Member of the National Academy of Sciences, U.S.A.  
Emeritus Professor of Medicine and former Dean University of California  
513 Parnassus Avenue, Room S-357  
San Francisco, California 94143-0410, USA  
Tel. +01 • 415 • 4762342, Fax. +01 • 415 • 4760689  
\*Expanded and updated text of a previously published article in  
**World Journal of Gastroenterology**, vol. 4, Suppl. 2, Pages 1-3,  
**October 1998.**  
Received 1999-05-01

wide spectrum of clinical expression that is seen in many inherited diseases. For example, homozygous Wilson disease, copper storage disease, may clinically present as progressive cirrhosis, as a severe chronic disease of the central nervous system, or as acute hemolytic anemia. This phenotypic variability probably reflects the polygenic nature of this disease, a hypothesis which is likely to be resolved by the successful sequencing of the human genome. Another example of highly variable expression of a genetic defect is observed in  $\alpha$ -1 antitrypsin deficiency type ZZ. Here, only 20% of the patients homozygous for the defect actually develop progressive liver disease and cirrhosis. In the majority of patients, the liver merely exhibits scattered hepatocytes bearing variable amounts of defective and hence misfolded and precipitated antitrypsin which accumulates in the cells, eventually killing them by apoptosis. The variation in phenotypic expression of this hereditary defect may reflect genetic differences in the activity of cellular metalloproteases fitted to degrade the precipitated antitrypsin. Again, the genome project is likely to resolve this puzzle.

Another benefit of the genome project will be identification of the genetic factors which determine individual susceptibility to environmental assaults, such as viral, bacterial or fungal infections or exposure to toxins or poisons. Clearly, different people respond to such noxious assaults differently. For example, some experts believe that inflammatory bowel disease, such as ulcerative colitis or Crohn's disease, may be the result of a genetically determined aberration of the immune response to the trillions of microorganisms inhabiting the intestinal lumen. To date, no such genetic immune defect has been identified but the sequencing of the genome may change this. A similar differentiated response is also observed in chronic alcoholism. Surprisingly, only 25% of chronic alcoholics develop cirrhosis of the liver. Why is it that the majority escapes hepatic injury? It clearly is not due to dietary factors or to a preferred alcoholic beverage. Rather, I suspect that this striking difference is caused by genetic factors which determine how the liver is reacting to the metabolic products or reactive oxygen radicals which are produced when alcohol is metabolized. Here, too, the sequencing of the genome in the next century may provide plausible answers.

The Human Genome Project is of importance also for the future of gene therapy for inherited diseases. This is because it will facilitate identification of the nature of the genetic error in a mutated gene e.g., transposition of a base pair, missense mutations, deletion of several nucleotide sequences etc. This information is crucial for construction of the new gene to be transposed. As you are aware, somatic gene therapy *in vivo* has

been used successfully in many animal models and in a few highly selected genetic defects in humans. There are still problems which need to be addressed, but I am confident that they will be resolved in the not too distant future. One of these problems concerns the vehicle or vectors which are used to transport the replacing gene to the targeted cells or organ. At present, this is usually accomplished by packaging it into liposomes, adeno or retroviruses, or more recently, adeno-associated viroids. But these RNA viruses often cause immune or toxic reactions which limit their usefulness as vectors. Moreover, it is difficult to target live viruses to specific cells or tissues in which the mutation is being expressed.

As an attractive alternative a highly imaginative new approach has been proposed (Kren *et al.* Nature Medicine, March 1998) which employs a chimeric RNA/DNA oligonucleotide embedded in a short stretch of DNA. This is coated with a polycation containing a ligand that permits targeting of specific cells. And it is the cells' own DNA mismatch repair mechanism which is used for integration of the new oligonucleotide into the cells' DNA. This new technology has been tested successfully for site-specific introduction of a single base-pair mutation in rat hepatocytes *in vitro* and *in vivo*. It is very promising particularly for gene therapy of hereditary diseases expressed in the liver and it undoubtedly will play a commanding role in the next century.

A second problem with current gene therapy is that the somatic cells selected for gene repair have a limited natural life span and then undergo apoptosis. A repaired gene therefore can be expressed no longer than the life span of its cell, which may range from a few days for intestinal mucosa cells to several hundred days for hepatocytes. To overcome this major limitation, one would need to repair the genetic defect in embryonic germ cells, an approach which at present is neither possible nor ethically justifiable. A more promising design might be to target gene therapy to an organ's stem cell compartment. Stem cells are undifferentiated pluripotential progenitor cells, which can either replicate themselves or undergo differentiation to more mature cells. (Science, March 5, 1999). Such pluripotential stem cells have been identified in, or isolated from, a variety of animal and human tissues, including bone marrow, intestinal mucosal crypts and brain. In the liver, unequivocal identification of stem cells has not yet been reported, but so-called oval cells have been identified and isolated (Petersen *et al.* Hepatology, February 1998). Ovalocytes are believed to represent stem cell-derived intermediary precursor cells which are able to differentiate into hepatocytes or bile ductular cells (Matsusake *et al.* Hepatology, March 1999). They typically are found in regenerating liver under experimental conditions in

which replication of mature hepatocytes has been blocked. Since ovalocytes' differentiation potential is limited, identification of the authentic hepatic stem cell compartment currently is a top research priority. Once this has been accomplished, it should be feasible to transpose new genetic information into the stem cells' genome thereby making it available indefinitely to daughter cells. I am confident that in the coming century, such technology will become available which would represent a true breakthrough in gene therapy of a large number of hereditary diseases. At present, of course, permanent cure of hereditary diseases of the liver, such as Crigler-Najjar disease, OTC deficiency and hereditary analbuminemia, can be accomplished only by orthotopic liver transplantation.

Other new and promising applications of gene therapy recently have been described for the treatment of malignant tumors or cancer metastases in the liver. The trick here obviously is to package the genetic information to be transposed in a vehicle that is able to recognize specific molecular features of cancer cells, particularly cell membrane receptors or membrane-bound antigens. The majority of malignant tumor cells exhibits mutations in genes expressing so-called cancer repressor proteins, such as p53, p16 and others, which act primarily by controlling the cells' mitotic cycle. When these genes are mutated or lost, the result is unregulated cell replication and tumor growth. In animal models, gene therapy targeted specifically to surface receptors of malignant cells was able to successfully reconstitute functioning p53 or p16 genes, resulting in sustained tumor shrinkage and prolonged survival. In an alternative approach, the DNA sequence to be transposed into tumor cells was coupled to a monoclonal antibody which recognized a glycoprotein abundantly expressed in hepatocellular carcinomas (Mohr *et al. Hepatology*, January 1999). Although to date, these and other novel techniques of gene therapy have been tested only in experimental animals or in cell cultures, they obviously have great promise for cancer therapy of the future and eventually may substitute for surgery, radiation or chemotherapy.

I have discussed the Human Genome Project and particularly gene therapy in some detail because within their frame of reference both will have an epochal impact on the future practice of Gastroenterology and Hepatology. But the enormous advances in the basic biomedical sciences, particularly in molecular and cell biology and in molecular virology and genetics, will literally revolutionize the way physicians of the future will think about mechanisms of disease. And the next generation of gastroenterologists and hepatologists will be handed a staggering array of new therapeutic modalities, most of which have not yet been invented. To illustrate what I mean, I arbitrarily

have chosen for discussion three recent major scientific contributions which I believe have the potential to make an immense impact on clinical medicine of the future.

The first scientific break-through is the so-called nucleic acid or naked DNA vaccine. As you know, most of the currently available antiviral vaccines consist of attenuated live DNA or RNA viruses which have lost most of their virulence but retained their antigenic potential. Examples are vaccines against viral hepatitis, poliomyelitis, measles, varicella, yellow fever, etc. All of these, of course, are modeled, as it were, after Edward Jenner's classic experiment with cowpox as protection against the deadly smallpox. Although most of these live vaccines are highly protective, reservations often are expressed whether avirulent viruses could spontaneously undergo back mutation to a more virulent form; or whether attenuated live viruses could cause unsuspected morbidity decades after they had been used in a vaccine. The advent of recombinant DNA technology now has made it possible to design novel vaccines which provide strong and sustained antigen expression but exclude these lingering doubts about live-vaccines' safety.

The principle of this new approach is relatively simple. A gene from a pathogenic microbe encoding a microbial antigen, is spliced into a bacterial plasmid. The vaccine consisting of the plasmid bearing the spliced gene, is injected into muscle tissue where it directs the muscle cells to manufacture microbial antigen. The latter evokes a sustained immune response, involving both, antibody formation and a T-cell response. Although, to date, this new naked DNA vaccine has been tested only in experimental animals, persistent high titers of circulating antibodies have been obtained and the animals were protected against infection. It is thus evident that this new approach to vaccination has great promise and is likely to be a relatively inexpensive procedure. Indeed, naked DNA vaccine looks like the vaccine of the 21st century.

## TRANSPLANTATION OF ISOLATED SYNGENEIC HEPATOCYTES

The second subject I have selected for discussion is still in its experimental phase but its great potential for future medical applications already is unmistakable. It concerns the transplantation of isolated syngeneic hepatocytes into a recipient's liver *in vivo*. Development of such a technique for clinical use obviously would open new avenues not only for correction of genetic defects, but also for the management of acute hepatic failure. It eventually may contend with, if not substitute for, orthotopic liver transplantation which in view of the scarcity of available organs might be a solace.

The first satisfactory technique for isolation of intact and functioning hepatocytes from

experimental animals was developed by Berry and Friend in 1969 (J Cell Biol, vol. 43). It stimulated a profusion of attempts to culture such isolated cells in vitro or to introduce them into various organs of congenic recipients *in vivo*, but with few exceptions, the cells failed to survive, let alone to proliferate. In 1982, Mito *et al* in Japan (Gastroenterology, Vol. 82) reported the exciting finding that in rats, syngeneic hepatocytes transferred into a recipient's spleen not only survived and retained their characteristic physiologic functions, but also proliferated. In fact, partial hepatectomy of the recipient a few days after transfer of hepatocytes into its spleen greatly magnified the number of mitotic figures in the transplanted cell population. And then, in 1991, Gupta *et al* (Proc Natl Acad Sci USA, Vol. 88) announced the surprising observation that a major fraction of the hepatocytes extant in the spleen eventually migrated to the host's liver where they were fully integrated into existing liver cell plates, properly functioning and apparently surviving indefinitely (Hepatology, February 1999).

Since the spleen is a relatively small organ, only a limited number of donor hepatocytes can be transferred to the liver with this procedure. Nonetheless, in rats and mice, it was able to at least partially correct genetic defects such as analbuminemia and unconjugated hyperbilirubinemia. Fortunately, a complementary experimental stratagem has been developed (Laconi *et al*. Am J Pathol, Vol. 153, 1998) which allows for a significant increase of the number of donor hepatocytes which can be delivered to the liver via the spleen. This consists of preparatory treatment of the designated recipient animal with the pyrrolizidine alkaloid retrorsine which is taken up selectively by the liver. It blocks the resident hepatocytes' cell cycle and therefore suppresses their proliferative potential. When combined with a subsequent two-third hepatectomy, the proliferative thrust generated by this resection is lost on the blocked resident hepatocytes thereby greatly favoring the transplanted cells. In preliminary studies with this approach, one to two months after the procedure, up to 80 percent of the recipient liver's cells consisted of transplanted hepatocytes and their progeny.

Although these are unusually exciting experimental findings, in its present form, this technology clearly is far from being applicable to clinical medicine. Nonetheless, I believe that on the basis of the new scientific information and technical expertise gained from these experiments, it will only be a question of time until a clinically acceptable and promising version of this approach will be developed. Given the rapid progress in research on inducible immune tolerance, it even may become possible to use allogeneic hepatocytes for transplantation instead of being limited to

syngeneic donor cells. To start with, I can think of two important groups of liver diseases in which hepatocyte transplantation via the spleen may be the therapeutic approach of choice. One is fulminant hepatic failure of variable etiology, including potentially fatal tylenol poisoning, in which the number and/or condition of surviving liver cells during the acute phase may be insufficient to sustain life and eventual recovery. The other consists of genetic defects expressed in the liver for which conventional gene therapy may be unavailable or lacking promise. These include  $\alpha$ -1 antitrypsin deficiency type ZZ, Wilson disease, analbuminemia, Crigler-Najjar disease and several others. Two different technical approaches are possible. One is to transplant hepatocytes obtained from a syngeneic donor; the other is to use the patients' own hepatocytes after the genetic defect had been corrected *ex vivo* with DNA supplied by an unrelated donor. Either approach would seem attractive and technically feasible. I am confident that in the next century, this cellular approach to liver transplantation will become a very important and frequently used procedure.

#### ACTIVE BIDIRECTIONAL EXCHANGE OF NUCLEATED BLOOD CELLS BETWEEN FETUS AND MOTHER

The third scientific issue that I wish to discuss is really a working hypothesis, but one that is supported by powerful, though indirect, evidence. It concerns the recent demonstration that in pregnancy there often an active bidirectional exchange of nucleated blood cells between fetus and mother, producing what has been called microchimerism. In the maternal circulation, immune-competent fetal cells are detectable not only during pregnancy but often for several decades thereafter (Bianchi *et al*. Proc Natl Acad Sci USA, Vol. 93, 1996). It is unknown, of course, how these immunologically foreign cells are able to survive and proliferate in the mother and what consequences, if any, this may have for her own immune system.

The original discovery in maternal blood of cyncytial trophoblasts derived from fetal placenta was recorded in 1959 (Lewis Thomas *et al*. Trans Assoc Am Phys, Vol. 72). At that time, identification of these giant multinucleated cells was possible only by morphological means. But in the last decade, much more refined technology has become available for cell identification and isolation, such as polymerase chain reaction and fluorescence-activated cell sorters. With these new methods, forty middle-aged women were studied, all of whom had given birth to at least one son over the past three decades. The DNA of the Y chromosome was used for identification of male fetal cells in the mother's blood. Quantitative results were expressed in terms of the number of male fetal-cell DNA equivalents identified in a

specified sample of maternal blood (Nelson *et al.* The Lancet, Vol. 351, 1998). In the blood of healthy women aged 35.61, the range of male cell DNA equivalents was found to be very low (range 0.2, mean 0.38). But surprisingly, in women with established systemic sclerosis, a presumably autoimmune disease, the values were 30 times higher (range 0.61, mean 11.1, *P value* = 0.0007). In a comparable albeit less carefully controlled study of a larger group of women suffering from systemic sclerosis, male DNA sequences were identified in maternal blood in 46 percent, but only in 4 percent of healthy controls (Artlett *et al.* N Engl J Med, Vol. 338, 1998). These striking findings demonstrate not only a much higher incidence of fetal microchimerism in women with systemic sclerosis, but also a much more elevated level of fetal-cell DNA equivalents in the patients as compared to healthy controls.

To interpret these startling novel observations, Nelson in 1996 proposed the bold but attractive hypothesis that many chronic diseases of supposedly autoimmune nature in fact may be the result of allogeneic fetal cells which during pregnancy had gained access to the maternal blood and subsequently had engrafted and are surviving in the mother for decades (Arthritis Rheum, Vol. 39, 1996). This almost heretic hypothesis is bolstered by a number of supporting observations, such as the following:

① Many diseases of supposedly autoimmune etiology have a strong female predilection, particularly those affecting the liver, such as autoimmune hepatitis, primary sclerosing cholangitis, systemic sclerosis and primary biliary cirrhosis; the last has a female-to-male ratio of almost 10:1.

② All of these presumably autoimmune diseases exhibit morphological, immunological and chemical features characteristic of graft-versus-host disease which is a chimeric condition observed in recipients of allogeneic stem cell or bone marrow transplantations.

③ Moreover, in most of these supposedly autoimmune diseases and in graft versus host disease, intrahepatic bile ducts are a principal target of the pathological process. Furthermore, all of the above diseases tend to be associated with accessory "autoimmune" phenomena, such as Sj-gren's syndrome, systemic sclerosis, the CREST syndrome, thyroid dysfunction and others.

Although these diverse clinical observations persuasively imply a common pathogenic mechanism for this group of diseases, by themselves they of course do not prove this novel hypothesis. But I believe that in the coming century, this issue will receive great attention and will emerge as one of immunology's leading scientific problems. And when all the scientific information is in, I would not be surprised if Nelson's hypothesis would turn out to be

correct.

The three novel scientific contributions which I have discussed above are examples of work that has passed through most of its experimental phase and whose exciting potential for clinical application is quite obvious. It seems just a matter of time until it will be ready for testing in humans. But we should realize that there still are countless obscure diseases for whose full exploration we currently lack the required intellectual basis and experimental tools. It is in these areas that I expect molecular and cell biology, virology and genetics of the future to provide the necessary conceptual framework and methodology to make progress and achieve scientific breakthroughs.

One of these areas is the vast field of viral hepatitis, particularly of the types B and C which world-wide are causing immense morbidity and mortality. Despite recent remarkable advances, we still do not understand how these viruses are surviving indefinitely and how they are causing chronic liver injury nor do we have effective, reliable and safe therapies to arrest their progression, let alone to achieve permanent cure. Some of us are old enough to recall the complete failure of steroid treatment of chronic active hepatitis B which only a few decades ago had been flaunted as the ultimate therapy for this chronic liver disease. Against this background, the current hyperbole about interferon treatment of chronic viral hepatitis appears somewhat uncritical, if not misleading. I hope and actually anticipate that early in the next century, new scientific information and technology will become available which will allow development of a definitive therapy for chronic viral hepatitis which causes no more than minor side effects to the patient and whose costs are affordable.

## MOLECULAR DIAGNOSTICS

And finally, the rapid evolution of molecular biology has created a new discipline, molecular diagnostics, which is offering an ever-increasing number of tests of previously unthinkable variety, sophistication and sensitivity. For example, molecular techniques already are used to quantitate viral loads in viral hepatitis. But one of molecular diagnostics' most promising applications will be in the search for new infectious agents which to date have escaped detection by available staining or immunological methods. As you are aware, several gastrointestinal diseases, previously of unknown etiology, have recently been found to be caused by newly discovered microorganisms. These include, of course, peptic ulcer, but also Whipple's disease, bacillary angiomatosis and most recently, nanobacteria which cause connective tissue calcification in systemic sclerosis, sclerosing cholangitis and the CREST syndrome associated with primary biliary cirrhosis (Kajander, *et al.*

Proc Natl Acad Sci USA, July 1998). But there are several other gastrointestinal diseases of unknown etiology whose clinical and pathological features seem consistent with, if not suggestive of, an infective origin. These certainly include Crohn's disease, ulcerative colitis, granulomatous hepatitis and sarcoidosis and perhaps primary biliary cirrhosis and sclerosing cholangitis. Many experts of course have postulated an immunologic origin of these diseases and a recent report, that an antibody to tumor necrosis factor  $\alpha$  is profoundly down-regulating inflammation in Crohn's ileocolitis is supporting, but of course not proving, this hypothesis. (Baert *et al.* Gastroenterology, January 1999). Now, that highly sensitive molecular RNA and DNA probes and PCR have become available, I am confident that the hunt for elusive microorganisms will be intensified. And I would not be surprised if one or more of these diseases eventually would be discovered to have an infectious etiology.

#### DIAGNOSTIC AND THERAPEUTIC INSTRUMENTS AND MECHINERY

Predicting the future of Gastroenterology and Hepatology would be incomplete without briefly considering what new diagnostic and therapeutic instruments and machinery may become available in the next century. Here, progress, driven by intense market competition, is so rapid that precise predictions are quite impossible. Nonetheless, some trends seem to become detectable. Radiology is likely to progress by leaps and bounds, particularly spiral computerized tomography and three-dimensional imaging. They increasingly will replace invasive diagnostic procedures, including fiberoptic endoscopy. The only exception may be fiberoptic, laser-induced fluorescence spectroscopy which uses either tissue-intrinsic or extrinsically-elicited fluorescence; this is a novel procedure which appears to greatly enhance diagnostic accuracy. On the other hand, Magnetic Resonance Imaging, with its very expensive equipment, appears to be taking a back seat. And in gastrointestinal surgery, an ever-increasing proportion of invasive procedures will be performed by laparoscopy, which often makes hospitalization unnecessary and thereby reduces costs.

#### ECONOMICS OF HEALTH CARE

And this brings me to a true megafactor which in a major way will shape and restrain the practice of Gastroenterology in the next century. This is the economics of health care. All over the world, per capita costs of medical care are rising steeply, far outpacing the rate of inflation. To a considerable extent, this is due to the accelerated appearance on the market of new or advanced but always more

expensive machines, procedures and drugs which seem necessary to keep up with contemporary medicine. In the US, this continuing price increase has driven health care costs to a level, equaling 15% of gross domestic product (GDP), and other developed countries are not far behind. Although in the developing world, health care costs generally are lower, the cost increase in proportion is at least similar. It seems evident that if this trend should continue, health care eventually will consume a major part of the GDP. But I am afraid that as long as medical care continues to be unregulated or is remaining a competitive market commodity, it will be very difficult, if not impossible to bring quality of medical care and its costs into some sort of reasonable balance. Consider, for example, who would be qualified and publicly acceptable as decision makers. Would it fall to third party payers, that is insurance companies or health maintenance organizations. Or to employers who are funding the costs of health care Or to the medical care establishment, that is to physicians and hospitals Or perhaps to the government. However this paramount issue will be resolved, it will have an enormous impact on the future practice of Gastroenterology and Hepatology, both in the developed and in the developing world. As developing countries are striving to catch up with modern Western medicine, they rapidly are coming on mainstream, offering an almost unlimited market for aggressive pharmaceutical and medical equipment industries. This of course is further destabilizing the rapidly rising costs of adequate medical care.

#### CONCLUSION

In concluding, I believe that this brief glimpse into the science and practice of Gastroenterology and Hepatology in the next century is offering us a mixed perspective, one of an ever-widening disparity between rising opportunities on the one hand, and strained resources on the other. I am afraid that unless this serious imbalance will be dealt with early in the next century, the practice of Gastroenterology and the quality of health care world-wide will suffer. We need to learn how to reduce expenses by voluntarily lowering our dependence on technical procedures and complex equipment, and by avoiding use of expensive but only marginally effective medications and surgical interventions. And last but not least, in hopelessly ill patients, we should have the courage to abstain from using every possible means at our disposal to prolong dying and suffering, as unreasonable terminal care is one of modern health system's most expensive components. These, I am afraid, will be painful adjustments for the medical establishment but they must be faced better sooner than later.

# Escherichia *Coli* O157: H7 and Shiga-like-toxin-producing Escherichia Coli in China \*

XU Jian-Guo, CHENG Bo-Kun and JING Huai-Qi

**Subject headings** Escherichia coli O157:H7; Shiga-like-toxin; enteritis

*Escherichia coli* (*E. coli*) is one of the facultative anaerobes of the human intestinal tract, usually harmless. Infections due to pathogenic *E. coli* may result in urinary tract infections, sepsis, meningitis and enteric disease. Diarrheagenic *E. coli* has been classified into several categories, such as enterotoxigenic *E. coli* (ETEC), entero-invasive *E. coli* (EIEC), entero-pathogenic *E. coli* (EPEC), entero-aggregative *E. coli* (EaggEC) and entero-hemorrhagic *E. coli* (EHEC). A variety of virulence or potential virulence factors for diarrheagenic *E. coli* have been identified. The nomenclature of diarrheagenic *E. coli* is based on virulence factors<sup>[1,2]</sup>.

In 1977 Konowalchuk *et al*<sup>[3]</sup> reported that some strains of pathogenic *E. coli* O26 : H11 produced a toxin with a profound cytopathic effect on Vero cells, and named it verotoxin (VT). O'Brien *et al* noted<sup>[4]</sup> that the VT reported by Konowalchuk *et al*<sup>[3]</sup> was strikingly similar to Shiga toxin (Stx) produced by *Shigella dysenteriae* type 1, and it could be neutralized by anti-Stx, thus a new nomenclature, Shiga-like toxin (SLT), appeared. An alternative nomenclature is "Shiga toxin" (ST), which indicated that the specific cytotoxin described by Konowalchuk *et al*<sup>[3]</sup> is essentially identical at the genetic and protein levels with the Stx produced by *S. dysenteriae* I discovered some 100 years ago. Consequently, SLT, ST and VT have been used interchangeably, resulting in the name of verotoxin-

producing *E. coli* (VTEC), shiga-like-toxin-producing *E. coli* (SLTEC) and shiga-toxin-producing *E. coli* (STEC) coexisted in literature<sup>[5]</sup>. However, it must be noted that *E. coli* O157 : H7 is the main serotype of EHEC recognized at present<sup>[1,2,6]</sup>. Hemorrhagic colitis (HC) and hemolytic uremic syndrome (HUS) are life threatening, which are often caused by STEC or EHEC. So far as the diseases are concerned, *E. coli* O157 : H7 should belong to EHEC. All of the EHEC strains are believed to be pathogenic. As for its toxin, *E. coli* O157 : H7 should belong to VTEC, SLTEC or STEC. However, not all of the STEC strains could cause HC or HUS<sup>[7]</sup>. The confusion from the nomenclature may be clarified in future when the pathogenic mechanisms of bacteria are fully understood.

Food-borne outbreaks of SLTEC disease appear to be increasing in the world. Mass-produced and mass-distributed food can involve large numbers of people in short time. SLTEC strains belong to a very diverse range of serotypes, among which O157 : H7 is most commonly associated with large outbreaks<sup>[8]</sup>. In the summer of 1996 in Japan, a largest outbreak in the world caused by *E. coli* O157 : H7 was reported, in which about 10 000 cases were identified<sup>[9]</sup>. Chinese government and society became aware of the importance of *E. coli* O157 : H7 from the Japanese outbreak. An informal national network for detection of *E. coli* O157 : H7 was organized in April 1997, involving about 30 public health laboratories from different provinces and municipalities.

## *E. Coli* O157 : H7 IN CHINA

The studies of *E. coli* O157 : H7 in China can be divided into two phases. In phase 1, starting from 1986 up to August 1996, the bacteriologists who studied the pathogen were mainly motivated by their scientific interests, few organized projects were carried out<sup>[2]</sup>. In phase 2, starting from August 1996 up to now, the public health authorities and most of the scientists have paid more attention to *E. coli* O157 : H7, and a new trend of isolation of *E. coli* O157 : H7 has been attempted in various parts of China.

The first group of patients with HC caused by *E. coli* O157 : H7 were identified in Beijing in 1988,

Key Laboratory of Molecular Medical Bacteriology, Ministry of Health, Institute of Epidemiology and Microbiology, Chinese Academy of Preventive Medicine, Beijing 102206, China

Dr. XU Jian-Guo, male, born on 1952-04-19 in Pinglu County, Shanxi Province, graduated from Shanxi Medical University as a medical student in 1976, from Chinese Academy of Medical Sciences as graduate student with Master degree in 1982, from Chinese Academy of Preventive Medicine with doctoral degree in 1993, now professor of microbiology, majoring medical bacteriology, having 70 papers published.

**\*Supported by Outstanding Young Scientist Award from National Natural Science Foundation of China, Grant No. 39625001.**

**Correspondence to:** Professor XU Jian-Guo, Key Laboratory of Molecular Medical Bacteriology, Ministry of Health, Institute of Epidemiology and Microbiology, Chinese Academy for Preventive Medicine, Beijing 102206, China

Tel. +86 • 10 • 61739579, Fax. +86 • 10 • 61730233

Email. xujg@public.bta.net.cn

**Received** 1999-02-05

as the etiologic agents isolated in Xuzhou city, Jiangsu Province of China<sup>[10]</sup>. In the three years from 1986 to 1988, 24 of 486 sporadic diarrhea patients were diagnosed as having HC, 5 strains of *E.coli* O157 : H7 were isolated, all of which were hybridized with SLT1, SLT2 and EHEC specific probe<sup>[10]</sup>. In 1993, two strains of *E.coli* O157 : H7 were isolated from a patient with HC and a patient with HUS, in Shandong Province. In the same period, several groups of scientists failed to isolate *E.coli* O157 : H7 in other cities of China, possibly due to lack of proper diagnostic techniques and reagents. Kain *et al*<sup>[11]</sup> reported that, in a study carried out in Beijing, about 7% of fecal samples were collected from diarrhea children hybridized with EHEC probe pCVD419<sup>[6]</sup>. However, similar amount of positive samples were also observed in the control group, but without strain isolation. The 168 strains of EPEC isolated before 1982 were detected with SLT1, SLT2 and EHEC specific probes, no EHEC or STEC was found<sup>[2]</sup>.

In 1997, a Chinese national network for detection of *E.coli* O157 : H7 was organized, *E.coli* O157 : H7 strains were isolated from diarrhea patients in Zhejiang, Anhui Provinces and Ningxia Autonomous Region. Nine strains were isolated from pigs in Fujian Province. It was interesting to note that all of the 9 strains from pig source were negative for SLT1, SLT2, and Hly genes. In 1998, several public health laboratories in China have attempted to isolate *E.coli* O157 : H7 from various sources, such as diarrhea patients, pigs, cattle, food and cow's milk. A total of 48 strains were isolated from cattle, pigs and milk. Some strains were found to be hybridized with Hly, Slr1 or Slr2 gene probes, most of the strains, however, were not. And, this result was demonstrated and confirmed by PCR method in the reference laboratory. The *E.coli* O157 : H7 isolation data in China are summarized in Table 1.

**Table 1** *E.coli* O157 : H7 strains isolated in China

No. Strains	Year	Source	Hly <sup>a</sup>	SLT1	SLT2	Province
5	1986-1988	HC	+	+	+	Jiangsu
3	1993	HC, HUS	+	+	+	Shandong
1	1997	Diarrhea	+	+	+	Anhui
1	1997	Diarrhea	+	-	-	Zhejiang
1	1997	Diarrhea	+	ND	ND	Ningxia
1	1997	Diarrhea	-	-	-	Passenger
9	1997	Cattle	-	-	-	Fujian
2	1997	Food	+	+	+	Fujian
1	1998	Milk	+	+	+	Guangdong
2	1998	Food	ND	ND	ND	Guangdong
4	1998	Pig				Liaoning
1	1998	Cattle	+	+	+	Liaoning
2	1998	Cattle	+	ND	ND	Hebei
14	1998	Cattle	ND	ND	ND	Ningxia

<sup>a</sup>Hly: hemolysin gene.

strains have been isolated from samples of beef, lamb, deer, wild boar, ostrich, partridge, antelope, and reindeer<sup>[11,12]</sup>. Cattles have long been regarded as the principal reservoir of *E.coli* O157 : H7. STEC strains were found prevalent in the gastrointestinal tracts of other domestic animals, including sheep, pig, goat, dog, and cat<sup>[2,5]</sup>. Many domestic animals carrying pathogens are asymptomatic. Strains of *E.coli* O157 : H7 have also been detected in cats and dogs with diarrhea<sup>[2,5]</sup>. *E.coli* O157 : H7 can potentially enter the human food chain from a number of animal sources, most commonly by contamination of meat with feces or intestinal contents after slaughter. One of the most common sources of human *E.coli* O157 : H7 infections is hamburger patty, made from ground beef. Hence, most of the outbreaks of *E.coli* O157 : H7 infection all over the world have been linked to hamburgers. In the outbreak of United States in 1993, more than 700 people were infected, and over 50 cases of HUS were diagnosed. So far, this is the largest outbreak of *E.coli* O157 : H7 associated with hamburger.

In China, only few sporadic cases of *E.coli* O157 : H7 infections have been identified. No outbreak as yet has been reported. The strains of *E.coli* O157 : H7 were isolated from cattle, pigs and milk. These results suggest that risk of infection with these microbes existed in China. It occurred to us that the prevalence of *E.coli* O157 : H7 seems to be higher in pigs than one expected. It should be emphasized that the consumption of pork in China is very popular and the risk seems to be much higher than that from beef. Further investigation of *E. coli* O157 : H7 in pigs should be conducted in China. Fortunately, no known virulence gene was found in the strains isolated from pigs in China such as SLT1, SLT2 and hemolysin gene as well. However, it was reported recently that the SLT2 containing phage from sewage, as the phage containing virulence gene, could infect non-pathogenic *E.coli* rather easily. The risk of such microbe infection seems fairly high.

#### SLTEC OTHER THAN O157 : H7 IN CHINA

*E.coli* O157 : H7 has not been recognized as a big public health problem in China up to now. However, STEC seems to be serious<sup>[13]</sup>. In clinical or public health bacteriological laboratories, only EPEC, ETEC and EIEC used to be diagnosed by serotyping techniques. Nevertheless, it has been noted not infrequently that almost pure cultures of *E.coli* were seen and new varieties of *E.coli* were isolated from certain fecal samples of diarrheal patients, which could not be serotyped with the

It is shown in literature, that *E.coli* O157 : H7



typesera available. Whether they should be recognized as pathogenic *E.coli* or not still remains a question. We assumed that some of these strains isolated as *E.coli* might be pathogenic in nature, which had been overlooked because of lacking proper techniques for identification. In order to verify this hypothesis, we collected 174 named nonpathogenic *E.coli* strains in Beijing from 1988 to 1990 and detected them with DNA probes<sup>[14]</sup>. The DNA probes covered almost all the virulence genes reported, such as heat-stable toxin (ST) heat-labile toxin (LT), EPEC adherence factor (EAF), diffuse adherence gene (DA), EHEC specific probe pCVD419, EAggEC specific probe, 2.5 Kb specific probe for invasive plasmid (INV) of EIEC and Shigella-species, shiga-like toxin 1 or 2 (SLT1 or SLT2), EPEC attaching and effacing genes (eae). It was observed that 59.3% strains tested were hybridized with at least one of the used probes, with a higher percentage of (29.7%) *E.coli* strains hybridized with SLT2 and INV probes<sup>[13,14]</sup>.

In general, strains of EHEC and some of EPEC hybridize with SLT1 or/and SLT2 probe. INV probe is a 2.5-Kb fragment derived from the invasive plasmid of *S.flexneri* 2a, and used as a diagnostic tool specific for Shigella species and EIEC strains<sup>[14,15]</sup>. The fragment was subsequently sequenced and named invasive associated locus (ial). However, none of the known EIEC or Shigella flexneria species was found to hybridize SLTs probes<sup>[16]</sup>. To clarify the relationship between EIEC and some of our strains isolated, the invasive plasmid antigen BCD (ipaBCD), the key genes for invasive ability of EIEC and Shigella, were synthesized by PCR labeled by Digoxin and used as probe. The absence of DNA hybridization signals indicated a lack of ipaBCD genes in *E.coli* F171. We also found that *E.coli* F171 could not provoke keratoconjunctivitis in guinea pigs. Sereny test was used as a critical marker for virulence of EIEC and Shigella species. However, with HEP-2 cell assay, the *E.coli* F171 is able to invade the epithelial cells. The data suggested that the genes encoding invasive ability of *E.coli*-F171 differed from EIEC, and *E.coli* F171 was therefore not a member of EIEC<sup>[13,14]</sup>.

Adherence of bacteria to epithelial cells has been recognized as a virulence characteristic of enteric pathogen<sup>[1]</sup>. Three adherence patterns were defined i.e., localized adherence, diffuse adherence and aggregative adherence<sup>[17]</sup>. Many of our *E.coli* strains hybridized with SLT2 and INV DNA probes demonstrated HEP-2 cell aggregative adherence pattern<sup>[13,14]</sup>. However, none of them were hybridized with EAggEC specific probe, which

was derived from the genes encoding EAggEC adherence factor I (EAF/I), and used as an identification marker for EAggEC. The aggregative adherence pattern to HEP-2 cells is the characteristic feature as EAggEC strains<sup>[18]</sup>. Under electron microscope, a unique kind of fimbria was observed on the surface of cells of *E.coli* F171. The subunit size of the fimbriae protein was 19KDa, and the genes encoding the fimbriae were located on a 60 MDa plasmid. *E.coli* HB101 cells containing the cloned genes were able to adhere onto the HEP-2 cells. The analysis of N terminal amino acid sequence indicated that *E.coli* F171 has its unique features<sup>[14]</sup>.

The shiga-like toxins have been demonstrated as the virulence factors for *E.coli* strain, which could cause HC and HUS<sup>[19]</sup>. Many of EPEC and EHEC strains contain genes for SLT1 or SLT2. The toxin producing ability of *E.coli* F171 was studied with Vero cell assay, which was originally used for study SLTs since *E.coli* F171 was hybridized with SLT2 probe. Both cell culture filtrate and a crude toxin preparation of *E.coli* F171 were found toxic to Vero cells. The Vero cell toxicity of *E.coli* F171 could not be neutralized by SLT2 antibody. The fact that hybridization of *E.coli* F171 with SLT2 probe suggested that it has DNA fragment homologous to SLT2 gene or it has an entire SLT2 gene<sup>[14]</sup>.

The invasiveness, toxin production activity and epithelial cell adherence ability have been described as key features for EIEC, ETEC and EAggEC respectively<sup>[20]</sup>. *E.coli* F171 could adhere onto and invade into HEP-2 cells and produce toxins. It combines many key features of EIEC, EHEC, EPEC, and EAggEC. Based on the data obtained, it seems that *E.coli* F171 represents a new variety of STEC. Hence the name of enteric SLTs-producing and invasive *E.coli* (ESIEC) was proposed. Since 31.4% of collected *E.coli* strains were tested in our studies shared similar features as *E.coli* F171, infections presumably caused by this kind of pathogenic *E.coli* seems to be an important public health problem in China.

In order to confirm the virulence and pathogenesis to human beings, a study in adult volunteers was carried out. By oral intake of  $10^9$ - $10^{10}$  colony forming units (CFU) of *E.coli* F171, all of 8 volunteers developed diarrhea, 3 of 8 developed high fever ( $39.8^{\circ}\text{C}$ ). The incubation period ranged from 7 to 49 hours. Unformed stools were 3-6 times a day. The volumes of stools of 4 volunteers were above 1 000 mL a day. Antibiotic therapy was given to 5 of the 8 volunteers. No diarrhea was observed for the control group consisting of 4 volunteers, who ingested  $10^9$  CFU of

non-pathogenic strain *E.coli*-HB101. Typical clinical symptoms for ESIEC in volunteers were bowel movement, diarrhea, general abdominal pain, moderate fever and unformed stool. It was revealed that ingested *E.coli* F171 could colonize and replicate for up to 7 days. By examining the stool samples of the volunteers, it was observed that the bacteria could reach an amount of  $2.74 \times 10^{12}$  CFU. The strains isolated from the patient stool samples of volunteers were confirmed as *E.coli* F171 by specific antiserum in animal against it.

Although the human pathogenic nature of *E.coli* F171 was recognized, the key virulence factors of ESIEC have not been studied in detail. The pathogenic mechanism of ESIEC, for instance, has not been understood. The "pathogenicity island", which refers to the large chromosomal segment carrying genes involved in pathogenicity, has recently revolutionized our understanding of bacterial pathogenesis<sup>[21]</sup>. The GC content of pathogenesis islands is different from that of the other host chromosome, suggesting that they may originate from horizontal transfer between different bacterial general. The number of gram-negative bacterial species known to harbor pathogenicity islands has grown steadily, including uropathogenic *E.coli* (UPEC), EHEC, EPEC, *Helicobacter pylori*, *salmonella typhimurium* and *Vibrio cholerae*<sup>[21]</sup>. It is believed that there is no pathogenicity island in the non-pathogenic *E.coli*. We must investigate the pathogenicity island so as to confirm the medical significance of ESIEC. Recently, we have observed an *irp2* gene in many strains of ESIEC. The *irp2* gene is involved in iron uptake and has been considered as one of the virulence genes located on the high pathogenicity island (HPI) of *Yersinia*-species<sup>[22]</sup>. This gene was observed in many strains of adherent *E.coli* and in *E.coli* isolated from blood, but rarely observed in EPEC, EIEC or ETEC. No *-irp2-* was found in EHEC, *Shigella* and *Salmonella enterica* strains. It seems that pathogenicity island existed in ESIEC. The HPI of the *Y. pestis* is disseminated among species of the Enterobacteriaceae family which are pathogenic to humans.

## REFERENCES

- Levine MM. *Escherichia coli* that cause diarrhea: enterotoxigenic, enteropathogenic, enteroinvasive, enterohemorrhagic, and enteroadherent. *J Infect Dis*, 1987;155:377-389
- Xu JG, Qi GM. The clinical and epidemiological features of enterohemorrhagic *E.coli* and its diagnostic methods. *Chin J Epidemiol*, 1996;12:367-369
- Konowalchuk J, Speirs JJ, Stavric S. Vero response to a cytotoxin of *Escherichia coli*. *Infect Immun*, 1977;18:775-779
- O'Brien AD, Holmes RK. Shiga and Shiga-like toxins. *Microbiol Rev*, 1987;51:206-220
- James CP, Paton AW. Pathogenesis and diagnosis of Shiga toxin-producing *Escherichia coli* infections. *Clin Microbiol Rev*, 1998; 11:450-479
- Levine MM, Xu J, Kaper JB, Lior H, Prado V, Ball T. A DNA probe to identify enterohemorrhagic *Escherichia coli* of O157 : H7 and other serotypes that cause hemorrhagic colitis and hemolytic uremic syndrome. *J Infect Dis*, 1987;156:175-182
- Xu JG, Chen BK, Wu YP, Huang LB, Deng QD, Lai XH. A new bacterial pathogen: entero adherent-invasive-toxigenic *E.coli*. *Chin Med J*, 1996;109:16-17
- Griffin PM, Tauxe RV. The epidemiology of infections caused by *Escherichia coli* O157 : H7, other enterohemorrhagic *E.coli*, and the associated hemolytic uremic syndrome. *Epidemiol Rev*, 1991; 13(suppl):60-98
- Fukushima H, Hashizume T, Kitani T. The massive outbreak of enterohemorrhagic *E.coli* O157 infections by food poisoning among the elementary school children in Sakai, Japan. 3rd International Symposium and Workshop on Shiga Toxin (Verotoxin) Producing *Escherichia coli* Infections. Melville, NY: Lois Joy Galler Foundation for Hemolytic Uremic Syndrome Inc. 1997: 111
- Xu JG, Quan TS, Xiao DL, Fan RR, Li LM, Wang CA. Isolation and characterization of *Escherichia coli* O157 : H7 strains in China. *Curr Microbiol*, 1990;20:299-303
- Kain KC, Barteluk RL, Kelly MT, He X, Hua G, Ge YA. Etiology of childhood diarrhea in Beijing, China. *J Clin Microbiol*, 1991;29: 90-95
- Clarke RC, Wilson JB, Read SC, Renwick S, Rahn K, Johnson RP. Verocytotoxin producing *Escherichia coli* (VTEC) in the food chain: preharvest and processing perspectives. In: Karmali, MA, Goglio AG eds. Recent advances in verocytotoxin producing *Escherichia coli* infections. Amsterdam, The Netherlands: Elsevier Science BV, 1994:17-24
- Xu JG, Cheng BQ, Wu YP, Huang LB, Lai XH, Liu BY. Cell adherence patterns and DNA probe types of *E.coli* strains isolated from diarrheal patients in China. *Microbiol Immunol*, 1996;40: 88-99
- Xu JG, Wu YP, Deng QD, Xiao HF, Hall R, Lai XH. Characterization of a Shiga -like toxin producing and invasive *Escherichia coli* strain: a possible new variety of diarrheagenic pathogen. In: Keusch GT, Kawakami M, eds. Cytokines, cholera and the gut. OMN Ohmsha, Japan: IOS Press, 1996:321-328
- Small PL, Falkow S. Development of a DNA probe for the virulence plasmid of *Shigella* spp. and enteroinvasive *Escherichia coli*. In: Leive L, Bonventre PF, Morello JA, Silver SD, Wu WC, eds. Microbiology. Washington D.C: American Society for Microbiology, 1986:121-124
- Smith HR, Scotland SM, Chart H, Rowe B. Vero cytotoxin production and presence of VT genes in strains of *Escherichia coli* and *Shigella*. *FEMS Microbiol Lett*, 1987;42:173-177
- Nataro JP, Kaper JB, Robins-Browne B, Prado V, Vial P, Levine MM. Patterns of adherence of diarrheagenic-*Escherichia coli* to HEp-2 cells. *Pediatr Infect Dis J*, 1987;6:829-831
- Vial PA, Robins-Browne B, Lior H, Prado V, Kaper JB, Nataro JP. Characterization of enteroadherent aggregative *Escherichia coli*, a putative agent of diarrheal disease. *J Infect Dis*, 1988;158:70-78
- Karmali MA. Infection by verotoxin-producing *Escherichia coli*. *Clin Microbiol Rev*, 1989;2:15-38
- Nataro, JP, Kaper JB. Diarrheagenic *Escherichia coli*. *Clin Microbiol Rev*, 1998;11:142-201
- Hacker J, Blum-Oehler G, Mühldorfer I, Tsch-pe H. Pathogenicity islands of virulent bacteria: structure, function and impact on microbial evolution. *Mol Microbiol*, 1997;23:1089-1097
- Schubert S, Rakin A, Karch H, Carniel E, Heesemann J. Prevalence of the "high pathogenicity island" of *Yersinia* species among *Escherichia coli* strains that are pathogenic to humans. *Infect Immun*, 1998;66: 480-485

Edited by MA Jing-Yun

# The Hsp90 chaperone complex-A potential target for cancer therapy ?

Beatrice D. Darimont

See article on page 199

## ORIGINAL ARTICLE

Down-regulation of Hsp90 could change cell cycle distribution and increase drug sensitivity of tumor cells.

## MAJOR POINTS OF THE COMMENTED ARTICLE

Using an antisense RNA approach, Liu *et al* studied the consequence of lowering Hsp90  $\beta$  expression in two human gastric (SGC7901, SGC7901/VCR), one hepatic (HCC7402) and one esophageal (Ec109) cancer cell line. For two of the investigated cell lines (SGC7901/VCR and Ec109) cell growth slowed down upon decrease of the Hsp90  $\beta$  level due to an increase in G1 cell phase. The growth rate of the SGC7901 cell line was unaffected by lowering the concentration of Hsp90  $\beta$ , however the duration of G1 was decreased while G2 increased. No Hsp90  $\beta$  dependent change in the growth was detectable for the hepatic cancer cell line HCC7402, which expressed Hsp90  $\beta$  in lower levels than the other cell lines. Upon lowering the Hsp90  $\beta$  concentration, all cell lines became more sensitive to chemotherapeutic drugs. Increases in the efficacy of mitomycin C (MMC) and cyclophosphamide (CTX) were generally modest (0-5 fold), although the SGC7901 cell line exhibited a 24.8 fold increased sensitivity to MMC. With the exception of the cell line SGC7901/VCR, dramatic effects were observed on the sensitivity of the cell lines to adriamycin (ADR) and vincristine (MMC) with a  $10^4$  fold and  $3 \times 10^4$  fold increase in sensitivity of SGC7901 to VCR, or Ec109 to ADR, respectively.

## COMMENTARY

Molecular chaperones are one of the life-guards of a living cell. They coordinate and execute basic and essential cell functions, such as facilitation of protein folding and oligomeric assembly of proteins, as well as the regulation of ligand binding and

release, subcellular localization and turnover of proteins<sup>[1,2]</sup>. They are important for cell viability, and have been proposed to act as evolutionary tools, that produce a pool of mutant proteins under stress conditions<sup>[3,4]</sup>. Not surprisingly, aberrant chaperone action has been linked to numerous diseases<sup>[5-8]</sup>, and the clinical interest in chaperones as targets for drug based treatments is increasing.

### *Hsp90 assembles into multiprotein complexes*

Hsp90, a highly conserved and ubiquitously expressed chaperone of animal and plant cells, is one of the most abundantly expressed proteins (1%-2% of the cytosolic protein in unstressed mammalian cells)<sup>[2,9-11]</sup>. Most eukaryotic cells contain at least two Hsp90 isoforms-the heat shock induced Hsp90  $\beta$  and the usually less regulated Hsp90  $\beta$ <sup>[12]</sup>. Another close relative, Grp94, is expressed in the endoplasmic reticulum<sup>[11,13]</sup>. Hsp90 assembles into large multiprotein complexes, that have partially overlapping compositions and include other chaperones such as Hsp70, Hip ("Hsp70-interacting protein"), Hop ("Hsp90-Hsp70 organizing protein", also called p60, Sti1), p23, and one of three large immunophilins FKBP51, FKBP52 (Hsp56), or Cyp40, which are peptidyl prolyl isomerases<sup>[2,10]</sup>.

### *Hsp90 folds and controls the activity of regulatory proteins involved in signaling*

The predominant role of these complexes may be to facilitate the maturation, functional regulation, cellular localization and stress-dependent protection and repair of proteins rather than to assist the folding of de novo synthesized proteins<sup>[14-16]</sup>. Interestingly, many of the substrates of these Hsp90 chaperone complexes are regulatory proteins, or proteins involved in structural organization such as actin and tubulin<sup>[2]</sup>. One of the best studied substrates of Hsp90 chaperone complexes are intracellular receptors, especially but not exclusively steroid receptors<sup>[10,17-22]</sup>. *In vivo* association of unliganded steroid receptors with Hsp90 chaperone complexes is required for optimal steroid binding<sup>[23-25]</sup>, and may also affect receptor subcellular trafficking<sup>[26]</sup>. Hsp90 chaperone complexes also assist in the folding, maturation, membrane localization and degradation of many

Department of Cellular and Molecular Pharmacology, University of California, San Francisco, USA

**Correspondence to:** Beatrice D. Darimont, Department of Cellular and Molecular Pharmacology, University of California, San Francisco, CA 941430450, USA

Fax: 415-502-8644

E-mail: darimon@itsa.ucsf.edu

**Received** 1999-05-17

protein kinases<sup>[2,10,20]</sup>, such as v-Src<sup>[27]</sup>, Raf<sup>[28]</sup>, eIF-2- $\alpha$ -kinase<sup>[29]</sup>, casein kinase II (CK II)<sup>[30]</sup>, mitogen-activated protein kinase (MEK)<sup>[31]</sup>, cyclin-dependent kinase 4 (CDK4)<sup>[32,33]</sup>, and the cyclin-dependent kinase regulator Wee1<sup>[34]</sup>. Association of these kinases with Hsp90 chaperone complexes is mediated by p50 cdc37, an homolog of the yeast cell cycle control protein, cdc37<sup>[33,35]</sup>. The ability to interact functionally with a wide variety of regulatory proteins suggests that Hsp90 chaperone complexes may also coordinate and establish crosstalk between different signal transduction pathways. A recent study by Le Bihan *et al*<sup>[36]</sup> gave evidence for modulation of progesterin- and glucocorticosteroid receptor-mediated transcription by calcium/calmodulin kinases (CaMK types II and IV), presumably through Hsp90 chaperone complexes.

#### ***The role of Hsp90 in cell cycling and cancer***

Hsp90 action has been connected to cell cycle and cell differentiation<sup>[2,37,38]</sup>, most likely as a consequence of their role in folding and functional regulation of intracellular receptors, protein kinases and other potential substrates such as p53<sup>[9,39]</sup>. Moreover, the expression pattern of Hsp90 itself can be cell cycle dependent<sup>[40]</sup>. Increased levels of Hsp90 (mostly Hsp90  $\alpha$ ) have been found in various malignant cell lines and cancers and usually correlate with vigorous proliferation of the malignant cells<sup>[2,41-44]</sup>.

In a complementary study Liu *et al*<sup>[45]</sup> (this issue) investigate the consequence of lowering Hsp90  $\beta$  expression in several human cancer cell lines using an antisense RNA approach. In agreement with the trend seen in other studies<sup>[41-44]</sup>, they find that in some but not all cancer cell lines growth slows upon decrease of the Hsp90  $\beta$  level, with various changes in cell cycle phasing. For one cell line, the hepatic cancer cell line HCC7402, growth and cell cycle phasing is not affected by reduced expression of Hsp90  $\beta$ . Thus, overexpression of Hsp90 is not essential for cancerous growth. In fact, in an invasive and tumorigenic subline of 8701-BC breast cells down-regulation of Hsp90  $\beta$  has been observed<sup>[46]</sup>. In view of the differences in the regulation of Hsp90  $\alpha$  and Hsp90  $\beta$ , it would be interesting to extend the studies of Liu *et al* to Hsp90  $\alpha$ , whose expression is usually more directly linked to the cell cycle than that of Hsp90  $\beta$ .

#### ***Hsp90 as target for anti-tumor drugs***

Pharmacologically, the influence of Hsp90 activity on tumor growth is well established. Hsp90 chaperone complexes are targets for several pharmacological drugs<sup>[2,9,47]</sup>. The antibiotic geldanamycin is an anti-tumor drug that binds to the

ATP/ADP binding site in the N-terminal domain of Hsp90<sup>[48]</sup>. Geldanamycin interferes with the folding, maturation, cellular localization and degradation of various intracellular receptors and kinases<sup>[2,9,47]</sup>, and initially was described as an inhibitor for cell cycle kinases<sup>[49]</sup>. Another, unrelated antibiotic, Radicicol, also binds to the ATP-ADP-binding site of Hsp90 and suppresses transformation by diverse oncogenes such as Src, Ras and Mos<sup>[50,51]</sup>. Geldanamycin prevents binding of p23 to Hsp90<sup>[19]</sup>, however whether its anti-tumor activity is due directly to this interference remains to be investigated. Although the role of ATP/ADP in the function of Hsp90 is not fully understood, the functional consequence of the binding of these structurally unrelated antibiotics to the Hsp90 ATP/ADP-binding site marks this site as an interesting target for drug design. Other potential and probably more selective drug targets in the Hsp90 chaperone complex are the immunophilins FKBP51, FKBP52 or Cyp40 that bind the immunosuppressants FK506, rapamycin or cyclosporin A<sup>[10,19]</sup>.

#### ***Hsp90 mediated multidrug resistance***

In addition of being target for several pharmacological drugs, Hsp90 chaperone complexes influence the sensitivity of cells to many drugs, and high Hsp90 expression is often associated with multidrug resistance<sup>[52]</sup>, a major impediment of successful cancer chemotherapy. In their present study, Liu *et al*<sup>[45]</sup> demonstrate that upon lowering the Hsp90  $\beta$  concentration the sensitivity of cancer cell lines to chemotherapeutic drugs increases, however the extent of these changes was strongly dependent on the drug. With exception of some cancer cell lines, their Hsp90  $\beta$  dependent increases in the efficacy are generally modest (0-5-fold) for the drugs mitomycin C and cyclophosphamide, and more dramatic (up to  $3 \times 10^4$ -fold) for the drugs adriamycin and vincristine.

The mechanisms underlying multidrug resistance appear to be complex and are not well understood. In many tumor cells multidrug resistance is associated with overexpression of either the 170 kDa P-glycoprotein (Pgp) or members of the ATP-binding cassette transporter superfamily, such as the multidrug resistance protein (MRP) or the breast cancer resistance protein (BCRP), that act as drug export pumps<sup>[53-55]</sup>. A third form of multidrug resistance (atypical MDR) correlates with quantitative or qualitative alterations in topoisomerase II  $\alpha$ , that actively participates in the lethal action of cytotoxic drugs<sup>[56,57]</sup>. The mechanism of Hsp90 mediated multidrug resistance remains largely to be characterized. The contribution of Hsp90 might be a general strengthening of the stress response and the cellular

resistance to cytotoxic drugs. However, in some drug resistant cell lines Hsp90  $\beta$  was found to stabilize and enhance the function of Pgp<sup>[52]</sup> suggesting a more direct role of Hsp90 in regulating multidrug resistance.

## CONCLUSIONS AND PERSPECTIVES

Hsp90 chaperone complexes are vital and versatile coordinators and regulators of multiple signal transduction pathways. In higher organisms their action goes beyond that of a single cell and also affects complex regulatory systems such as the immune response. Hsp90, Grp94 and Hsp70 bind peptides and deliver them to MHC class I molecules, which increases the efficiency of the immune response<sup>[58]</sup> and often enhance tumor immunogenicity<sup>[59]</sup>. These pleiotropic functions make Hsp90 chaperone complexes ideal targets for the treatment of cancers.

Antisense Hsp90 mRNA expression, as used by Liu *et al*<sup>[45]</sup> is a powerful tool for regulating Hsp90 expression and reducing proliferation in some cancer cell lines. However, the inherent difficulty of selectively targeting antisense constructs to tumor cells impedes the usage of this strategy for clinical therapy. In contrast, the role of Hsp90, Grp94 and Hsp70 in tumor immunogenicity may offer new strategies for anti-tumor vaccination. Presently, the most promising strategy for an Hsp90 targeted therapy is the functional regulation of Hsp90 by drugs such as geldanamycin or radicicol. The solution of the molecular structures of Hsp90 : ATP/ADP and Hsp90 : geldanamycin complexes<sup>[48,60]</sup> allows the identification of structural features required for Hsp90 binding, and to develop new drugs with different pharmacological properties by structure based design. Other attractive targets for drug based regulation of Hsp90 chaperone complexes are the sites for the interaction with the kinase specific p50<sup>cdc37</sup> or immunophilins that appear to mediate specificity by directing Hsp90 chaperone complexes to particular substrates. Future elucidation of the composition, structure and function of those complexes will certainly open new possibilities for the treatment of cancer.

## REFERENCES

- Hartl FU. Molecular chaperones in cellular protein folding. *Nature*, 1996;381:571-579
- Csermely P, Schnaider T, Söiti C, Prohászka Z, Nardai G. The 90-kDa molecular chaperone family: structure, function, and clinical applications. A comprehensive review. *Pharmacol Ther*, 1998; 79:129-168
- Csermely P. Proteins, RNAs, chaperones and enzyme evolution: a folding perspective. *Trends Biochem Sci*, 1997;22:147-149
- Rutherford SL, Lindquist S. Hsp90 as a capacitor for morphological evolution. *Nature*, 1998;396:336-342
- Welch WJ. Mammalian stress response: cell physiology, structure/function of stress proteins, and implication for medicine and disease. *Physiol Rev*, 1992;72:1063-1081
- Burdon RH. Heat shock proteins in relation to medicine. *Mol Aspects Med*, 1993;14:83-165
- Jindal S. Heat shock proteins: applications in health and disease. *Trends Biotechnol*, 1996;14:17-20
- Brooks DA. Protein processing: a role in the pathophysiology of genetic disease. *FEBS Lett*, 1997;409:115-120
- Scheibel T, Buchner J. The Hsp90 complex-a super-chaperone machine as a novel drug target. *Biochem Pharmacol*, 1998;56: 675-682
- Pratt WB. The Hsp90 based chaperone system: involvement in signal transduction from a variety of hormone and growth factor receptors. *Proc Soc Exper Biol Med*, 1998;217:420-434
- Scheibel T, Buchner J. The Hsp90 family: an overview. In: Gething MJ, ed. Guidebook to molecular chaperones and protein catalyses. Oxford: Oxford University Press, 1997:147-151
- Krone PH, Sass JB. Hsp90  $\alpha$  and Hsp90  $\beta$  genes are present in the zebrafish and are differentially regulated in developing embryos. *Biochem Biophys Res Comm*, 1994;204:746-752
- Gupta RS. Phylogenetic analysis of the 90kD heat shock family of protein sequences and an examination of the relationship among animals, plants, and fungi species. *Mol Biol Evol*, 1995; 12:1063-1073
- Nair SC, Toran EJ, Rimerman RA, Hjermstad S, Smithgall TE, Smith DF. A pathway of multi-chaperone interactions common to diverse regulatory proteins-estrogen receptor, fcs tyrosine kinase, heat shock transcription factor, HSF1, and the aryl hydrocarbon receptor. *Cell Stress Chaperones*, 1996;1: 237-250
- Johnson JL, Craig EA. Protein folding in vivo: unraveling complex pathways. *Cell*, 1997;90:201-204
- Nathan DF, Vos MH, Lindquist S. *In vivo* function of the *Saccharomyces cerevisiae* Hsp90 chaperone. *Proc Natl Acad Sci USA*, 1997;94:12949-12956
- Smith DF, Toft DO. Steroid receptors and their associated proteins. *Mol Endo*, 1993;7:4-11
- Bohen SP, Yamamoto KR. Modulation of steroid receptor signal transduction by heat shock proteins. In: The biology of heat shock proteins and molecular chaperones. Cold Spring Harbor: Cold Spring Harbor Laboratory Press, 1994:313-334
- Pratt WB, Toft DO. Steroid receptor interactions with heat-shock protein and immunophilin chaperones. *Endo Rev*, 1997;18:306-360
- Pratt WB. The role of the Hsp90 based chaperone system in signal transduction by nuclear receptors and receptors signaling via MAP kinase. *Annu Rev Pharmacol Toxicol*, 1997;37: 297-326
- Holley SJ, Yamamoto KR. A role for Hsp90 in retinoid receptor signal transduction. *Mol Biol Cell*, 1995;6:1833-1842
- Pongratz I, Mason GG, Poellinger L. Dual roles of the 90-kDa heat shock protein Hsp90 in modulating functional activities of the dioxin receptor. Evidence that the dioxin receptor functionally belongs to a subclass of nuclear receptors which require Hsp90 both for ligand binding activity and repression of intrinsic DNA binding activity. *J Biol Chem*, 1992;267: 13728-13734
- Picard D, Khurshed B, Garabedian MJ, Fortin MG, Lindquist S, Yamamoto KR. Reduced levels of Hsp90 compromise steroid receptor action *in vivo*. *Nature*, 1990;348:166-168
- Bohen SP, Yamamoto KR. Isolation of Hsp90 mutants by screening for decreased steroid function. *Proc Natl Acad Sci USA*, 1993; 114:24-11428
- Nathan DF, Lindquist S. Mutational analysis of Hsp90 function: interactions with a steroid receptor and a protein kinase. *Mol Cell Biol*, 1995;15:3917-3925
- DeFranco DB, Ramakrishnan C, Tang Y. Molecular chaperones and subcellular trafficking of steroid receptors. *J Steroid Biochem Molec Biol*, 1998;65:51-58
- Xu Y, Lindquist S. Heat-shock protein Hsp90 governs the activity of pp60v-src kinase. *Proc Natl Acad Sci USA*, 1993;90: 7074-7078
- van der Straten A, Rommel C, Dickson B, Hafen E. The heat shock protein 83 (Hsp83) is required for Raf-mediated signalling in *Drosophila*. *EMBO J*, 1997;16:1961-1969
- Uma S, Hartson SD, Chen JJ, Matts RL. Hsp90 is obligatory for the hemeregulated eIF-2 $\alpha$  kinase to acquire and maintain an activable conformation. *J Biol Chem*, 1997; 272:11648-11656
- Miyata Y, Yahara I. The 90-kDa heat shock protein, Hsp90, binds and protects casein kinase II from selfaggregation and enhances its kinase activity. *J Biol Chem*, 1992;267: 7042-7047
- Stancato LF, Silverstein AM, Owens-Grillo JK, Chow YH, Jove R, Pratt WB. The Hsp90 binding antibiotic geldanamycin decreases Raf levels and epidermal growth factor signaling without disrupting

- formation of signaling complexes or reducing the specific enzymatic activity of Raf kinase. *J Biol Chem*, 1997;272:4013-4020
- 32 Dai K, Kobayashi R, Beach D. Physical interaction of mammalian CDC37 with CDK4. *J Biol Chem*, 1996;271:22030-22034
  - 33 Stephanova L, Leng X, Parker SB, Harper JW. Mammalian p50Cdc37 is a protein kinase-targeting subunit of Hsp90 that binds and stabilizes Cdk4. *Genes Dev*, 1996;10:1491-1502
  - 34 Aligue R, Akhavan-Niak H, Russell P. A role for Hsp90 in cell cycle control: wee 1 tyrosine kinase requires interaction with Hsp90. *EMBO J*, 1994;13:6099-6106
  - 35 Kimura Y, Rutherford SL, Miyata Y, Yahara I, Freeman BC, Yue L, Morimoto RI, Lindquist S. Cdc37 is a molecular chaperone with specific functions in signal transduction. *Genes Dev*, 1997;11:1775-1785
  - 36 Le Bihan S, Marsaud V, Mercier Bodard C, Baulieu EE, Mader S, White JH, Renoir JM. Calcium/calmodulin kinase inhibitors and immunosuppressant macrolides rapamycin and FK506 inhibit progesterin and glucocorticosteroid receptor-mediated transcription in human breast cancer T47D cells. *Mol Endo*, 1998;12:986-1001
  - 37 Sato N, Torigoe T. The molecular chaperones in cell cycle control. *Annals New York Acad Sci*, 1998;851:61-66
  - 38 Galea-Lauri J, Latchman DS, Katz DR. The role of the 90-kDa heat shock protein in cell cycle control and differentiation of the monoblastoid cell line U937. *Exp Cell Res*, 1996;226:243-254
  - 39 Sepehrnia B, Paz IB, Dasgupta G, Momand J. Heat shock protein 84 forms a complex with mutant p53 protein predominantly within a cytoplasmic compartment of the cell. *J Biol Chem*, 1996;271:15084-15090
  - 40 Jerome V, Vourc'h C, Baulieu EE, Catelli MG. Cell cycle regulation of the chicken Hsp90 $\alpha$  expression. *Exp Cell Res*, 1993;205:44-51
  - 41 Ferrarini M, Heltai S, Zocchi MR, Rugarli C. Unusual expression and localization of heat shock proteins in human tumor cells. *Int J Cancer*, 1992;51:613-619
  - 42 Yufu Y, Nishimura J, Nawata H. High constitutive expression of heat shock protein 90 $\alpha$  in human acute leukemia cells. *Leuk Res*, 1992;16:597-605
  - 43 Franzen B, Linder S, Alaiya AA, Eriksson E, Fujioka K, Bergman AC, Jornvall H, Auer G. Analysis of polypeptide expression in benign and malignant human breast lesions. *Electrophoresis*, 1997;18:582-587
  - 44 Nanbu K, Konishi I, Komatsu T, Mandai M, Yamamoto S, Kuroda H, Koshiyama M, Mori T. Expression of heat shock proteins HSP70 and Hsp90 in endometrial carcinomas. Correlation with clinicopathology, sex steroid receptor status, and p53 protein expression. *Cancer*, 1996;77:330-338
  - 45 Liu XL, Xiao B, Yu ZC, Guo JC, Zhao QC, Xu L, Shi YQ, Fan DM. Down-regulation of Hsp90 could change cell cycle distribution and increase drug sensitivity of tumor cells. *W J G*, 1999;199-208
  - 46 Luparello C, Noel A, Pucci-Minafra I. Intratumoral heterogeneity for Hsp90 beta mRNA levels in a breast cancer cell line. *DNA Cell Biol*, 1997;16:1231-1236
  - 47 Cardenas ME, Sanfridson A, Cutler NS, Heitman J. Signal-transduction cascades as targets for therapeutic intervention by natural products. *Trends Biotechnol*, 1998;16:427-433
  - 48 Stebbins CE, Russo AA, Schneider C, Rosen N, Hartl FU, Pavletich NP. Crystal structure of an Hsp90 geldanamycin complex: targeting of a protein chaperone by an antitumor agent. *Cell*, 1997;89:239-250
  - 49 Uehara Y, Murakami Y, Suzukake-Tsuchiya K, Moriya Y, Sano H, Shibata K, Omura S. Effects of herbimycin derivatives on src oncogene function in relation to antitumor activity. *J Antibiot (Tokyo)*, 1988;41:831-834
  - 50 Sharma SV, Agatsuma T, Nakano H. Targeting of the protein chaperone, Hsp90, by the transformation suppressing agent, radicicol. *Oncogene*, 1998;16:2639-2645
  - 51 Roe SM, Prodromou C, O'Brien R, Ladbury JE, Piper PW, Pearl LH. Structural basis for the inhibition of the Hsp90 molecular chaperone by the antitumor antibiotics radicicol and geldanamycin. *J Med Chem*, 1999;42:260-262
  - 52 Bertram J, Palfner K, Hiddemann W, Kneba M. Increase of P-glycoprotein-mediated drug resistance by Hsp90 beta. *Anti-Cancer Drugs*, 1996;7:838-845
  - 53 Persidis A. Cancer multidrug resistance. *Nature Biotech*, 1999;17:94-95
  - 54 Bradshaw DM, Arceci RJ. Clinical relevance of transmembrane drug efflux as a mechanism of multidrug resistance. *J Clin Oncol*, 1998;16:3674-3690
  - 55 Doyle LA, Yang W, Abruzzo LV, Krogmann T, Gao Y, Rishi AK, Ross DD. A multidrug resistance transporter from human MCF-7 breast cancer cells. *Proc Natl Acad Sci USA*, 1998;95:15665-15670
  - 56 Volm M. Multidrug resistance and its reversal. *Anticancer Res*, 1998;18:2905-2917
  - 57 Nooter K, Stoter G. Molecular mechanisms of multidrug resistance in cancer chemotherapy. *Pathol Res Practice*, 1996;192:768-780
  - 58 Multhoff G, Botzler C, Issels R. The role of heat shock proteins in the stimulation of an immune response. *Biol Chem*, 1998;379:295-300
  - 59 Campbell FA, Redmond HP, Bouchier-Hayes D. The role of tumor rejection antigens in host antitumor defense mechanisms. *Cancer*, 1995;75:2649-2655
  - 60 Prodromou C, Roe SM, O'Brien R, Ladbury JE, Piper PW, Pearl LH. Identification and structural characterization of the ATP/ADP binding site in the Hsp90 molecular chaperone. *Cell*, 1997;90:65-75

Edited by MA Jing-Yun

# Down-regulation of Hsp90 could change cell cycle distribution and increase drug sensitivity of tumor cells

LIU Xian-Ling<sup>1</sup>, XIAO Bing, YU Zhao-Cai, GUO Jian-Cheng, ZHAO Qing-Chuan, XU Li, SHI Yong-Quan and FAN Dai-Ming

See invited commentary on page 195

**Subject headings** Hsp90; antisense RNA; cell cycle; gene transfection; drug resistance, multiple

## Abstracts

**AIM** To construct Hsp90 antisense RNA eukaryotic expression vector, transfect it into SGC7901 and SGC7901/VCR of MDR-type human gastric cancer cell lines, HCC7402 of human hepatic cancer and Ec109 of human esophageal cancer cell lines, and to study the cell cycle distribution of the gene transected cells and their response to chemotherapeutic drugs.

**METHODS** A 1.03kb cDNA sequence of Hsp90 $\beta$  was obtained from the primary plasmid pHSP90 by EcoR I and BamH I nuclease digestion and was cloned to the EcoR I and BamH I site of the pcDNA by T4DNA ligase and an antisense orientation of Hsp90 $\beta$  expression vector was constructed. The constructs were transfected with lipofectamine and positive clones were selected with G418. The expression of RNA was determined with dot blotting and RNase protection assay, and the expression of Hsp90 protein determined with western blot. Cell cycle distribution of the transfectants was analyzed with flow cytometry, and the drug sensitivity of the transfectants to Adriamycin (ADR), vincristine (VCR), mitomycin (MMC) and cyclophosphamide (CTX) with MTT and intracellular drug concentration of the transfectants was determined with flow

## cytometry.

**RESULTS** In EcoR I and BamH I restriction analysis, the size and the direction of the cloned sequence of Hsp90 $\beta$  remained what had been designed and the gene constructs were named pcDNA-Hsp90. AH-SGC790, AH-SGC7901/VCR, AH-HCC7402 and AH-Ec109 cell clones all expressed Hsp90 anti-sense RNA. The expression of Hsp90 was down-regulated in AH-SGC7901, AH SGC7901/VCR, AH-HCC7402 and AH-Ec109 cell clones. Cell cycle distribution was changed differently. In AH-SGC7901/VCR and AH-Ec109 cells, G1 phase cells were increased; S phase and G2 phase cells were decreased as compared with their parental cell lines. In AH-SGC7901 cell, G1 phase cells were decreased, G2 phase cells increased and S phase cells were not changed, and in AH-HCC7402 cells G1, S and G2 phase cells remained unchanged as compared with their parental cell lines. The sensitivity of AH SGC7901, AH-SGC7901/VCR, AH-HCC7402 and AH-Ec109 to chemotherapeutic drugs, the sensitivity of AH-SGC7901/VCR to ADR, VCR, MMC and CTX the sensitivity of AH-HCC7402 to ADR and VCR, and the sensitivity of Ec109 to ADR, VCR and CTX all increased as compared with their parental cell lines. The mean fluorescence intensity of ADR in AH-SGC7901, AH-SGC7901/VCR, AH-HCC7402 and AH-Ec109 was also significantly elevated ( $P < 0.05$ ).

**CONCLUSION** Down-regulation of Hsp90 could change cell cycle distribution and increase the drug sensitivity of tumor cells.

## INTRODUCTION

Heat shock proteins (HSPs) are a highly conserved group of intracellular proteins whose synthesis is increased in response to a variety of stressful stimuli<sup>[1]</sup>. HSPs are classified by molecular weight into groups of HSP110, HSP90, HSP70, HSP60, small molecular HSP and ubiquitin. HSP90 is a main chaperone protein in the cell plasma<sup>[2]</sup>. Recent studies have suggested that HSP90

<sup>1</sup>Institute of Digestive Diseases, Xijing Hospital, Fourth Military Medical University, Xi'an 710032, Shaanxi Province, China

Dr. LIU Xian-Ling, female, born on 1962-04-12 in Shaanxi Province, received Ph.D. degree in 1998 from Fourth Military Medical University, now attending physician in the department of gastroenterology, having 10 papers published.

\*Project supported by the National Natural Science Foundation of China, No. 39570806 and National Excellent Youth Scientific Foundation, No. 3952020.

**Correspondence to:** LIU Xian-Ling, Institute of Digestive Diseases, Xijing Hospital, Fourth Military Medical University, 15 Western Chang Le Road, Xi'an 710032, Shaanxi Province, China  
Tel. +29 • 3375226

Received 1999-01-03 Revised 1999-03-19

expression is increased in tumor tissues<sup>[3,4]</sup> and is closely related to multi-drug resistance protein P-gp<sup>[5,6]</sup>. To further investigate the biological roles of HSP90 in the processes of carcinogenesis and the possibility of down regulation of HSP90 to reverse the drug resistance of tumor cells, we have constructed the Hsp90 antisense RNA eukaryotic expression vector, transfected it into SGC7901 of human gastric cancer SGC7901/VCR of multi-drug resistant human gastric cancer, HCC7402 of human hepatic cancer and Ec109 of human esophageal cancer cell lines. We also studied the cell cycle distribution of the gene transected cells and their response to chemotherapeutic drugs.

## MATERIAL AND METHODS

### Materials

**Reagents** EcoR I and BamH I nuclease was purchased from Sino-American Biotech Inc T4 DNA ligase from Promega Company. Other reagents included guanidinium isothiocyanate lysis solution (guanidinium isothiocyanate, citric acid sodium, sarkosyl, ( $\gamma$ -<sup>32</sup>P) ATP, T4 phage polynucleotide kinase, 20 × SSC (NaCl, citric acid sodium), 50 × Denhardt (Ficoll, N-Polyvinylpyrrolidone and BSA), pre-hybridization solution (6 × SSC, 0.5% SDS, 5 × Denhardt, 100 mg/L salmon sperm DNA) TBE (89 mmol/L Tris-boric acid, 2 mmol/L EDTA), 5 × hybridization buffer (200mM-PIPES pH 6.4, 2mM-NaCl, 5mM EDTA), formamide hybridization buffer (formamide: 5 × hybridization buffer = 4:1), RNase S<sub>1</sub>, RNase S<sub>1</sub> buffer (10mM Tris-Cl pH 7.5, 300mM NaCl, 5mM EDTA), 50mg/L proteinase K, 0.5% SDS (w/v), phenol, chloroform, RNA loading buffer (80% formamide, 1mM EDTA pH 8.0, 0.1% bromophenol blue, 0.1% Xylene Cyanol), acrylamide, bisacrylamide, 10% saturated ammonium sulfate, urea, lipofactamine, G418, RPMI1640, goat anti-human HSP90  $\beta$  monoclonal antibody, HRP-labeled donkey anti-goat IgG, Lysis buffer (50 mmol/L Tris • Cl, pH 8.0, 150 mmol/L NaCl, 0.02% NaN<sub>3</sub>, 0.1% SDS, 100  $\mu$ L/mL PMSF, 1 mg/L aprotinin, 1% NP-40, 0.5% deoxycholic acid), TEMED, Tris-glycine working solution (25 mmol/L Tris • Cl, 250 mmol/L glycine, 0.1% SDS), 2 × SDS gel-loading buffer (100 mmol/L Tris • Cl, pH 6.8, 200 mmol/L DTT, 4% SDS, 0.2% bromophenol blue, 20% glycerol), electroblotting buffer (39 mmol/L glycine, 48 mmol/L Tris • Cl, 0.037% SDS, 20% methanol), tetrachloride naphenol, propidium iodide, adriamycin (ADR), vincristine (VCR), Mitomycin (MMC) and cyclophosphamide (CTX).

**Cell lines** SGC7901 of human gastric cancer cell line was provided by the Military Medical Scientific Chinese Academy, of Military Medical Sciences, SGC7901/VCR of MDR-type

human gastric cancer cell line was from our institute, HCC7402 of human hepatic cancer cell line from Pathological Department of Fourth Military Medical University (FMMU). Ec109 of human esophageal cancer cell line was from Biochemical Department of FMMU.

### Methods

**Construction of HSP90 antisense RNA eukaryotic expression vector** phHSP90 of HSP90 cDNA plasmid was supplied by YAMAMOTO. Eukaryotic expression vector pcDNA 3.1(+) was supplied by Yang Jing-Hua. E.coli JM109 was introduced by original source of our institute. ① Plasmid map analyses: Analysis of the nuclease site of phHSP90 plasmid map of HSP90 prokaryotic expression vector found that there were two EcoR I nuclease sites and one BamH I nuclease sites in the gene sequence of HSP90 cDNA, of which EcoR I nuclease site is located at 0.99kb and 1.07kb respectively and BamH I nuclease site is located at 2.1kb. There was another EcoR I nuclease site at prime 3 of the phHSP90 plasmid following the stop codon of HSP90 cDNA (Figure 1). There was one EcoR I and one BamH I nuclease site on the multi-clonal nuclease sites of prokaryotic expression vector pcDNA 3.1(+), of which EcoR I is located at prime 3 and BamH I is located at prime 5 (Figure 2). With EcoR I and BamH I nuclease, a 1.03kb fragment of 1.07kb-2.1kb could be digested from HSP90 cDNA (EcoR I was at prime 3, BamH I at prime 5). By inserting the digested fragment (1.03kb) into EcoR I and BamH I nuclease site of pcDNA 3.1(+), the HSP90 antisense RNA eukaryotic expression vector could be constructed.

② The primary plasmid phHSP90 was extracted by alkali lysis. First, phHSP90 was digested by EcoR I and electrophoresed on agarose-gel. Two fragments of 1.43kb and 3.99kb could be seen under ultraviolet from the gel. Of them, the 1.43kb-DNA was excised from the gel and purified by the frozen-melting method. The purified DNA was further digested by BamH I nuclease and electrophoresed, and a 1.3kb fragment (EcoR-I was at prime 3, BamH I was at prime 5) was obtained. The specific fragment (0.5  $\mu$ g) and 0.1  $\mu$ g-pcDNA 3.1(+) linearized by EcoR I and BamH I nuclease was ligated by T4 DNA ligase under 16°C for 18 h (Figure 3). The ligated products were transformed into the sensitized *E.coli* JM109, grew on ampicilline resistant agarose gel. Positive clones were selected and amplified and a small amount of plasmid was extracted. The reconstructed plasmid was digested by either EcoR I or BamH I or by both EcoR I and BamH I nuclease to determine the size and the direction of the fragment.



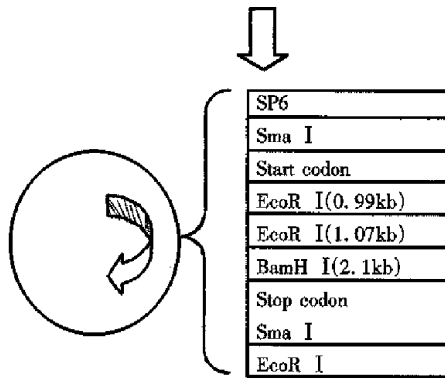


**Figure 1** Plasmid map of phHSP90.

Vector: pSP64(3kb); Inserts: human HSP90 $\beta$  cDNA (2.5kb); Insert site: Sma I of multiclonal enzyme restriction site of pSP64; Promoter: SP6; Drug resistance: Amp

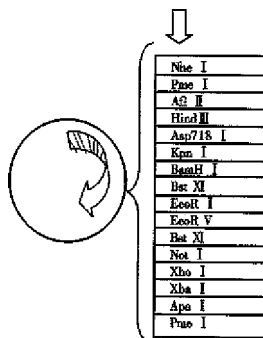


**Figure 2** Plasmid map of eukaryotic expression vector pcDNA 3.1 (+). (5.4kb)

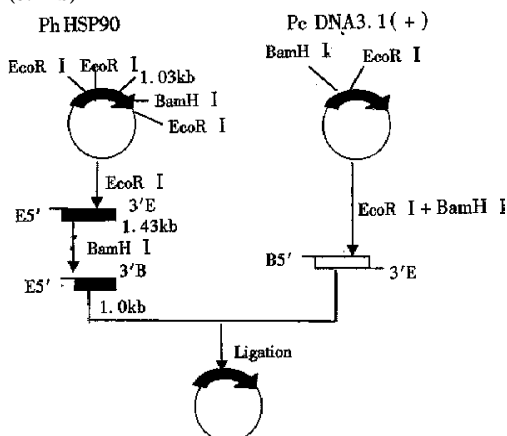


**Figure 3** Construction of pcDNA-HSP90 of HSP90 antisense RNA eukaryotic expression vector.

**Gene transfection and clone selection.** The pcDNA-HSP90 of HSP90 anti-sense RNA constructs was extracted by the alkali lysis method, purified by PEG, transfected into SGC7901, SGC7901/VCR, HCC7402 and Ec109 by Lipofectamine and selected by G418. In a six-well culture plate, seed  $1 \times 10^5$  cells per well in 2 mL appropriate complete growth

medium. Incubate the cells at 37°C in a CO<sub>2</sub> incubator until the cells are 80% confluent. After rinsing the cells with serum free and antibiotics-free medium, add pcDNA-HSP90-Lipofectamine mixture (or pcDNA 3.1(+)Lipofectamine mixture as control). Incubate the cells at 37°C in a CO<sub>2</sub> incubator for 6 hours. Then change the medium with RPMI1640 culture medium containing 10% fetal bovine serum. G418 (400 mg/L) was added to select the resistant clone after 48-72 hours. The medium was changed every 3-4 days and colonies were collected approximately 3 weeks later.

**RNA analyses.** ① Probe designing and synthesizing. Reading 30bp from 1641<sup>st</sup> bp of HSP90 cDNA, the gene sequence is 5' ATT GAC GAG TAC TGT GTG CAG CAG CTC AAG-3'. This gene fragment was matched with the gene bank from the Internet. We found that this sequence could only match with the HSP90 gene, and no homology with any other available genes. So this selected sequence was used as a probe and was synthesized by the Shanghai Biotech Company.  $\beta$ -actin was donated by Dr. Zhao Qing-Chuan and the sequence is  $\beta$ -actin-2095: 5'-ACT ATG TTT GAG ACC TTC AA-3'. ② Oligonucleotide probes labeled by T4 phage polynucleotide kinase. Add pure water to a total volume of 19.5  $\mu$ L in 10pmol/ $\mu$ L Oligonucleotide (1.0  $\mu$ L),  $10 \times$  T4 buffer (2.0  $\mu$ L) and 10pmol [ $\gamma$ -<sup>32</sup>P]ATP (5.0  $\mu$ L). After being mixed, suck 0.5  $\mu$ L-10  $\mu$ L 10 mmol/L Tris-Cl (pH 8.0) to assay the radioactivity ratio. Then 1  $\mu$ L T4 phage polynucleotide kinase was added and mixed and bathed in 37°C for 45 min, then bathed in 68°C for 10min to inactive T4 phage polynucleotide kinase. Afterwards, suck 0.5  $\mu$ L above solution and added to 10  $\mu$ L 10 mmol/L Tris-Cl (pH 8.0) to assay the radioactivity ratio. Precipitate the probes with ethanol and resubalalyzed to 20  $\mu$ L 1mmol/L EDTA deionized water and stored at -20°C. Radioactivity ratio of the oligonucleotide was assayed by the TCA method<sup>[7]</sup>. ③ RNA isolation. Total RNA was obtained from the cells by the guanidium isothiocyanate-phenol-chloroform extraction method. Cells of  $1 \times 10^6$  were collected and washed with PBS, guanidinium isothiocyanate lysis solution 500  $\mu$ L, 3 mol/L- NaAc 100  $\mu$ L, water saturated phenol and chloroform each 500  $\mu$ L-were added, ice bathed for 20 min and centrifuged at 4°C (12 000r/min) for 15 min. The upper water layer was sucked up to another eppendoff tube, extracted with anequal volume of phenol/chloroform (1/1), precipitated by isopropanol, centrifuged at 4°C (12 000r/min) for 15 min, washed with 70% ethanol once, resuspended to three-evaporated water, treated by

50  $\mu$ L DEPC quantitated and stored at  $-20^{\circ}\text{C}$ . ④ RNA dot blotting. The quantitated RNA was denatured by formaldehyde and was dropped to the nitrocellulose membrane and was dried in  $80^{\circ}\text{C}$  dry oven for 2 h. After pre-hybridization at  $68^{\circ}\text{C}$  water bathing for 2 h, probes were added to the hybridization bag and water bathed for 16 h-24 h at  $68^{\circ}\text{C}$ . The hybridization membrane was picked out and washed with  $2 \times \text{SSC}$  and 0.1% SDS for 20 min at room temperature and with  $0.2 \times \text{SSC}$  and 0.1% SDS at  $68^{\circ}\text{C}$  3 times for 10 min. Then the nitrocellulose membrane was dried by filter paper and was covered by fresh-keeping film. The membrane was exposed to X-ray film in the presence of intensifying screens at  $-20^{\circ}\text{C}$  for 48 h-72 h. The film was then developed to observe the results. ⑤ RNase protection assay<sup>[8]</sup>. RNA (10  $\mu$ L) from the cells were precipitated and resuspended in 30  $\mu$ L formamide hybridization buffer. Radiolabeled Oligonucleotide probes (1  $\mu$ L) and  $\beta$ -actin probes (1  $\mu$ L) diluted to  $1 \times 10^5$  cpm with hybridization buffer were added to the total RNA. The mixture was heated at  $85^{\circ}\text{C}$  for 5 min and the RNAs hybridized at  $45^{\circ}\text{C}$  or  $50^{\circ}\text{C}$  overnight. After hybridization, 2  $\mu$ L RNase S1 buffer, 16  $\mu$ L water and 2  $\mu$ L RNase S1 (2 mg/L) were added and the mixture was incubated at  $37^{\circ}\text{C}$  for 60 min. The solution, which now contained RNase protected fragments, was deproteinized with 50 mg/L proteinase K and 0.5% SDS (w/v) at  $37^{\circ}\text{C}$  for 15 min, extracted with an equal volume of phenol/chloroform (1/1), coprecipitated with 10  $\mu$ g yeast RNA, and resuspended in 8  $\mu$ L loading buffer. The samples were electrophoresed on a 18% acrylamide/6M urea polyacrylamide sequencing gel (200 v, 120 min). Gels were radioautographed at  $-20^{\circ}\text{C}$  for 48 h. Its size was determined according to the standard molecular weight marker.

**Protein analyses** Cells were lysed by lysis buffer and the protein was quantitated. Then SDS-PAGE and immunoblot was performed as usual. Goat anti-HSP90- $\beta$  (1:100) was reacted with the electroblotting for 2 h and HRP-labeled donkey anti-goat IgG (1:500) reacted with the electroblotting for 1 h at room temperature. After washing with PBS (0.01 mol/L pH 7.4), tetrachloride nephrol was used to develop the protein strip and photographed.

**Growth analyses** The pcDNA-HSP90 gene transfected cells and the parental cells were seeded into 24-well plates as pairs at a concentration of  $1 \times 10^4$ /well, 2 mL each well, and cultured in the incubator with a condition of 5%  $\text{CO}_2$ ,  $37^{\circ}\text{C}$ . The cell morphology and growth feature were observed

under microscope. Three wells of each kind of cells were digested by 0.25% trypsin and counted, and its mean value was used to draw the growth curve. Cell doubling time of the exponential phase was calculated by Patterson's formula,  $T_d = T \cdot \lg 2 / \lg (N_1/N_0)$ . Here  $T_d$  is cell doubling time (hour),  $T$  is the time needed for cell growth from  $N_0$  to  $N_1$ .

**Cell cycle analyses.** Cells growing well were digested by 0.25% trypsin, washed by PBS, fixed by cold ethanol at  $4^{\circ}\text{C}$  and dyed with PI, and then were analyzed by flow cytometry.

**The drug sensitivity analyses.** MTT methods were used. The pcDNA-HSP90 gene transfected cells and their parental cells were seeded into 96well plates as pairs at a concentration of  $5 \times 10^3$ /well, 200  $\mu$ L each well, cultured in the incubator with a condition of 5%  $\text{CO}_2$ ,  $37^{\circ}\text{C}$  overnight. Add adriamycin, vincristine, mitomycin or cyclophosphamide at a concentration of 2  $\mu$ g/ $\mu$ L, 2  $\mu$ g/ $\mu$ L, 2  $\mu$ g/ $\mu$ L and 400  $\mu$ g/ $\mu$ L according to the peak plasma concentration of different antineoplastic drugs, and diluted at a ratio of 1:10 respectively and seed 3 weeks for each concentration. Forty-eight hours later, add tetrazolium blue 20  $\mu$ L to each well at a concentration of 5 mg/L PBS. Culturing was continued for 4 hours and the supernatant was removed. Add 150  $\mu$ L DMSO to react for 15 minutes. ELISA reader was used to measure the OD value of each well at 490 nm and the ratio of living cells. The living cell ratio = A490 of the experimental well/that of control well. Dose-effector curve was drawn and  $\text{IC}_{50}$  and resistant index (RI) were determined.  $\text{RI} = \text{IC}_{50}$  of parental cells/that of the gene transfected cells.

**Intracellular drug concentration analyses** In a 35 mm tissue culture plate, seed  $3 \times 10^5$  cells in to 2 mL complete growth medium. Incubate the cells at  $37^{\circ}\text{C}$  in a  $\text{CO}_2$  incubator until the cells are 70% confluent. Add adriamycin to make its final concentration to 10 mg/L. After culture for 1 hour, cells were digested by 0.25% trypsin, washed by PBS and were analyzed by flow cytometry at 575 nm.

#### Statistical analysis

The growth of pcDNA-HSP90 transfectants and their associated controls were compared using two sample *t* tests. Cell cycle fractions, sensitivity of tumor cells to chemotherapeutic drugs and intracellular drug concentrations of pcDNA-HSP90 transfectants and their associated controls were compared using ANOVA.

#### RESULTS

### ***The constructed HSP90 antisense RNA expression vector***

Two gene fragments of 1.43kb and 3.99kb were isolated by agarose-gel electrophoresis after the primary plasmid pHSP90 was digested by EcoR. After the 1.43kb gene fragment was further digested by BamH I, a 1.03kb fragment was obtained, of which BamH I was at its prime 3, EcoR I was at its prime 5. The eukaryotic expression vector pcDNA 3.1(+) was digested by EcoR I and BamH I nuclease and formed linearized plasmid, of which EcoR I was at its prime 3 and BamH I was at its prime 5. With the ligated positive reconstructs digested by EcoR I and BamH I nuclease, we could obtain a 5.4kb vector DNA and 1.03kb inserted fragment. If the ligated positive reconstructs were digested by either EcoR I or BamH I nuclease, we could see a linearized reconstructs (Figure 4). These results indicated that the size and the direction of the inserted HSP90 cDNA fragment was what had been expected. The reconstructed expression vector was named pcDNA-HSP90.



**Figure 4** Nuclease restriction analysis of pcDNA-HSP90 of HSP90 anti-sense RNA eukaryotic expression vector.

1. pHSP90; 2. pHSP90/EcoR I; 3. HSP90/EcoR I-BamH I; 4.  $\lambda$  DNA/EcoR I+Hind III marker (21227, 5148, 4268, 2027, 1375, 125bp); 5. pcDNA 3.1(+); 6. pcDNA 3.1 (+)/EcoR I+BamH I; 7. pcDNA-HSP90; 8. pcDNA-HSP90/EcoR I+BamH; 9. pcDNA-HSP90/EcoR I; 10. pcDNA-HSP90/BamH I

### ***Gene transfection and clone selection***

The positive colonies were selected approximately 3 weeks later. pcDNA-HSP90 of HSP90 anti-sense RNA constructs transfected cell lines were named AH-SGC7901, AH-SGC7901/VCR, AH-HCC7402 and AH-Ec109 respectively (Figure 5). pcDNA3.1 (+) transfected cell lines were named SGC7901-pcDNA, SGC7901/VCR-pcDNA, HCC7402 pcDNA and Ec109-pcDNA.

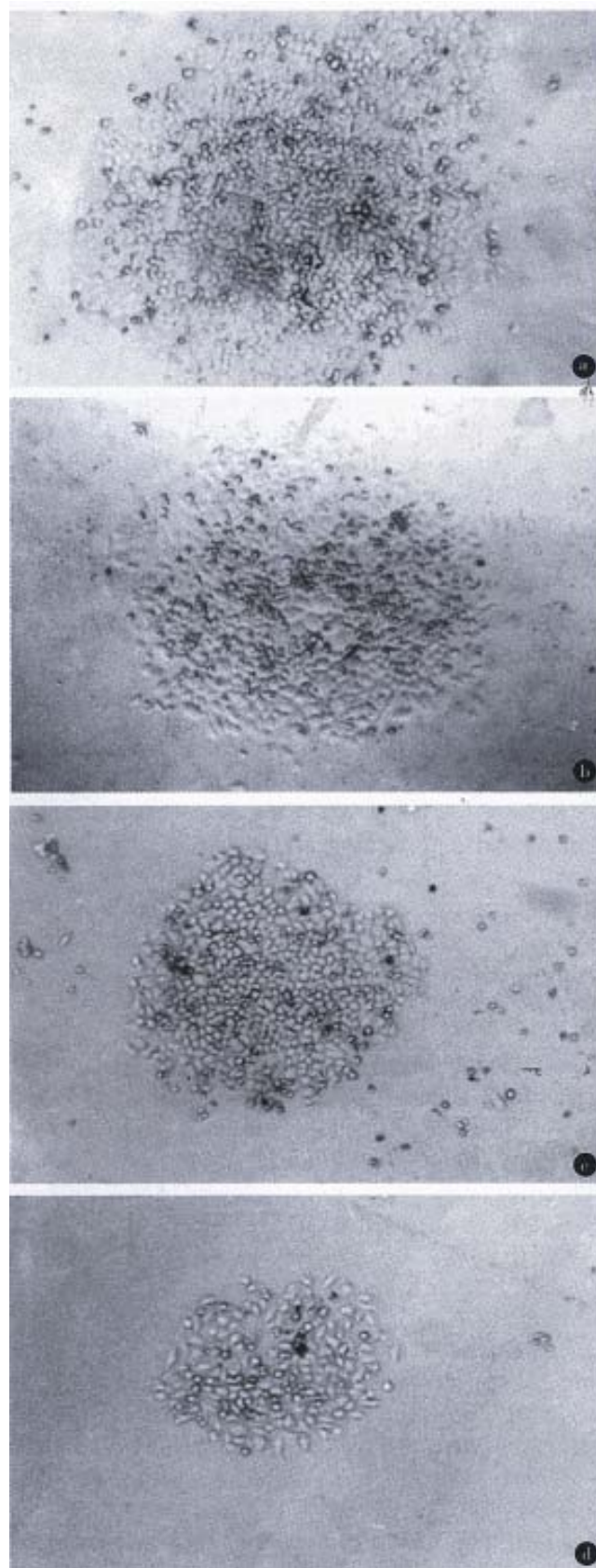


**Figure 5** SGC7901, SGC7901/VCR, HCC7402 and Ec109 cells transfected with pcDNA-HSP90 of HSP90 antisense RNA constructs, selected by G418, positive clones were obtained and were named a. AH-SGC7901; b. AH-SGC7901/VCR; c. AH-HCC7402; d. AH-Ec109.

### Dot blotting and RNase protection assay

**Dot blotting.** All three groups of pcDNA-HSP90 transfectants, pcDNA3.1(+) transfectants and their parental cells had positive signals of  $\beta$ -actin (Figure 6). Only pcDNA-HSP90 transfected cell group had positive signals of HSP90 anti-sense RNA (Figure 7), indicating that pcDNA-HSP90 transfected cell group had the expression of HSP90 anti-sense RNA.

**RNase protection assay (Figure 8).** HSP90 anti-sense RNA transfectants AH-SGC7901/VCR (1), AH-SGC7901 (4), AH-HCC7402 (7) and AH-Ec109 (10) cells had two positive stripes (Hsp90 anti-sense RNA,  $\beta$ -actin) while pcDNA3.1(+) transfected group and the blank control cell group (parental cell line) had only one positive stripe ( $\beta$ -actin), also indicating that pcDNA-HSP90 transfected cell group had the expression of HSP90 anti-sense RNA and further confirmed that pcDNA-HSP90 had been transfected into the aim cells and had the expression of HSP90 anti-sense RNA.

**The expression of Hsp90 protein in the gene transfected cells.** Western blot results showed that the expression of Hsp90 $\beta$  in pcDNA 3.1(+) transfected cells and in their parental cells were almost the same. In Hsp90 antisense RNA transfected cells (AH-SGC7901, AH-SGC7901/VCR, AH-HCC7402 and AH-Ec109), Hsp90 $\beta$  expression was lower than that of their parental cells and pcDNA3.1(+) transfected cells (Figure 9).

**Growth of the gene transfected cell lines.** Compared with their parental cells, the growth of pcDNA-HSP90 gene transfected cells was inhibited in different degrees (Figure 10). The growth inhibiting rate of the 10th day AH-SGC7901 to SGC7901 was 24.28%, of AH-SGC7901/VCR to SGC7901/VCR 27.58%, AH-HCC7402 to HCC7402 10.51% and AH-Ec109 to Ec109 66.91%.

In SGC7901 and AH-SGC7901, the Td calculated from the cell growth curve was 26.6 h and 27.72 h, respectively. The Td of AH-SGC7901 was prolonged 1.12 has compared with its parental cell SGC7901. Td of SGC7901/VCR and AH-SGC7901/VCR was 55.53 h and 72.22 h, respectively. Td of HCC7402 and AH-HCC7402, and Ec109 and AH-Ec109 was 40.66 h and 43.40 h, and 25.03 h and 41.00 h, respectively. These results indicated that the Td of AH-SGC7901/VCR and AH-Ec109 was significantly longer than that of their parental cells ( $P < 0.05$ ), while that of AH-SGC7901 and AH-HCC7402 had no obvious changes as against that of their parental cells ( $P > 0.005$ ).

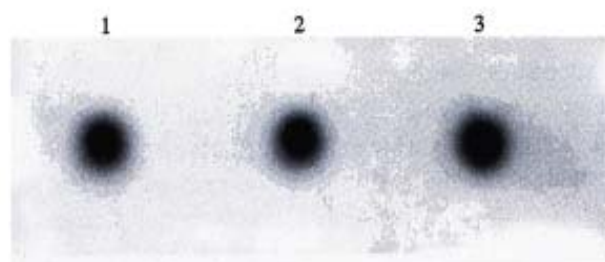


**Figure 6** The expression of  $\beta$ -actin mRNA in AH-SGC7901 of pcDNA-HSP90 transfected cell line, SGC7901-pcDNA of pcDNA 3.1(+) transfected cell line and its parental cell line SGC7901 by Dot blot. 1: SGC7901; 2: SGC7901-pcDNA; 3: AH-SGC7901

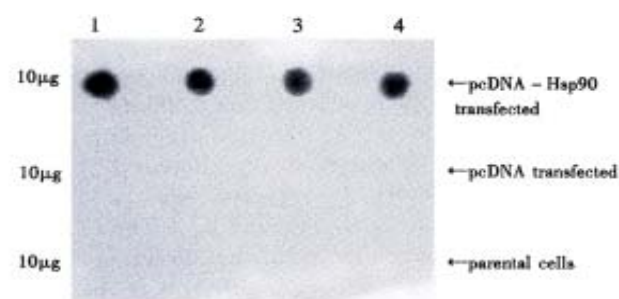


**Figure 7** The expression of HSP90 anti-sense RNA in pcDNA-HSP90 transfected, pcDNA 3.1(+) transfected and the parental cell lines of SGC7901, SGC7901/VCR, HCC7402 and Ec109 by Dot blot. 1: SGC7901; 2: SGC7901/VCR; 3: HCC7402; 4: Ec109

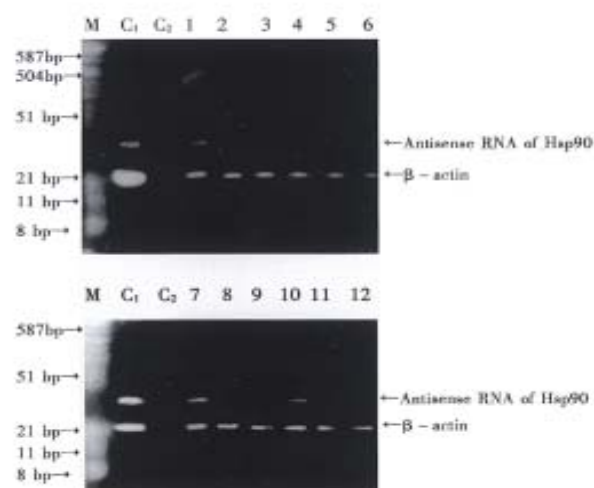


**Figure 8** Expression of hsp90 anti-sense RNA by RNase protection assay. M: PBR322 DNA/Hae III Marker; C1: Positive control,  $\beta$ -actin (20bp) and HSP90 probe (30bp); C2: negative control, probe plus RNase S1, no RNA. 1. AH-SGC7901/VCR; 2. SGC7901-pcDNA/VCR; 3. SGC7901/VCR; 4. AH-SGC7901; 5. SGC7901-pcDNA; 6. SGC7901; 7. AH-HCC7402; 8. HCC7402-pcDNA; 9. HCC7402; 10. AH-Ec109; 11. Ec109-pcDNA; 12. Ec109



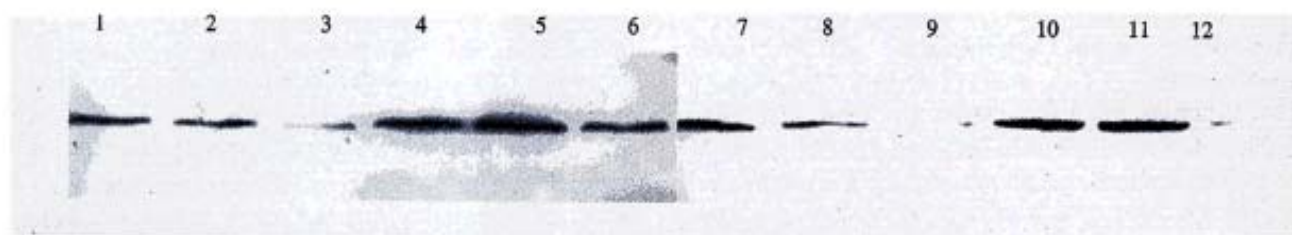


**Figure 9** The expression of HSP90 protein in pcDNA-HSP90 transfected cells. 1. SGC7901; 2. SGC7901-pcDNA; 3. AH-SGC7901; 4. SGC7901/VCR; 5. SGC7901/VCR-pcDNA; 6. AH-SGC7901/VCR; 7. HCC7402; 8. HCC7402pcDNA; 9. AH-HCC7402; 10. Ec109; 11. Ec109pcDNA; 12. AHEc109

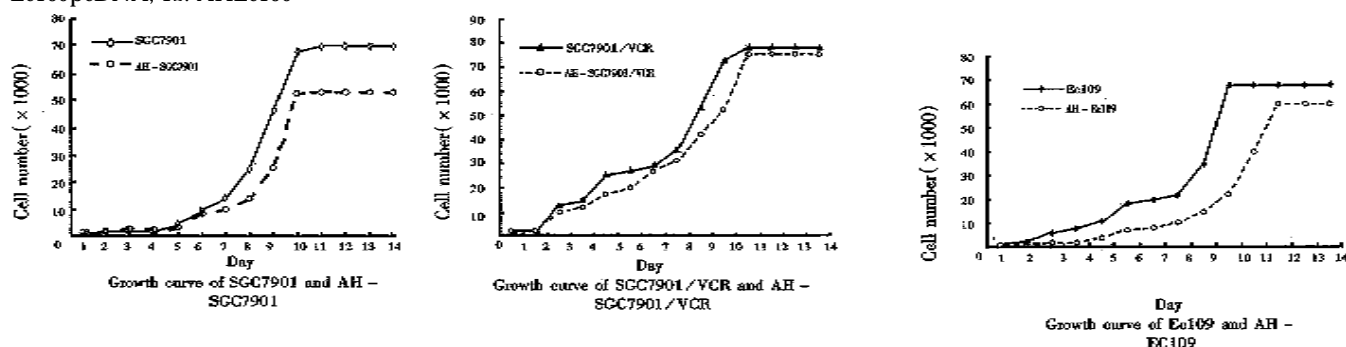


**Figure 10** Growth of gene transfected cell lines.

**Cell cycle distribution of the transfected cells (Table 1).** We can see from Table 1 that G<sub>1</sub> phase cells of AH-SGC7901 were decreased, G<sub>2</sub> phase cells were increased and S phase had no obvious change as compared with their parental cells, while G<sub>1</sub> phase cells of AH-SGC7901/VCR were increased and S phase and G<sub>2</sub> phase cells were decreased. G<sub>1</sub> phase, S phase and G<sub>2</sub> phase cell of AH-HCC7402 had no obvious changes and G<sub>1</sub> phase cells of AH-Ec109 were increased, S and G<sub>2</sub> phase cells were significantly decreased as compared with their parental cells.

**Table 1** Kinetics of pcDNA-HSP90 transfected cells and their parental cells analyzed with flow cytometry

Cell lines	Cell cycle fraction (%)		
	G0-G1	S	G <sub>2</sub> -M
SGC7901	61.6	28.0	10.4
AH-SGC7901	55.7	28.1	16.2
SGC7901/VCR	62.2	23.5	14.3
AH-SGC7901/VCR	74.7	13.6	11.7
HCC7402	70.7	21.1	8.2
AH-HCC7402	69.5	20.0	10.4
Ec109	56.2	29.5	14.8
AH-Ec109	72.5	19.5	8.0

**Drug sensitivity of the gene transfectants.** IC<sub>50</sub> of SGC7901 to ADR, VCR, MMC and CTX was 1.58 × 10<sup>-6</sup>, 1.99 × 10<sup>-3</sup>, 3.10 × 10<sup>-2</sup> and 630 mg/L and IC<sub>50</sub> of AH-SGC7901 to ADR, VCR, MMC and

CTX was 1.58 × 10<sup>-7</sup>, 1.99 × 10<sup>-7</sup>, 1.25 × 10<sup>-3</sup> and 630 mg/L respectively. RI of SGC7901 to ADR, VCR, MMC and CTX was 10, 10 000, 24.8 and 1 compared with AH-SGC7901, i.e., the sensitivity of AH-SGC7901 to ADR, VCR and MMC increased 10, 10 000 and 24.8 times respectively as compared with their parental cell lines, and the sensitivity to CTX had no obvious changes.

IC<sub>50</sub> of SGC7901/VCR to ADR, VCR, MMC and CTX was 0.398, 1.25, 0.199 and 3981.07 mg/L, IC<sub>50</sub> of AH-SGC7901/VCR to ADR, VCR, MMC and CTX was 0.1, 0.199, 0.063 and 794.32 mg/L. RI of SGC7901/VCR to ADR, VCR, MMC and CTX was 3.98, 6.28, 3.15 and 5.01 as compared with AH-SGC7901.

IC<sub>50</sub> of HCC7402 to ADR, VCR, MMC and CTX was 1.20 × 10<sup>-3</sup>, 6.33 × 10<sup>-4</sup>, 3.0 × 10<sup>-2</sup> and 1258.92 mg/L and IC<sub>50</sub> of AH-HCC7402 to ADR, VCR, MMC and CTX was 2.51 × 10<sup>-6</sup>, 6.33 × 10<sup>-5</sup>, 3.00 × 10<sup>-2</sup> and 1258.92 mg/L. RI of HCC7402 to ADR, VCR, MMC and CTX was 477.7, 10, 1 and 1 or the sensitivity of AH-HCC7402 to ADR and VCR increased 477.7 and 10 times respectively compared with their parental cell lines, and its sensitivity to MMC and CTX had no obvious changes.

IC<sub>50</sub> of Ec109 to ADR, VCR, MMC and CTX was 1.0 × 10<sup>-1</sup>, 44.66, 1.99 and 1258.92 mg/L and IC<sub>50</sub> of Ec109 to ADR, VCR, MMC and CTX was 3.16 × 10<sup>-6</sup>, 1.99, 1.99 and 398.10 mg/L respectively. RI of Ec109 to ADR, VCR, MMC and CTX was 31 622.77, 22.44, 1.00 and 3.16.

**Intracellular drug concentration of the gene transfectants.** The mean fluorescence intensity of ADR was  $0.286 \pm 0.02$  in SGC7901,  $0.290 \pm 0.026$  in AH-SGC7901 and  $0.279 \pm 0.009$  in SGC 7901 control, which was significantly increased in AH-SGC7901 ( $P < 0.05$ ).

The mean fluorescence intensity of ADR in SGC7901/VCR was  $0.320 \pm 0.050$ ,  $0.323 \pm 0.054$  in AH-SGC7901/VCR which was significantly increased ( $P < 0.05$ ).

The mean fluorescence intensity of ADR was  $0.480 \pm 0.122$  in HCC7402, and significantly increased in AH-HCC7402 ( $0.503 \pm 0.188$ ) ( $P < 0.05$ ).

The mean fluorescence intensity of ADR was  $1.300 \pm 0.361$  in Ec109, and significantly increased in AH-Ec109 ( $1.680 \pm 0.590$ ) ( $P < 0.05$ ).

## DISCUSSION

Antisense RNA is the RNA that is complementary with the mRNA. The antisense RNA could combine with mRNA specifically and inhibit the translation of the RNA. It is one of the gene expression and modulating modes in prokaryotic cells. Antisense RNA also exists in eukaryotic cells but its function is still unknown. Antisense RNA technich is to tranfect artificially-composed antisense RNA into the eukaryotic cells, transcript antisense RNA, block the translation of the gene, inhibit the expression of the specific gene and block the function of the gene, and to evaluate the influence of the gene to the cell growth and cell differentiation. In comparison of the ribozyme technich<sup>[8]</sup>, antisense RNA technich has the advantages of simple designing, strong specificity, easy operating, and being economic and time saving. According to the two common nuclease EcoR I and BamH I and their different directions of pHSP90 and pcDNA 3.1(+), the nuclease digested fragment was inserted to pcDNA 3.1(+), and the nuclease restriction analysis showed that the gene clone was successful. This study has laid ground for further understanding the biological roles of HSP90 in tumor cells.

In order to determine whether the HSP90 antisense RNA gene transfected and G418 selected cell clones had the expression of HSP90 antisense RNA, a 30-bp oligonucleotide was synthesized and was labeled with ( $\gamma$ -<sup>32</sup>P) ATP by T4 phage polynucleotide kinase. RNA isolated from the selected clones was first analyzed by dot blotting with the labeled probes. The results showed that the pcDNA-HSP90 transfected cell group had positive signals while the pcDNA 3.1(+) transfected cell group and the blank control cell group had no positive signals, indicating that the pcDNA-HSP90 transfected cell group had the expression of HSP90 antisense RNA.

RNase protection assay<sup>[9,10]</sup> or RNase mapping

is a highly sensitive method for gene expression analysis. This method was primarily used to analyze and quantitate specific RNAs. In the research of gene's characters, it is used to determine the size of the exons. The principle of RNase protection assay is: the labeled oligonucleotide probes were hybridized with cell total RNA or mRNA. The unhybridized single chain RNA was digested by RNase S1. The hybridized double chain was protected and could not be digested by RNase S1. Electrophoresis on acrylamide/urea polyacrylamide sequencing gel, the protected chain could be isolated. Radioauto graph could develop the protected chain. Its size could be determined according to the standard-molecular-weight-marker. By this method, 0.1pg globin RNA could be assayed. Its specificity and sensitivity is far greater than Northern blot. In this research, RNase protection assay was also used to determine the expression of HSP90 antisense RNA in the gene transfected and the control cells. The results showed that pcDNA-HSP90 transfected cells had the expression of HSP90 antisense RNA. Analysis of RNA by RNase protection assay is simpler than Northern blot and more specific than Dot blot.

Western blot showed that the expression of HSP90  $\beta$  in AH-SGC7901, AH-SGC7901/VCR, HCC7402 and Ec109 was decreased as compared with their parental cells and their pcDNA transfected groups. This indicated that the antisense RNA of HSP90 has partly blocked the mRNA of HSP90 and inhibited the translation of HSP90 protein.

Both Dot blot and RNase protection assay showed that pcDNA-HSP90 transfected AH-SGC7901, AH-SGC7901/VCR, AH-HCC7402 and AH-Ec109 all had the expression of HSP90 antisense RNA, and with western blot, the expression of HSP90 $\beta$  protein in these cells was decreased when compared with their parental cells and their pcDNA transfected groups. This has established a cell model for further studying the role of HSP90 in these cell lines.

It is known that cell growth is closely related to cell cycle distribution, and cell cycle is regulated by many factors. Oesterreich S<sup>[11]</sup> and Mairesse N<sup>[12]</sup> showed in their studies that hsp27 may be involved in the regulation of cell growth. Fuse *et al*<sup>[13]</sup> had investigated the alternations of cytokinetics and HSP70 expression by hyperthermia in the in vitro experimental systems, using two rat glioma cell lines, two human glioblastoma cell lines and rat glioblast cells. They found that HSP70 was increased in all the heat-treated cells. S phase and/or G2/M phase cells were increased in these heat-treated cells. Faassen<sup>[14]</sup> suggested that *in vivo* aging of human T cells resulted in a general defect in the

induction of gene products required for transition from quiescence into the S phase of the cell cycle. This conclusion is supported by observations of diminished inducibility of the lymphokine IL-2 and its receptor during aging. Faassen's study demonstrated that decreased proliferative response to phytohemagglutinin (PHA) was also paralleled by decreased induction during the prereplicative interval of two of the most strongly enhanced proteins in mitogen-activated T cells: HSP90 and P73, which are also members of the heat shock protein family. Diminished induction of HSP90 and p73 was observed in lymphocytes from older subjects (mean age 75 years), regardless of differences in health status of the subject populations.

The above two researches indicated that HSP plays a regulation role in cell growth. Hyperthermic treatment could induce the expression of HSP70, promote the synthesis of DNA and increase the S phase and G2/M-phase cell and is beneficial to cell proliferation. In the aged subjects, T cell proliferative response was decreased because of the defects in the induction of HSP90 and P73.

In order to further understand whether decreased expression of HSP90 could influence the tumor growth, we used the cell model we had established and studied their growth. From the cell growth curve it can be seen that the cell growth of the HSP90 antisense RNA transfectants was inhibited in different degrees. Among them, the growth of AH-SGC7901/VCR and AH-Ec109 was significantly decreased as compared with their parental cells, and the cell doubling time prolonged 16.69 h and 15.97 h respectively. The growth of AH-SGC7901 was also inhibited to some degree as compared with its parental cells.

Cell cycle analyses showed that, G<sub>1</sub> phase cells of AH-SGC7901/VCR and AH-Ec109 were increased and S phase cells were decreased as compared with their parental cells, indicating that there was G<sub>1</sub> arrest, causing the growth inhibition of the above two cell groups. G<sub>1</sub> phase cells of AH-SGC7901 were diminished, G<sub>2</sub> phase cells were increased and S phase had no obvious change, indicating that there was G<sub>2</sub>/M arrest, causing slower mitosis, and the decrease of cell mitosis and proliferation. G<sub>1</sub> phase S phase and G<sub>2</sub> phase of AH-HCC7402 all had no obvious changes compared with their parental cells. These results indicate that the expression of HSP90 $\beta$  is related to cell growth. Low expression of HSP90 could cause G<sub>1</sub> arrest and inhibit the synthesis of DNA or cause G<sub>2</sub>/M-arrest and inhibit cell mitosis, therefore inhibiting the cell growth and proliferation. The different inhibition rate in different cell lines may be because of the different heritage background and different blocking rate of HSP90 antisense RNA to HSP90

gene in these gene transfected cells. We concluded that down-regulate the expression of HSP90 $\beta$  could change the cell cycle distribution and inhibit the tumor cell growth.

The development of resistance of tumor cells to anti-cancer drugs is one of the critical issues for successful chemotherapy. Multi-drug resistance is an adaptable reaction of tumor cells to chemotherapeutic drugs. Various kinds of protein expression and/or the changes of enzyme activity could be seen in MDR-type tumor cells. Through the changes of these proteins, tumor cells could avoid being killed by chemical agents. Much evidence suggests that the heat shock proteins (hsp) may be involved in drug resistance<sup>[5,6,11,15-17]</sup>. In our study, the sensitivity of the pcDNA-HSP90 transfected cells to chemotherapeutic drugs increased more significantly than their parental cells. This means that lowered expression of HSP90 could increase sensitivity of the tumor cells to chemotherapeutic drugs. We also found that drug accumulation was increased in the pcDNA-HSP90 transfected cells. HSP90 might be related to the efflux of chemical agents. When HSP90 is decreased, the retention of chemical agents is increased and the intracellular drug concentration is increased, so is the sensitivity of the cells to the anti-cancer drugs. HSP90 is a major cytoplasmic chaperone protein and is related to many protein substrates, e.g. actin, tubulin, protein kinase and steroid receptor<sup>[18,19]</sup>. HSP90 may form hetero-oligomeric complex with some plasmic proteins such as HSP70, p60, Hip/p48, p23, FKBP52, FKBP51 and Cyp-40, involve protein folding, transportation and degradation, and regulate the activity of the protein<sup>[20-25]</sup>.

We thought that HSP90 may regulate the sensitivity of tumor cells to chemotherapeutic drugs through regulating the activity and function of P-gp. Bertram J and co-workers have reported that heat-shock protein hsp90 beta is associated with the P-glycoprotein (P-gp or P170), one of the most prominent components of the drug resistance machinery. They demonstrated that hsp90 beta can be co-precipitated along with P-gp and vice versa. In native agarose gels, both proteins migrated together as one single band as shown by Western blot analysis. This intracellular protein-protein interaction may present a mechanism for the modulation of P-gp function possibly by a stabilization of the protein which seems to be attributed to hsp90 beta. This study supports our research.

Oesterreich S and co-workers<sup>[1]</sup> found that when hsp was induced by elevated temperatures, resistance to doxorubicin (Dox), but not to other commonly used chemotherapeutic agents, was

induced in breast cancer cells. To evaluate the role of hsp27 in this phenomenon, they have transfected MDA-MB-231 breast cancer cells, which normally express low levels of hsp27, with a full-length hsp27 construct. These hsp27-overexpressing cells now display a 3-fold elevated resistance to Dox. They have also derived a MCF-7 breast cancer cell line with amplified endogenous hsp27 which is highly resistant to Dox. When these cells were transfected with an antisense hsp27 construct, they were rendered sensitive to Dox (3-fold). These results suggest that hsp27 specifically confers Dox resistance in human breast cancer cells. Our studies showed that HSP90 was related to MDR, and lowered expression of HSP90 could increase the drug sensitivity of tumor cells by 3-30 000 times indicating that regulation of HSP90 is more effective than hsp27 in this aspect. In different cells with different chemicals, the effect is different, possibly because of the different biological characteristics of the tumor cells and the different mechanism of the anti-cancer drugs.

The mechanisms of HSP90 in sensitizing tumor cells to anti-cancer drugs need to be further studied. This study gives some clues in using HSP inhibitors as a sensitizer to increase the sensitivity of tumor cells to anti-cancer drugs. In conclusion, down-regulation of HSP90 could change the cell cycle distribution and slow the tumor cell growth and increase the sensitivity of tumor cells to anti-cancer drugs.

## REFERENCES

- Schlesinger MG. Heat shock proteins. *J Biol Chem*, 1990;265:12111-12114
- Jill L, Elizabeth AC. Protein folding *in vivo*: unraveling complex pathways. *Cell*, 1997;90:201-204
- Yano M, Naito Z, Tanaka S and Asano G. Expression and roles of heat shock protein in human breast cancer. *Jpn J Cancer Res*, 1996;87:908-915
- Jameel A, Skilton RA, Campbell TA. Clinical and biological significance of Hsp90 $\beta$  in human breast cancer. *Int J Cancer*, 1992;50:409-415
- Bertram J, Palfner K, Hiddemann W, Kneba M. Increase of P-glycoprotein-mediated drug resistance by hsp 90 beta. *Anticancer Drug*, 1996;7:838-845
- Kim SH, Hur WY, Kang CD, Lim YS, Kim DW, Chung BS. Involvement of heat shockfactor in regulating transcriptional activation of MDR1 gene in multidrug-resistance cell. *Cancer Letters*, 1997;115:9-14
- Zhou DY. Experimental methods of molecular biology. *Beijing: People's Military Medical Publishing House*, 1995:42
- Lau ET, Kong RY, Cheah KSE. A critical assessment of the RNase protection assay as a means of determining exon sizes. *Analytical Biochem*, 1993;209:360-366
- Altman S. RNA enzyme-directed gene therapy. *Pro Natl Acad Sci USA*, 1993;90:10898-10900
- Sambrook J, Fritsch EF, Maniatis T. Molecular cloning: a laboratory manual. 2nd ed. Cold Spring Harbor: *Cold Spring Harbor Laboratory Press*, 1989:374
- Oesterreich S, Weng CN, Qiu M, Hilsenbeck SG, Osborne CK, Fuqua SAW. The small heat shock protein Hsp27 is correlated with growth and drug resistance in human breast cancer cell lines. *Cancer Res*, 1993;53:4443-4448
- Mairesse N, Horman S, Mosselmans R, Galand P. Antisense inhibition of the 27kDa heat shock protein production affects growth rate and cytoskeletal organization in MCF-7 cells. *Cell Biol Int*, 1996;20:205-212
- Faassen AE, O'Leary JJ, Rodysill KJ, Bergh N, Hallgren HM. Diminished heat-shock protein synthesis following mitogen stimulation of lymphocytes from aged donors. *Exp Cell Res*, 1989;183:326-334
- Ciocca DR, Fuqua SA, Lock Lim S, Toft DO, Welch WJ, McGuire WL. Response of human breast cancer cells to heat shock and chemotherapeutic drugs. *Cancer Res*, 1992;52:3648-3654
- Ciocca DR, Oesterreich S, Chamness GC, McGuire WL, Fuqua SA. Biological and clinical implications of heat shock protein 27000 (Hsp27): a review. *J Natl Cancer Inst*, 1993;83:1558-1570
- Sliutz G, Karlseder J, Tempfer C, Orel L, Holzer G, Simon MM. Drug resistance against gemcitabine and topotecan mediated by constitutive hsp70 overexpression *in vitro*: implication of quercetin as sensitizer in chemotherapy. *Brit J Cancer*, 1996;74:172-177
- Smith DF. Dynamics of heat shock protein 90-progesterone receptor binding and the disactivation loop model for steroid receptor complexes. *Mol Endocrinol*, 1993;7:1418-1429
- Xu Y, Lindquist S. Heat-shock protein Hsp90 governs the activity of pp60v-src kinase. *Proc Natl Acad Sci USA*, 1993;90:7074-7078
- Yhonehara M, Minami Y, Kawata Y. Heat-induced chaperone activity of Hsp90. *J Biol Chem*, 1996;271:2641-2645
- Wiech H, Buchner J, Zimmermann R, Jakob U. Hsp90 chaperones protein folding *in vitro*. *Nature*, 1992;358:169-170
- Jakob U, Buchner J. Assisting spontaneity: the role of Hsp90 and small HSPs as molecular chaperones. *TIBS*, 1994;19:205-211
- Pennisi E. Expanding the eukaryote's Cast of chaperones. *Science*, 1996;274:1613-1614
- Freeman BC, Toft DO, Morimoto RI. Molecular chaperone machine: chaperone activities of cyclophilin Cyp-40 and the steroid aporeceptor-associated protein p23. *Science*, 1996;274:1718-1720
- Johnson J, Corbisier R, Stensgard B. The involvement of p23, hsp90, and immunophilins in the assembly of progesterone receptor complexes. *J Steroid Biochem Mol Biol*, 1996;56:21-37
- Jakob U, Lilie H, Meyer I. Transient interaction of Hsp90 with early unfolding intermediates of citrate synthase. Implications for heat shock *in vivo*. *J Biol Chem*, 1995;270:7288-7294

Edited by MA Jing-Yun



# Cyclosporin A protects Balb/c mice from liver damage induced by superan tigen SEB and D-GalN

YIN Tong<sup>1</sup>, TONG Shan-Qing<sup>2</sup>, XIE Yu-Cai<sup>3</sup> and LU De-Yuan<sup>2</sup>

**Subject headings** cyclosporin A; liver necrosis; apoptosis; staphylococcal enterotoxin B; D-galactosamine

## Abstract

**AIM** To investigate the pathogenic effect of SEB and D-GalN on liver and the protection of cyclosporin A, the relationship between hepatic apoptosis and necrosis and the possible mechanism of acute hepatic necrosis.

**METHODS** After staphylococcal enterotoxin B (SEB) mixed with D-galactosamine (D-GalN) were injected intraperitoneally into Balb/c mice and those previously treated with cyclosporin A, blood samples were collected and livers were isolated at 2, 6, 12, 24h. Patterns of hepatocellular death were studied morphologically and biochemically, circulating cytokines (TNF- $\alpha$ , IFN- $\gamma$ ) and mice mortality within 24h was assessed.

**RESULTS** The SEB could induce the typical apoptotic changes of hepatocytes, the D-GalN could induce hepatocytes apoptosis and degeneration at the same time, and the mice having received the SEB+D-GalN injections developed apoptosis at 2 and 6h, but after 12h hepatocytes were characterized by severe injury, whereas all the examinations in the cyclosporin A treated mice were normal.

**CONCLUSION** Hepatic cell apoptosis might be related to necrosis, and massive hepatocyte apoptosis is likely the initiating step of acute hepatic necrosis in mice. The effects induced by SEB and D-GalN on hepatocytes might be mediated by T cells, and could be prevented by cyclosporin A.

## INTRODUCTION

Patterns of cell death are defined as apoptosis and necrosis<sup>[1]</sup>. After staphylococcal enterotoxin B (SEB) together with D-Galactosamine (D-GalN) were injected ip. into BALB/c mice as well as those previously treated with cyclosporin A, we studied the patterns of hepatocellular death to investigate the pathogenic effect of SEB and D-GalN on liver and the protection of cyclosporin A, the relationship between hepatic apoptosis and necrosis, and the possible mechanism of acute hepatic necrosis.

## MATERIALS AND METHODS

### Main reagents

Cyclosporin A was given by Prof. Fan Li-An, Shanghai Institute of Immunology. D-GalN was purchased from Sigma Chemical Co. SEB was purchased from Institute of Microbiology and Epidemiology, Academy of Military Medical Sciences.

### Mice

Six-week-old male Balb/c mice weighing 20 g were purchased from the Department of Experimental Animal, Shanghai Institute of Biological Products, Ministry of Health of China.

### Groups

Mice were randomly divided into 6 groups: NS, CSA, SEB, D-GalN, SEB+D-GalN and CSA+SEB+D-GalN. Each group was divided into 4 subgroups each containing 6 mice according to 2, 6, 12 and 24 h. After pretest, SEB amount was set at 50  $\mu$ g/mice; D-GalN, 16 mg/mice; and CSA, 0.5 mg/mice. CSA was injected 0.5 h earlier. After mixed *in vitro*, SEB and D-GalN were injected. Control group was treated with normal saline in the same way. All drugs were injected intraperitoneally.

### Light microscopic examination

Livers were isolated at 2, 6, 12 and 24 h, and immediately fixed in 100 mL/L formalin, 5  $\mu$ m thick sections were stained with HE for light microscopic examination. Incidence of apoptosis bodies (ABs) was counted<sup>[2]</sup>.

### Transmission electron microscopic examination

Immediately after sacrifice, 1 mm<sup>3</sup> section from the

<sup>1</sup>Faculty of Medical Laboratory Sciences, Ruijin Hospital, Shanghai Second Medical University, Shanghai 200025, China

<sup>2</sup>Department of Microbiology, Shanghai Second Medical University, Shanghai 200025, China

<sup>3</sup>Department of Internal Medicine, Ruijin Hospital, Shanghai Second Medical University, Shanghai 200025, China

YIN Tong, female, born on 1967-07-28 in Zhenjiang City, Jiangsu Province, graduated from Shanghai Second Medical University as a postgraduate in 1996, lecturer, majoring infection and immunology, having 4 papers published.

\*Supported by Shanghai Institute of Immunology Foundation, No.9508.

**Correspondence to:** YIN Tong, Faculty of Medical Laboratory Sciences, Ruijin Hospital, Shanghai Second Medical University, Shanghai 200025, China

Tel. +86 • 21 • 63846590 Ext. 470

Received 1999-01-04

liver were fixed in 20 g/L glutaraldehyde. After stained, ultrathin sections were examined under a 200CX electron microscope.

#### **Agarose gel electrophoresis of hepatocellular DNA**

DNA was purified from hepatocytes and subsequently analyzed on 10 g/L agarose gels<sup>[3]</sup>.

#### **Serum alanine aminotransferase (ALT) assay**

Serum ALT activities were measured by a CX4 automatic biochemical analyzer (Beckman).

#### **Serum tumor necrosis factor (TNF- $\alpha$ ) assay**

It was performed according to L929 cell-killing method<sup>[4]</sup>.

#### **Serum interferon $\gamma$ (IFN- $\gamma$ ) assay**

IFN- $\gamma$  assay was made by cytopathic effect reduction method<sup>[5]</sup>.

#### **Statistical analysis**

Statistical significance was evaluated according to paired student's *t* test.

### **RESULTS**

#### **Tissue histology**

Hepatocytes of SEB 2 h and 6 h groups showed nuclear pycnosis (Figure 1A) and no necrosis was found in 12 h and 24 h, suggesting that SEB only induce hepatocyte apoptosis in Balb/c-mice. Hepatocytes of D-GalN 2 h group developed chromatin condensation and organelle edema (Figure 1B), 6 h group showed hepatocyte coexistence of degeneration and apoptosis bodies, no necrosis occurred after 12 h. Hepatocytes of SEB+D-GalN 2 h group showed nuclear pycnosis, nucleus was fragmented in 6 h group, after 12 h, besides some hepatocytes apoptosis, necrosis characters such as widespread destruction of the liver structure, massive erythrocyte agglutination, etc (Figure 1C) were found. Hepatocytes of the CSA+SEB+D-GalN group were normal (Figure 1D).

In SEB and D-GalN group, the incidence of ABs was strikingly raised at 6 h, rapidly decreased after 6 h, and decreased to normal in 24 h. But in SEB+D-GalN group it continuously increased till 24 h, and in CSA+SEB+D-GalN group it had no obvious changes.

#### **Agarose gel electrophoresis of hepatocellular DNA**

The groups of SEB 6 h, D-GalN 6 h, SEB+D-GalN 6h and, 12 h showed typical "ladder" pattern, but SEB+D-GalN 24 h present "smear" pattern, and no abnormalities were found in CSA+SEB+D-GalN group (Figure 2).

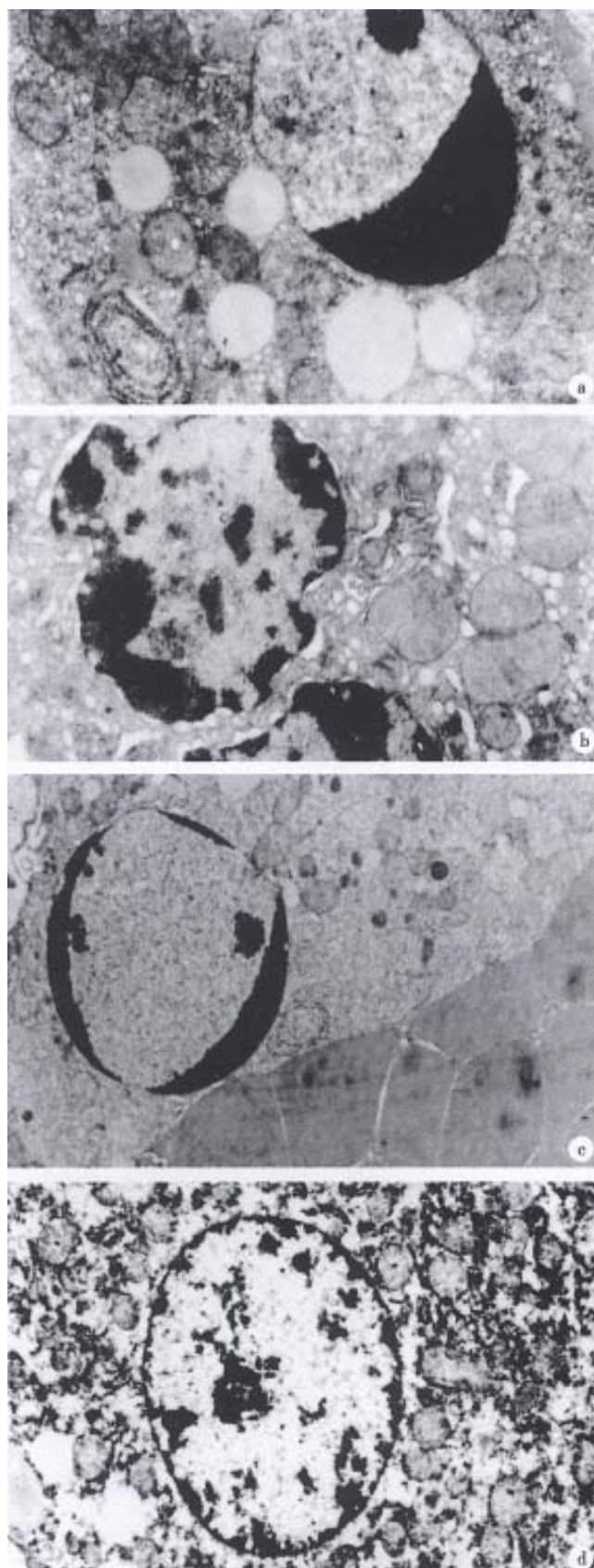


**Figure 1** Hepatocytes of Balb/c mice under TEM.

A. SEB 6 h, chromatin condensation,  $\times 10\,000$ ; B. D-GalN 2 h, nuclear pycnosis and organelle edema,  $\times 10\,000$ ; C. SEB+D-GalN 12 h, nuclear pycnosis and erythrocyte agglutination,  $\times 4\,000$ ; D. CSA+SEB+D-GalN 6 h, nuclear of hepatocyte,  $\times 6\,000$

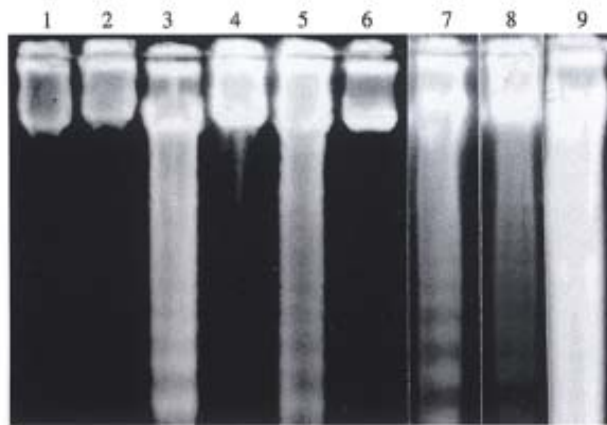


**Figure 2** DNA agarose gel electrophoresis in livers of Balb/c mice. 1. CSA 6 h; 2. CSA+SEB+D-GalN 6 h; 3. SEB+D-GalN 6 h; 4. CSA+SEB+D-GalN 12 h; 5. SEB+D-GalN 12 h; 6. NS; 7. SEB 6 h; 8. D-GalN 6 h; 9. SEB+D-GalN 24 h.

### Serum ALT assay

Compared with control group, there was very obvious difference in the activities of serum ALT of SEB+D-GalN 6 h and 12 h groups ( $P<0.01$ ), and there was obvious difference in D-GalN 2, 6 h and SEB+D-GalN 2 h groups ( $P<0.05$ ), but there was no difference in each of SEB groups, CSA, CSA+SEB+D-GalN, D-GalN 12 h and 24 h groups ( $P<0.05$ ). Among these groups, activities of serum ALT of SEB+D-GalN 12 h even up to several thousand units (Table 1).

### Circulating cytokine levels

Serum TNF- $\alpha$  levels of SEB 2 h ( $210 \text{ ng/L} \pm 80 \text{ ng/L}$ ) and SEB+D-GalN 2 h ( $300 \text{ ng/L} \pm 110 \text{ ng/L}$ ) reached a peak, thereafter sharply decreased in SEB 6 h ( $50 \text{ ng/L} \pm 30 \text{ ng/L}$ ) and SEB+D-GalN 6 h ( $50 \text{ ng/L} \pm 20 \text{ ng/L}$ ). Serum IFN- $\gamma$  levels of SEB and SEB+D-GalN groups began to increase after 2 h of administration (SEB 2 h  $400 \text{ ng/L} \pm 120 \text{ ng/L}$ , SEB+D-GalN 2 h  $400 \text{ ng/L} \pm 150 \text{ ng/L}$ ), and peaked at 6 h-12 h (SEB 6 h  $1480 \text{ ng/L} \pm 480 \text{ ng/L}$ , 12 h  $1620 \text{ ng/L} \pm 590 \text{ ng/L}$ , 24 h  $780 \text{ ng/L} \pm 350 \text{ ng/L}$ , SEB+D-GalN 6 h  $1360 \text{ ng/L} \pm 520 \text{ ng/L}$ , 12 h  $1860 \text{ ng/L} \pm 680 \text{ ng/L}$ , 24 h  $790 \text{ ng/L} \pm 320 \text{ ng/L}$ ). Our data showed that there was no difference in the kinetics of appearance of serum cytokines between mice of SEB and SEB+D-GalN groups ( $P<0.05$ ). In CSA+SEB+D-GalN groups both serum of TNF- $\alpha$  or IFN- $\gamma$  levels were negative.

### Twenty-four lethality

None of the Balb/c mice died at a dose of SEB up to  $150 \mu\text{g}/\text{mouse}$  alone, and D-GalN of  $16 \text{ mg}/\text{mouse}$  within 24 h, whereas the lethality was elevated within 24 h with increased dose of D-GalN when the two were used in combination, for example,  $50 \mu\text{g}$  SEB caused death in about half of the mice,  $150 \mu\text{g}$  SEB up to 100%. But pretreated with CSA 0.5 h earlier, the mice were all survived (Table 2).

**Table 1** Serum ALT activities of Balb/c mice in different time (IU/L,  $1 \text{ IU/L} = 16.67 \text{ nmol} \cdot \text{s}^{-1}/\text{L}$ )

t/h	NS	CSA	SEB	D-GalN	SEB+D-GalN	CSA+SEB+D-GalN
2	$51.8 \pm 16.4$	$51.5 \pm 17.8$	$59.5 \pm 18.8$	$71.3 \pm 25.7^a$	$69.0 \pm 24.6^a$	$54.2 \pm 24.5$
6	$56.0 \pm 21.3$	$63.0 \pm 18.1$	$60.5 \pm 20.3$	$81.3 \pm 24.7^a$	$95.7 \pm 38.7^b$	$60.7 \pm 29.4$
12	$54.8 \pm 14.9$	$55.5 \pm 27.5$	$56.5 \pm 16.9$	$63.8 \pm 22.8$	$4109.2 \pm 1910.1^b$	$60.5 \pm 26.7$
24	$59.7 \pm 24.5$	$59.0 \pm 24.7$	$59.5 \pm 24.7$	$60.7 \pm 26.3$		$65.7 \pm 24.2$

<sup>a</sup> $P<0.05$ , <sup>b</sup> $P<0.01$  vs normal saline.

**Table 2** Lethality within 24 hours

D-GalN (mg/mice)	SEB ( $\mu\text{g}/\text{mice}$ )	CSA (mg/mice)	24 h lethality (death/total)
	10		0/3
	50		0/6
	100		0/3
	150		0/3
16			0/6
16	10		0/3
16	50		3/6
16	100		2/3
16	150		3/3
16	50	0.5	0/6
		0.5	0/6
			0/6 <sup>a</sup>

<sup>a</sup>Mice treated with normal saline.

## DISCUSSION

Hepatocytes of SEB groups only showed apoptosis morphologically, and the course seems to finish within 12 hours, DNA agarose gel electrophoresis of hepatocytes exhibited the "ladder" pattern at 6 h-12 h, but activities of serum ALT were always normal. This result indicates that SEB caused hepatocytes nuclear pycnosis while membrane was intact. Mice lethality within 24 hours is 0. Because SEB did not exhibit any direct toxic effect on hepatocytes<sup>[6]</sup>, we analysed the mechanism of SEB-induced hepatocyte apoptosis may be related to biological features of superantigen nonspecific stimulating massive T cell proliferation and

releasing cytokines (TNF- $\alpha$ , IFN- $\gamma$ , etc.). D-GalN could induce both hepatocyte apoptosis and degeneration morphologically. The result of DNA agarose gel electrophoresis was similar to that of SEB groups, but activities of ALT rose between 2 and 6 hours, probably due to ( $P<0.05$ ), hepatocyte degeneration which elevated membrane permeability. Mice lethality within 24 hours is 0. D-GalN is a kind of indirect toxin to liver, which can cause a selective depletion of urine nucleotides in mouse liver, thus leading to secondary hepatic injury. High doses can cause hepatocyte injury in mice resembling human viral hepatitis<sup>[1]</sup>.

Balb/c mice treated with SEB+D-GalN showed typical features of hepatocyte apoptosis within 6 hours, but after 12 hours, extensive cell necrosis was prominent besides apoptosis in a few hepatocyte. After 12 hours, the incidence of ABs became too high to count because a majority of hepatocytes were destructed. In biochemistry, DNA agarose gel electrophoresis demonstrated typical "ladder" between 6 and 12 hours, but a "smear" pattern at 24 hours. Serum ALT increased from the 2nd hour ( $0.01<P<0.05$  at 2 hours, as compared  $P<0.01$ , at 6 hours  $68 \mu\text{mol} \cdot \text{s}^{-1} \cdot \text{L}^{-1}$  to at 12 hours. This indicated a great amount of hepatocytes were destructed, with a 24 h lethality of 50% whereas the mice pretreated with CSA were all normal. Superantigen had no direct toxic effect on hepatocytes, only nonspecifically stimulated massive T cell proliferation and released cytokines while CSA can inhibit T lymphocyte releasing cytokines. Therefore, we think that the acute injury to hepatocytes is mediated by T cells thus it can be inhibited by CSA.

Leist<sup>[7]</sup> reported that D-GalN+LPS/TNF induced hepatocyte apoptosis in Balb/c mice in the early stage and necrosis in the late stage. Our results are in agreement with Leist's. Based on the studies of transgenic mice in literature<sup>[8]</sup> and our experiment, we assume that the process of hepatic

injury induced by SEB+D-GalN is: massive hepatocyte apoptosis occurred, then the neutrophils and macrophages were attracted by endogenous mediators and activated by apoptotic hepatocytes releasing massive cytokines, and finally, the secondary acute hepatic necrosis, occurred leading to the death of mice. D-GalN in addition to its sensitization of hepatocyte, D-GalN may prevent the rapid uptake of apoptotic cells by neighboring hepatocytes and Kupffer's cells<sup>[7]</sup>. Gantner<sup>[9]</sup> reported apoptotic hepatocytes can induce procoagulant activities in endothelial cells and platelets that eventually result in thrombin deposition and sinusoidal congestion. Therefore, there might be some relationship between apoptosis and necrosis. If the number of apoptotic hepatocytes is small and can be rapidly phagocytized by the nearby hepatocytes and Kupffer's cells, secondary necrosis will not occur while if it is massive and can not be phagocytized rapidly, secondary necrosis will develop.

## REFERENCES

- 1 Alison MR, Sarraf CE. Liver cell death: pattern and mechanisms. *Gut*, 1994;35:577
- 2 Faa G, Ledda-Columbano GM, Ambu R, Congiu T, Coni P, Riva A. An electron microscopic study of apoptosis induced by cycloheximide in rat liver. *Liver*, 1994;14:270
- 3 Sambrook J, Fritsch EF, Maniatis T. Molecular cloning, 2nd ed. *Beijing: Science and Technology Press*, 1993:309
- 4 Hu BY, Zhang BZ, Zhu YM. Assay of TNF induced by whole blood. *Shanghai J Immunol*, 1991;11:160
- 5 Yong TP, Yi XN. Practical immunology, 1st ed. *Changchun: Changchun Publishing House*, 1994:596
- 6 Uchiyama T, Yan XJ, Imanishi K, Imanishi KI, Yagi J. Bacterial superantigen-mechanism of T cell activation by the superantigen and the role in the pathogenesis of infectious diseases. *Microbiol Immunol*, 1994;38:245
- 7 Leist M, Gantner F, Bohlinger I, Tiegs G, Germann PG, Wendel A. Tumor necrosis factor-induced hepatocyte apoptosis precedes liver failure in experimental murine shock models. *Am J Pathol*, 1995; 146:120
- 8 Chisari FV. Hepatitis B virus transgenic mice: insights into the virus and the disease. *Hepatology*, 1995;22:1316
- 9 Gantner F, Leist M, Jilgs S, Germann PG, Freudenbeg MA, Tiegs G. Tumor necrosis factor-induced hepatic DNA fragmentation as an early marker of T cell-dependent liver injury in mice. *Gastroenterology*, 1995;109:166

Edited by MA Jing-Yun

# Nitric oxide synthase distribution in esophageal mucosa and hemodynamic changes in rats with cirrhosis

HUANG Ying-Qiu<sup>1</sup>, XIAO Shu-Dong<sup>2</sup>, ZHANG De-Zhong<sup>2</sup> and MO Jian-Zhong<sup>2</sup>

**Subject headings** esophagus; nitric oxide synthase; liver cirrhosis; hemodynamics

## Abstract

**AIM** To observe the nitric oxide synthase (NOS) distribution in the esophageal mucosa and hemodynamic changes in cirrhotic rats.

**METHODS** NOS distribution in the lower esophagus of rats with carbon tetrachloride-induced cirrhosis was assessed by using NADPH-diaphorase (NADPH-d) histochemical method. Concentration of NO in serum were measured by fluorometric assay. Mean arterial pressure (MAP), cardiac output (CO), cardiac index (CI), splanchnic vascular resistance (SVR), and splanchnic blood flow (SBF) were also determined using <sup>57</sup>Co-labeled microsphere technique.

**RESULTS** Intensity of NOS staining in the esophageal epithelium of cirrhotic rats was significantly stronger than that in controls. There was a NOS-positive staining area in the endothelia of esophageal submucosal vessels of cirrhotic rats, but the NOS staining was negative in normal rats. NO concentration of serum in cirrhotic rats were significantly higher in comparison with that of controls. Cirrhotic rats had significantly lower MAP, SVR and higher SBF than those of the controls.

**CONCLUSION** Splanchnic hyperdynamic circulatory state was observed in rats with cirrhosis. The endogenous NO may play an important role in development of esophageal varices and in changes of hemodynamics in cirrhosis.

## INTRODUCTION

Cirrhosis with portal hypertension is associated with hyperdynamic circulation characterized by generalized vasodilation and increased cardiac output and splanchnic regional blood flows. Endogenous NO, a very potent vasodilator factor, may play a very important role in the pathogenesis of hemodynamic changes in cirrhosis. It is unclear whether NO is involved in the pathogenesis of esophageal varices as one of severe complications of hepatic cirrhosis. The present study was aimed at investigating the effects of endogenous NO on esophageal varices and hemodynamic changes in cirrhotic rats.

## MATERIALS AND METHODS

### *Experimental animal*

Male Sprague-Dawley (SD) rats (supplied by the Shanghai Laboratory Animal Center of Chinese Academy of Sciences) weighing between 250 g and 300 g were used. Cirrhotic rat model was induced by injection of 60% CCl<sub>4</sub> oily solution twice weekly subcutaneously (0.3 mL/100 g, first time 0.6 mL/100 g) for two months<sup>[1]</sup>. After the model was established, there were 8 cirrhotic rats in experimental group and 8 normal SD rats served as controls.

### *Hemodynamic studies*<sup>[2]</sup>

Under Ketamine anesthesia (100 mg/kg intramuscularly), the right femoral artery and the femoral vein were cannulated with a polyethylene 50 catheters, which went forward respectively to the abdominal aorta and inferior vena cava. The left ventricle was catheterized under pressure monitoring through the right carotid artery with a polyethylene 50 catheter for injection of <sup>57</sup>Co-labeled microspheres. All catheters were connected to highly sensitive pressure transducers that were calibrated before each study, and blood pressures were registered on a multichannel recorder (Lifescope 6). An abdominal incision (1.5 cm-2.0 cm) was performed, and the portal pressure (PP) was indirectly measured through puncture of spleen with a No.4 needle<sup>[3]</sup>. Cardiac output and splanchnic blood flows were measured by using <sup>57</sup>Co-labeled microspheres technique. A reference blood sample was obtained from the femoral artery

<sup>1</sup>Department of Gastroenterology, General Hospital of Benxi Iron & Steel Co., Benxi 117000, China

<sup>2</sup>Shanghai Institute of Digestive Diseases, Renji Hospital, Shanghai Second Medical University, Shanghai 200001, China

HUANG Ying-Qiu, male, born on 1962-03-30 in Benxi City, Liaoning Province, graduated from Shanghai Second Medical University, with a master degree in 1997, now chief of Department of Gastroenterology, General Hospital of Benxi Iron & Steel Co., physician and associate professor of China Medical University, member of Liaoning Digestive Branch of Chinese Medical Association (CMA), and member of Liaoning Internal Medicine Branch of CMA, majoring digestive medicine, having 30 papers published.

**Correspondence to:** Dr. HUANG Ying-Qiu, Department of Gastroenterology, General Hospital of Benxi Iron & Steel Co., Benxi 117000, China

Received 1999-02-05 Revised 1999-04-14



catheter for 70 seconds at a constant rate of 1 mL/min with a continuous-withdrawal pump (model WZ-50, Zhejiang Medical University, China). Meanwhile, approximately 50 000 microspheres labeled with  $^{57}\text{Co}$ -labeled microspheres (diameter,  $15\ \mu\text{m} \pm 0.6\ \mu\text{m}$ , Du Pont Co., USA) were injected into the left ventricle 10 seconds after the start of blood withdrawal. Then 2 mL blood sample was withdrawn from the right femoral vein and stored at  $-70^\circ\text{C}$  for determination. The rats were then killed, the lower esophagus was quickly excised and quick-frozen in nitrogen solution for NADPH-d histochemical staining, and then liver specimens were fixed in 10% formalin for histologic examination. Other abdominal organs and mesentery were also taken out, weighed, and cut into small pieces, and placed in  $\gamma$  counter (model GP1, Shanghai Electronic Apparatus Co., China) for determining the radio-activity (cpm).

### Calculations

Cardiac output (CO) (mL/min) = injected  $^{57}\text{Co}$  (cpm)  $\times$  reference blood sample (mL/min)/reference blood  $^{57}\text{Co}$  (cpm).

Cardiac index (CI) (mL  $\cdot$  min $^{-1}$   $\cdot$  100 g-1BW) = CO (mL/min)/100 g BW.

Splanchnic blood flow (SBF) (mL/min) = organ  $^{57}\text{Co}$  (cpm)  $\times$  reference blood sample (mL/min)/reference blood  $^{57}\text{Co}$  (cpm).

Portal vein blood flow (PVF) (mL/min) = the sum of gastric, splenic, intestinal, mesenteric and pancreatic venous flows.

Splanchnic vascular resistance (SVR) (kPa  $\cdot$  mL $^{-1}$   $\cdot$  min $^{-1}$ ) = [MAP-PP (kPa)]/PVF (mL/min).

### NADPH-d histochemical staining<sup>[4]</sup>

Esophageal samples were fixed in 4% paraformaldehyde and 0.4% picric acid in 0.16 mol/L sodium phosphate buffer, pH 6.9, for 4 hours. Then they were transferred to 10% sucrose in 0.1% mol/L sodium phosphate buffer, pH 7.2, at  $4^\circ\text{C}$  for 24 hours. Cryostat sections (10  $\mu\text{m}$  thick,  $-20^\circ\text{C}$  Minotome cryostat, USA) were immersed for 10 minutes in 0.01 mol/L phosphate buffer, pH 8.0, and were incubated for 40 minutes at  $37^\circ\text{C}$  in prewarmed solution consisting of 0.01 mol/L phosphate buffer, pH 8.0; 0.3% Triton X100; 0.5 mmol/L nitroblue tetrazolium (NBT, Sigma, USA); and were 1.0 mmol/L NADPH (Sigma, USA). After washing in 0.01 mol/L phosphate buffer, pH 7.4, the sections were dehydrated with graded alcohol and mounted on microscopic glass slides.

### Serum NO determination

This assay is a modification of the method of

Damiani and Burini<sup>[5]</sup> for the fluorometric determination of nitrite. Briefly, the serum sample is added with 20% sodium sulfosalicylic acid to remove protein. After centrifugation, the filtrate is added with 0.01 mol/L EDTA and 2,3-Diaminonaphthalene (DAN, Fluka, Switzerland) hydrochloric acid solution. The reaction is terminated after 10 min at  $20^\circ\text{C}$  by addition of 2.8 mol/L-NaOH solution. The intensity of fluorescent signal of 1(H) naphthotriazole in the serum sample were obtained in a luminescence spectrofluorometer (Model F-4 000, Hitachi, Japan) with excitation at 365 nm, emission at 420 nm and slits at 3 nm. Nitrite levels in samples were then calculated as a standard curve for nitrite.

### Liver histologic examination

The liver samples were fixed in 10% formalin, processed routinely, and embedded in paraffin. The sections were stained with HE and were then observed using a microscope.

### Statistical analysis

The results were expressed as  $\bar{x} \pm s$ , and were analyzed with Student's *t* test.  $P < 0.05$  was regarded as of statistical significance.

## RESULTS

The liver histology of all the animals treated with CCl<sub>4</sub> in the study had a granulated surface, and histological examination showed the characteristic features of cirrhosis.

Areas with a positive reaction for NADPH diaphorase were stained dark blue. The reaction was negative in specimens stained without NADPH. NADPH-diaphorase histochemical staining showed that intensity of NOS staining in lower esophageal epithelium of cirrhotic rats was significantly stronger than that in normal SD rats. There was a NOS positive staining area in the endothelium of esophageal submucosal vessels, but the NOS staining was negative in normal controls (Figures 1, 2).

Hyperdynamic circulatory status associated with portal hypertension was observed in all rats with cirrhosis (Tables 1, 2). Serum NO level in cirrhotic rats were significantly higher than that in normal controls ( $4.204\ \mu\text{mol/L} \pm 1.253\ \mu\text{mol/L}$  vs  $0.532\ \mu\text{mol/L} \pm 0.257\ \mu\text{mol/L}$ ,  $P < 0.01$ ).

**Table 1 Hemodynamics parameters ( $\bar{x} \pm s$ )**

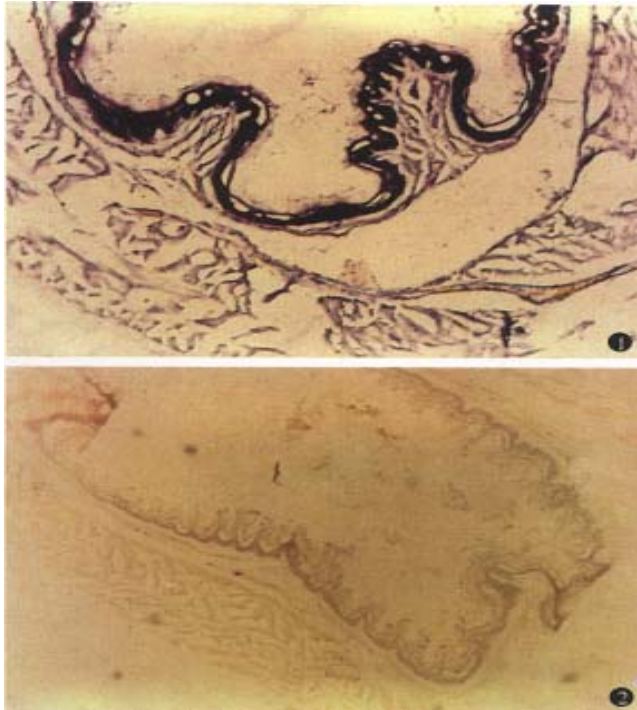
	Controls ( <i>n</i> = 8)	Cirrhotic rats ( <i>n</i> = 8)
MAP (kPa)	$17.05 \pm 0.34$	$14.42 \pm 0.47^a$
PP (kPa)	$1.123 \pm 0.096$	$1.665 \pm 0.067^a$
CO (mL/min)	$135.5 \pm 3.55$	$189.99 \pm 9.26^a$
CI (mL $\cdot$ min $^{-1}$ $\cdot$ 100 g-1 BW)	$39.68 \pm 1.64$	$55.89 \pm 1.82^a$
PVF (mL $\cdot$ min $^{-1}$ $\cdot$ 100 g-1 BW)	$3.762 \pm 0.094$	$4.295 \pm 0.155^a$
SVR (kPa $\cdot$ mL $^{-1}$ $\cdot$ min $^{-1}$ )	$4.234 \pm 0.118$	$2.974 \pm 0.186^a$

<sup>a</sup> $P < 0.01$ , compared to control group.

**Table 2** Blood flow of splanchnic organs ( $\text{mL} \cdot \text{min}^{-1} \cdot \text{g}^{-1}$ ,  $\bar{x} \pm s$ )

Organ	Controls ( $n = 8$ )	Cirrhotic rats ( $n = 8$ )
Stomach	$0.544 \pm 0.045$	$0.881 \pm 0.065^a$
Spleen	$0.946 \pm 0.060$	$0.725 \pm 0.057^a$
Pancreas	$0.819 \pm 0.031$	$0.998 \pm 0.055^a$
Intestine & mesentery	$1.451 \pm 0.037$	$1.686 \pm 0.057^a$
Kidney	$0.465 \pm 0.038$	$0.686 \pm 0.046^a$

<sup>a</sup> $P < 0.01$ , compared to control group.

**Figure 1** Esophageal NADPH-d histochemical staining in cirrhotic rats.  $\times 200$ **Figure 2** Esophageal NADPH-d histochemical staining in normal rats.  $\times 200$ 

## DISCUSSION

Lower esophageal varices are the main clinical manifestation and the cause of upper gastrointestinal hemorrhage in cirrhosis associated with portal hypertension. Cirrhosis with portal hypertension is often associated with hyperdynamic circulation characterized by generalized vasodilation and increased cardiac output and splanchnic regional blood flows. However, the mechanisms responsible for the development of lower esophageal varices and the hyperdynamic circulatory status are still unclear.

Our study showed that intensity of NOS staining in esophageal epithelium of cirrhotic rats associated with portal hypertension was significantly stronger than that in normal SD rats. There was a NOS positive staining area in the endothelium of esophageal submucosal vessels, but the NOS staining

was negative in normal rats. In addition, we also found that the levels of serum NO were all significantly elevated in cirrhotic rats as compared to normal rats. The hyperdynamic circulatory state of cirrhosis with portal hypertension could provide continuous stimuli (such as a progressive increase in blood flow, high oxygenation in portal blood, or endotoxemia) for nitric oxide synthase (NOS) induction in the portal collateral bed<sup>[6]</sup>. Our findings suggest that NO may play an important role in the collateralization of the portal system because inhibition of NO synthesis reduces portal systemic shunting without affecting portal pressure in cirrhotic rats<sup>[7]</sup>. Therefore, overexpressed NOS in the mucosa of the lower esophagus of cirrhotic rats significantly shows a mechanism for the predisposition of collaterals to develop at this site by enhancing NO production. Therefore, greater NOS content in the lower esophageal mucosa of cirrhotic rats would produce increased amounts of NO, adding to the hyperdynamic circulation in the region.

In order to determine NOS, we used a kind of histochemical staining method depended on the presence of diaphorase. The technique of “diaphorase” staining is based on the ability of the C-terminal portion of nitric oxide synthase to transfer electrons from NADPH to nitroblue tetrazolium (NBT) reducing the substrate NBT to an insoluble purple formazan product giving the characteristic “diaphorase” reaction<sup>[8]</sup>. Other studies showed that the overexpressed of NOS visualized by immunohistochemical staining and of NADPH-d staining in brain and peripheral tissues were identical<sup>[9,10]</sup>. It seems that the NADPH-d staining technique is a useful and simple method to determine the expression of NOS<sup>[11]</sup>. In the present study, we found a strong expression of NADPH-d activity in the lower esophagus, reflecting NOS. The findings are identical to Tanoue’s report<sup>[4]</sup>. Tanoue *et al* found that expression of NOS proteins in endothelia of submucosal veins was markedly higher in portal-hypertensive rats than in controls. We postulate that because NO is a very potent vasodilator factor, overexpression of NOS may be an important cause of esophageal varice rupture to give rise to hemorrhage.

In the present study, increment of splanchnic blood flow associated with portal hypertension was observed in all 8 rats with cirrhosis except that splenic vein flow was lower than controls. Moreover, there were 6 cirrhotic rats with ascites in the 8 rats with cirrhosis. Although the cause of this hyperdynamic circulation is still a matter of

controversy, it seems that vasodilatation, induced by increased activity of endothelia-independent and endothelia-dependent vasodilators, initiates the hyperdynamic state. Recently, a role of endogenous nitric oxide in the regulation of blood flow and vascular tone of the systemic and splanchnic circulations in portal hypertension has been suggested by several *in vivo* and *in vitro* studies, implying that excessive synthesis of NO could be responsible for the these circulatory abnormalities. Our previous studies had suggested that an excessive release of NO may be involved in the splanchnic hyperemia<sup>[12]</sup>.

In conclusion, the results of the present study show that endogenous NO may play an important role in development of esophageal varices and in changes of hemodynamics pattern in cirrhosis.

## REFERENCES

- Huang YQ, Zhang DZ, Mo JZ, Xiao SD, Li RR. Effects of nitric oxide on hemodynamics in cirrhotic rats. *Chin J Hepatol*, 1997;5: 153-155
- Nagasawa M, Kawasaki T, Yoshimi T. Effects of calcium antagonists on hepatic and systemic hemodynamics in awake portal hypertensive rats. *J Gastroenterol*, 1996;31:366-372
- Benoit JN, Womack WA, Hernandez L. "Forward" and "backward" flow mechanisms of portal hypertension. Relative contributions in the rat model of portal vein stenosis. *Gastroenterology*, 1985;89:1092-1096
- Tanoue K, Ohta M, Tarnawski AS, Wahlstrom KJ, Sugimachi K, Sarfeh IJ. Portal hypertension activates the nitric oxide synthase gene in the esophageal mucosa of rats. *Gastroenterology*, 1996; 110:549-557
- Damiani P, Burini G. Fluorometric determination of nitrite. *Talanta*, 1986;33:649-652
- Miller VM, Aarhus LL, Vanhoutte PM. Modulation of endothelium-dependent responses by chronic alteration of blood flow. *Am J Physiol*, 1986;251:H520-H527
- Lee FY, Albilos A, Colombato LA, Groszmann RJ. The role of nitric oxide in the vascular hyporesponsiveness to methoxamine in portal hypertensive rats. *Hepatology*, 1992;16:1043-1048
- Norris PJ, Charles IJ, Scorer CA, Emson PC. Studies on the localization and expression of nitric oxide synthase using histochemical techniques. *Histochemical J*, 1995;27:745-756
- Dawson TM, Bredt DS, Fotuhi M, Hwang PM, Snyder SH. Nitric oxide synthase and neuronal NADPH diaphorase are identical in brain and peripheral tissues. *Proc Natl Acad Sci USA*, 1991;88: 7797-7801
- Hope BT, Maichel JG, Knigge KM, Vincent SR. Neuronal NADPH diaphorase is a nitric oxide synthase. *Proc Natl Acad Sci USA*, 1991;88:2811-2814
- Ward SM, Xue C, Shuttleworth W, Bredt DS, Snyder SH, Sanders KM. NADPH diaphorase and nitric oxide synthase colocalization in enteric neurons of canine proximal colon. *Am J Physiol*, 1992; 263:G277-G284
- Huang YQ, Xiao SD, Zhang DZ, Mo JZ. Effects of erythropoietin or nitric oxide synthesis inhibitor on hyperdynamic circulatory state in cirrhotic rats. *Natl Med J China*, 1998;78:139-142 (in Chinese with English abstract)

Edited by MA Jing-Yun



# Expression of perforin and granzyme B mRNA in judgement of immunosuppressive effect in rat liver transplantation \*

ZHANG Shao-Geng<sup>1</sup>, WU Meng-Chao<sup>2</sup>, TAN Jing-Wang<sup>1</sup>, CHEN Han<sup>2</sup>, YANG Jia-Mei<sup>2</sup> and QIAN Qi-Jun<sup>2</sup>

**Subject headings** liver transplantation; immunosuppression; perforin granzyme B genes; graft rejection

## Abstract

**AIM** To explore the expression of perforin and granzyme B genes mRNA to judge the effect of immunosuppression in acute rejection of liver transplantation.

**METHODS** The expression of perforin and granzyme B genes mRNA was examined by reverse transcription-polymerase chain reaction (RT-PCR) in hamster to rat liver grafts under the immunosuppression of cyclosporine or/and splenectomy. Histological findings were studied comparatively.

**RESULTS** Cyclosporine could obviously decrease the cellular infiltration, and completely repress the expression of mRNA for perforin and granzyme B, but could not change severe hepatocyte necrosis and hemorrhage. Splenectomy could significantly lighten hepatocyte necrosis, and completely eliminate hemorrhage, but not affect the cellular infiltration and the expression of perforin and granzyme B genes mRNA. Cyclosporine or splenectomy alone could not prolong the survival time, however, their combination could completely repress the rejection of liver grafts. The survival time of animals were significantly prolonged (37.1 days). The architecture of hepatic lobules was preserved. There was slight

**cellular infiltration in the portal tracts and no expression of perforin and granzyme B genes mRNA could be seen in three weeks after transplantation.**

**CONCLUSION** Perforin and granzyme B genes are valuable in judging the effect of immunosuppression in liver transplantation.

## INTRODUCTION

Rejection is one of major factors influencing the outcome of the patients after liver transplantation, and acute rejection is more harmful to the grafts and recipients. The cellular immunity has been proved to be a chief mechanism in rejecting liver transplantation, and cytotoxic T lymphocyte (CTL) is the major effector cell, the perforin lytic pathway to granzyme B, plays a critical role in the T-cell immune response<sup>[1]</sup>. It is a hot issue of the moment to search for special early markers to judge the effect of immunosuppression in acute rejection of liver transplantation. In this study, the expression of perforin and granzyme B mRNA was examined by reverse transcriptase-polymerase chain reaction (RT-PCR) under the immunosuppression of Cyclosporine (CsA) and splenectomy based on the establishment of a stable and reliable model of hamster to rat concordant xenogeneic orthotopic liver transplantation.

## MATERIALS AND METHODS

### Animals

Female golden hamsters weighing 150 g-180 g were the donors of liver xenografts, and male Wistar rats weighing 230 g-260 g were the recipients. The animals were purchased from Xi Bi Experimental Animal Centre and Shanghai Experimental Animal Centre of Chinese Academy of Sciences.

### Liver transplantation

Orthotopic liver transplantation was performed according to simplified three-cuff technique<sup>[2]</sup> with some modifications. Donor cholecystectomy was performed at the time of cuff preparation, without reconstruction of hepatic artery, and splenectomy at the time of transplantation with simple ligation of the splenic hilum and excision. No microscope was

<sup>1</sup>The Department of Hepatobiliary Surgery, Fuzhou Military General Hospital, Fuzhou 350025, Fujian Province, China

<sup>2</sup>Shanghai East Hepatobiliary Hospital of Second Military Medical University, Shanghai 200433, Shanghai, China

Dr. ZHANG Shao-Geng, male, born on 1964-02-16 in Nanchang city, Jiangxi Province, graduated from Shanghai Second Military Medical University in 1997, under the instruction of professor Wu Meng-Chao, he was engaged in the studies of liver transplantation and obtained M.D. and Ph.D. Now he is working in the Department of Hepatobiliary Surgery, Fuzhou Military General Hospital.

\*Project supported by the National Natural Science Foundation of China, No. 39500152.

**Correspondence to:** Dr. ZHANG Shao-Geng, Department of Hepatobiliary Surgery, Fuzhou Military General Hospital, 156 Xi Huan Bei Road, Fuzhou 350025, Fujian Province, China

Tel. +86 • 591 • 3709089

Received 1999-02-05

used for all the operations.

### Experimental groups

Liver xenografts were studied in four groups: A, untreated controls ( $n = 8$ ); B, treated with cyclosporine 30mg/kg/daily ( $n = 6$ ); C, treated with splenectomy ( $n = 6$ ); D, treated with splenectomy and cyclosporine 30 mg · kg · day ( $n = 7$ ).

### Immunosuppressants

CsA was administered to recipients intramuscularly beginning on the first day of operation, at an interval of 12 hours. Splenectomy was done at the time of transplantation.

### Histology

Postoperative specimens at rejection and specimens taken at sacrifice were fixed in 10% formalin and stained with hematoxylin and eosin.

### RNA extraction

Total RNA was extracted according to the Qiagen kit directory. In brief, after homogenization and lysis with lytic buffer RLT in QIA shredder, same volume of 70% ethanol were added. Samples were then moved into RNeasy spin column and centrifuged for 15sec at  $8\,000 \times g$ , buffer RW1 and buffer PRE were added and centrifuged for 15 sec at  $8\,000 \times g$  step by step. Finally, RNA was eluted with diethylpyrocarbonate (DEPC)treated water and centrifuged for 1min at  $8\,000 \times g$ . The approximate quantity of RNA was determined with an OD 260 nm and the purity was confirmed with an OD ratio of 260 : 280 to be greater than 1.8 in all specimens. RNA was extracted from rat splenocytes stimulated in culture for 18 hours with PHA (10 mg/L), Con A (10 mg/L) and IL-2 (20 units/mL) for the positive control. The RNA of normal rat liver served as negative control.

### Reverse transcription and polymerase chain reaction

The cDNA synthesis was performed with GIBCOL BRL kit. RNA mixtures were prepared as follows: 2 µg of total RNA and 0.5 µg of oligo (dT) 12-18, were added with DEPC-treated water and diluted to 12 µL, water bathed at 70°C for 10 min and incubated on ice for at least 1min, then added with 2 µL of  $10 \times$  PCR buffer, 2 µL of 25mM MgCl<sub>2</sub>, 1 µL of 10mM dNTP, and 2 µL of 0.1M DTT and incubated at 42°C for 5 min. 200U Super Script II RT was added and incubated at 42°C for 50 min and the reaction was terminated at 70°C for 15 min and chilled on ice, and finally 1 µL of Rnase H was added to each tube and incubated for 20 min at 37°C. The cDNA was stored at -20°C.

The DNA was amplified using RT-PCR on a

Perkin-Elmer 2 400 thermocycler, and RT-PCR primer was designed according to the exon of rat gene sequences. The primer set for perforin was ① 5' GCCATCCTGCGTCTGGACCTG3', ② 5' CATTTGCGGTGCACG ATGGAG3'; primer set for the granzyme was ① GACTTTGTGCTGACTGCTGC TCAC3', ② 5' TTGTCCATAGGAGACGATGCCC GC3'; and for the β-actin: ① 5' TGCTAC ACTGCCA CT CGGTCA3', ② 5' GCATGCTCTGTGGAGCTGT TA3'<sup>[3]</sup>. The reaction mixture contained 2 µL cDNA, 1 µL of 10 mmol/L dNTP, 3 µL of 25 mmol/L MgCl<sub>2</sub>, 5 µL of  $10 \times$  buffer, 1 µL Taq polymerase, 2 µL each of the forward and reverse primer, and 34 µL of dual-distilled water for each 50 µL amplification reaction. Reactions were performed for 30 cycles. The conditions were 94°C for 3 min prior to cycling, denaturing at 95°C for 15 sec, annealing at 60°C for 20 sec and extension at 70°C for 30 sec. Following amplification, ten µL PCR products were run on a 1.5% agarose gel stained with ethidium bromide, gene specific bands were visualized by photography under UV fluorescence.

## RESULTS

### Survival time

Graft survival is shown in Table 1. Groups A, B and C showed rejection in 6-9 days. Groups B and C had rejection with a time course similar to group A ( $P > 0.05$ ). Survival in group D was significantly prolonged to  $37.1 \pm 9.9$  days ( $P > 0.01$ ).

**Table 1 Survival of hamster to rat liver transplantation**

Groups	Therapy	Survival (days)	$\bar{x} \pm s$
A	None	6,7,7,7,7,7,7	$6.9 \pm 0.4$
B	CsA 30 mg · kg · day	6,7,7,7,8,9	$7.3 \pm 1.0$
C	Splenectomy	6,7,7,7,7,8	$7.0 \pm 0.6$
D	CsA 30mg · kg · day+splenectomy	27,29,30,35,39,46,54	$37.1 \pm 9.9^a$

<sup>a</sup> $P < 0.01$  as compared with groups A, B and C.

### Histological examination

The liver xenografts in group A showed diffuse mononuclear cell infiltration, massive necrosis and interstitial hemorrhage (Figure 1A). In group B, CsA at dose of 30 mg · kg · day obviously decreased cellular infiltration, but severe hepatocyte necrosis and hemorrhage remained unchanged (Figure 1B). Splenectomy (group C) significantly alleviated hepatocyte necrosis and hemorrhage, but did not change diffuse mononuclear cell infiltration (Figure 1C). In group D, CsA and splenectomy abated cellular infiltration and hepatocyte necrosis and hemorrhage, the architecture of the hepatic lobule was preserved, but there was slight cellular infiltration in the portal tracts (Figure 1D).

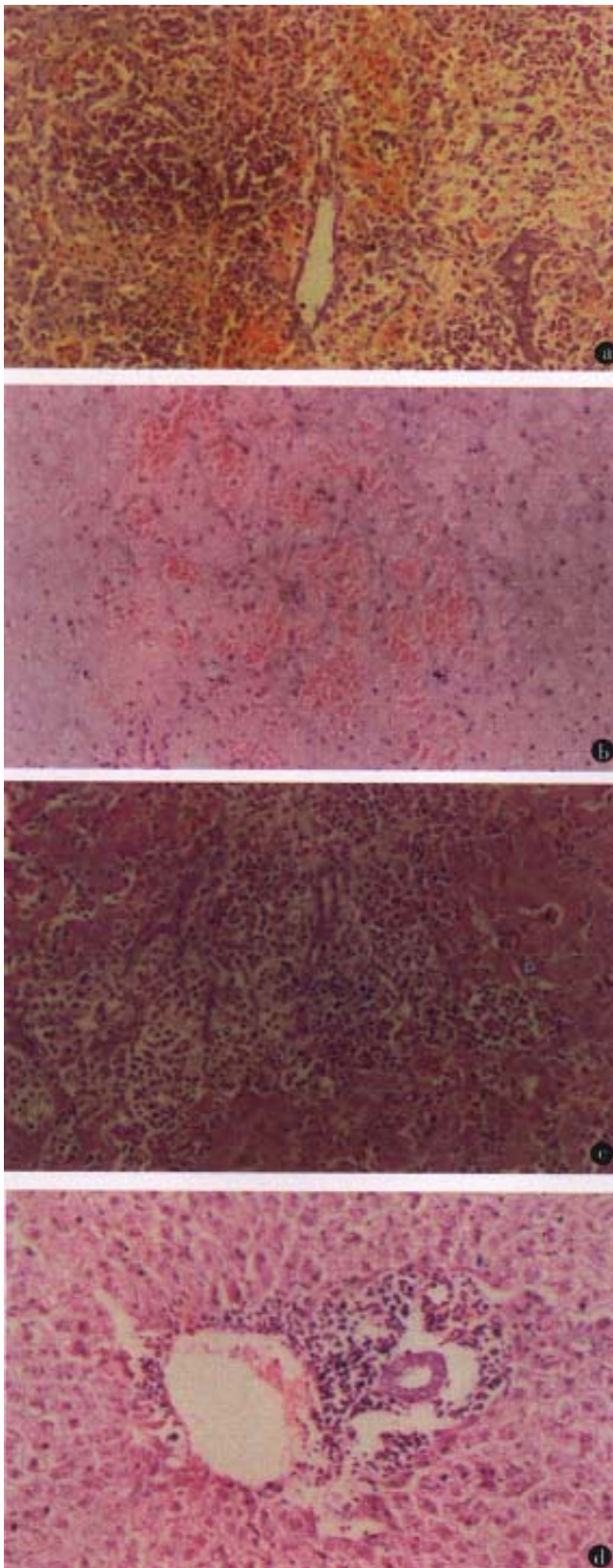


**Figure 1** Histology of liver grafts. (A) Diffuse mononuclear cell infiltration, massive necrosis and interstitial hemorrhage; (B) Cellular infiltration obviously decreased, but severe hepatocyte necrosis and hemorrhage unchanged; (C) Splenectomy significantly alleviated hepatocyte necrosis and hemorrhage, but did not change diffuse mononuclear cell infiltration; (D) The architecture of the hepatic lobule was preserved, but there was slight cellular infiltration in the portal tracts.

### Expression of perforin and granzyme B genes mRNA

All recipients had the expression of perforin and granzyme B genes mRNA in group A on post-transplantation day (POD) 5; only one (1/6) in group B expressed mRNA of these genes on POD 5; and five recipients (5/6) in group C expressed mRNA of both genes on POD 5. There was no expression of both genes in group D on POD 5 and 14, but only one recipient (1/7) expressed mRNA of perforin and granzyme B genes on POD 21 (Figure 2).

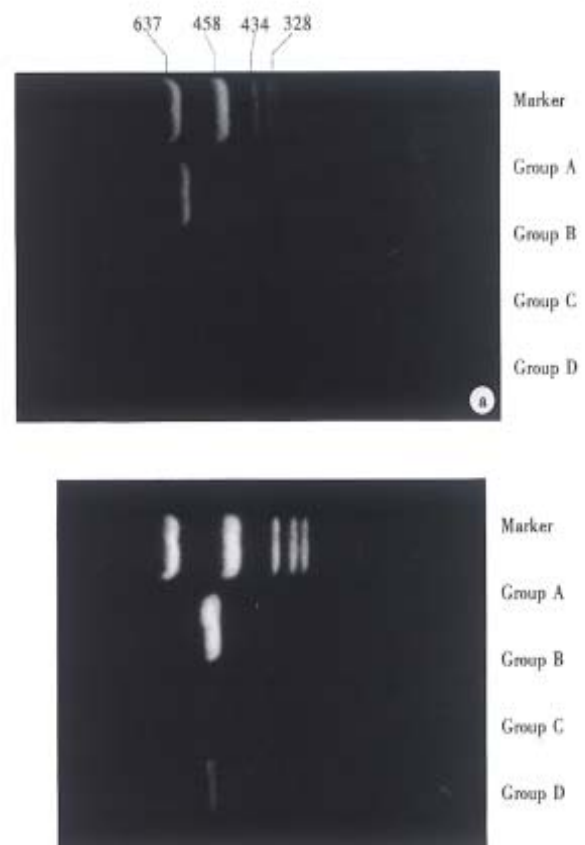


**Figure 2** Expression of perforin and granzyme B genes in liver xenografts on POD 7. A. Perforin; B. Granzyme B.

### DISCUSSION

Gold hamster to rat orthotopic liver transplantation is concordant and heterotransplantation and presents with acute rejection. The recipient's survival can not prolong until both cellular and humoral rejection are depressed due to its dual-immune mechanism. Splenectomy can effectively inhibit antibody formation, obviously abated hepatocyte necrosis and hemorrhage, but is unable to improve the diffuse mononuclear cellular infiltration in the grafted liver. CsA can significantly decrease cellular infiltration, but can not improve hepatocyte necrosis and hemorrhage,

neither of them can prolong the recipient's survival when used alone, but they can inhibit both cellular and humoral rejection, normalize the architecture of the grafted liver, and significantly prolong the recipient's survival to 37.1 days when used in combination. The result is better than that reported abroad<sup>[4]</sup>.

CTL is believed to play an important role in the mechanism of rejection, and effect mechanism of perforin and granzyme B, in spite of the regulatory and effect mechanism underlying the rejection process, remains incompletely understood. Effect of immunosuppression on the expression of perforin and granzyme B mRNA has become a hot topic in recent years. Mueller *et al*<sup>[5]</sup> analyzed the expression of perforin and granzyme A genes in situ hybridization in cellular infiltrates of MHC mismatched mouse heart transplants both in immunosuppressed recipients treated with CsA and untreated recipients. In untreated grafts, there were many perforin and granzyme A-expressing cells and heart transplants were completely rejected on POD 10. In contrast, CsA treatment significantly decreased the positive cells and prolonged survival of the transplants to 30 days. CsA did not obviously decrease infiltration of CD8<sup>+</sup> cells but significantly reduced the number of perforin and granzyme A-positive cells. It shows that CsA treatment mainly depressed the activation of CTL rather than decreased the number of infiltrating cells. Rapamycin can completely block

the expression of granzyme B gene in infiltrating cells of grafts, obviously prolong the survival of grafts<sup>[6]</sup>.

Our experimental results show that combined CsA and splenectomy could effectively depress rejection in hamster to rat orthotopic liver transplantation. The architecture of the hepatic lobule was undamaged, and the survival was significantly prolonged, and there were no expression of perforin and granzyme B genes mRNA.

In conclusion, expression of the CTL-associated gene perforin and granzyme B provides two valuable markers to judge the effect of immunosuppression in acute rejection of liver transplantation. But this should be further confirmed clinically.

## REFERENCES

- 1 Griffiths GM, Mueller C. Expression of perforin and granzymes *in vivo*: potential diagnostic markers for activated cytotoxic cells. *Immunol Today*, 1991;12:415-419
- 2 Zhang SG, Tan JW, Yang JM. Three cuff in hamster to rat orthotopic liver transplantation. *J Sec Milit Med Univ*, 1998;19:89-90
- 3 McDiarmid SV, Farmer DG, Kuniyoshi JS. Perforin and granzyme B. *Transplant*, 1995;59:762-766
- 4 Valdivia L, Monden M, Gotoh M. Prolonged survival of hamster-to-rat liver xenografts using splenectomy and cyclosporine administration. *Transplant*, 1987;44:759-763
- 5 Mueller C, Shao Y, Altermatt HJ. The effect of cyclosporine treatment on the expression of genes encoding granzyme A and perforin in the infiltrate of mouse heart transplants. *Transplant*, 1993;55:139-145
- 6 Wieder KJ, Hancock WW, Schmidbauer G. Rapamycin treatment depresses intragraft expression of RC/MMP 2, granzyme B and IFN gamma in rat recipients of cardiac allografts. *J Immunol*, 1993;151:1158-1166

Edited by MA Jing-Yun

# Cultivation of human liver cell lines with microcarriers acting as biological materials of bioartificial liver \*

GAO Yi, XU Xiao-Ping, HU Huan-Zhang and YANG Ji-Zhen

**Subject headings** bioartificial liver; liver cell lines; microcarrier

## Abstract

**AIM** To improve the cultivation efficiency and yield of human liver cell line CL-1.

**METHODS** High-density cultivation of CL-1 on microcarriers was carried out with periodic observation of their growth and proliferation. The specific functions of human liver cell were also determined.

**RESULTS** Cells of CL-1 cell line grew well on microcarrier Cytodex-3 and on the 7th day the peak was reached. The amount of CL-1 cells was  $2.13 \times 10^8$  and the total amount of albumin synthesis reached 71.23  $\mu\text{g}$ , urea synthesis 23.32 mg and diazepam transformation 619.7  $\mu\text{g}$  respectively. The yield of CL-1 on microcarriers was 49.3 times that of conventional cultivation. The amounts of albumin synthesis, urea synthesis and diazepam transformation were 39.8 times, 41.6 times and 33.3 times those of conventional cultivation, respectively.

**CONCLUSION** The human liver cell line CL-1 can be cultivated to a high density with Cytodex-3 and has better biological functions. High-density cultivation of CL-1 on microcarriers can act as the biological material of bioartificial liver.

## INTRODUCTION

The animal experiments of extracorporeal bioartificial liver suggested that the device could provide special assistance to hepatic functions, and the effects of its primary clinical application was encouraging<sup>[1-3]</sup>. Although few successful studies were reported on human cell line acting as the biological material of bioartificial liver, it is rather conspicuous<sup>[4,5]</sup>, and has opened up a new path for the study of bioartificial liver.

To meet the principal needs of bioartificial liver functions, microcarrier technique was used to cultivate high density human liver cell line to improve the cultivation efficiency and yield in this study. The growth of liver cells on microcarriers was observed and the specific functions of liver cells were determined periodically. The feasibility and value of human liver cell line cultivated on microcarriers as the biological material of bioartificial liver were inquired.

## MATERIALS AND METHODS

### Materials

The tissue of human liver cell line CL-1 was taken from normal adult liver. Microcarrier Cytodex-3 was produced by Pharmacia in Sweden. Magnetic stirrer (0r/min-200r/min) and stirring culture vessel was made by Bellco Biotechnology in USA. The culture matrix consisted of DMEM was soluted in 10% NCS and L-Glutamine at a concentration of 3 g/L, products of Gibco.

### Methods

**Common culture of CL-1** CL-1 cells 100mL, at a concentration of  $2 \times 10^5$  mL, were inoculated into a cubic culture flask. On the 1st, 3rd, 5th and 7th day the growth of cells was observed on an upside-down microscope and the cells were counted respectively. The amount of the cells in the culture system was also calculated. superficial clear liquid was obtained periodically to determine the functions of the liver cells.

**Microcarrier culture of CL-1** Cell suspension 100 mL, at a concentration of  $2 \times 10^5$  mL, was inoculated into a stirring culture vessel containing 500 mg Cytodex-3 and stirred intermittently for 8 hours. Then the culture system was placed into a fixed temperature culture case at a temperature of

Department of General Surgery, Zhujiang Hospital, First Military Medical University, Guangzhou 510282, Guangdong Province, China

Dr. GAO Yi, male, born on 1961-04-06 in Beijing, Han nationality, graduated from Second Military Medical University as M.D. in 1992, associate professor of general surgery, director of postgraduate.

\*Supported by the National Natural Science Foundation of China, No.39570212.

**Correspondence to:** Dr. GAO Yi, Department of General Surgery, Zhujiang Hospital, First Military Medical University, Guangzhou 510282, Guangdong Province, China

Tel. +86 • 20 • 84339888 Ext.43549

Received 1998-12-21

37°C and stirred continuously at a speed of 300 r/min. From the 2nd day on, whether to change the culture substrate or not and how much volume to change were determined by the color of the matrix and the value of its pH and the interval of changing liquid was about 24 hours-36 hours.

**Morphological observation and counting of the cells cultivated on microcarriers** On the 1st, 3rd, 5th, 7th and 9th day 0.1mL samples were taken at a well-distributed state of stirring, and growth of the cells was observed on the upside-down microscope. One mL samples were collected every other day to calculate the amount of cells in the culture system by means of crystal ester-calculating.

**Observation of cells cultivated on microcarriers under electron scanning microscope** On the 7th day cell sample was taken at a well-distributed state and culture matrix was discarded. After it was rinsed with phosphate buffer solution and fixed for 0.5 hour with 2 mL 2% pentanal, it was rinsed with phosphate buffer solution again, fixed for 0.5 hour with 1% osmic acid, dehydrated gradiently for 10 minutes each stage, exchanged with acetic isopental ester for 4 hours, and dried by CO<sub>2</sub> drier (HITACHI HCP-2, JAPAN). Finally it was splashed with ion platinum vacantly. Growth of the cells was observed under S-450 electron scanning microscope (JAPAN).

**Determination of albumin synthesis** When the culture substrate was changed, superficial clear liquid was obtained to determine the concentration of human albumin by radio-immunity competition.

**Determination of diazepam transformation** Standard diazepam was added to the culture vessel at a concentration of 20 µg/mL. The superficial clear liquid was taken periodically and the concentration of diazepam was determined according to XUE Guo-Zhu *et al*<sup>[6]</sup>. The amounts of diazepam transformation were calculated.

**Determination of urea in superficial clear liquid** Superficial clear liquid (0.2 mL) was taken and determined by BECKMAN biochemical auto-detector. The amount of urea was calculated on the basis of the culture volume.

## RESULTS

### Comparison of cell amounts after expanded by cultivation

After 1-3 days of cultivation, the CL-1 cells in common culture adhered and grew slowly, and part of them in suspension was devitalized. From then on the adhering CL-1 cells grew rapidly, and cell amount reached  $4.32 \times 10^6/100$  mL on the 5th day.

On the 7th day the amount decreased to  $3.83 \times 10^6/100$  mL while in the microcarrier culture the growth of CL-1 accelerated on the 3rd day and reached the peak of  $2.13 \times 10^8$  on the 7th day, and decreased to  $1.83 \times 10^8$  on the 9th day (Figure 1). The ratio of the peak amounts of CL-1 between microcarrier culture and common culture was 49.3:1.

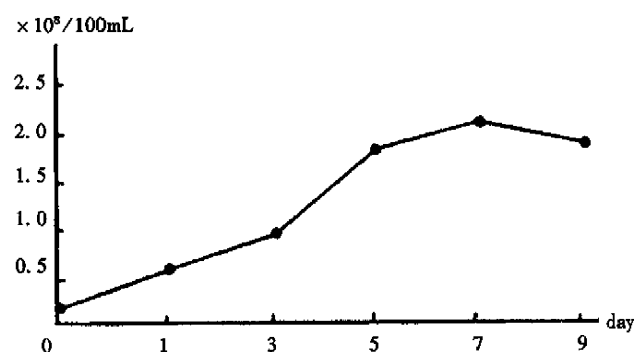


Figure 1 Change of the amount of CL-1 cultivated on microcarriers.

### Morphological observation of CL-1 cultivated on microcarriers

**Observation under upside-down microscope** On the 1st day over 50% microcarriers were attached with cells and the cells were beginning to expand. On the 5th day more than 80% microcarriers were covered with cells (Figure 2). The multi-morphological growth of liver cells could be observed under high-amplification microscope. On the 7th day the phenomenon of bridge-link could be observed between microcarriers, i.e., the microcarriers were linked to each other through cells (Figure 3).

**Observation under electron microscope** On the 7th day of cultivation, electron microscopy showed that the cells adhered fast to the microcarriers semi-spherically (Figure 4). The microvilli on the surfaces of the cells could be observed clearly.

**Changes of specific functions of cells** When CL-1 cells were cultivated on microcarriers, the specific functional indexes such as albumin synthesis, urea synthesis and diazepam transformation rose gradually along with the prolonging of the cultivation. On the 7th day these indexes peaked, and then decreased gradually, while CL-1 cells were commonly cultivated, the functional indexes as described above reached their peaks on the 5th day and decreased noticeably on the 7th day. All the functional indexes determined at various time points in microcarrier culture were obviously higher than those in common culture



(Tables 1, 2). When functional indexes of CL-1 cells reached their peaks on the 7th day, the albumin synthesis, urea synthesis and diazepam transformation of CL-1 in microcarrier culture were 39.8, 41.6 and 33.3 times over those in common culture on the 5th day.

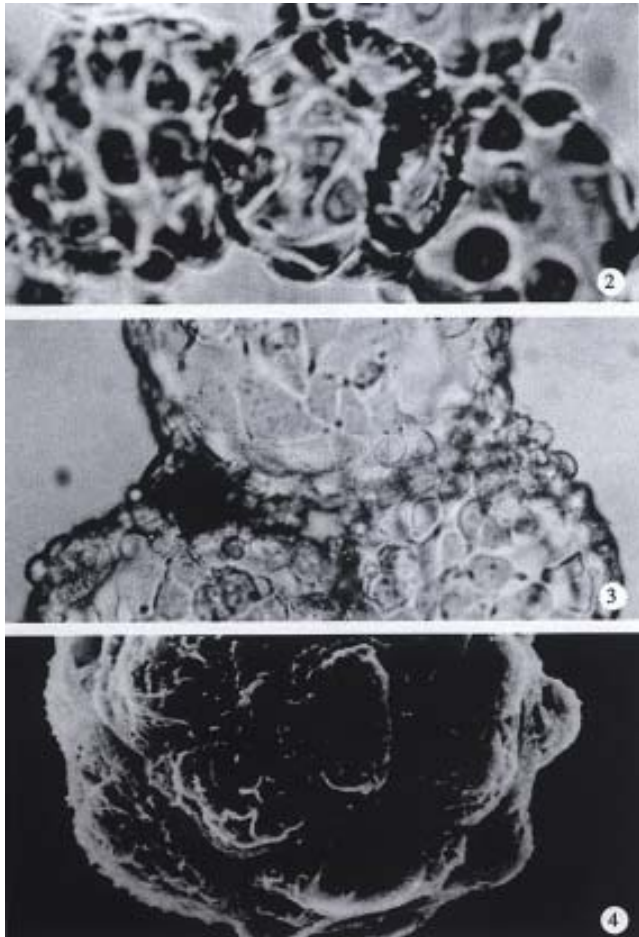


**Figure 2** On the 5th day more than 80% microcarriers were covered with CL-1 cells under upside-down microscope.  $\times 120$

**Figure 3** On the 7th day the phenomenon of bridge-link could be observed between microcarriers under upside-down microscope.  $\times 200$

**Figure 4** On the 7th day of cultivation, the electron microscope showed that the cells adhered fast to the microcarriers semi-spherically under scanning electronic microscope.  $\times 950$

**Table 1** Changes of specific functions of CL-1 under two culture conditions

Indexes of functions	1st day	3rd day	5th day	7th day	9th day
Albumin synthesis ( $\mu\text{g}$ )					
Microcarrier culture	21.34	35.87	58.35	71.32	67.98
Common culture	0.43	1.21	1.79	1.65	
Urea synthesis (mg)					
Microcarrier culture	7.45	11.49	19.62	23.32	20.18
Common culture	0.08	0.34	0.56	0.42	
Diazepam transformation ( $\mu\text{g}$ )					
Microcarrier culture	112.2	271.3	544.1	619.7	573.3
Common culture	3.4	8.9	18.6	13.5	

**Table 2** Comparison of peak function values of CL-1 under two culture conditions

Indexes of functions	Albumin synthesis ( $\mu\text{g}$ )	urea synthesis (mg)	Diazepam transformation ( $\mu\text{g}$ )
Microcarrier culture	71.23	23.32	619.7
Common culture	1.79	0.56	18.6
Ratio	39.8:1	41.6:1	33.3:1

## DISCUSSION

Microcarrier culture can improve the culture efficiency and yield. As the biological material of bioartificial liver, the liver cells must meet two needs: ① possessing the specific functions of liver; and ② providing biological function enough to satisfy the patients. The former demands high differentiation of the cells, and the latter sufficient amount of liver cells. Our primary study on the human liver cell line at early stage showed the characteristics of high differentiation and good specific liver functions of CL-1. It is extremely valuable as the biological material of bioartificial liver<sup>[6]</sup>. In common culture, however, the yield of human cell line can only reach the level of  $10^6$ - $10^7$ , not enough to meet the need of necessary amount to survive an individual. So the urgent question on the biological material of bioartificial liver is how to increase the amount of the cells. The technique of microcarrier culture in cell engineering makes cultivating the human liver cell line possible in high-density in that it possesses a high ratio of surface area to volume, which provides a comparatively large area for cells to adhere in small culture volume. Few successful cultivations of animal primary liver cells on microcarriers have been reported both at home and abroad<sup>[7,8]</sup>, while there was no report on cultivation of human liver cells on microcarriers yet. Microcarrier culture of CL-1 was studied by using Cytodex-3 and slow stirring in our work. After 100 mL suspension of CL-1 was inoculated at a concentration of  $2 \times 10^5/\text{mL}$ , the cells grew and adhered to the microcarriers in great amount and reached the peak on the 7th day. The maximal yield of cells cultivated on microcarrier was 49.3 times over that in 100 mL common cubic flask. The reasons for the increase of cell yield in a big margin when CL-1 was cultivated on microcarrier were as follows: ① The surface area in the culture system for cells to grow was greatly improved by using microcarriers. 0.5 g Cytodex-3 was added into 100 mL culture matrix each and the cultivating surface area could reach 2 300  $\text{cm}^2$ ; while the efficient surface area of the common culture flask was only 28  $\text{cm}^2$ . The quantity of the cells increased correspondingly with the improvement of the cultivating surface; ② Cytodex-

3 is primarily characterized by a thin layer of collagen chemically coupled to a matrix of cross-linked dextran, so that it can attach the liver cells strongly, stimulate the expanding and growth of them and promote their growth<sup>[5,9]</sup>; and ③ Low speed stirring employed to cultivate CL-1 cells made them easy to adhere to the surfaces of the suspending microcarriers and expand to mono-layers gradually.

The overall functions of CL-1 cultivated in microcarrier system were improved. Due to the marked increase of the amount of cells, the function indexes of CL-1 cultivated on microcarrier were greatly improved and predominated over those in common culture. Such improvement was the prerequisite for CL-1 cultivated on microcarrier to act as the biological material of bioartificial liver. Furthermore, the time for the highest cell amount and function indexes in microcarrier culture was later than that in common culture. It may be due to the improvement of efficient surface area for cultivating which delayed the peak of growth and reproduction of CL-1 afterwards.

Further improvement is needed in microcarrier culture of liver cells. Matsumura held that about 25 g-75 g liver cell ( $2.5 \times 10^9$ - $7.5 \times 10^9$  liver cells) was enough to provide the necessary liver functions to survive an individual when his liver weight was 1 200 g<sup>[10]</sup>. Although the amount of CL-1 had been

greatly improved to the level of  $2 \times 10^8$  in a culture volume of 100 mL in this study, it can not meet the need of the bioartificial liver yet. Expansion of the volume of microcarrier culture to several or even several tens of liters is to be further studied. Perfusion culture with microcarrier is promising.

## REFERENCES

- 1 Sussman NL, Finegold MJ, Kelly JH. Recovery from syncytial giant-cell hepatitis (SGCH) following treatment with an extracorporeal liver assist device (ELAD). *Hepatology*, 1992;15:51A
- 2 Rozga J, Holzmann MD, Ro MS. Development of a hybrid bioartificial liver. *Ann Surg*, 1993;217:502-511
- 3 Demetriou AA, Rozga J, Podesta L, Lepage E, Morsiani E, Moscioni AD, Hoffman A, McGrath M, Kong L, Rosen H. Early clinical experience with a hybrid bioartificial liver. *Scand J Gastroenterol Suppl*, 1995;208:111-117
- 4 Sussman L, Kelly JH. Artificial liver: a forthcoming attraction. *Hepatology*, 1994;17:1163-1164
- 5 Nyberg SL, Rimmel RP, Mamn HJ. Primary hepatocytes outperform HepG2 cells as the source of biotransformation function in a bioartificial liver. *Ann Surg*, 1994;220:59-67
- 6 Xue GZ, Gao Y, Yang JZ. Primary study on human cell line acting as the biological material of artificial liver. *J Chin Infil Artif Organ*, 1996;7:1-4
- 7 Rozga J, Williams F, Ro MS, Neuzil DF, Giorgio TD, Backfisch G, Moscioni AD, Hakim R, Demetriou AA. Development of a bioartificial liver: properties and function of a hollow module inoculated with liver cells. *Hepatology*, 1993;17:258-265
- 8 Wang YJ, Li MD, Wang YM. Cultivation of rat liver cells adhered on microcarriers. *J Chin Exp Surg*, 1997;14:61
- 9 Kasai S, Sawa M, Mito M. Is the biological artificial liver clinically applicable. A historic review of biological artificial liver support system. *Artif Organ*, 1994;18:348-354
- 10 Matsumura KN, Guevara GR, Huston H, Hamilton WL, Rikimaru M, Yamasaki G, Matsumura MS. Hybrid bioartificial liver in hepatic failure: preliminary clinical report. *Surgery*, 1987;101:99-103

Edited by WANG Xian-Lin



# CT arterial portography and CT hepatic arteriography in detection of micro liver cancer

LI Li, WU Pei-Hong, MO Yun-Xian, LIN Hao-Gao, ZHENG Lie, LI Jin-Qing, LU Li-Xia, RUAN Chao-Mei and CHEN Lin

**Subject headings** liver neoplasms/diagnosis; CT arterial portography; CT hepatic arteriography

## Abstract

**AIM** To recognize the characteristic findings of micro-liver cancer (MLC) and to evaluate the effect of CT arterial portography (CTAP) and CT hepatic arteriography (CTHA) in diagnosis of MLC.

**METHODS** Between April 1996 to December 1998, CTAP and CTHA were performed in 12 patients with MLC, which were not detected by conventional CT examinations. After CTHA, 3 mL-5 mL mixture of lipiodol, doxorubicin and mitoycin C were injected into hepatic artery through the catheter, and the followed up by CT three or four weeks later (Lipiodol CT Lp-CT).

**RESULTS** A total of 22 micro-tumors (0.2 cm-0.6 cm in diameter) were detected in 12 patients, which manifested as small perfusion defects in CTAP and small round enhancement in CTHA. The rate of detectability of CTAP and CTHA was 68.2% (15/22) and 77.3% (17/22) respectively, and the rate of the simultaneous use of both procedures reached 86.4% (19/22). All micro-tumors were demonstrated as punctate lipiodol deposit foci in Lp-CT. After Lp-CT, the elevated serum level of  $\alpha$ -fetoprotein (AFP) dropped to the normal level in all patients.

**CONCLUSION** The CTAP and CTHA are the most sensitive imaging methods for detecting micro-liver cancer. Confirmed by the change of the elevated serum AFP level and lipiodol deposit foci in Lp-CT, small perfusion defects in CTAP and punctate enhancement in CTHA may suggest micro-liver cancer.

Cancer Center, Sun Yat-Sen University of Medical Sciences, Guangzhou 510060, Guangdong Province, China

Dr. LI Li, male, born on 1968-10-08 in Changsha City, Hunan Province, graduated from Sun Yat-Sen University of Medical Sciences as a postgraduate in 1996, now attending doctor of medical imaging, majoring oncological imaging diagnosis and interventional radiology, having 8 papers published.

\*Supported by "9 • 5" National Major Project of National Committee of Sciences and Technology, No. 96-907-03-02.

**Correspondence to:** Dr. LI Li, Department of Imaging & Interventional Radiology, Cancer Center, Sun Yat-Sen University of Medical Sciences, 651 Dongfeng Road E, Guangzhou 510060, Guangdong Province, China

Tel. +86 • 20 • 87765368 Ext 3216, Fax. +86 • 20 • 87754506

Email. Liliixj@public.guangzhou.gd.cn

Received 1998-10-08

## INTRODUCTION

With combined the findings of diagnostic imaging and elevated serum AFP level, more and more small liver cancer were detected earlier, and the therapeutic effect was significantly improved<sup>[1,2]</sup>. Except for other causes, such as hepatitis and teratoma, the elevated serum AFP level (higher than 400  $\mu$ g/L) strongly suggests the occurrence of primary hepatocellular carcinoma. However, sometimes no tumors could be found on conventional CT scanning (contrast material administered by intra-venous injection). These patients were further examined with were CTAP and CTHA. From April 1996 to December 1998, 12 patients with micro-cancer were examined with CTAP and CTHA in our hospital.

## MATERIALS AND METHODS

### Materials

From April 1996 to December 1998, 12 patients (10 men, 2 women) suspected to have liver cancer were examined with CTAP and CTHA. They ranged in age from 23 to 54 years (mean age, 36.4 years). The serum level of AFP was elevated in all the patients with a range of 201  $\mu$ g/L to 1 405  $\mu$ g/L (including 8 cases > 400  $\mu$ g/L, 4 cases < 400  $\mu$ g/L). Cirrhosis occurred in 7 cases. The tumors were 0.2 cm-0.6 cm in size with a mean of 0.46 cm. Multiple nodules were found in 7 cases.

### Methods

CTAP examinations were performed with incremental scanning of the liver in cranial-to-caudal direction with 2.7 mm to 8 mm collimation on bi-spiral-Elscint Twin Flash scanner (Elscint-Corp.). CT images were obtained 25sec-35sec after the initiation of transcatheter (5-F) superior mesenteric artery injection of 30 mL-40 mL of non-ionic contrast medium at a rate of 2.5 mL/sec-3.0 mL/sec with an automatic power injector (Medrad, Pittsburgh). During the catheterization, contrast medium administered before CT scanning was limited to 5 mL-10 mL injected by hand to visualize any aberrant vessels and to facilitate proper catheter placement.

CTHA examinations were done by injecting contrast medium into proper hepatic artery or

common hepatic artery. Twenty mL to 30 mL of contrast medium was injected at a rate of 3.0 mL/sec-3.5 mL/sec. Consecutive scanning of the liver was started 6sec-8sec after the initiation of injection of the contrast medium. After CTHA examinations, 3 mL-5 mL mixture of lipiodol, doxorubicin (10 mg-15 mg), and mitoycin C (2 mg-4 mg) were injected into hepatic artery, and the follow-up CT was performed three or four weeks later (Lp-CT). The serum AFP level was detected in all the patients two or three weeks later, and all returned to normal within 1-6 months.

## RESULTS

### *Detectable rate of micro-tumors*

A total of 22 micro-tumors were found in our group. The tumors measured 0.2 cm-0.6 cm with a mean of 0.46 cm. CTAP and CTHA images were carefully interpreted by two experienced radiologists. Fifteen tumors were demonstrated as fleckly perfusion defects on CTAP images with a detectable rate of 68.2%, and 17 manifested as punctate enhancement foci on CTHA with a detectable rate of 77.3%. Nineteen were found by simultaneous use of both procedures with a detectable rate of 84.4%. But 3 tumors were not detected by CTAP and CTHA in 2 patients. All 22 micro-tumors manifested as punctate lipiodol deposit foci in Lp-CT, which was performed two or three weeks later. Because the tumors in our series were extremely small, no pathologic diagnosis was acquired in all patients.

### *Follow-up of patients*

The serum AFP level was examined two or three weeks after Lp-CT. The AFP level dropped to the normal level in all the patients. Within 1-6 months. All survived without any signs of recurrence in our group, and the survival period ranged from 3 to 33 months (mean, 15.2 months).

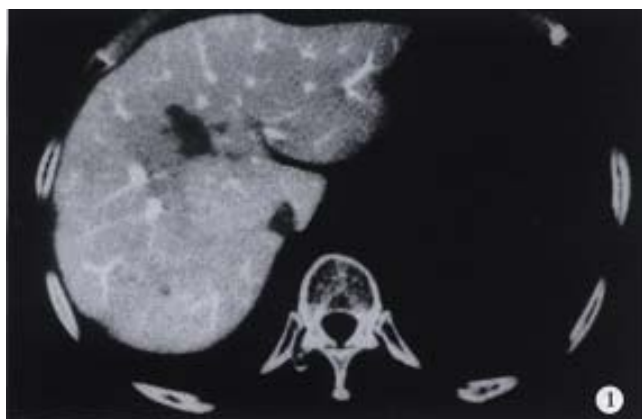


**Figure 1** CTAP image obtained in a 40-year-old man with liver micro-cancer shows a punctuate perfusion defect in right lobe.

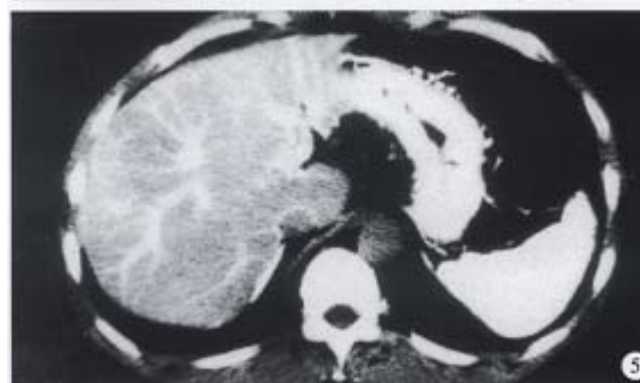
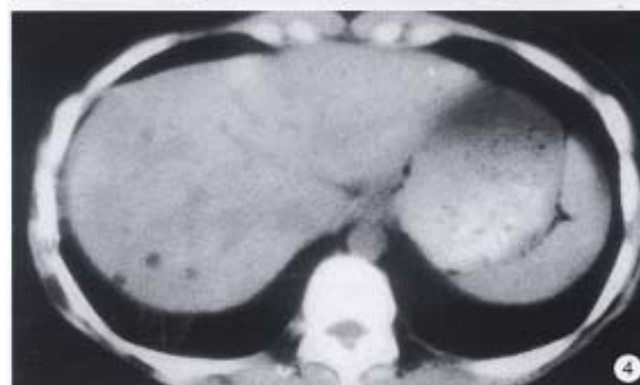
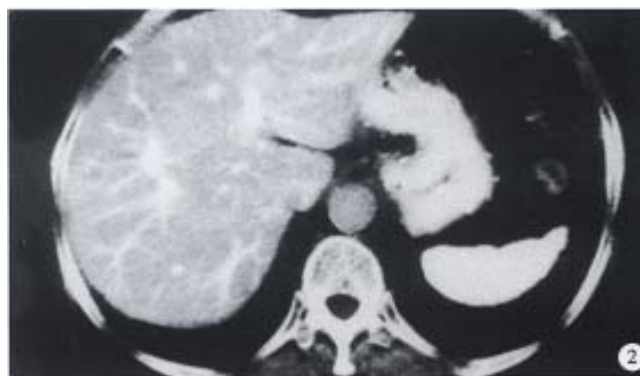


**Figure 2** CTHA image obtained on the same slice to Figure 1, the micro-tumor manifested as an small round enhancement nodule.

**Figure 3** CTHA in a 45-year-old man shows a micro-cancer with a diameter of 0.3 cm.

**Figure 4** A punctuate lipiodol deposit focus with 0.2 cm in diameter is shown on Lp-CT in a 28-year-old woman with elevated serum AFP level of 860  $\mu\text{g/L}$  detects which was not detected by CTAP and CTHA.

**Figure 5** CTHA in a 35-year-old man shows two punctuate non-pathologic enhancement foci on the edge of right lobe.

## DISCUSSION

In some of our patients found with elevated serum level by AFP, no tumors were detected by conventional CT scanning. For those patients, CTAP and CTHA examinations were recommended. Fleckly perfusion defects were found on CTAP (Figure 1) and punctate enhancement foci on CTHA (Figure 2). After CTHA examination, 3 mL-5 mL mixture of lipiodol and anticancer drug was tentatively injected in to hepatic artery for Lp-CT diagnosis, which was repeated three or four weeks later. Micro-foci of lipiodol deposit was found with elevated serum AFP level, which dropped continuous to normal. The prognosis of these patients was very good. Since April 1996, 12 patients with such findings have been examined in our hospital. All patients were surviving without any signs of recurrence, and the longest survival being 33 months. Due to its special clinical significance, we suggested the definition of micro-cancer in liver (0.2cm-06cm in diameter) which includes: ① elevated serum AFP level ( $\text{AFP} \geq 400 \mu\text{g/L}$ , or rising continuously); ② no micro-tumors were detected by conventional imaging methods, but by CTAP and CTHA; ③ Punctate lipiodol deposit foci were demonstrated on Lp-CT; and ④ after Lp-CT, serum AFP level lowered continuous or turned to normal level. CTAP and CTHA are considered as the most sensitive imaging methods for detecting small hepatocellular carcinoma<sup>[3]</sup>. The development of spiral CT technique greatly facilitated procedures and improved the quality of CT images<sup>[4]</sup>. Detectability of CTAP and CTHA for very small tumors (as small as 0.2 cm in diameter, Figure 3) was high, being 68.2% and 77.3% respectively, and that of simultaneous use of both procedures was 84.4%. But there were still some cases of micro-tumors which could not be detected by CTAP and CTHA. In a 28-year-old female patient with elevated AFP level of  $860 \mu\text{g/L}$ , no tumors were found either on conventional CT scanning or on CTAP and CTHA images. Three weeks later, Lp-CT detected a punctate lipiodol deposit focus of 0.2 cm in diameter in her left lobe with AFP continuous dropping to normal level (Figure 4). This patient had survived for 33 months without any signs of recurrence. With the widespread use of CTAP and CTHA, there have been more reports on non-pathologic perfusion defects detected with CTAP and non-pathologic enhancement detected with CTHA. Due to aberration of blood supply for some parts of the liver, such as arterio-portal shunt<sup>[5]</sup>, cirrhotic nodule, focal nodular hyperplasia, and focal fatty infiltration, the normal tissue could manifest as perfusion defects in CTAP, especially in the

medial segment of the left lobe<sup>[6]</sup>. Peterson *et al* reported that perfusion defects on CTAP were sometimes nonspecific, and peripheral flat or wedge-shaped perfusion defects indicated benignity<sup>[7]</sup>. In our study, the occurrence rate of non-pathologic perfusion defects detected with CTAP was 15.1%, and peripheral wedge-shaped perfusion defects were most common<sup>[8]</sup>. Similar to findings of CTAP, pseudo-lesion enhancement of normal liver tissue also occurred in CTHA. Kanematsu *et al* supposed that local non-pathologic enhancement detected with CTHA might result from the cystic venous drainage or peripheral arterio-portal shunts<sup>[9]</sup>. In our study, the occurrence rate of non-pathologic enhancement detected with CTHA was 22.0%, and small round peripheral enhancement was seen most commonly<sup>[8]</sup> (Figure 5). Thus, we do not recommend to use CTAP or CTHA alone to interpret small hepatocellular carcinomas. The combined use of both procedures can help distinguish micro-cancer from the false-positive findings on CTAP and CTHA, and increase the accuracy of diagnosis for small hepatocellular carcinoma<sup>[10]</sup>. Besides the findings on CTAP and CTHA images, combination of lipiodol deposit foci on Lp-CT and dropping of elevated serum AFP level are also helpful for the establishment of diagnosis for liver micro-cancer.

## REFERENCES

- 1 Wu MC. Clinical research advantage in primary liver cancer. *WJG*, 1998;4:471-474
- 2 Tang ZY. Advances in clinical research of hepatocellular carcinoma in China. *WCJD*, 1998;6:1013-1016
- 3 Hori M, Murakami T, Oi H, Kin T, Takahashi S, Matsushita M. Sensitivity in detection of hypervascular hepatocellular carcinoma by helical CT with intra-arterial injection of contrast medium, and by helical CT and MR imaging with intravenous injection of contrast mediums. *Acta Radiol*, 1998;39:144-151
- 4 Murakami T, Oi H, Hori K, Kim T, Takahashi S, Tomoda K. Helical CT during arterial portography and hepatic arteriography for detecting hypervascular hepatocellular carcinoma. *AJR*, 1997; 169:131-135
- 5 Tamura S, Kihara Y, Yuki Y, Sugimura H, Shimice T, Adjei O. Pseudolesion on CTAP secondary to arterio portal shunts. *Clin Imaging*, 1997;21:359-365
- 6 Matusi O, Kadoya M, Yashikawa J, Gadate T, Kawanori Y. Posterior aspect of hepatic segment IV: Patterns of portal venule branching at helical CT during arterial portography. *Radiology*, 1997; 205:159-162
- 7 Peterson MS, Baron RL, Dodd III GD, Zajko AJ, Oliver JH, Miller WJ. Hepatic parenchymal perfusion defects detected with CTAP: imaging-pathologic correlation. *Radiology*, 1992;185:149-155
- 8 Li L, Wu PH, Lin HG, Li JQ, Mo YX, Zheng L. Findings of non-pathologic perfusion defects by CT arterial portography and non-pathologic enhancement of CT hepatic arteriography. *WJG*, 1998; 4:513-515
- 9 Kanematsu M, Hoshi H, Imado T, Yamawaki Y, Mizuno S. Non-athological focal enhanced on spiral CT hepatic angiography. *Abdom Imaging*, 1997;22:55-59
- 10 Irie T, Takeshita K, Wada Y, Kisano S, Terahata S, Tamai S. Evaluation of hepatic tumors: comparison of CT with arterial portography, CT with infusion hepatic arteriography, and simultaneous use of both techniques. *AJR*, 1995;164:1407-1412

# Effect of apolipoprotein E gene Hha I restricting fragment length polymorphism on serum lipids in cholecystolithiasis

LIN Qi-Yuan, DU Jing-Ping, ZHANG Ming-Yi, YAO Yu-Gwei, Li Lin, CHENG Nan-Sheng, YAN Lu-Nan and XI-AO Lu-Jia

**Subject headings** apolipoprotein E; polymorphism; lipids; cholecystolithiasis; polymerase chain reaction

## Abstract

**AIM** To investigate the role of apolipoprotein E (apoE) polymorphism in the lithogenesis of gallstone and the hereditary pathogenesis of the disease.

**METHODS** Polymerase chain reaction (PCR) was used to study apoE phenotypes and allele frequencies in patients with gallstones and control, and the fasting serum lipids of subjects were also measured by enzymatic methods.

**RESULTS** The levels of triglyceride (TG) and very low density lipoprotein cholesterol (VLDL-C) were much higher in E<sub>2</sub>/E<sub>3</sub> patients than that in E<sub>2</sub>/E<sub>3</sub> control. E<sub>3</sub>/E<sub>3</sub> patients were accompanied with remarkably low levels of high density lipoprotein cholesterol (HDL-C) and its subforms. But in E<sub>3</sub>/E<sub>4</sub> patients there were only slight changes in levels of VLDL-C and low density lipoprotein cholesterol (LDL-C).

**CONCLUSION** Different apoE phenotype patients with gallstones have different characteristics of dyslipidemia and the average level of serum lipids in patients with gallstones are higher than subjects without gallstones in the same apoE gene phenotype. ε<sub>2</sub> allele is possibly one of the dangerous factors in the lithogenesis of cholecystolithiasis.

Department of General Surgery, First Hospital, West China University of Medical Sciences

Dr. LIN Qi-Yuan, Male, born on 1964-01-01 in Nanchong City, Sichuan Province, graduated from West China University of Medical Sciences and earned a Doctor degree in 1996, now an associate professor, majoring hepatic-biliary-pancreatic surgery having 16 articles published.

\*Project supported by National Natural Science Foundation of China a, No. 39670709.

**Correspondence to:** LIN Qi-Yuan, Department of General Surgery, First University Hospital, West China University of Medical Sciences, Chengdu 610041, Sichuan Province, China

Tel. +86 • 28 • 5551078, Fax. +86 • 28 • 5530724

Received 1999-01-20

## INTRODUCTION

The apolipoprotein E (apoE) gene locus possesses three alleles, ε<sub>2</sub>, ε<sub>3</sub> and ε<sub>4</sub>, which are inherited in co-dominant fashion and code for three isoprotein E<sub>2</sub>, E<sub>3</sub> and E<sub>4</sub> making up six phenotypes, three heterozygous E<sub>2</sub>/E<sub>3</sub>, E<sub>3</sub>/E<sub>4</sub> and E<sub>2</sub>/E<sub>4</sub>, three homozygous E<sub>2</sub>/E<sub>2</sub>, E<sub>3</sub>/E<sub>3</sub> and E<sub>4</sub>/E<sub>4</sub><sup>[1-7]</sup>. The differences of these main isoprotein alter the receptor-binding affinity of the apolipoprotein-containing lipoproteins and affect the metabolism of cholesterol and lipids<sup>[2,4]</sup>. It is putative that apoE polymorphisms are closely related to hyperlipidemia<sup>[5]</sup>, coronary heart disease<sup>[6]</sup> and diabetes mellitus<sup>[7]</sup>. The formation of gallstones is frequently associated with the changes in biliary lipid compositions, the lithogenic bile being usually supersaturated with cholesterol and decreased with bile acids and lecithin<sup>[8,9]</sup>. A prerequisite for the formation of gallstones is the lithogenic bile, which is often the result of disorders in lipid metabolism or dyslipidemia. The important role of apoE in the regulation of lipid metabolism raises the possibility that apoE polymorphisms may be involved in the formation of gallstones. This case-control cohort study is designed to investigate the significance of apoE polymorphisms as a predisposing factor in the pathogenesis of cholecystolithiasis.

## SUBJECTS AND METHODS

### Subjects

Eighty-seven consecutive patients with gallstones were investigated. The treatment group consisted of 39 men and 48 women (mean age 52 years, ranging from 16 to 83 years). All of them suffered from non-symptomatic cholecystolithiasis and underwent operation in the First Hospital from January 1994 to December 1995. The control group included 50 subjects with 27 men and 23 women (mean age 49 years, ranging from 15 to 78 years), and they were also matched in sex and age distribution with the patients with gallstones.

### DNA amplification

Leukocyte DNA of venous blood collected in EDTA tubes were extracted by Hixson slotting-out method<sup>[10]</sup>. Model DNA was amplified by polymerase chain reaction (PCR) thermal cycles using oligonucleotides primers F4 (5'-ACAGAATTCGCC CCGGCTGGTACAC-3') and F6 (5'-TAAGCTTGG CACGGCTG TCCAAGGA-3'). Each amplification reaction system contained 1 μg DNA, 1 pmol/L

of each primer and 25 kilo units/L of Taq-polymerase up to a final volume of 30  $\mu$ L. Each reaction mixture was heated at 95°C for 5 minutes for predenaturation, and followed by 30 cycles of amplification for annealing at 60°C for 1 minute, elongation at 70°C for 2 minutes, denaturation at 95°C for 1 minute, and then a prolonged elongation time up to 7 minutes at 56°C.

### Analysis of restricting fragment length polymorphism for apoE

Twenty-five  $\mu$ L of PCR amplified products in each reaction system were mixed with 5 units of Hha I enzyme for digestion apoE sequences at 37°C for 1 hour. Each reaction mixture was loaded onto 85 g/L polyacrylamide gel, after electrophoresis for 3 hours under constant current (45 mA) and visualized by ultraviolet light. The size of apoE Hha I restricting fragment length polymorphisms were estimated by comparison with marker DNA PBR32. On the basis of the size and the number of various fragments, apoE phenotypes were determined as E2 with 91bp, and 83bp E3 with 91bp, 48bp and 35bp, as well as E4 with 72bp, 48bp and 35bp.

### Lipids analysis

Serum total cholesterol (TC) and total triglyceride (TG) were determined by enzymatic methods with the OUL 3 000 automatic analyzer. High density lipoprotein cholesterol (HDL-C) was measured enzymatically and formed in the serum supernatant after precipitation of low density lipoprotein cholesterol (LDL-C) and very low density lipoprotein cholesterol (VLDL-C) with dextrin sulfate and  $MgCl_2$ . The LDL-C and VLDL-C levels were calculated according to Friedwald's formula<sup>[11]</sup>.

### Statistical analysis

All results were expression as  $\bar{x} \pm s$ . The *F* test and  $\chi^2$  test were used for statistical analysis, *P* values less than 0.05 were regarded as significant.

## RESULTS

### Distribution of apoE phenotypes and allele frequencies

In the six common apoE phenotypes, E<sub>2/3</sub>, E<sub>3/3</sub> and E<sub>3/4</sub> phenotypes existed in either patients with gallstones or control subjects. There were only 2 E<sub>2/2</sub> phenotype cases in the control, and no E<sub>2/2</sub> and E<sub>4/4</sub> were detected in both groups. The overall distribution of apoE phenotypes and apoE allele frequencies in the patients with gallstones were analogous to that of the control (Table 1).

**Table 1 Apolipoprotein E phenotype distributions and allele frequencies in patients with gallstones and controls**

Groups	<i>n</i>	Phenotype				Allele		
		E <sub>2/3</sub> (%)	E <sub>2/4</sub> (%)	E <sub>3/3</sub> (%)	E <sub>3/4</sub> (%)	ε2(%)	ε3(%)	ε4(%)
Patients	87	10(11.4)	0	69(79.4)	8(9.2)	5.8	89.6	4.6
Male	39	4(10.2)	0	31(79.4)	4(10.2)	5.1	89.8	5.1
Female	48	6(12.5)	0	38(79.1)	4(8.9)	6.3	89.6	4.2
Controls	50	5(10.0)	2(4.0)	37(74.1)	6(12.0)	7.0	85.0	8.0
Male	27	3(10.0)	1(3.7)	20(74.0)	3(11.0)	7.4	85.2	7.4
Female	23	2(8.6)	1(4.3)	17(74.6)	3(13.0)	6.5	84.8	8.7

### Serum lipids

The levels of TG (1.43 mmol/L) and VLDL-C (0.68 mmol/L) in E<sub>2/3</sub> patients with gallstones were markedly higher than that in E<sub>2/3</sub> control (1.06 mmol/L, *P*<0.05 and 0.48 mmol/L, *P*<0.05). LDL-C (1.41 mmol/L) was significantly lower in E<sub>2/3</sub> patients than that in the control (2.04 mmol/L, *P*<0.05). No statistical differences were noted in TC, HDL-C, HDL2-C and HDL3-C between E<sub>2/3</sub> patients and control subjects (Table 2).

In E<sub>3/3</sub> patients with gallstones, the HDL-C (0.89 mmol/L), HDL2-C (0.49 mmol/L) and HDL3-C (0.39 mmol/L) were significantly decreased as compared with that in E<sub>3/3</sub> control (1.28 mmol/L, *P*<0.05; 0.73 mmol/L *P*<0.001; and 0.55 mmol/L, *P*<0.001). LDL-C and VLDL-C showed no difference in both groups (Table 2). E<sub>3/3</sub> female patients had lower levels of HDL-C (0.82 mmol/L), HDL2-C (0.46 mmol/L) and HDL3-C (0.36 mmol/L) than E<sub>3/3</sub> female controls (1.33 mmol/L, *P*<0.001; 0.77 mmol/L, *P*<0.01; and 0.57 mmol/L, *P*<0.01). Serum lipid levels were not changed in E<sub>3/3</sub> male patients and controls (Table 3).

LDL-C increased (1.92 mmol/L) and VLDL-C decreased (0.42 mmol/L) in E<sub>3/4</sub> patients with gallstones as compared with E<sub>2/3</sub> patients (LDL-C-1.41 mmol/L, VLDL-C-0.68 mmol/L) and E<sub>3/3</sub> patients (LDL-C 1.87 mmol/L, VLDL-C 0.46 mmol/L), but the differences were not significant. No obvious changes occurred in TC or HDL-C and its subforms among E<sub>2/3</sub>, E<sub>3/3</sub> and E<sub>3/4</sub> patients with gallstones (Table 2).

**Table 2 Comparisons of lipid levels in E<sub>2/3</sub>, E<sub>3/3</sub>, E<sub>3/4</sub> both gallstone patients and controls**

Lipids (mmol/L)	E <sub>2/3</sub>		E <sub>3/3</sub>		E <sub>3/4</sub>	
	Patients (n=10)	Controls (n=5)	Patients (n=69)	Controls (n=37)	Patients (n=8)	Controls (n=6)
TG	1.43 ± 0.35 <sup>a</sup>	1.06 ± 0.10	0.97 ± 0.21	0.64 ± 0.44	1.11 ± 0.33	0.92 ± 0.16
TC	2.99 ± 0.65	2.52 ± 0.53	3.14 ± 0.59	3.67 ± 0.76	3.94 ± 0.45	3.62 ± 0.63
LDL-C	1.41 ± 0.56 <sup>a</sup>	2.04 ± 0.16	1.87 ± 0.49	2.43 ± 0.67	1.92 ± 0.64	2.46 ± 0.32
VLDL-C	0.68 ± 0.26 <sup>a</sup>	0.48 ± 0.20	0.46 ± 0.20	0.30 ± 0.11	0.42 ± 0.13	0.44 ± 0.10
HDL-C	0.95 ± 0.23	1.02 ± 0.15	0.89 ± 0.30 <sup>a</sup>	1.28 ± 0.23	0.86 ± 0.21	0.90 ± 0.36
HDL2-C	0.53 ± 0.13	0.62 ± 0.22	0.49 ± 0.18 <sup>b</sup>	0.73 ± 0.13	0.44 ± 0.19	0.55 ± 0.18
HDL3-C	0.42 ± 0.12	0.56 ± 0.28	0.39 ± 0.12 <sup>b</sup>	0.55 ± 0.11	0.40 ± 0.13	0.46 ± 0.12

<sup>a</sup>*P*<0.05, <sup>b</sup>*P*<0.01, vs controls; *F* test.

**Table 3 The comparisons of lipid levels in E<sub>3/3</sub> same gender either gallstone patients or controls**

Lipids (mmol/L)	Male		Female	
	Patients (n = 31)	Controls (n = 20)	Patients (n = 38)	Controls (n = 17)
TG	0.85 ± 0.50	0.53 ± 0.22	1.10 ± 0.30	0.72 ± 0.57
TC	3.05 ± 0.44	0.41 ± 0.57	3.23 ± 0.85	3.87 ± 0.63
LDL-C	1.86 ± 0.68	2.71 ± 0.49	1.89 ± 0.86	2.20 ± 0.56
VLDL-C	0.40 ± 0.24	0.25 ± 0.10	0.52 ± 0.14	0.35 ± 0.17
HDL-C	0.94 ± 0.33	1.21 ± 0.28	0.82 ± 0.27 <sup>b</sup>	1.33 ± 0.19
HDL2-C	0.52 ± 0.22	0.69 ± 0.16	0.46 ± 0.15 <sup>b</sup>	0.77 ± 0.10
HDL3-C	0.42 ± 0.12	0.52 ± 0.13	0.36 ± 0.12 <sup>b</sup>	0.57 ± 0.10

<sup>b</sup>P<0.01, vs controls, F test.

## DISCUSSION

E<sub>2/3</sub>, E<sub>3/3</sub>, and E<sub>3/4</sub> are three common apolipoprotein E gene phenotypes, accounting for more than 50%, E<sub>2/4</sub> and E<sub>4/4</sub> for less than 6.2%<sup>[12]</sup>. In the present study, only 2 E<sub>2/4</sub> phenotype cases were detected in control, and no E<sub>2/2</sub> and E<sub>4/4</sub> homozygotes were found in both groups. The results show that ε2 and ε4 alleles resulting from the inheritary variations of apoE gene existed mainly in heterozygous way in population.

There were racial differences in the distribution of apoE alleles and phenotypes. In this study and Wang's literature<sup>[13]</sup>, the frequencies of E<sub>3/3</sub> phenotype were 85%-86% in healthy Chinese people, but 75% in Finnish people. Frequencies of ε4 were lower in Chinese people (8%-9%) than 20% in the Finnish (20%). The frequencies of E<sub>3/3</sub> phenotype in Chinese patients with gallstones were 79.3% as compared with 62.2% in Finnish, and E<sub>3/4</sub> phenotype in Chinese patients with gallstones were 9.2% but 28.9% in Finnish<sup>[14]</sup>. Kambath<sup>[15]</sup> also reported that there may be some variations of apoE allele and phenotype in different regional population from western to oriental countries.

Patients of different apoE phenotype with gallstones had different characteristics of dyslipidemia. Higher mean serum TG, VLDL-C levels and lower mean LDL-C levels were found in E<sub>2/3</sub> patients. The E<sub>3/3</sub> patients, especially in women, had markedly lower concentrations of HDL-C, HDL2-C and HDL3-C, while E<sub>3/4</sub> patients had only slight lower levels of VLDL-C and higher levels of LDL-C as compared with the E<sub>2/3</sub> and E<sub>3/3</sub> patients with gallstones.

The difference in the changes of serum lipid levels in different apoE phenotype patients with gallstone may be associated with apoE locus gene polymorphisms. E2, E3 and E4 isoproteins resulted from the single amino acid interchange between 112 site cysteine and 118 site arginine, E3 with cysteine at 112 site and arginine at 18 site, E2 with cysteine and E4 with arginine at either 112 site or 118 sites. Because of arginine bearing positive charge, E4 possessed more than one charge, the activity of receptor-binding to apoE-contained lipoprotein was stronger than E3. On the contrary, E2 possessed less than one charge, the activity of receptor-binding was lower<sup>[1-3]</sup>. Accordingly, ε2 allele

predisposes to serum triglyceride elevation<sup>[7]</sup>, the correlative change to serum lipid levels can be found in E<sub>2/3</sub> patients with gallstones in this study. ε4 allele was responsible for the increase of serum cholesterol<sup>[16]</sup>, but in E<sub>3/4</sub> phenotype patients, the increments of VLDL-C had no statistical difference, this may be associated with the low frequency of ε4 allele in population.

E<sub>3/3</sub> phenotype is putative normal type, but the E<sub>3/3</sub> patients with gallstones possessed the low level of HDL-C and its subforms as well. The changes may be related to other pathogenesis except apoE polymorphisms<sup>[17]</sup>. The results suggest that cholecystolithiasis may be a multigenic disease but not a monogenic one.

This study demonstrates that patients of different apoE phenotype with gallstones possess different dyslipidemia. The average level of serum lipids are much higher in patients with gallstones than that in non-gallstone subjects in the same apoE phenotype population. ε2 allele is likely one of the high-risk factors in the lithogenesis of cholecystolithiasis.

## REFERENCES

- Weisgraber KH. Apolipoprotein E distribution among human plasma lipoproteins: role of the cysteine-arginine interchange at residue 112. *J Lipid Res*, 1990;31:1503-1511
- Gajra B, Candlish JK, Saha N, Heng CK, Soemantri AG, Tay JS. Influence of polymorphisms for apolipoprotein B (ins/del, Xba I, EcoR I) and apolipoprotein E on serum lipids and apolipoproteins in a Javanese population. *Genet Epidemiol*, 1994;11:19-27
- Miettinen TA. Impact of apoE phenotype on the regulation of cholesterol metabolism. *Ann Med*, 1992;23:181-186
- Rall SC Jr, Mahley RW. The role of apolipoprotein E genetic variants in lipoprotein disorders. *J Intern Med*, 1992;231:653-659
- Walden CC, Hegele RA. Apolipoprotein E in hyperlipidemia (comments). *Ann Intern Med*, 1994;120:1026-1036
- Lenzen HJ, Assmann G, Buchwalds R, Schulte H. Association of apolipoprotein E polymorphism, low-density lipoprotein cholesterol, and coronary artery disease. *Clin Chem*, 1986;32:778-781
- Ukkola O, Kervinen K, Salmela PI, Von Dickschhoff K, Laakso M, Kesaniemi YA. Apolipoprotein E phenotype is related to macro and microangiopathy in patients with non-insulin-dependent diabetes mellitus. *Atherosclerosis*, 1993;101:9-15
- Johnston DE, Kaplan MM. Pathogenesis and treatment of gallstones. *New Eng J Med*, 1993;116:412-421
- Carey MC. Pathogenesis of gallstones. *Am J Surg*, 1993;165:410-419
- Hixson JE, Vernier DT. Restriction isotyping of human apolipoprotein E by gene amplification and cleavage with Hha I. *J Lipid Res*, 1990;31:548
- Friedewald WT, Levy RI, Friedrickson DS. Low-density lipoprotein cholesterol estimation of the concentration of in plasma without use of the preparative ultracentrifuge. *Clin Chem*, 1972;18:499-502
- Wilson PW, Myers RH, Larson MG, Ordovas JM, Wolf PA, Schaefer EJ. Apolipoprotein E alleles, dyslipidemia, and coronary heart disease. The Framingham offspring study. *JAMA*, 1994;272:1666-1671
- Wang KQ, He JL, Xie YH. Studies on human apolipoprotein E genetic isoform and their phenotypes among the Chinese population. *Proc CAMS and PUMC*, 1987;2:133-139
- Juononen T, Kervinen K, Kairaluoma MI, Lajunen LH, Kesaniemi YA. Gallstone cholesterol content is related to apolipoprotein E polymorphism. *Gastroenterology*, 1993;104:1806-1813
- Kamboh MI, Aston CE, Ferrell RE, Hamman R. Impact of apolipoprotein E polymorphism in determining interindividual variation in total cholesterol and low density lipoprotein cholesterol in Hispanics and non-Hispanic whites. *Atherosclerosis*, 1993;98:201-211
- Jikkanen MJ, Huttunen JK, Ehnholm C, Pietidnen. Apolipoprotein E4 homozygosity predisposes to serum cholesterol elevation during high fat diet. *Arteriosclerosis*, 1990;10:285-288
- Juononen T, Savolainen MJ. ApoA1 and cholesteryl ester protein gene loci in patients with gallbladder disease. *J Lipid Res*, 1995;36:80

Edited by MA Jing-Yun



# Studies on the flow and distribution of leukocytes in mesentery microcirculation of rats \*

JIANG Yong, LIU Ai-Hua and ZHAO Ke-Seng

**Subject headings** microcirculation; leukocyte; leukocyte-endothelium interaction; mesentery

## Abstract

**AIM** To study the effect of leukocyte-endothelium interaction (LEI) on the flow and distribution of leukocytes in microcirculation under physiological condition.

**METHODS** A microcirculation image multiple parameter computer analysis system (MIMPCAS) was used to study the flow and distribution of leukocytes in mesentery microcirculation of rats *in vivo*.

**RESULTS** The difference of visible leukocyte flux (VLF) was as high as 131 times in the arterioles and venules with similar diameter and blood velocity. The visible leukocytes rolled along the blood vessel wall as a "jerky" movement. The frequency distribution of the visible leukocyte velocity (VLV) showed a "two-peak" curve. The low peak value was on 10  $\mu\text{m/s}$ -15  $\mu\text{m/s}$  while the high peak fell between 25  $\mu\text{m/s}$ -30  $\mu\text{m/s}$ . With the increase of diameter of venules, VLF increased while the VLV remained at the same level. With the increase of RBC velocity, VLV trends to elevate and VLF to fall down.

**CONCLUSION** The results herein might provide a basic theory for the study on the mechanism of LEI under physiological condition and novel methods for the prevention and treatment of high LEI in many pathological processes.

Chinese PLA Key Laboratory for Shock and Microcirculation, The First Military Medical University Guangzhou 510515, China  
Dr. JIANG Yong, male born on 1964-10-25 in Henan Province, graduated and got a Ph.D. degree from the Academy of Military Medical Sciences in 1997, now professor of pathophysiology, majoring shock and cellular signal transduction, having more than 50 papers published in international or national major journals.

\*Project supported by National Natural Science Foundation of China, No. 39270852.

**Correspondence to:** Dr JIANG Yong, Chinese PLA Key Laboratory for Shock and Microcirculation, The First Military Medical University, Guangzhou 510515, China.

Tel. +86 • 20 • 85148376, Fax. +86 • 20 • 87705671

Received 1999-01-20

## INTRODUCTION

Leukocyte-endothelium interaction (LEI) exists in many pathophysiological processes, such as inflammation, burns, tumor and shock<sup>[1,2]</sup>. In the recent two decades, quantitative studies on the interaction of leukocyte-endothelium have been carried out and the change of the flow and distribution of leukocytes is the basis for the abnormal increase of LEI<sup>[3-5]</sup>. High level LEI would bring about the blockage of blood vessels and decrease of blood perfusion<sup>[6,7]</sup>. Therefore, it is important to study the flow and distribution of leukocytes in microcirculation. We used a microcirculation image multiple parameter computer analysis system (MIMPCAS)<sup>[4]</sup> to study the characteristic of the flow and distribution of leukocytes in mesentery microcirculation of rats, and analyzed its influencing factors.

## MATERIALS AND METHODS

Five Sprague-Dawley rats were anesthetized with a mixture of 133 g/L urethane and 10 g/L chloralose (6 mL/kg, im)<sup>[4]</sup>. The abdomen of rats was open by the incision on the midline under the xiphoid. Small intestinal loops were pulled out and the mesentery was mounted on a hollowed transparent pedestal for observation. The specimen was suffused with a balanced 37°C Krebs's solution to maintain relatively normal condition in temperature and environment.

An Olympus microscope with a halogen lamp and Leitz long distance lens (20 × ) was used to observe the third order arterioles and venules. Being transmitted through a low-light level camera of model 1319, the signal was displayed on a Hitachi color monitor. A JVC recorder was used for off line measurement. Each specimen was recorded no more than 30 minutes so as not to affect the mesentery microcirculation<sup>[3]</sup>. The MIMPCAS was used to measure the diameter (D) of blood vessels, the velocity of red blood cells (V<sub>rbc</sub>), the visible leukocyte velocity (VLV), the visible leukocyte flux (VLF) and the adhesive leukocyte count (ALC) following the procedure described previously<sup>[4]</sup>.

The following formula was used to calculate the parameters of microcirculation<sup>[4,6,9]</sup>: 1. mean blood velocity,  $V_{\text{mean}} = V_{\text{rbc}}/1.6$ ; 2. flow volume of blood,

$F = V_{\text{mean}} \times \pi \times D^2/4$ ; 3. shear rate,  $\dot{\gamma}_w = 8 \times (V_{\text{mean}}/D)$ ; 4. total leukocyte flux,  $\text{TLF} = (60 \times F) \times K \times 10^{-6}$ ,  $K$  is the amount of leukocytes in the blood<sup>[7]</sup>; 5. invisible leukocyte flux,  $\text{ILF} = \text{TLF} - \text{VLF}$ .

The results were represented by mean  $\pm$  standard deviation ( $\bar{x} \pm s$ ) and the significance of difference was judged by Student's  $t$  test.

## RESULTS

### *Leukocytes flow and distribution in microcirculation of rat mesentery under physiological condition*

Twenty arterioles with a diameter between 11  $\mu\text{m}$ -45  $\mu\text{m}$  were selected for observation. Only one leukocyte rolled along the wall and there was no leukocyte sticking on it in the third order arterioles. In the 20 capillaries with an average diameter of  $6.3 \mu\text{m} \pm 1.7 \mu\text{m}$ , the visible leukocyte flux was  $0.2 \text{ cells/min} \pm 0.4 \text{ cells/min}$  and there were no plugging leukocytes. In the 20 venules with a diameter of 10  $\mu\text{m}$ -50  $\mu\text{m}$ , the visible leukocyte flux was  $13.3 \text{ cells/min} \pm 7.2 \text{ cells/min}$  and there were about  $0.3 \pm 0.3$  leukocytes sticking on the wall within a length of 94  $\mu\text{m}$  of blood vessels (Table 1). Under the physiological condition, the flow and distribution of leukocytes in different blood vessels varies to a large extent. The visible leukocyte flux (VLF) differed significantly between the venules and arteries with comparable diameter and blood velocity and the value of VLF in venules was as high as 131 times that of arterioles. Due to the interaction of leukocyte and endothelium which mainly occurred in venules, further studies were carried out on the flow and distribution of leukocytes in mesentery venules.

**Table 1** The flow and distribution of leukocytes in the mesentery microvasculature of rats under physiological condition

	Arteriole	Capillary	Venule
Number	20	20	20
D( $\mu\text{m}$ )	$22.6 \pm 9.1$	$6.3 \pm 1.7$	$25.1 \pm 10.6$
Vmean(mm/s)	$1.07 \pm 0.3$	$0.45 \pm 0.12$	$0.86 \pm 0.27$
Flow(pL/s)	$440.1 \pm 439.2$	$14.1 \pm 6.7$	$430.7 \pm 412.4$
$\dot{\gamma}_w(\text{s}^{-1})$	$371.1 \pm 212.8$	$570.4 \pm 189.7$	$272.1 \pm 189.2$
TLF(cells/min)	$91.1 \pm 90.9$	$2.9 \pm 1.4$	$89.2 \pm 85.4$
VLF(cells/min)	$0.1 \pm 0.2^b$	$0.2 \pm 0.4$	$13.1 \pm 7.2^b$
ILF(cells/min)	$91.0 \pm 90.9$	$2.7 \pm 1.3$	$76.1 \pm 77.8$
ALC(cells/94 $\mu\text{m}$ )	0	0	$0.3 \pm 0.3$

<sup>b</sup> $P < 0.01$ ,  $t = 8.07$ .

### *The characteristic of the flow and distribution of visible leukocytes*

**The space characteristic of the flow and distribution of visible leukocytes** Ten sampling lines on vessel with equal distance were set perpendicular to the longitudinal

vessel and the velocity of leukocyte passing through each line was measured. The variation of the velocity of leukocyte reflected the characteristic of its temporal distribution. Each leukocyte passing through the sampling lines with a large variation on velocity suggested that leukocyte rolling along the wall of blood vessels took a "jerky" movement (Figure 1). However, the average velocity for a leukocyte passing through a vessel with a definite length was similar, about 20  $\mu\text{m/s}$ .

**The time characteristic of the flow and distribution of visible leukocytes** For the measurement, one line was set on a third order venule (D: 37  $\mu\text{m}$ ) of mesentery of rat. The velocity and flux of all the visible leukocytes passing the measuring line were determined in 10s as one unit, and measurements were continuously performed 6 times in 1 minute. It was found that visible leukocyte velocity and visible leukocyte flux changed temporarily (Figure 2).

**Frequency distribution of VLV** The velocities of 400 visible leukocytes in 30 third branch venules were measured, of which the frequency distribution is shown in Figure 3. The frequency distribution of VLV presented with the characteristic of double peaks. Low peak value was about 10  $\mu\text{m/s}$ -15  $\mu\text{m/s}$  while the high peak was around 25  $\mu\text{m/s}$ -30  $\mu\text{m/s}$ . Leukocytes with velocity below 5  $\mu\text{m/s}$  or above 50  $\mu\text{m/s}$  were rarely found.

### *The influence of vessel diameter and blood velocity on the flow and distribution of leukocytes*

Visible leukocyte flux and visible leukocyte velocity were measured in 20 capillaries of mesentery of rats. Eight venules with similar blood velocity (Vrbc:  $1.2 \text{ mm/s} \pm 0.1 \text{ mm/s}$ ) and vessel diameter (D: 10  $\mu\text{m}$ -50  $\mu\text{m}$ ) were selected for the observation of influence of vessel diameter on the flow and distribution of leukocytes. It was found that with the increase of blood vessel diameter, visible leukocyte flux increased while visible leukocyte velocity remained relatively stable. Twelve venules with similar diameter ( $31.5 \mu\text{m} \pm 1.1 \mu\text{m}$ ) were selected for the observation of the influence of blood velocity on the flow and distribution. The blood velocity in these vessels ranged from 0.27 mm/s to 1.38 mm/s. Following the increase of Vrbc, visible leukocyte velocity increased while visible leukocyte flux decreased as shown in Figure 4.

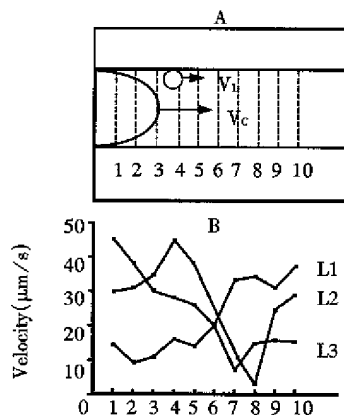


**Figure 1** Leukocytes rolling along the blood vessel wall showed a “jerky” movement. (A. Multiple sampling scheme for the velocity determination used by MIMPCAS; B. Three leukocytes passed through 10 sampling lines with a large variation of velocity.)

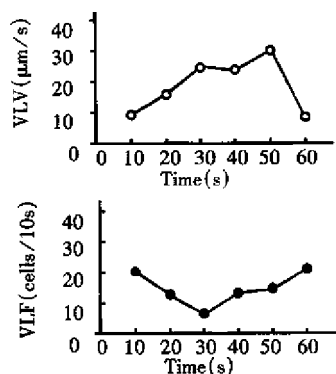


**Figure 2** The time-dependent changes of VLV and VLF in the third order venules of rat mesentery.

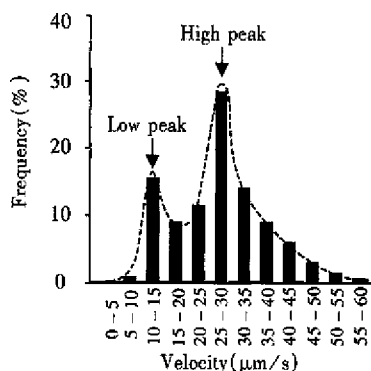


**Figure 3** The frequency histogram of VLV.

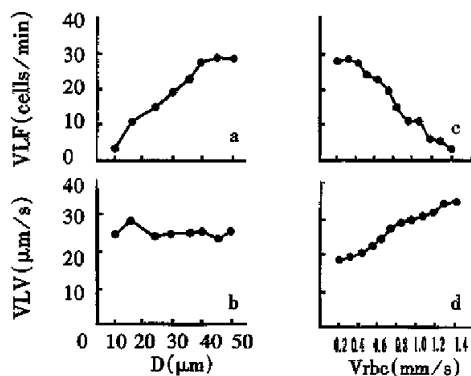


**Figure 4** Effect of vessel diameter and red blood cell velocity on the flow and distribution of visible leukocytes in the venules of rats.

## DISCUSSION

Recently, wide interest has been shown in the research of leukocyte-endothelium interaction. Studies on the rheological behavior of leukocytes in the microcirculation have promoted the understanding on the mechanism of cellular adhesion. These studies mainly involved two aspects, i.e., one is the interaction between leukocytes and red blood cells and the other is that between leukocytes and endothelial cells<sup>[6,7]</sup>.

It was found in this study that leukocytes scarcely rolled on the wall or firmly stuck in arterioles. Under normal condition, sticking leukocytes in venules were rarely observed while some leukocytes rolled along the vessel wall in the marginal stream, suggesting that the flow and distribution of leukocyte in venules and arterioles was significantly different. There exist some interactions between leukocytes and endothelium in venules, for which the major phenomenon is the leukocytes rolling on the endothelium of venule wall. The development of leukocyte rolling and sticking on endothelium depends on two forces: leukocyte-endothelium adhesive forces and hemodynamic dispersal forces, i.e., shear stress<sup>[1,8]</sup>. Mayrovitz had suggested that the adhesion of leukocytes on the vessel wall might be mainly related to shear stress, for the adhesion of leukocytes existed on the wall of post-capillary venules<sup>[7]</sup>. However, the results herein showed that VLV varied to a large extent even in the arterioles and venules with a similar shear stress, suggesting that under physiological condition the difference of leukocyte flow and distribution in different vessels mainly came from the characteristic of endothelial cells and the micro-environment around leukocytes<sup>[9]</sup>.

The rolling of leukocytes along the walls presented with an uneven “jerky” movement. The balance between adhesive forces and dispersal forces was broken by the non-homogeneity of endothelium and that of hemodynamic forces, which brought about the rolling of leukocytes with the characteristic of non-stable speed<sup>[3,8,10]</sup>. The factors that influence homogeneity of endothelium include non-even surface of endothelium, local characteristic of endothelium, surface distribution of charge, the concentration of reactive substances, etc., while that for hemodynamic force, were temporal variation of blood velocity and local concentration of red blood cells. The results from the analysis on the frequency of VLV showed that the rolling leukocytes with a velocity lower than 10  $\mu\text{m/s}$  had a potential to stick on the endothelium of blood vessels, while the rolling leukocytes with

a speed higher than 30  $\mu\text{m/s}$  tended to merge into the central stream of blood. The two peaks of the distribution of VLV suggested that there were at least two kinds of adhesive molecules with different property, by which two different velocities of leukocyte rolling along the walls were mediated. However, the adhesive molecules involved in the leukocyte-endothelium interaction are waiting to be identified and it is also necessary to pay more attention to the study on the mechanism of cellular adhesion.

In this study, the impact of diameter of blood vessels and blood flow of venules on the flow and distribution of leukocytes was analyzed. The diameter of blood vessels were found to have a significant effect on the flow and distribution of leukocytes. In the blood vessels with a larger diameter, visible leukocyte flux (VLF) increased significantly, but the visible leukocyte velocity (VLV) kept stable. Atherton had suggested that the temporal contact between leukocyte and endothelium should be taken as an inelastic collision<sup>[3]</sup>. The increase of adhesion force would bring about more chances of random collision and higher degree of inelastic collision between leukocytes and endothelium. Visible leukocyte flux mainly reflects the random collision between leukocyte and endothelium, while visible leukocyte velocity indicates the degree of inelastic collision. In the larger vessels, the leukocyte flux and the area of endothelium are also larger, so the random contact chances increase to bring about high flux of visible leukocyte. The change of diameter would not impact the adhesion force, so visible leukocyte velocity was the same.

Given a certain extent of blood viscosity, shear stress is determined by blood velocity under the condition of definite vessel diameter<sup>[2,6,8,10]</sup>. The

shear stress is high in the blood vessels with fast flow of blood, which will reduce the chance of collision between leukocyte and endothelium. Therefore in the vessels with fast blood flow, visible leukocyte flux is low while visible leukocyte velocity is high.

In summary, the flow and distribution of leukocytes in the mesentery microcirculation of rats was studied *in vivo*, and the influential factors on which were explored under normal conditions. The result of this study is helpful for the understanding of the mechanism for leukocyte endothelium interaction in physiological state and provides theoretic basis for the study and treatment of increased LEI in pathological processes.

## REFERENCES

- 1 Harlan JM. Leukocyte-endothelial interactions. *Blood*, 1985;65: 513-525
- 2 Zhao K, Wu KY, Zhu ZJ, Huang XL. The role of leukocyte in the disorder of microcirculation during shock. *Natl Med J Chin*, 1986; 66:722-725 (Chin)
- 3 Atherton A, Born GVR. Quantitative investigations of the adhesiveness of circulating polymorphonuclear leukocytes to blood vessel walls. *J Physiol (Lond)*, 1972;222:447-474
- 4 Jiang Y, Zhao KS, Li SX. Computer assisted analysis of leukocyte rheological behavior in microvasculature. *Chin Med J*, 1993;106: 883-888
- 5 Zentl H, Sack FU, Intaglietta M, Messmer K. Computer assisted leukocyte adhesion measurement in intravital microscopy. *Int J Microcirc: Clin Exp*, 1989;8:293-302
- 6 House SD and Lipowsky HH. Leukocyte-endothelium adhesion: microhemodynamics in mesentery of the cat. *Microvasc Res*, 1987; 34:363-379
- 7 Mayrovitz HN, Kang SJ, Herscovici B, Sampsel RN. Leukocyte adherence initiation in skeletal muscle capillaries and venules. *Microvasc Res*, 1987;33:22-34
- 8 Zhao KS. Cytorheology-A new project for shock research. *Med J Chin PLA*, 1986;11:137-139 (Chin)
- 9 Schmid-Schibein GW, Usami S, Skalak R, Chen S. The interaction of leukocytes and erythrocytes in capillary and postcapillary vessels. *Microvasc Res*, 1980;19:45-70
- 10 Jones DA, Smith CW, and McIntire LV. Effect of fluid shear stress on leukocyte adhesion to endothelium cells. In: Granger DN and Schmid-Schonbein GW, eds. Physiology and pathophysiology of leukocyte adhesion. 1st ed. New York: Oxford University Press, 1995:148-168

Edited by MA Jing-Yun

# Study on the quality of recombinant proteins using matrix-assisted laser desorption ionization time of flight mass spectrometry \*

ZHOU Guo-Hua<sup>1</sup>, LUO Guo-An<sup>1</sup>, SUN Guo-Qing<sup>2</sup>, CAO Ya-Cheng<sup>2</sup> and ZHU Ming-Sheng<sup>3</sup>

**Subject headings** recombinant proteins; molecular weight; flight mass spectrometry; erythropoietin tryptic digests

## Abstract

**AIM** To study the possibility of matrix-assisted laser desorption/ionization time of flight mass spectrometry (MALDI-TOF MS) for controlling the quality of recombinant proteins.

**METHODS** By using MALDI-TOF MS, the molecular weights and purity of recombinant bioactive proteins were analyzed.

**RESULTS** The molecular weights and purity were obtained in nine recombinant bioactive proteins, including interleukin 2, tumor necrosis factor  $\alpha$ , granulocyte-macrophage colony stimulating factor, interferon  $\alpha 2b$ , interferon  $\alpha 1$ , erythropoietin, calmodulin and its fragment, and neuronal nitric oxide synthase were obtained. MALDI-TOF MS was also used to assay specific proteins in the mixtures and to characterize the erythropoietin tryptic digests.

**CONCLUSION** The results showed that MALDI-TOF MS can be employed for the effective quality control of recombinant proteins.

## INTRODUCTION

Since Hillenkamp *et al*<sup>[1]</sup> first introduced matrix-assisted laser desorption/ionization time of flight mass spectrometry (MALDI-TOF MS) to analyze proteins with molecular masses greater than Mr 10 000, MALDI-TOF MS has been widely used to study different classes of biomolecules such as proteins, oligonucleotides, polysaccharides and polymers<sup>[2-5]</sup>. Compared to the traditional techniques, such as sodium dodecyl sulfate polyacrylamide gel electrophoresis (SDS-PAGE), MALDI-TOF MS has several advantages in the determination of protein molecular weight (Mr), peptide mapping, and purity.

In the present report, MALDI-TOF MS was used to accurately determine the Mr and purity of nine biological samples including recombinant bioactive proteins, such as: interleukin-2 (IL-2), interferon- $\alpha 2b$  (IFN $\alpha 2b$ ), interferon- $\alpha 1$  (IFN $\alpha 1$ ), erythropoietin (EPO), granulocyte-macrophage-colony stimulating factor (GM-CSF), tumor necrosis factor  $\alpha$  (TNF $\alpha$ ), calmodulin (CaM) and its fragment, and neuronal nitric oxide synthase (nNOS). In addition, the protein mixtures and EPO peptide mapping were characterized by the technique.

## MATERIALS AND METHODS

### Materials

**Chemicals** 3,5-dimethoxy-4-hydroxycinnamic acid (Sinapinic acid), 2,5-dihydroxybenzoic acid (DHB) and acetonitrile were produced by Sigma (St. Louis, USA). Trifluoroacetic acid (TFA) was from Merk-Schuchardt. Ammonium hydrogencarbonate, acetic acid and ethanol were produced by Nanjing Chemical Reagent Plant (Nanjing, China). All water used in the experiment was ultra high quality produced by a Milli-Q Plus Ultra Pure Water System.

**Proteins** Horse heart myoglobin, carbonic anhydrase B,  $\beta$ -lactoglobulin, bovine serum albumin and trypsin were obtained from Sigma (St. Louis, USA). IL-2 (*E.coli*), IFN $\alpha 1$  (Silkworm cell), GM-CSF (*E.coli*), IFN $\alpha 2b$  (*E.coli*), EPO (CHO), nNOS, and CaM and its fragments were supplied by the East China Institute for Medicine and Biotechnology (Nanjing, China).

<sup>1</sup>Department of Chemistry, Tsinghua University, Beijing 100084 Beijing, China

<sup>2</sup>Institute of Soil Science, Chinese Academy of Sciences, Nanjing 210018, Jiangsu Province, China

<sup>3</sup>Huadong Research Institute for Medicine and Biotechnics, No. 293 Zhongshan East Road, Nanjing 210002, Jiangsu Province, China.

Dr. ZHOU Guo-Hua, male, born on 1964-12-03 in Nantong County, Jiangsu Province, Han nationality, graduated from Tsinghua University as a Ph.D graduate in 1998, associate professor of Pharmacy, majoring in drug analysis, having 30 papers published.

\*Supported by the National Natural Science Foundation of China, No. 692350220.

**Correspondence to:** Prof. LUO Guo-An, Department of Chemistry, Tsinghua University, Beijing 100084 Beijing, China

Tel. +86 • 10 • 62784764 or +86 • 25 • 4540665, Fax. +86 • 10 • 62784764 or +86 • 25 • 4541183

Email: galuo@sam.chem.tsinghua.edu.cn or GHZHOU@publicl.ptt.js.cn

Received 1999-01-04

## Methods

**Tryptic digestion of EPO** Approximately 200 µg EPO protein was lyophilized and dissolved in 200 µL 1% ammonium bicarbonate (pH 8.5). Trypsin protease was added to the solution which was incubated at 37°C for 16h in a substrate: enzyme ratio of 50:1 (w:w). The digestion was quenched by storing the sample at -70°C. The sample was lyophilized and reconstituted in 50 µL 10% acetic acid before use.

**MALDI-TOF MS** Analyses were performed on a Finnigan Laser MAT 2 000 time-of-flight mass spectrometer (Finnigan MAT, Hemel Hempstead, Herts, UK). The system used a nitrogen laser (337 nm, 2 ns pulse) to desorb ions from the sample specimen. The desorbed ions were accelerated to 20kV into a free long tube. The time recorded for a molecule to travel the length of the tube to a detector was proportional to the mass of the ion, which was its molecular weight. All spectra were obtained using the positive-ion mode. Standard stainless-steel targets (with a sample application area of about 3.14 mm<sup>2</sup>) obtained from the manufacturer were employed for all analyses. The lasermat software allowed the user to irradiate one of the four possible target regions or quadrants of about 0.02 mm<sup>2</sup>. The spectra in this study were calibrated using instrumental calibration, based on the parameters determined from analysis of a number of standard proteins and peptides.

**Sample preparation for MALDI-TOF MS determination** The samples of each protein were prepared to 0.8 g/L-1.0 g/L in dilute TFA (0.05%, 0.09 mol/L sinapinic acid in acetonitrile-ethanol-water(60:4:36, v/v/v) was used as protein matrix and 0.1 mol/L 2,5-dihydroxybenzoic (DHB) in formic acid-water (9:1, v/v) was used as peptide matrix. The matrix solution was kept in the dark and prepared fresh every few days.

The samples for mass spectrometric analysis were mixed with the matrix in an Eppendorf tube. Typically, 5 µL of sample solution was added to a tube containing 10 µL of matrix solution. The solution was stirred in a vortex mixer, and then approximately 0.5 µL of sample solution was applied to the target and followed by drying at room temperature and atmospheric pressure. For some protein samples in which the buffer contained salts at high concentrations, the dried sample/matrix preparation on the target was washed by depositing a droplet of cold distilled water for a few seconds on the sample spot surface to dissolve excess salt crystals, and followed by removing the droplet.

## RESULTS AND DISCUSSION

### *Mr measurement for purified proteins*

**Nonglycosylated proteins** The *M<sub>r</sub>* of recombinant proteins, IL-2, TNFα, GM-CSF, TNFα-2b, CaM fragments and nNOS expressed in *E.coli* were determined using MALDI-TOF MS. Table 1 shows the number of amino acids, theoretical *M<sub>r</sub>*, measured *M<sub>r</sub>* and relative determination error for these nonglycoproteins.

**Table 1** *M<sub>r</sub>* of non-glycoproteins measured by MALDI-TOF MS

Protein	Number of amino acids	Theoretical <i>M<sub>r</sub></i>	Measured <i>M<sub>r</sub></i>	Relative error (%)
IL-2	134 <sup>a</sup>	15478	15610	2.8
GM-CSF	127	14477	15451	5.56
TNF-α	158 <sup>a</sup>	17484	17517	0.18
nNOS	199 <sup>a</sup>	22248	22306	0.26
IFN-α2b	166 <sup>a</sup>	19378	19533	0.79
CaM fragment	95	10846	10851	0.05

<sup>a</sup>An additional methionine at the NH-2-terminal.

As table 1 shows, the *M<sub>r</sub>* relative error of the protein GM-CSF was 5.56%, which was much higher than the systematic error of the instrument. In addition, the peak in the GM-CSF mass spectrum was very sharp, indicating that the product was very pure. However, the results of Edman sequencing showed that there were 8 additional amino acids, MMKSDNSH, at the NH-2-terminus. The relative error was 0.12% when the 8 amino acids were added to the regular GM-CSF amino acid sequence. The relative errors of interleukin-2 and interferon α2b were approximately 0.8%. The increased mass was approximately equal to the *M<sub>r</sub>* of an amino acid, which may have been added during the modifications, such as phosphorylation and cystinylation. The details were not achieved in the present report. An asymmetric single charged peak was observed in the interferon α2b mass spectrum (Figure 1), with an unresolved impurity peak on the left side that could be seen when the mass spectrum was amplified partially. This may be caused by partially removing N terminal methionine residue in the interferon α2b.

**Glycosylated proteins** Proteins expressed in mammal cells are generally glycosylated. Because of the microheterogeneity of the carbohydrates, the final product is a complicated heterogeneous mixture. In some cases, the functions of the biomolecules depend on the carbohydrate components<sup>[11,12]</sup>. For example, recombinant human erythropoietin will lose its *in vivo* bioactivity without sialic acid residues<sup>[13,14]</sup>. Thus, it is very important to characterize the carbohydrate parts in glycoproteins<sup>[15,16]</sup>. In this article, MALDI-TOF MS



was used to determine  $M_r$  and carbohydrate percentages of erythropoietin (EPO) and interferon  $\alpha 1$  (Table 2).

**Table 2**  $M_r$ s of glycoproteins measured by MALDI-TOF MS

Protein	Number of amino acids	Measured $M_r$	Carbohydrate content (%)
EPO	166	28 707	35.6
IFN $\alpha 1$	166	20 465	5.2

As can be seen in Figure 2, the half-intensity-width of EPO was much larger, indicating that EPO was a heterogeneous protein. The carbohydrate percentage was so high that electrospray mass spectrometry could not be employed to determine the heterogeneity. The  $M_r$  obtained using MALDI-TOF MS was 28 707, while the  $M_r$  obtained using the traditional SDS-PAGE technique was about 34 000. The mass difference of 5 293 suggested that SDS-PAGE could measure the apparent  $M_r$  of the glycoprotein with high carbohydrate content. Since the results of SDS-PAGE for the molecular weight were related to the gel concentration, the determination procedure was difficult to control. The degree of glycosylation for biomolecules expressed in silkworm cells was generally lower, with only 5.2% carbohydrates found in recombinant protein interferon  $\alpha 1$  by MALDI-TOF MS, which was consistent with theoretical calculations. The TOF mass spectra for EPO and IFN $\alpha 1$  showed that the half-intensity-widths were 8 000 and 3 000, respectively, much wider than that of nonglycoproteins in Table 1, Figures 4 and 5. Ordinarily the half-intensity-widths are produced by isotopes, and are no more than 500<sup>[17]</sup>. Therefore, half-intensity-widths of 500 in singly charged MS peaks may be employed as a simple criterion to evaluate the heterogeneity of glycoproteins. The MS peak width will increase as glycoprotein becomes more heterogeneous.

#### Determination of protein mixture

##### Mixture composed of known standard proteins

Methods used to analyze each component in multi-protein mixtures without tedious separation are of great value. The advantage of MALDI-TOF MS in multicomponent characterization is the ability to simultaneously determine the  $M_r$  of each ingredient during one scan. However, singly charged oligomers with multiply charged monomers and multiply charged oligomers would complicate the mass spectra. Peaks could be specified only according to their  $M_r$  and the number of charges.

Figure 3 shows the MALDI-TOF mass spectrum for mixed proteins composed of myoglobin from horse heart, carbonic anhydrase B,  $\beta$ -lactoglobulin

and bovine serum albumin. Both molecular ion and the multiply charged monomers or oligomers were observed. The  $M_r$  measurement accuracy for the four proteins was 0.0%, 0.04%, 0.12%, and 0.18%, respectively.

#### Determination of a specific protein in mixtures

The mass spectrum of *E. coli* expressed products containing calmodulin in Figure 4, showed a protein mixture containing a protein with an observed  $M_r$  of 16 934, together with a doubly charged monomer and a singly charged dimer, indicating that the mixture contained calmodulin with a theoretical  $M_r$  of approximately 17 000. In addition, the spectrum showed that there was very little singly charged dimer, because calmodulin seldom formed dimers.

#### Measurement of the purity of expressed products and the relative content of impurities

Since MALDI-TOF MS can give the  $M_r$  of all components in a mixture, the relative purity of the expressed product, along with the  $M_r$  of the impurity and its abundance, can be obtained from the mass spectrum. Figure 5 shows the mass spectrum of calmodulin fragment expressed in *E. coli* had small amounts of impurities with  $M_r$  of 9643.8 and 9074.0. In addition, few impurities were observed in the recombinant proteins, IL-2, TNF $\alpha$ , GM-CSF, IFN $\alpha 2b$ , nNOS, IFN $\alpha 1$  and EPO.

#### Characterization of tryptic peptide mapping for erythropoietin

The MALDI-TOF peptide mapping strategy has been used successfully to analyze proteins in enzymatic digests and has thus been applied to verify the primary structure of some proteins<sup>[18]</sup>. As a technique, it offers a number of advantages over conventional peptide mapping with HPLC since it reduces the actual analysis time and also provides a means of assigning peptide fragments from their respective  $M_r$ . Peptide mapping is the "fingerprint" of the protein, so it can be employed to rapidly identify the correctness of the primary structure of protein during expression or purification<sup>[19]</sup>. This report introduces the peptide map of recombinant human erythropoietin by MALDI-TOF MS. Protease trypsin can theoretically digest the erythropoietin into 21 peptide fragments, including three glycopeptide fragments and two disulfide bonds (one between fragments T<sub>1</sub> and T<sub>20</sub>, and another inside T<sub>5</sub>). The proteolytic digests were subjected directly to MALDI-TOF MS analysis without any prior purification. Figure 6 shows the mass spectrum of the tryptic digest with 13 peaks corresponding to peptide fragments. The observed mass values of the digests were consistent with the theoretical mass values as calculated from the amino acid sequence of rhEPO (Table 3). The mass value

of 1612.7 indicated the formation of a disulfide bond between  $T_1$  nor  $T_{20}$ , which was verified by the fact that neither  $T_1$  nor  $T_{20}$  was observed. Peptide mixtures generated by enzymatic digestion do not always allow for complete evaluation of peptide fragments by MALDI-TOF MS. As can be seen in Table 3, about 76.5% of the entire amino acid sequence was confirmed. In the lower mass range (below  $m/z$  400), analyte molecules could not be identified since the matrix peaks overlap with the signals from the analytes. In addition, the three glycosylated peptides were also not observed, because EPO was heterogeneous and the MS sensitivity to carbohydrates was much lower than that of peptides. Several matrices, including 2,5-dihydroxy benzoic acid (DHB), 2-aminobenzoic acid and  $\alpha$ -cyano-4-hydroxycinnamic acid, were tested to obtain the best resolution and sensitivity in the mass spectrum measurement. The results in Figures 6, 7 and 8, show that the best matrix was DHB, which produced large analytical signals with good resolution. The 2-aminobenzoic acid matrix gave signals with lower sensitivity and poorer resolution, but it was better than the  $\alpha$ -cyano-4-hydroxycinnamic acid matrix that is more suitable for "big" proteins rather than "small" peptides. The matrix concentration also affects the mass resolution and analyte signals. For example, with saturated DHB solution employed as the matrix, only two main peaks with mass values of about 480 and 2550 were obtained, possibly due to poor crystallization over the entire sample area in the target.

In general, the choice of MALDI-TOF matrix is very critical to the homogeneous crystallization and the homogeneous embedding of the analyte molecules in the matrix. In addition, the matrix is responsible for the high mass resolution and high analyte signals.

**Table 3** MALDI-TOF-MS analysis of the tryptic digests of EPO

rhEPO peptide	Position	Calculated mass value	Observed mass value	Relative mass value error (%)
$T_1$	1-4	439.5	440.5	0.23
$T_3$	11-14	515.6	517.8	0.39
$T_4$	15-20	735.9	735.5	-0.05
$T_5$	21-45	glycopeptide		
$T_6$	46-52	927.1	928.4	0.14
$T_7$	53	174.2		
$T_8$	54-76	2525.3	2525.5	0.01
$T_9$	77-97	glycopeptide		
$T_{10}$	98-103	601.7	600.8	-0.15
$T_{11}$	104-110	802.5	803.4	0.11
$T_{12}$	111-116	586.3	585.5	-0.14
$T_{13}$	117-131	glycopeptide		
$T_{14}$	132-139	923.0	923.5	0.05
$T_{15}$	140	146.2		
$T_{16}$	141-143	434.5	*	
$T_{17}$	144-150	898.0	899.1	0.12
$T_{18}$	151-152	203.2		
$T_{19}$	153-154	259.3		
$T_{21}$	163-166	447.4	*	
$T_2$ -S-S- $T_{20}$	1615.8	1612.7		-0.19

\*A wide unresolved peak caused by  $T_1$ ,  $T_{16}$  and  $T_{21}$ .

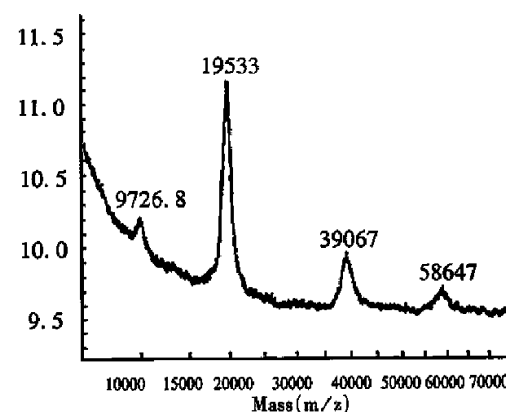


**Figure 1** MALDI-TOF mass spectrum of interferon  $\alpha 2b$  using sinapinic acid as matrix.

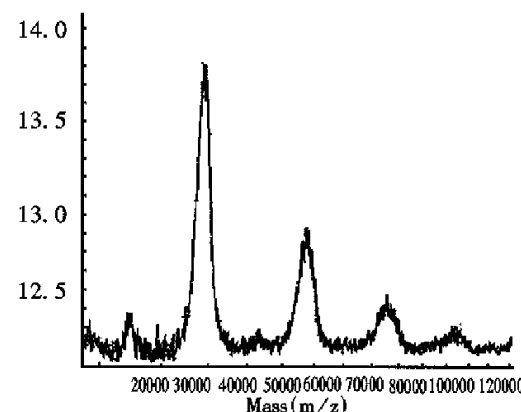


**Figure 2** MALDI-TOF mass spectrum of recombinant human erythropoietin using sinapinic acid as matrix.

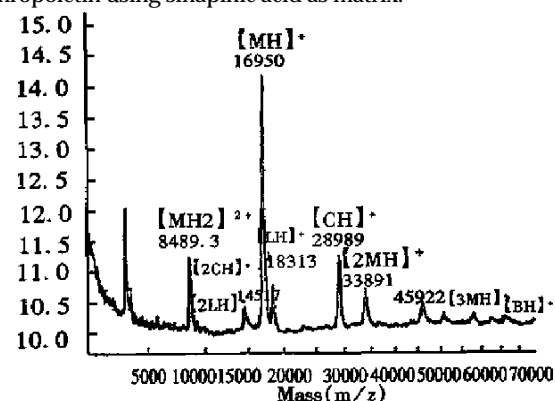


**Figure 3** MALDI-TOF mass spectrum of standard protein mixtures using sinapinic acid as matrix. M: Myoglobin; C: Carbonic anhydrase B; L:  $\beta$ -lactoglobulin; B: Bovine serum albumin.

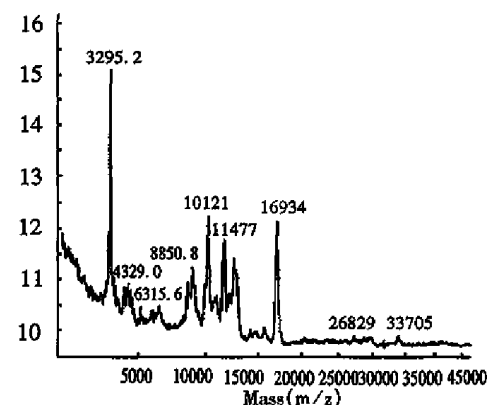


**Figure 4** MALDI-TOF mass spectrum of mixtures containing calmodulin using sinapinic acid as matrix.

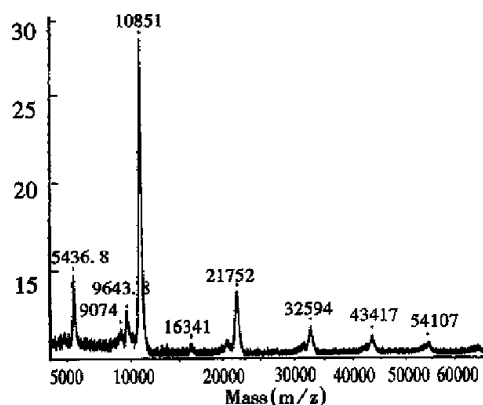


**Figure 5** MALDI-TOF mass spectrum of calmodulin fragment using sinapinic acid as matrix.

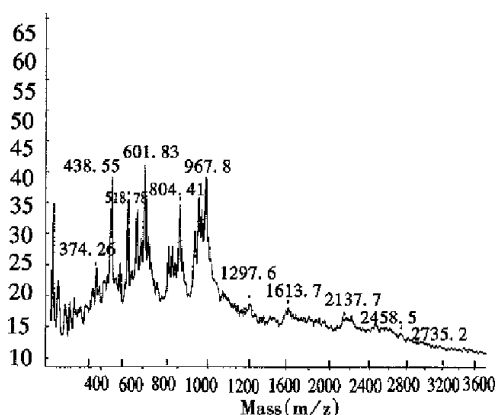


**Figure 6** MALDI-TOF mass spectrum of tryptic digests of recombinant human erythropoietin using 100mM DHB as matrix.

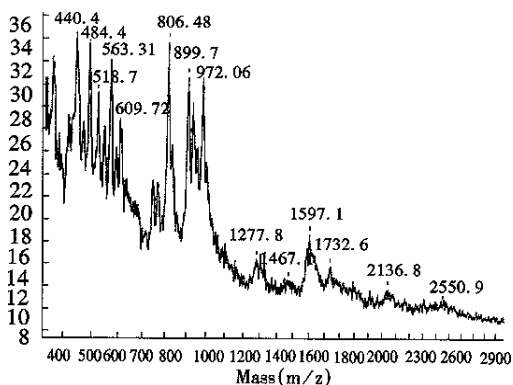


**Figure 7** MALDI-TOF mass spectrum of tryptic digests of recombinant human erythropoietin using 2-Aminobenzoic acid as matrix.

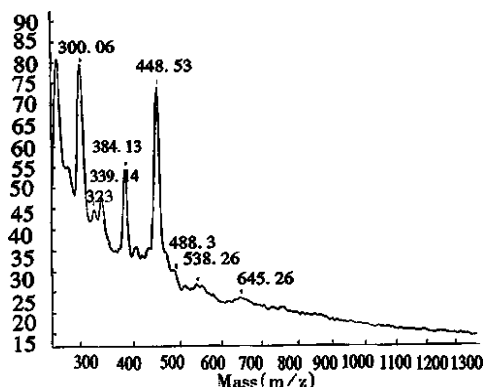


**Figure 8** MALDI-TOF mass spectrum of tryptic digests of recombinant human erythropoietin using  $\alpha$ -cyano-4-hydroxycinnamic acid as matrix.

## CONCLUSION

The present investigations clearly show that MALDI-TOF MS is a powerful tool for measuring protein molecular weight, identifying unknown components in mixtures, determining purity and the relative content of impurities, and characterizing peptide mapping. The MALDI-TOF analysis validated that SDS-PAGE is unreliable in determining the  $M_r$  of glycoproteins. Since the broad MS peaks reflect the carbohydrate heterogeneity, half-intensity widths, MALDI-TOF MS peaks are recommended as a criterion to evaluate the heterogeneity of glycoproteins. The advantages of MALDI-TOF MS were described in this paper, such as its accuracy, small volume sample consumption and rapid response. It is suggested that this technique should be the first choice when studying the quality of scarce or precious samples during the early stages in the development of engineered proteins.

## REFERENCES

- 1 Karas M, Hillenkamp F. Laser desorption/ionization of proteins with molecular masses exceeding 10000 daltons. *Anal Chem*, 1988; 60:2299-2301
- 2 Papac DI, Wong A, Jones AJS. Analysis of acidic oligosaccharides and glycopeptides by matrix-assisted laser desorption/ionization time-of-flight mass spectrometry. *Anal Chem*, 1996; 68:3215-3223
- 3 Karas M, Bahr U, Strupat K, Hillenkamp F. Matrix dependence of metastable fragmentation of glycoproteins in MALDI TOF mass spectrometry. *Anal Chem*, 1995; 67:675-679
- 4 Feistner GJ, Faull KF, Barofsky DF, Roepstorff P. Mass spectrometric peptide and protein charting. *J Mass Spectrom*, 1995; 30: 519-530
- 5 Harmon BJ, Gu X, Wang DIC. Rapid monitoring of site-specific glycosylation microheterogeneity of recombinant human interferon- $\gamma$ . *Anal Chem*, 1996; 68:1465-1473
- 6 Russell DH, Edmondson RD. High-resolution mass spectrometry and accurate mass measurements with emphasis on the characterization of peptides and proteins by matrix-assisted laser desorption/ionization time-of-flight mass spectrometry. *J Mass Spectrom*, 1997; 32:263-276
- 7 Powell, AK, Harvey DJ. Stabilization of sialic acids in N-linked oligosaccharides and gangliosides for analysis by positive ion matrix-assisted laser desorption/ionization mass spectrometry. *Rapid Commun Mass Spectrom*, 1996; 10:1027-1032
- 8 Rosinke B, Strupat K, Hillenkamp F, Rosenbusch J, Dencher N, Krüger U, Galla HJ. Matrix-assisted laser desorption/ionization mass spectrometry (MALDI-MS) of membrane proteins and non-covalent complexes. *J Mass Spectrom*, 1995; 30:1462-1468
- 9 Tang X, Sadeghi M, Olumee Z, Vertes A, Braatz JA, McIlwain LK, Dreifuss PA. Detection and quantitation of  $\beta$ -2-microglobulin glycosylated end products in human serum by matrix-assisted laser desorption/ionization mass spectrometry. *Anal Chem*, 1996; 68: 3740-3745
- 10 Edmondson RD, Russell DH. Evaluation of matrix-assisted laser desorption/ionization-time-of-flight mass measurement accuracy by using delayed extraction. *J Am Soc Mass Spectrom*, 1996; 7: 995-1001
- 11 Wasley BC, Timony G, Murtha P, Stoudemire J, Dorner AJ, Caro J, Kriege M, Kaufman RJ. The importance of N- and O-linked oligosaccharides for the biosynthesis and in vitro and in vivo biologic activities of erythropoietin. *Blood*, 1991; 77:2624-2632
- 12 Yamaguchi K, Akai K, Kawanishi G, Ueda M, Masuda S, Sasaki R. Effects of site directed removal of N-glycosylation sites in human erythropoietin on its production and biological properties. *J Biol Chem*, 1991; 266:20434-20439

- 13 Higuchi M, Oh-eda M, Kuboniwa H, Tomonoh K, Shimonaka Y, Ochi N. Role of sugar chains in the expression of the biological activity of human erythropoietin. *J Biol Chem*, 1992;267:7703-7708
- 14 Takeuchi M, Takasaki S, Shimada M, Kobata A. Role of sugar chains in the in vitro biological activity of human erythropoietin produced in recombinant Chinese hamster ovary cells. *J Biol Chem*, 1990;265:12127-12130
- 15 Narhi LO, Arakawa T, Aoki KH, Elmore R, Rohde MF, Boone T, Strickland TW. The effect of carbohydrate on the structure and stability of erythropoietin. *J Biol Chem*, 1991;266:23022-23026
- 16 Lai PH, Everett R, Wang FF, Arakawa T, Goldwasser E. Structural characterization of human erythropoietin. *J Biol Chem*, 1986;261:3116-3121
- 17 Depaous AM, Advani JV, Sharma BG. Characterization of erythropoietin dimerization. *J Pharmac Sci*, 1995;84:1281-1284
- 18 Apffel A, Chakel J, Udiavar S, Hancock WS, Soubers C, Jr EP. Application of capillary electrophoresis, high performance liquid chromatography, on line electrospray mass spectrometry and matrix assisted laser desorption ionization time of flight mass spectrometry to the characterization of single chain plasminogen activator. *J Chromatogr A*, 1995;717:41-60
- 19 Rush RS, Derby PL, Strickland TW, Rohde MF. Peptide mapping and evaluation of glycopeptide microheterogeneity derived from endoproteinase digestion of erythropoietin by affinity high-performance capillary electrophoresis. *Anal Chem*, 1993;65:1834-1842

Edited by WANG Xian-Lin

# Cloning and identification of an angiostatic molecule IP-10/crg-2 \*

LIU Zhi-Guo<sup>1</sup>, YANG Jing-Hua<sup>2</sup>, AN Hua-Zhang<sup>1</sup>, WANG Hai-Yan<sup>1</sup>, HE Feng-Tian<sup>1</sup>, HAN Zhe-Yi<sup>1</sup>, HAN Ying<sup>1</sup>, WU Han-Ping<sup>1</sup>, XIAO Bing<sup>1</sup> and FAN Dai-Ming<sup>1</sup>

**Subject headings** IFN- $\alpha$ ; IFN- $\gamma$ ; inducible protein; cytokine responsive gene-2; DNA

## Abstract

**AIM** To obtain human and murine cDNAs encoding IFN- $\gamma$  inducible protein 10 (IP-10) and cytokine responsive gene-2 (Crg-2).

**METHODS** The encoding genes of IP-10 and Crg-2 were amplified by RT-PCR from cultured human fibroblast cells and Balb/c mouse liver treated by IFN- $\gamma$  and TNF- $\alpha$ , respectively, and cloned into plasmids of pUC19 and pGEM3Zf(+).

**RESULTS** The nucleotide sequences of the amplified DNA were confirmed by endonucleases digestion and sequencing.

**CONCLUSION** Recombinant IP-10/crg-2 gene clones with 306 bp and 314 bp inserts were established for further research on biological activities and ligands of hIP-10/mCrg-2.

## INTRODUCTION

Angiogenesis plays an important role in tumorigenesis and metastasis, and gene therapy targeting vasculature of neoplasms has become a hot topic<sup>[1]</sup>. Many new molecules, including endostatin and angiostatin, were discovered with significant inhibitory effect on neovascularization of tumor. Besides these molecules, some 'old' cytokines were also found to possess the bioactivity of inhibiting angiogenesis, including IP-10/Crg-2<sup>[2]</sup>. Human IP-10 belongs to a superfamily called chemokines and Crg-2 is its murine analogue. As a member of chemokines, IP-10/Crg-2 was primarily characterized as a proinflammatory molecule. However, recent findings showed that IP-10/Crg-2 had a powerful inhibitory effect in neovascularization of tumor, and tumor regression induced by IL-12 was closely related with high level of IP-10 expression and subsequent vasculature destruction<sup>[3]</sup>. However, little has been known about its properties, especially the mechanisms of its inhibitory effect on endothelium, since the receptor of IP-10/Crg-2, CXCR3, was predominantly distributed in activated T cells, but not in endothelial cells<sup>[4]</sup>. To further clarify the bioactivity of IP-10/Crg-2 and explore its potential application in gene therapy against angiogenesis, we amplified the gene sequence encoding IP-10 and Crg-2 by RT-PCR from primary human fibroblast cells and mouse liver, and cloned them into pUC19 and pGEM3Zf(+) vector, respectively.

## MATERIAL AND METHODS

### Material

Recombinant human IFN- $\gamma$  was purchased from Bonding Co., Beijing. Recombinant TNF- $\alpha$  was kindly provided by Genetic Diagnosis Institute of our University. Endonucleases, T4 ligase and reverse transcriptase were purchased from Gibco BRL. Taq DNA polymerase was obtained from Perkin Elmer. 100bp PCR marker was purchased from New England Biolabs. The kit for purification of plasmids and PCR products were obtained from Promega. Primers were synthesized by the Shanghai Bioengineering Center of Chinese Academy of Sciences. Host bacterial cell line DH5 $\alpha$ , cloning vector pUC19 and pGEM3Zf(+) were stored in our lab.

<sup>1</sup>Department of Gastroenterology, Xijing Hospital, the Fourth Military Medical University, Xi'an 710032, China

<sup>2</sup>Department of Cellular and Molecular Biology, Harvard University, USA

Dr. LIU Zhi-Guo, male, born on 1974-03-24 in Harbin of China, graduated from Department of Medicine, the Fourth Military Medical University (FMMU) with bachelor degree of medicine in 1997, and now as a postgraduate in Department of Gastroenterology of Xijing Hospital, FMMU.

\*Supported by the Outstanding Youth Fund from National Natural Science Foundation of China, No. 39625023.

**Correspondence to:** Dr. FAN Dai-Ming, Department of Gastroenterology, Xijing Hospital, The Fourth Military Medical University, Xi'an 710032, Shaanxi Province, China

Tel. +86 • 29 • 2539041, Fax. +86 • 29 • 2539041

Email. zhiguoliu@163.net

Received 1998-12-03 Revised 1999-03-01

## Methods

### Template preparation of human and mouse cDNA

Human primary fibroblast cell was obtained by cultured surgically resected specimens of normal adult. Four hours before RNA extraction, human IFN- $\gamma$  was added to reach a final concentration of  $1 \times 10^6$  U/L for cell culture and Balb/c mice was individually injected with TNF- $\alpha$   $5 \times 10^6$  U. The total RNAs were then purified from fibroblast cells and mouse liver respectively by the method of guanidium/phenol, and reverse-transcribed to cDNA according to literature<sup>[5]</sup>.

### PCR amplification of IP-10 and Crg-2 encoding sequence

Primers were designed according to the sequence of IP-10/crg-2. For human IP10, endonuclease sites were introduced: 5' primer GGGCGCTAGC (*Nhe* I)CATATG(*Nde* I) AATCAAAGTGGCGATTCTGATT, 3' primer AAGCTT(*Hind* III) GGTACC(*Kpn* I) TTAA GGAGATCTTTTAGACATTTC. For murine crg-2, no endonucleases were introduced: 5' primer ACCATGAACCCAAGTGCTGC; 3' primer GCTTCACTCCAGTTAAGGAG. PCR cycle parameters: 94°C 45s, 60°C 45s, 72°C 45s, 30 cycles in all. PCR reaction mixture consists of cDNA template (human or murine origin) 2  $\mu$ L, 25 mmol/L MgCl<sub>2</sub> 8  $\mu$ L, 10XPCR buffer 10  $\mu$ L, 10 mmol/L dNTPs 4  $\mu$ L, Taq DNA polymerase 2  $\mu$ L, 50  $\mu$ mol/L upstream and downstream primers 2  $\mu$ L each, and distilled water was supplemented to 100  $\mu$ L.

### Construction of human IP-10 recombinant plasmid

PCR amplification product was digested by endonucleases *Nhe* I and *Kpn* I, meanwhile pUC19 was cut by *Xba* I and *Kpn* I. After purification by agarose electrophoresis, these two fragments were ligated by cohesive ends and then the recombinant plasmid was introduced into *E. coli* line DH5 $\alpha$ . Clones were picked randomly by blue/white screening, and identified by endonucleases digestion of *Xba* I/*Eco*R I and *Hind* III/*Bgl* II.

### Construction of murine crg-2 recombinant plasmid

Murine crg-2 recombinant plasmid was constructed by T/A cloning according to literature<sup>[6]</sup>. Five  $\mu$ g pGEM3Zf(+) was digested by *Sma* I. After purification by electrophoresis, 10  $\mu$ L 10 $\times$  PCR buffer, 1  $\mu$ L 100 mmol/L dTTP, 1  $\mu$ L Taq DNA polymerase and distilled water were added to make a final volume of 100  $\mu$ L and incubated at 75°C for 2 h. The PCR product was ligated with vector and the recombinant was transformed into DH5 $\alpha$ , clones

were selected by blue/white screening, minipreps were extracted and the right insert was confirmed by endonuclease digestion with *Bam*H I or *Hin* d III.

**Sequence analysis** DNA sequence analyses were conducted in the Central Lab of our university with automatic DNA analyzer (PE373-A, USA) according to the methods of Sanger.

## RESULTS

### PCR amplification of IP-10/Crg-2 encoding sequence

PCR reactions were carried out using the obtained cDNAs of human fibroblast and murine liver treated by IFN- $\gamma$  or TNF- $\alpha$  as the templates. Electrophoresis of PCR products indicated that fragments of about 300bp were amplified in each of the reaction mixture, which were consistent with our expectation of 322bp and 314bp (Figure 1).



**Figure 1** Amplification of human IP-10 and murine crg-2 gene by PCR.

1. crg-2 gene fragment (306 bp); 2. IP-10 gene fragment (314 bp); 3. 100 bp PCR marker (1500, 1200, 1000, 900, 800, 700, 600, 500, 400, 300, 20 and 100 bp fragment, from top to bottom. The 500 and 1000 bp fragments serve as reference bands).

### Construction and identification of recombinant plasmids

For recombinant construction of human IP-10, purified PCR product was ligated with endonucleases-digested pUC19, and the recombinant was transformed into *E. coli* line DH5 $\alpha$ . White clones were picked and confirmed by dual endonucleases digestion with *Xba* I/*Eco*R I and *Hin* d III/*Bgl* II. Electrophoresis of 20 g/L showed that fragments of about 237 bp and 318 bp were released respectively. This clone was identified as positive and named pUC19/h-IP-10 (Figure 2, lane 1-3). For vector construction of crg-2, the amplified fragment was ligated directly with pGEM3Zf(+) T vector, and recombinants were analyzed by single endonuclease digestion with



*Bam* H I or *Hin* d III. Electrophoresis of 20 g/L showed that a fragment of 251 bp or 204 bp was released the positive clones were named pGEM3Zf(+)/*crg*-2 (Figure 2, lane 5-7).

### Sequence analysis

Minipreps of pUC19/IP-10 and pGEM3Zf(+)/*crg*-2 were prepared according to the manual of Promega Wizard Minipreps kit. Samples were analyzed with automatic sequence analyzer. Sequencing results showed that the 306 bp and 314 bp inserts were completely identical with reported sequences of IP-10<sup>[7]</sup> and *crg*-2<sup>[8]</sup>, flanked by introduced endonuclease sites or added single T (Figure 3).

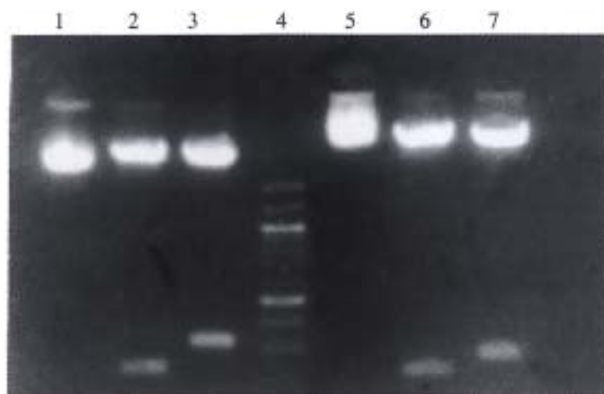


**Figure 2** Identification of pUC 19/IP-10 and pGE M3Zf(+)/*crg*-2 recombinant clones by restriction endonucleases digestion. 1. pUC19/IP-10 control; 2. pUC19/IP-10 by *Xba*-I+*Eco* R I; 3. pUC19/IP-10 by *Hin* d III+*Bgl* II; 4. 100bp PCR marker; 5. pGEM3Zf(+)/*crg*-2 control; 6. pGEM3Zf(+)/*crg*-2 by *Hin* d III; 7. pGEM3Zf(+)/*crg*-2 by *Bam* H I.

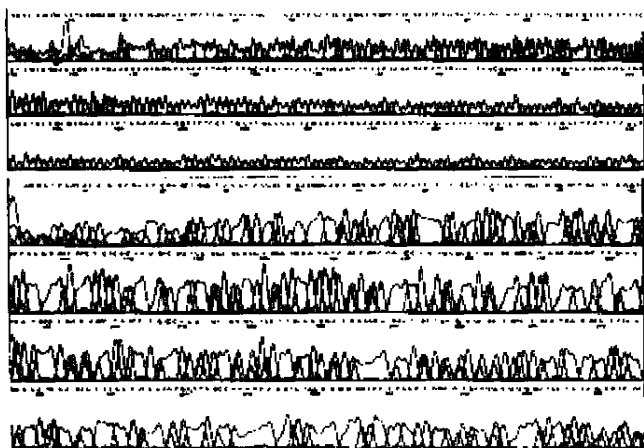


**Figure 3** The nucleotide sequence of IP-10/*crg*-2 gene encoding region. Human IP-10 sequence (above); murine-*crg*-2 sequencing (below).

### DISCUSSION

The growth of tumor is dependent on the vasculature for nutrition and oxygen. Destruction of established vasculature will lead tumor cells to necrosis or apoptosis, that is the main idea of angiostatic therapy. Tumor cells are highly heterogenic and multiple drug resistance (MDR) is very likely to be induced. But its endothelium, is more stable and susceptible to treatment and causes little<sup>[9]</sup> MDR. In normal adult, endothelium remains in dormant status except for wound-healing and menstruation. So inhibiting the process of active angiogenesis of tumor will eventually selectively cure the neoplasms and its metastasis without induction of MDR.

IP-10 was initially identified in 1985 as a member of CXC subfamily in chemokine superfamily<sup>[7]</sup>. The family of chemokines is characterized by 4 highly conservative cysteines at the N terminus of protein. Most chemokines are basic heparin binding protein possessing the activity of chemotaxis, which play important roles in inflammation and wound healing. According the different structures, gene location and bioactivities, this family can be divided into 2 subfamilies, CC and CXC subfamily. The first 2 cysteines of CC subfamily are adjacent with each other, while in CXC subfamily the cysteines were separated by a single random residue. IP-10/Crg-2 is a secreted protein consisting of 98 amino acids, of which the first 21 amino acids represent a signal peptide, with a  $M_r$  of 6000-7000 for mature form. Its receptor CXCR3 was successfully cloned in 1996<sup>[4]</sup>. The receptor belonging to seven transmembrane G-protein coupled receptors expressed primarily on activated T cell. The best-described bioactivities of IP-10/Crg-2 include angiogenesis inhibition, bone marrow hemopoietic stem cell inhibition, chemotaxis for activated T cell and monocyte-macrophage<sup>[10]</sup>. Among them, the most attracting property is the effect on vasculature, especially after it is found to be the downstream molecule for IFN- $\gamma$  or IL-12 to induce the regression of tumor<sup>[3, 11]</sup>. But most researches are focused on its induction or its effects on various kinds of tissues and cells, and are far from the insight of its biological activity and signal transduction process.

We amplified the complete cDNA sequences of IP-10/Crg-2. The target gene clones were established and confirmed by endonuclease digestion and sequence analysis. This will help us further clarify the bioactivity of IP-10/Crg-2 and the downstream mechanism after receptor binding.

## REFERENCES

- 1 Folkman J. Antiangiogenic gene therapy. *Proc Nat Acad Sci USA*, 1998;95:9064-9066
- 2 Keane MP, Arenberg DA, Lynch JP, Whyte RI, Iannettoni MD, Wilke CA, Morris SB, Glass MC, DiGiovine B, Kunkel SL, Strieter RM. The CXC chemokines, IL-8 and IP-10, regulate angiogenic activity in idiopathic pulmonary fibrosis. *J Immunol*, 1997;159:1437-1443
- 3 Sgadari C, Angiolillo AL, Tosato G. Inhibition of angiogenesis by interleukin 12 is mediated by the interferon-inducible protein 10. *Blood*, 1996;87:3877-3882
- 4 Marcel L, Basil G, Pius L, Simon AJ, Luca P, Ian C, Marco B, Bernhard M. Chemokine receptor specific for IP-10 and Mig: structure, function and expression in activated T lymphocytes. *J Exp Med*, 1996;184:963-969
- 5 Sambrook J, Fritsch EF, Maniatis T. Molecular cloning: a laboratory manual. 2nd ed. New York: Cold Spring Harbor Laboratory Press, 1989:60-87
- 6 Borovkov AY, Rivkin MI. Xcm I-containing vector for direct cloning of PCR products. *Bio Techniques*, 1997;22:812-814
- 7 Andrew DL, Jay CU, Jeffrey VR.  $\gamma$ -interferon transcriptionally regulates an early response gene containing homology to platelet proteins. *Nature*, 1985;315:672-676
- 8 Vanguri P, Farber JM. Identification of CRG-2: An interferon inducible mRNA? predicted to encode a murine monokine. *J Biol Chem*, 1990;265:15049-15057
- 9 Thomas B, Judah F, Timothy B, Michael SO. Antiangiogenic therapy of experimental cancer does not induce acquired drug resistance. *Nature*, 1997;390:404-407
- 10 Baggiolini M, Dewald B, Moser B. Human chemokines: an update. *Annu Rev Immunol*, 1997;15:675-705
- 11 Yu WG, Ogawa M, Mu J, Umehara K, Tsujimura T, Fujiwara H, Hamaoka T. IL-12 induced tumor regression correlates with in situ activity of IFN- $\gamma$  produced by tumor-infiltrating cells and its secondary induction of anti-tumor pathways. *J Leukoc Biol*, 1997;62:450-457

Edited by MA Jing-Yun

# Pathogenic effects of O-polysaccharide from *Shigella flexneri* strain \*

ZHONG Qi-Ping

**Subject headings** *Shigella flexneri* strain;bacterial antigen;O-polysaccharide,virulence

## Abstract

**AIM** To investigate the specific pathogenesis of O-polysaccharide (O-PS) which is on the outer membrane of lipopolysaccharides (LPS) from *Shigella flexneri*.

**METHODS** The O-PS was isolated and purified from *Shigella flexneri*- 5 M90T by enzymatic hydrolysis and gel chromatography. Effects of O-PS were observed by *in vitro* experiment, (HeLa cell culture), and *in vivo* experiment (rabbit ileal loop assay).

**RESULTS** *In vitro* and *in vivo* experiments with the purified O-PS from *Shigella flexneri*-revealed that the O-PS alone was toxic to HeLa cells and caused mucosal inflammation and hemorrhagic exudation in ileal loop of rabbit.

**DISCUSSION** O-PS might be one of the factors causing diarrhea and its mechanism was different from endotoxin reaction of LPS. The molecular mechanism of O-PS need further studies.

## INTRODUCTION

*Shigella flexneri* is one of the pathogens which causes diarrhea and its pathogenic mechanism is still unclear, even though extensive investigations were carried out worldwide. It has been known that the invasive outer membrane protein encoded by its plasmid DNA plays a primary role in bacterial infection. The roles of other factors, especially lipopolysaccharides (LPS), were also better understood. The specific pathogenesis of O-polysaccharide (O-PS) which is on the outer membrane of lipopolysaccharides remains unclear. To understand the pathogenesis of the O-PS of *Shigella flexneri*, we isolated and purified the O-PS from *Shigella flexneri*- 5 M90T and observed the pathogenesis of O-PS *in vitro* and *in vivo*.

## MATERIALS AND METHODS

### Materials

**Strain** Wild-type *Shigella flexneri* 5 M90T was provided by Pasteur Institute (French).

**Medium** Lauria-Bertani (LB) medium.

**Reagents** Proteinase K was purchased from Merck, Sephadex G50 from Sigma, fetal bovine serum (FBS) from Institute of Hematology, Chinese Academy of Medical Sciences, 1640 medium from GIBCO, and nuclease from Huamei.

### Methods

**Preparation of O-PS** ① Cultivation of bacteria and harvest. A single colony of *Shigella flexneri*- 5 M90T was inoculated onto LB plates, incubated at 37°C overnight and harvested into a clean centrifuge tube. The bacteria were washed with 20 mmol/L Tris-HCl (pH 7.4) buffer, lyophilised and ground to powder in a mortar. ② Isolation of LPS by enzymatic hydrolysis and gel chromatography<sup>[1,2]</sup>. Bacterium powder (25 mg) was suspended in 1.0 mL ddH<sub>2</sub>O, boiled for 15 min and centrifuged to remove cell debris. The supernatant was added with DNase (50 mg/L) and RNase (100 mg/L) and incubated at 37°C for 1 hour, then added with proteinase K (1mg), incubated at 60°C for 1 hour, boiled for 5 min and centrifuged for supernatant. The supernatant was then dialyzed against ddH<sub>2</sub>O overnight and centrifuged again. The supernatant, the crude LPS, was separated by a Sephadex G50 chromatography

Department of Microbiology, Tianjin Medical University, Tianjin 300070, China

ZHONG Qi-Ping, female, born on 1955-10-02 in Tianjin, graduated from Nankai University in 1982, graduated from Tianjin Medical University with a master degree in 1997, engaged in bacteriological research, now associate professor of microbiology, having 9 papers published.

\*Project supported by the National Natural Science Foundation of China, No. 39370040.

**Correspondence to:** ZHONG Qi-Ping, Department of Microbiology, Tianjin Medical University, Tianjin 300070, China

Tel. +86 • 22 • 23525615

**Received** 1998-12-13 **Revised** 1999-04-02

column with elution of ddH<sub>2</sub>O. The first peak was collected, lyophilized and stored at 4°C. ③ Preparation of O-PS by acid hydrolysis<sup>[2,3]</sup>. LPS was hydrolyzed in 1% acetic acid at 100°C for 2 hours. The solution was then centrifuged and the supernatant was separated by gel chromatography and O-PS was collected as described above.

**Quantification of carbohydrates by the sulfuric acid-phenol method<sup>[4]</sup>** A proper amount of O-PS was dissolved in 2 mL ddH<sub>2</sub>O, mixed well with 1 mL 5% phenol and then added with 5 mL sulfuric acid. The mixture was incubated at room temperature for 10 min and transferred to 25°C-30°C water bath for 10 min-20 min. The carbohydrate content was quantified by measuring absorbance at 480 nm with 10 mg/L-100 mg/L rhamnose as standard.

**Antigenicity measurement of O-PS by ELISA** Rabbit antisera against *-Shigella flexneri*-5 M90T and enzyme-conjugated goat antirabbit IgG were added to the plate coated with 50 mg/L O-PS. The antigenicity of O-PS was determined by color reaction density after adding TMB.

**Effects of O-PS on HeLa cell** With 1640 medium containing 10% bovine sera, penicillin and streptomycin, HeLa cells were cultured into monolayer and transferred into a 12 hole tissue culture plate. When cells grew onto the plate walls and formed small clumps, the medium was replaced by fresh one. O-PS was added to each hole to reach a final concentration of 100, 200, 500 and 1000 µg/L respectively and incubated under 5% CO<sub>2</sub> at 37°C. Growth and morphology of the HeLa cells were observed every 24 hours.

**Rabbit ileal loop assay** Rabbits were fasted for 24 hours. The rabbit ligated ileal loops (5 cm) were prepared in rabbits (weight 2 kg) anesthetized with procaine hydrochloride by local infiltration. Twenty µg O-polysaccharides in 0.5 mL saline was injected into the loop. Rabbits were sacrificed 24 hours later. Portions of tested loops were taken and fixed in 10% buffered formalin immediately. The pathologic slices of the specimen were prepared with standard procedures.

## RESULTS

**Purification of O-PS from *Shigella flexneri* 5 M90T** Separation of the crude O-PS by Sephadex G50 showed three major peaks of carbohydrates measured with the sulfuric acid-phenol method (Figure 1). According to references<sup>[3]</sup> and the

molecular weight, the peak I was thought to be the long-chain O-PS. This was confirmed by ELISA analysis which gave rise to positive results with peak I by using antisera against *-Shigella flexneri*-5 M90T. On the contrast, peak II yielded negative results with ELISA analysis. Peak III was not analyzed due to its small amount and low molecular weight. Therefore, it is plausible that peak II and III were the fragments generated in acid-hydrolysis. Peak I is the O-PS based on its molecular weight and antigenicity.

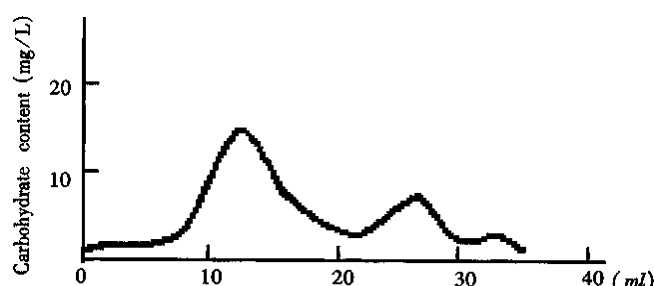


**Figure 1** The curve of carbohydrate content quantified. The crude O-PS was separated by Sephadex G50 with elution of ddH<sub>2</sub>O.

### *Toxicity of O-PS to HeLa cells*

The toxicity of O-PS to HeLa cells demonstrated as cell shrinking and falling off from plate walls within 48 hours. The cytopathic effect of HeLa cells was positively related to the concentration of O-PS in medium (Figure 2).

### *Effects of O-PS on ileal loop of rabbits*

After 24 hours of injection of 20 µg O-PS into ileal loop of rabbit, mucosal inflammation and hemorrhagic exudation in ileal loop of rabbit could be observed. When observing the pathologic slice of the specimen under light microscope, we could see inflammatory reaction, the mucosa and submucosa had moderate to severe hyperemia and infiltration of neutrophils and lymphocytes, the muscularis and serosa had mild hyperemia and infiltration of white blood cells. There were necrotic substances and hemorrhage in the lumen.

## DISCUSSION

*Shigella flexneri* is an intracellular pathogen which causes acute inflammation by infection of the

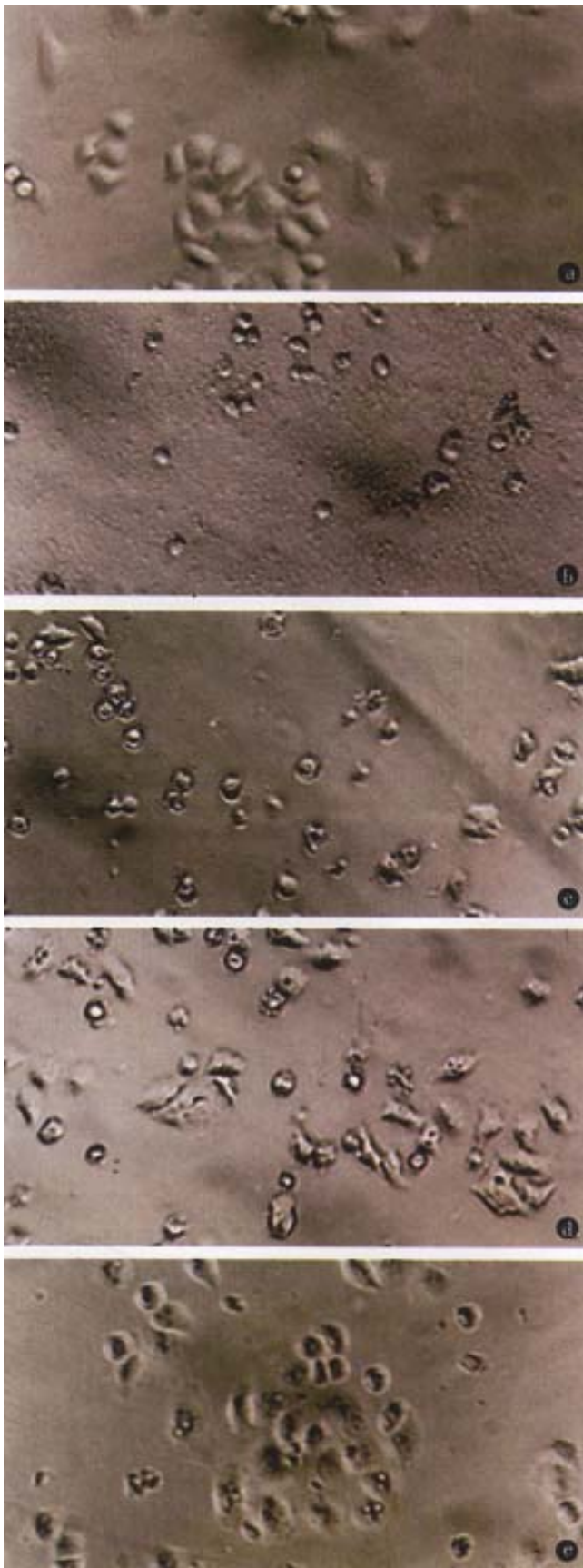


**Figure 2** Effect of various doses of O-PS on HeLa cell. Normal HeLa cells (A), and HeLa cells in the medium containing 1000 (B), 500 (C), 200 (D), 100 (E)  $\mu\text{g}/\text{mL}$  O-PS respectively.  $\times 200$

mucosal membrane of the large intestine and damages the mucosal epithelial cells, leading to ulcer. It has been shown that the infection of *Shigella flexneri* is accomplished by releasing the across membrane signals which induce aggregation of actin and polymerization of myosin to trigger the endocytosis. This will bring about the breakdown of membrane and allow bacteria to get into cells, proliferate and move in cells, diffuse into surrounding cells and eventually kill the cells infected by inhibiting respiration<sup>[5]</sup>. These functions were dependent on the presence of O antigen and involved in form a “tail-like” actin structure on the bacterium surface as a motile apparatus. As for the infection of *Shigella flexneri*, LPS plays an important role in inducing inflammation. For example, antibodies against LPS showed protective effects for inflammatory reaction and the mutants defective in O-antigen can not cause keratitis in guinea pigs, although it is able to invade HeLa cells. However, little is known about the roles and mechanisms of LPS played in the infection of cells.

LPS of gram negative bacteria is composed of lipoid A, core polysaccharide and O-PS. Among them, lipoid A, the principal component of LPS, causes pathological or physiological damages by inducing some cellular factors<sup>[6]</sup>. But O-PS is generally thought to determine the antigenicity of the bacterium and its resistance to the defence of the host cells<sup>[7]</sup>. In recent years, the specific pathogenesis of O-PS has received increasing attention worldwide<sup>[8,9]</sup>. There are reports using whole bacterium in the research, but the role played by each component of LPS has not been distinguished. For example, enteroinvasive *Escherichia coli* (EIEC) can be strongly recognized by the antisera against O-PS, suggesting that the structure of O-PS may be related to its toxicity. The *Shigella* vaccine of the same serotype was efficient; the mAb against O-PS of *Shigella flexneri* could inhibit contact hemolytic activity<sup>[10]</sup>. All these indicate the importance of O-PS in pathogenesis of *Shigella flexneri*. Therefore, it is important to investigate the pathogenesis by using purified O-PS.

In this paper, we studied *Shigella flexneri* pathogenesis by using purified O-PS both *in vitro* and *in vivo*. We have modified Eidhin's method to improve the preparation of crude LPS by conducting additional steps of nuclease digestion and Sephadex G50 gel chromatography. The experiment showed that M90 O-PS alone was toxic to HeLa cells and caused mucosal inflammation and hemorrhagic exudation of ileal loop in rabbits. It appears that the toxicity to HeLa cells and ileal loop pathogenesis resulted from a common factor. Our experiments

showed that *Shigella flexneri* O-PS may also be one of the factors which cause diarrhea. However, its molecular mechanism is still nuclear and need further investigations. The methods and results presented in this report provide a basis to study diarrhea pathogenesis and a new thought to develop diarrhea vaccines.

**Acknowledgments** We are grateful to Professor Chen En-Lin for his overall guide to this paper, to Mr. He Jian-Min for his technical assistance in preparing LPS, to Dr. Li Fang-Tao, Li Bao-Yan and Kang Ning for participating in the animal experiment, and Department of Pathology for pathological diagnosis.

## REFERENCES

- Eidhin DN, Mouton C. A rapid method for preparation of rough and smooth lipopolysaccharide from *Bacteroides*, *Porphyromonas* and *Prevotella*. *FEMS Microbiol Lett*, 1993;110:133-138
- Xu XP, Chen ZH, Su X. Study on immunogenicity of *S. sonnei* polysaccharide-protein conjugate. *Chin J Microbiol Immunol*, 1992;12:141-144
- Muller-Seitz E. Degradation studies on and investigation of O specific and core polysaccharides. *FEBS Lett*, 1968;1:311-314
- Blay K, Caroff M, Richards JC, Perry MB, Chaby R. Specific and cross-reacting monoclonal antibodies to *Bordetella parapertussis* and *Bordetella bronchiseptica* lipopolysaccharides. *Microbiology*, 1994;140(pt 9):2459-2465
- Sansonetti PJ. Genetic and molecular basis of epithelial cell invasion by *Shigella* species. *Rev Infect Dis*, 1991;13(Suppl 4):S285-292
- Jiao BH. Molecular endotoxicology. *Shanghai: Shanghai Scientific and Technological Publishing House*, 1995:151-156, 232-253
- Lindberg AA, Karnell A, Weintraub A. The lipopolysaccharide of *Shigella* bacteria as a virulence factor. *Infect Dis*, 1991;13(Suppl 4):S279-284
- Rajakumar K, Jost BH, Sasakawa C, Okada N, Yoshikawa M, Adler B. Nucleotide sequence of the rhamnose biosynthetic operon of *Shigella flexneri* 2a and role of lipopolysaccharide in virulence. *J Bacteriol*, 1994;176:2362-2373
- Sandlin RC, Lampel KA, Keasler SP, Goldberg MB, Stolzer AL, Maurelli AT. Avirulence of rough mutants of *Shigella flexneri*: requirement of O antigen for correct unipolar localization of IcsA in the bacterial outer membrane. *Infect Immun*, 1995;63:229-237
- Mei Y, Su X, Li H, Xu XP. Analysis of biological characteristics of monoclonal antibodies to *Shigella flexneri* 2a O-side chain of LPS. *Chin J Microbiol Immunol*, 1992;12:322-323

Edited by MA Jing-Yun



# The mechanism of actions of Octreotide, Bupleurum-Peony Cheng Qi decoction and Dan Shan in severe acute pancreatitis

WU Xie-Ning

**Subject headings** Pancreatitis/therapy; Octreotide; bupleurum peony Cheng Qi decoction

The pathogenesis of severe acute pancreatitis (necrotizing pancreatitis) is complicated and has not been elucidated up to date. In my opinion, it is multifactorial, and aggressive treatment should be directed to the multifaceted pathophysiology<sup>[1]</sup>. A cumulative series of twenty cases were treated with the regimen i.e., combined traditional Chinese and modern medicine. No death, almost no morbidity and no serious complications, such as ARDS and DIC occurred, only mental confusion as sequela occurred in a patient with previous cerebral infarction. The present article is to discuss the mechanism of actions of the medicines used in this treatment regimen.

## THE PATHOGENESIS OF SEVERE ACUTE PANCREATITIS

It involves ① the release of pancreatic and lysosomal enzymes by the pancreatic acini which induce pancreatic autodigestion; ② the increase of vascular permeability, resulting in microcirculatory impairment; and ③ overstimulation of macrophages and neutrophils with release of many cytokines, inflammatory mediators (leukotrienes, prostaglandins, platelet activating factor) and free radicals. These factors interact with one another producing pancreatic acinar damage and intestinal epithelial barrier dysfunction. If not corrected instantly, it might lead to gut barrier damage and translocation of intestinal bacteria and endotoxin, resulting in a "second attack" caused by infection and endotoxemia, producing multiorgan dysfunction syndrome and eventually multiorgan failure.

Severe acute pancreatitis is most frequently precipitated by gallstone, biliary sludge,

microlithiasis with or without bile reflux, obstruction of biliary-pancreatic common pathway, high fat and high protein diet, alcohol consumption and ischemia here in Shanghai, hence, I think it is multifactorial and multifaceted a disease. The detailed mechanism will be delineated in another paper.

## OCTREOTIDE AND SOMATOSTATIN

On reviewing the medical literature, octreotide and somatostatin are found to act on many facets. Either of them inhibits cholecystokinin which stimulates the synthesis, secretion and release of pancreatic enzymes<sup>[2]</sup>, concomitantly it also stimulates and activates the monocytic-macrophagic system, lower the endotoxin level in acute necrotizing pancreatitis<sup>[3]</sup>. An experimental study showed that somatostatin could cause the blockage of endotoxin, IL-1, IL-6, IL-2, TNF- $\alpha$  and restore them to a near normal level<sup>[4]</sup>. Microcirculatory impairment is the initiating as well as aggravating factor in necrotizing pancreatitis, octreotide could decrease the small intestinal and colonic blood flow, and cause redistribution intrapancreatically, as well as decrease of the blood flow to the islets and to the cells secreting hormones with vasodilating property<sup>[5]</sup>. This is a very important point in contrast to the viewpoint that octreotide decreased pancreatic blood flow in the past. Another experimental study also showed the pancreatic microcirculatory impairment mimicked the ischemia-reperfusion damage in humans, with impaired arteriolar perfusion, increased vascular permeability and aggregation and stasis of neutrophils in the postcapillary venules. Via the mediation of the adhesive molecules on the vascular endothelium, the neutrophils interacted with the endothelial cells, the oxygen free radicals produced by the neutrophils damaged the vascular endothelium, resulted in endothelial swelling, making the capillary lumen narrowed and obstructed, and the functional capillary density decreased. By given octreotide, the changes in the postcapillary venules were much lessened as compared with those not given octreotide, the statistical difference was significant<sup>[6]</sup>. No adhesion of neutrophils in the

Department of Gastroenterology, Shanghai First People's Hospital, Shanghai 200080, China

Dr. WU Xie-Ning, Professor of Medicine, B.S., M.D. Editor of Ten books on Hepatology and Gastroenterology, having 185 papers published.

**Correspondence to:** Dr. WU Xie-Ning, Department of Gastroenterology and Central Research Laboratory, Shanghai First People's Hospital, No. 85, Wujing Road, Shanghai 200080, China

**Received** 1999-04-08

postcapillary venules were seen, indicating that octreotide attenuated the interaction between neutrophils and endothelial cells, thus providing a protective effect. Octreotide also increased PGI<sub>2</sub> level<sup>[7]</sup>, inhibited the synthesis of vasoconstricting leukotrienes and decreased the eicosanoid products<sup>[6]</sup>. Basing on the above facts, octreotide or somatostatin is a requisite in the treatment of severe acute pancreatitis.

#### BUPLEURIUM-PEONY CHENG QI DECOCTION

The herbal mixture Bupleurium-Peony Cheng Qi decoction has seven constituents: *Bupleurum*, *White peony*, *Scutellaria*, *Rhubarb* (*Rhei Rhizome*), *Unripe bitter orange*, *Magnolia bark*, *Refined mirabilite*. This herbal mixture also acts on multifacets of the disease, among which, rhubarb is the major constituent<sup>[8]</sup>. It inhibits the secretion and activity of the pancreatic enzymes, such as trypsin, lipase, phospholipase A2, chymotrypsin, elastase, amylase, kallikren-kinin and is synergistic with octreotide (or somatostatin) in this aspect. It stabilizes the lysosomal membrane of acinar cells<sup>[9]</sup>, which is important in attenuating the acinar damage. It inhibits the inflammatory cytokines, its antihistamine derivative inhibits the phagocytic function of phagocytes, thereby inhibiting their overstimulation. As it is known, cytokines, such as IL-6, IL-1, IL-8 and TNF- $\alpha$ , are released by overstimulation of macrophages. A recent experimental study showed that acute phase proteins were induced by IL-6 and inhibited by rhubarb. Furthermore, the neutrophilic infiltration was only minimal in the necrotizing pancreatitis rats. The chemotactic effect of neutrophils on the inflamed area was by IL-8. Rhubarb can neutralize and expel the endotoxin, resulting in low blood endotoxin level with subsequent low release of TNF- $\alpha$ , these are the indirect evidences of rhubarb's inhibitory effect on cytokine release<sup>[4]</sup>. Rhubarb also inhibits vascular permeability, after oral administration, rhubarb is more concentrated in the pancreas, liver and kidney, whereas the brain and the lung are the next, and inhibition of the vascular permeability can cause cessation of exudation in the above organs and tissues. This is crucial in the prevention of local complications of the pancreas itself as well as prevention of leakage of fluid into the peritoneal cavity which causes peritonitis, hypovolemia and hypoalbuminemia, adult respiratory distress syndrome (ARDS) and pancreatic encephalopathy<sup>[5]</sup>. It also inhibits Na<sup>+</sup>, K<sup>+</sup>ATPase, impedes the transport of Na<sup>+</sup> from intestinal lumen into the cells and increases the volume of luminal contents, as the osmotic pressure increases within the colonic lumen, intestinal wall is

then stimulated and peristalsis increased. Concomitantly, the plasma oncotic pressure increases, water switches to the blood circulation from the tissue. In this recipe, bupleurum and unripe bitter orange can increase the gastric emptying and small intestinal propulsion, refined mirabilite can also promote small intestinal peristalsis. As a whole, the herbal mixture restores the gut motility and absorptive function of the GI tract, relieving intestinal paresis and even paralysis. Magnolia bark and white peony relax the gut smooth musculature to restrain the overaction of the rest constituents. When the tongue becomes moistened, it indicates the gut function is restored<sup>[6]</sup>. Rhubarb has also broad-spectrum antibiotic action, *in vitro* it inhibits bacteroid fragilis, streptococci, B.Coli etc., neutralizes and expels the endotoxin in the intestinal lumen. It is of particular importance in the prevention of dislocation of intestinal bacteria and endotoxin<sup>[7]</sup>. It decreases blood lipids, inhibits protein catabolism, reduces urea synthesis and promotes urinary excretion of urea and creatinine<sup>[8]</sup>. Rhubarb has another important effect, i.e., a powerful relaxant of Oddi's sphincter, it can antagonize and abolish the contracting effect of octreotide, in favor of pancreatic fluid and bile drainage. This is of particular importance in the management of severe acute pancreatitis especially in cases with stone in the common bile duct. One of the precautions is that rhubarb cannot be decocted too long, i.e., two minutes is enough, otherwise many of its beneficial effects will be lost.

Bupleurum has tranquilizing and analgesic effects, it also inhibits the growth of hemolytic streptococcus, staphylococcus aureus *in vitro*, also protects liver cells and decreases serum cholesterol and triglyceride, moreover, it enhances the intestinal contractility by acetylcholine. Another important effect is that it can stimulate the secretion of endogenous glucocorticoids<sup>[11]</sup> which can inhibit excessive secretion of cytokines and inflammatory mediators and protect acinar cells.

Unripe bitter orange has biphasic action on gut smooth muscle, low concentration stimulates, high concentration inhibits, which is dependent upon the functional status of the GI tract and the concentration of the herbal medicine. It has a synergistic effect on the GI musculature with bupleurum, refined mirabilite and rhubarb.

White peony inhibits amylase and has a weak relaxing effect on the Oddi's sphincter.

Scutellaria has antibiotic effect on staphylococcus aureus, streptococcus, B.Coli, pseudomonas bacillus, etc. It decreases free fatty acid, triglyceride, serum and hepatic cholesterol and transaminase levels. High fat diet is often one of the precipitating factors of severe acute

pancreatitis, free fatty acid can cause lipoperoxidation and damage the vascular endothelium and acinar cells, and scutellaria inhibits lipoperoxidation both via vitamin C-Fe and NADPH-ADP routes. It can also inhibit release of histamine by mast cells, and the cyclo-oxygenase and lipo-oxygenase pathways which produce inflammatory mediators. Besides, it inhibits thromboxane A<sub>2</sub> synthase, reduces platelet aggregation and its adhesive function, promotes PGE<sub>1</sub> and PGE<sub>2</sub> levels, and transformation of fibrinogen to fibrin and prevents endotoxin induced disseminated intravascular coagulation (DIC). Finally, scutellaria also has the effect of lowering the elevated temperature.

### SALVIA MILTIORRHIZA

*Salvia Miltiorrhiza* (Dan Shen) inhibits platelet aggregation, decreases blood viscosity, improves blood rheology and microcirculation, and inhibits the release of lysosomal enzymes and chemotacting neutrophils as well. Besides, it is an antioxidant as well as a calcium ion antagonist, the latter is also of great importance in improving the microcirculation. Experimental studies revealed that Ca<sup>2+</sup> influx occurred via the acinar cell membrane before the exocrine pancreatic secretion started<sup>[13]</sup>, and then some proteases were secreted. Ca<sup>2+</sup> influx also occurred before the macrophages produced and released the cytokines such as TNF- $\alpha$ , IL-6 and IL-1. TNF- $\alpha$  is the crucial mediator of systemic complications, it upregulates adhesive molecules and induces excessive nitric oxide formation and superoxide free radicals, damaging the pancreas substance and other organs. Furthermore, it causes increased vascular permeability inducing microcirculatory ischemia. Calcium ion antagonist inhibits the release of TNF- $\alpha$ , improves the ischemia and increases the vascular perfusion, and it also inhibits the acinar cells to produce protease, ameliorating the inflammation and tissue damage. In our experience, Dan Shen is also an important therapeutic agent in the management of severe acute pancreatitis.

By and large, the above seven constituents of the herbal mixture have an overall effect on interruption of the cascade in severe acute pancreatitis. The herbal mixture restores the gut

motility; inhibits release of cytokines and inflammatory mediators with subsequent attenuation of neutrophilic infiltration; improves pancreatic ischemia; prevents the dislocation of intestinal bacteria and endotoxin; and lowers blood lipoids, decreases lipoperoxidation and reduces damages of vascular endothelium and acinar cell membrane. Together with octreotide (or somatostatin) and Dan Shen, these would provide a synergistic as well as a complementary effect. During the treatment, the patients usually run a smooth course without fluctuation and recover uneventfully, hence, their combined use is of practical value and worth recommendation of wide use in clinical practice.

### REFERENCES

- 1 Wu XN. Management of severe acute pancreatitis. *WJG*, 1998;4: 90-91
- 2 Shiratori K, Watanabe SI, Takeuchi T. Somatostatin analogues SMS 201-995 inhibits pancreatic exocrine secretion and release of secretin and cholecystokinin in rats. *Pancreas*, 1991;6:23-30
- 3 Büchler MW, Binder M, Friess H. Role of somatostatin and its analogues in the treatment of acute and chronic pancreatitis. *Gut*, 1994;3(Suppl):S15-S19
- 4 Zhang QH, Cai D, Wu SC. Changes of inflammatory mediators in acute necrotizing pancreatitis rats and the effect of somatostatin. *Natl Med J China*, 1997;77:355-358
- 5 Carlsson PO, Jansson L. The long-acting somatostatin analogue octreotide decreases pancreatic islet blood flow in rats. *Pancreas*, 1994;9:361-364
- 6 Hoffmann TF, Uhl E, Messmer K. Protective effect of the somatostatin analogue octreotide in ischemic/reperfusion induced acute pancreatitis rats. *Pancreas*, 1996;12:286-293
- 7 Van Ooljen R, Tinga CT, Kat WJ. Effect of long-acting somatostatin analog (SMS 201-995) on eicosanoid synthesis and survival in rats with necrotizing pancreatitis. *Dig Dis Sci*, 1992;37: 1434-1440
- 8 Li YK, Jiang MY (eds). Pharmacology of Chinese herbal medicine. Traditional Chinese Medicine Publisher, 1992
- 9 Xu JY, Yu DJ, Jiang SH. Experimental study on the treatment of acute hemorrhagic necrotizing pancreatitis with target liposome of emodin. Shanghai International Conference of Gastroenterology, Nov. 28-30, 1996, Shanghai
- 10 Zhao Q, Quai NC, Li QK, Wu SZ. Clinical and experimental studies on the effect of Dachengqi decoction on acute phase protein levels in multiple organ dysfunction syndrome. *Chin J Integrated Tradit Western Med*, 1998;18:453-456
- 11 Kimura K, Shimosagawa T, Sasano H. Endogenous glucocorticoids decrease the acinar cell sensitivity to apoptosis during cerulein pancreatitis in rats. *Gastroenterology*, 1998;114:372-381
- 12 Zhen SS, Wei QJ, Wu HG. Study on the effects of Dan Shan and Anisodamine hydrochloride injection on early pulmonary damage in dogs with acute hemorrhagic necrotizing pancreatitis. *Chin J Integrated Western Med*, 1989;9:158-360
- 13 Hughes CB, El-Din MAB, Koto M. Calcium channel blockade inhibits release of TNF- $\alpha$  and improves survival in a rat model of acute pancreatitis. *Pancreas*, 1996;13:22-28

Edited by MA Jing-Yun

Review

# Diagnostic approach to patients with cholestatic jaundice

N Assy, G Jacob, G Spira and Y Edoute

**Subject headings** bile ducts, intrahepatic; biopsy; cholangiography; cholestasis; diagnosis, differential; jaundice; tomography, X-ray computed; ultrasonography

Conjugated hyperbilirubinemia due to any form of hepatobiliary disease is essentially the result of impairment in bile formation and/or bile flow, a condition known as cholestasis<sup>[1,2]</sup>. Cholestatic jaundice is often accompanied by a broad spectrum of laboratory, clinical, and histological abnormalities. Laboratory abnormalities include increased serum levels of alkaline phosphatase and gamma-glutamyltransferase (GGT), and variable elevation of bilirubin, serum copper, ceruloplasmin, cholesterol, lipoprotein X, and serum bile acids, as well as of prothrombin time, which is corrected by vitamin K supplementation. There is minimal or no elevation of aminotransferases. Clinically, pruritus, fatigue, xanthomas, back pain from osteoporosis, pale stools, or even steatorrhea may be present, with evidence of fat-soluble vitamin deficiency. Histologically, conjugated hyperbilirubinemia is characterized by bile plugs (bilirubinostasis), feathery degeneration of hepatocytes (cholestasis), small-bile-duct destruction, pericholangitis, portal edema, bile lakes and infarcts (typically with extrahepatic obstruction), and finally, biliary cirrhosis<sup>[1-3]</sup>.

## MECHANISM OF CHOLESTASIS

Bile formation originates in hepatocytes with the uptake and production of organic anions, bilirubin, and bile salts through diverse cellular transporters that may be either sodium-dependent or independent<sup>[4]</sup>. Bile salts taken up at the sinusoidal surface of the hepatocytes are generally conjugated to increase their water solubility and subsequently

are excreted into the biliary tree at the apical (canalicular) surface. Secretion is achieved via the combined process of Na<sup>+</sup> coupled, carrier-mediated, or vesicular-transport systems<sup>[4]</sup>. Multiple factors contribute to the impairment of bile flow: Endotoxins are potent stimuli for activating cytokine production from macrophages<sup>[5,6]</sup> and have acute cholestatic effects on hepatic bile production<sup>[7]</sup>. Endotoxins and several proinflammatory cytokines [tumor necrosis factor (TNF)alpha, interleukin (IL)-1, and IL-6 down-regulate hepatic transport mechanisms that determine bile acid-dependent bile flow, affecting both bile acid uptake and canalicular secretion<sup>[8,9]</sup>. These proinflammatory cytokines also promote the expression of MHC class II molecules on target cells, thereby enhancing target antigen presentation<sup>[10]</sup>. Proinflammatory cytokines activate neutrophils and T and B cells, increase the expression of intercellular adhesion molecules (ICAMs), and may promote tissue damage by direct action. It is proposed that these portal tract inflammatory events can contribute to the down-regulation of hepatocellular bile salt transport, and hence aggravate cholestasis. Unfortunately, there are few cases of cholestatic jaundice in which the specific cellular defect has been identified. For most cholestatic process, multiple defects may act in concert to produce disease.

## EVALUATION OF THE PATIENT WITH CHOLESTATIC JAUNDICE

The first question to be resolved is whether the cholestasis results from intrahepatic or extrahepatic disease process, bearing in mind that several intrahepatic causes of cholestatic jaundice can mimic extrahepatic obstruction to varying degree<sup>[2,11]</sup>. Comprehensive clinical evaluation comprising the history, physical examination, and basic laboratory tests and the additional information provided by ultrasonography (US) or computed tomography (CT) are highly successful in making this important distinction (Figure 1). Clinically important clues to extrahepatic obstructions include abdominal pain, a palpable gallbladder or upper abdominal mass, evidence of cholangitis, and a history of previous biliary surgery. Clinical clues to intrahepatic

Liver Disease Unit and Department of Internal Medicine C, Rambam Medical Center, Haifa, and Department of Anatomy, the Bruce Rappaport Faculty of Medicine, Technion-Israel Institute of Technology, Haifa, Israel

**Correspondence to:** Dr. Nimer Assy, P.O.Box 428, 25170 Fassouta, Upper Galilee, Israel  
Tel. +972 • 4 • 987 • 0080, Fax. +972 • 4 • 987 • 0080  
Email: drnimer@netvision.net.il

**Received** 1999-04-08

cholestasis include pruritus, as in primary biliary cirrhosis (PBC) and primary sclerosing cholangitis (PSC) patients<sup>[12]</sup>. Pruritus may be prominent in alcoholic hepatitis and has been reported in about 10% of patients with acute viral hepatitis<sup>[13]</sup>.

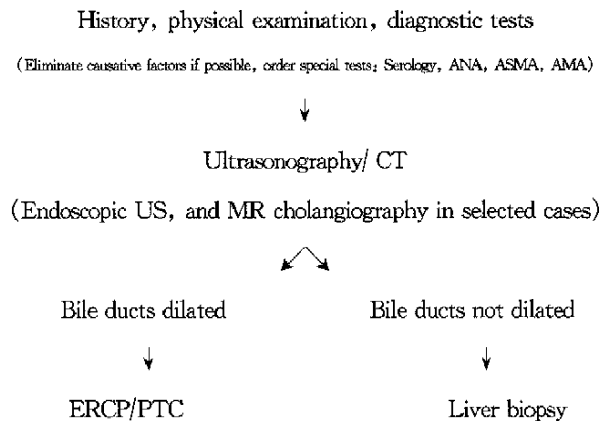


**Figure 1** Schematic of work-up of cholestatic jaundice. AFP, alpha-fetoprotein; AMA, antimitochondrial antibodies; ANA, antinuclear antibody; ASMA, anti-smooth muscle antibody; CT, computed tomography; ERCP, endoscopic retrograde cholangiography; MR, magnetic resonance; PTC, percutaneous transhepatic cholangiography; US, ultrasonography.

The patient should be asked about risk factors, including alcohol intake, medications, sexual contact, drug abuse, needle punctures, and travel history. The family history is of value in benign recurrent intrahepatic cholestasis (BRIC). Details regarding the onset of jaundice and its duration, whether intermittent or progressive, as well as its associated symptoms like darkening of the urine, acholic stools, arthralgia, rash, weight loss, fever, chills, and pain in the right upper quadrant should be obtained<sup>[3]</sup>. Physical examination should involve careful observation of stigmata of chronic liver disease, xanthelasma, clubbing, and lymphadenopathy. Hepatomegaly is usual in alcoholic liver disease, primary or secondary hepatic neoplasm, infiltrative disease, and primary biliary cirrhosis (PBC)<sup>[14,15]</sup>. Marked splenomegaly suggests cirrhosis with portal hypertension or lymphoproliferative disease<sup>[16,17]</sup>.

Laboratory work-up for cholestatic jaundice should include complete blood count with differential, urea, creatinine, electrolytes, and a liver panel including alkaline phosphatase, GGT, aminotransferases, albumin, bilirubin, and prothrombin time. Immunological markers such as AMA, ANA, ASMA, ANCA, and immunoglobulins and serological markers for viral hepatitis are

helpful. Serum alpha-fetoprotein, carcinoembryonic antigen, and CA19.9 may be increased in patients with malignancies<sup>[18]</sup>.

Clinical evaluation is quite sensitive, but has a positive predictive value of only about 75%; that is, about 25% of patients with suspected obstruction actually have hepatocellular disease<sup>[2]</sup>. The rare case of obstruction that is missed in the initial clinical evaluation will probably become apparent on follow-up evaluation, and the delay in establishing the correct diagnosis is unlikely to harm the patient. If, on the other hand, obstruction is suspected, then a more aggressive work-up is appropriate.

US and CT have comparable sensitivity (85%-96%) in detecting dilatation of the intrahepatic and extrahepatic biliary tree in patients with proven obstruction<sup>[3]</sup>. US is widely recommended as the first-line imaging procedure in the evaluation of cholestatic jaundice. Although gallbladder stones are readily detected by US, common bile duct stones may be missed in 60% of patients because of the interference caused by intestinal gas. Obesity may also lead to an unsatisfactory study. Moreover, with the exception of mass lesion in the head of the pancreas, US usually does not identify the type of obstruction.

CT is more likely to yield information regarding the level of the obstruction, localizing this in 90% of patients<sup>[3,19]</sup>. CT is also a reasonable first choice in patients with lymphoma, in whom it may provide information regarding retroperitoneal lymph node involvement<sup>[20]</sup>. Although a negative US or CT may represent a logical stopping point in the diagnostic work-up of a patient in whom obstruction is not strongly suspected on clinical grounds, a negative study should not dissuade the clinician from further evaluation of a patient in whom obstruction is considered highly likely. In patients in whom the clinical suspicion of biliary obstruction is supported by CT or US, direct visualization of the biliary tree with percutaneous transhepatic cholangiography (PTC) or endoscopic retrograde cholangiography (ERCP) is appropriate and necessary. PTC and ERCP have in common 99% sensitivity and specificity for the diagnosis of biliary obstruction, and both are capable of demonstrating the site and the nature of the obstruction in more than 90% of patients<sup>[21]</sup>. Both also provide therapeutic interventions including removal of stones, dilatation of strictures, and the placement of stents across obstructing lesions, as well as the placement of biliary drainage catheters<sup>[22]</sup>.

ERCP is the procedure of choice in suspected ampullary or duodenal lesions in pancreatic

carcinoma and when gallstone obstruction is suspected, in which case sphincterectomy and stone extraction can be implemented. Palliative stenting of neoplastic obstruction and temporary stenting of certain types of traumatic lesions of the common bile duct are frequently accomplished with ERCP<sup>[22]</sup>. ERCP is also a logical first procedure in patients with suspected PSC and in patients who have undergone cholecystectomy in whom jaundice is suspected on the basis of choledocholithiasis, since US is often unhelpful in this setting, as the stone is likely to be missed and ductal dilatation may be absent<sup>[23]</sup>.

PTC is often preferred when an obstructing lesion high in the biliary tree is anticipated, as it will permit visualization of the proximal extent of the lesion and enable immediate biliary drainage of obstructed intrahepatic ducts. PTC is also preferred in patients with previous gastrointestinal surgery like Billroth II gastrectomy<sup>[24]</sup>. PTC is usually contraindicated in patients with marked ascites and coagulopathy. In some instances, both PTC and ERCP may be used together in a combined therapeutic approach from above and below to maneuver guidewires and stents across a difficult obstruction. Sometimes hepatobiliary scintigraphy, which is of established value in the diagnosis of acute cholecystitis, may help in evaluating biliary leaks and congenital malformations<sup>[25]</sup>.

Recently, endoscopic CT and magnetic resonance cholangiography have been found to be very helpful in the diagnosis of biliary obstruction, especially in the setting of liver transplantation<sup>[26,27]</sup>. A negative study obtained by ERCP or PTC represents a reasonable endpoint to the work-up of obstruction in the jaundiced patient. Liver biopsy may be appropriate at this time point. Minor complications of a cutting needle biopsy, such as prolonged right upper quadrant pain, occur in up to 6% of cases<sup>[28]</sup>. Major complications such as clinically significant intra-abdominal bleeding are uncommon, and mortality (almost always from hemorrhage) is approximately 0.01%<sup>[29,30]</sup>. Cholestasis per se does not appear to increase the risk of a major complication. Percutaneous liver biopsy is contraindicated in patients with a significant coagulopathy or substantial ascites; in these instances, performance of a transjugular liver biopsy<sup>[31]</sup> or not performing a biopsy at all are alternatives. Weighing against these negative considerations are the potential benefits of obtaining histological information.

Liver biopsy may be of great value in differentiating hepatocellular cholestasis from obstructive cholestasis<sup>[32]</sup>. Unfortunately,

differentiating drug-induced cholestatic hepatitis from other causes cannot be performed histologically. A chief question in a patient with cholestatic jaundice is whether there is significant underlying chronic liver disease<sup>[33]</sup> or an infiltrative process, particularly granulomatous disease, lymphoma, or metastatic carcinoma<sup>[34]</sup>. Portal tract neutrophilic infiltrates seen in liver biopsy are a common accompaniment of biliary obstruction, ascending cholangitis, outright sepsis, cholangiolytic drug reactions, and hyperalimentation<sup>[35]</sup>. Finally, biopsy of the liver is particularly helpful in differentiating the cholestatic picture of alcoholic hepatitis from that of cholangitis<sup>[36]</sup>.

### DIFFERENTIAL DIAGNOSIS

Cholestatic liver disease can be broadly categorized as extra-or intrahepatic. The extrahepatic component is best approached anatomically. The intrahepatic component comprises intrinsic disease, infiltrative disease, systemic disease, and space-occupying lesions. Prevalent clinical abnormalities (Tables 1, 2) will be detailed in subsequent sections.

### EXTRAHEPATIC CAUSES OF CHOLESTATIC JAUNDICE

Among the extrahepatic causes of chronic cholestasis, secondary sclerosing cholangitis due to choledocholithiasis or biliary surgery is probably the most common. This is usually related to a single stricture of the common hepatic duct or common bile duct. Other causes of extrahepatic cholestasis are listed in Table 1.

**Table 1 Differential diagnosis of cholestasis and hyperbilirubinemia (cholestatic jaundice)**

CBD dilated: Best approach is anatomically
Ampulla of Vater
Stones, carcinoma of pancreas, chronic pancreatitis, ampullary neoplasm, diverticulum, pancreatic cyst, abscess of pancreas, sphincter of Oddi dysfunction
Common bile duct
Benign traumatic stricture, stones, choledochal cyst, cholangiocarcinoma, parasites, hemobilia, extrahepatic atresia
Gallbladder
Carcinoma of gallbladder
Portal nodes
Cholangiocarcinoma, lymphoma, metastatic carcinoma, cavernous portal vein

### CHOLEDOCHOLITHIASIS

Although gallstones produce jaundice by impaction in the common bile duct, acute cholecystitis is associated with mild jaundice in up to 20% of



patients. This is attributed to edema of the common duct (Mirizzi syndrome) or to direct involvement of the porta hepatis by inflammation<sup>[37]</sup>. Common duct stones retained after cholecystectomy may produce jaundice in the immediate postoperative period or even several years after cholecystectomy. Acute gallstone obstruction is often associated with pain from biliary colic or from acute pancreatitis resulting from ampullary obstruction. Sudden impaction of a stone in the common duct may be associated with a rapid rise in aminotransferases 20-50 above normal, followed by an equally rapid decline within 72 hours<sup>[38]</sup>. Cholangitis is relatively common in patients with choledocholithiasis and manifests as fever with chills, abdominal pain, and jaundice, a syndrome known as Charcot's triad, although jaundice may be absent in one third of patients with cholangitis<sup>[39]</sup>.

### BENIGN STRICTURES OF THE BILE DUCTS

Benign biliary stricture in adults following previous surgery and biliary atresia in the pediatric population are the two most common type of strictures<sup>[18]</sup>. PSC may produce multiple or diffuse strictures that are not associated with proximal ductal dilatation<sup>[40]</sup>. In patients with chronic alcoholic pancreatitis, a long stricture may develop in the intrapancreatic portion of the common duct, leading initially to cholestasis and eventually to secondary biliary cirrhosis<sup>[41]</sup>. Ampullary stenosis may result in patients with acquired immunodeficiency syndrome (AIDS)<sup>[42]</sup> or from the trauma of passing a stone. Cholangitis is frequent in patients with benign biliary obstruction, in contrast to its relative infrequency in the framework of malignant obstruction<sup>[18]</sup>.

### NEOPLASTIC OBSTRUCTION

Pancreatic carcinoma is the commonest neoplasm producing obstructive jaundice. Other tumors include cholangiocarcinoma, ampullary tumors, and carcinoma of the gallbladder<sup>[18,43]</sup>. Abdominal pain radiating into the back, along with loss of appetite and weight loss, may be present, but jaundice may also develop without pain (usually progressive and deep jaundice). Cholangiocarcinoma may obstruct the biliary system at any level, and the clinical presentation is similar to pancreatic cancer<sup>[44]</sup>. Cholangiocarcinoma of the extrahepatic bile ducts may be growing into the lumen. The sclerosing variant of cholangiocarcinoma, which frequently arises at the confluence of the right and left hepatic ducts (Klatskin's tumor), may be difficult to distinguish from PSC both radiologically and on biopsy. This tumor infiltrates early into the wall of

the bile duct, where it elicits a markedly sclerotic response<sup>[45]</sup>.

Tumors producing complete obstruction of the common bile duct may be accompanied by marked, palpable dilatation of the gallbladder (Courvoisier's law). Ampullary tumors may produce intermittent jaundice because of sloughing of the tumor and partial relief of the block. Metastatic cancer may obstruct the bile duct, as may lymphoma<sup>[46]</sup>. Hepatocellular carcinoma may uncommonly rupture into the biliary system and give rise to tumor emboli that lodge in and obstruct the common duct<sup>[47]</sup>. The extrahepatic ducts may be compressed by adjacent tumor, by peribiliary lymph node infiltrated by lymphoma, or by metastatic carcinoma of breast<sup>[46]</sup>. Direct infiltration of the ducts by lymphoma may also lead to obstruction<sup>[48]</sup>.

### UNCOMMON CAUSES OF OBSTRUCTIVE JAUNDICE

Choledochal cyst may first manifest as obstructive jaundice after 17 years of age<sup>[49]</sup>. A duodenal diverticulum is a rare cause of biliary obstruction. Hemobilia, mostly a result of hepatic trauma, including invasive procedures or neoplasm, presents with the triad of biliary colic, jaundice and gastrointestinal bleeding<sup>[50]</sup>. Invasion of the common bile duct with *Ascaris* or with liver flukes of the *Fasciola*, *Clonorchis*, or *Opisthorchis* genera may produce cholangitis<sup>[51]</sup>. Secondary sclerosing cholangitis due to opportunistic infection of immunodeficient patients has become increasingly common since the advent of AIDS. *Cryptosporidium parvum*, cytomegalovirus (CMV), and *Microsporidia* are the organisms most frequently found<sup>[52]</sup>.

### INTRAHEPATIC CAUSES OF CHOLESTATIC JAUNDICE

Intrahepatic cholestasis may arise from many sources and presents, therefore, a particular challenge when it develops in the seriously ill patient (Table 2). Many insults may cause local and systemic activation of the inflammatory cytokine system, and thus these proinflammatory events are potent inducers of intrahepatic cholestasis.

### INTRINSIC DISEASES

Drug-induced cholestasis. Drugs may be responsible for 2%-5% of cases of jaundice in in-patients, and this percentage is probably substantially higher in the elderly<sup>[53]</sup>. The clinical presentation may mimic viral hepatitis or biliary tract disease. Serum sickness like features, including rash, arthralgia, and eosinophilia, are clues to a drug-induced etiology<sup>[53]</sup>. Chronic cholestasis tends to occur as a rare idiosyncratic reaction to certain commonly used drugs, including ampicillin-clavulanic acid,

chlorpromazine, cotrimoxazole, erythromycin, flucloxacillin, phenytoin, and tetracycline (Table 3)<sup>[54]</sup>. The histological features vary from case to case and over time. Generally, in the acute phase there is parenchymal bilirubinostasis, in the chronic phase bilirubinostasis commonly resolves, and features of cholate stasis persist and ductopenia develops<sup>[55]</sup>. A different pattern of drug-induced liver injury leading to chronic cholestasis is drug-induced sclerosing cholangitis, as seen following floxuridine treatment<sup>[56]</sup>. Scolicidal agents, injected into intrahepatic hydatid cysts, may escape into the biliary system and cause stricture formation that may ultimately lead to biliary cirrhosis<sup>[57]</sup>. In patients taking numerous medicines, the only practical approach is to eliminate the drug with the highest likelihood of cholestatic injury and monitor for improvement.

**Table 2 (continued): Differential diagnosis of cholestatic jaundice**

Normal CBD
Extrahepatic
Stone too early, stone too late, cholangiocarcinoma, and primary sclerosing cholangitis
Intrahepatic
Intrinsic diseases
Drugs, alcoholic hepatitis, viral hepatitis, AIDS, primary biliary cirrhosis, autoimmune cholangitis, primary sclerosing cholangitis, idiopathic adulthood ductopenia, Autoimmune hepatitis, decompensated liver cirrhosis
Infiltrative diseases
Granulomatous hepatitis (Tuberculosis, amyloidosis), sarcoidosis, Lymphoma, leukemia, fatty liver
Systemic diseases
Sepsis, total parenteral nutrition (TPN), benign recurrent intrahepatic cholestasis (BRIC), cholestasis of pregnancy, cystic fibrosis, disappearing intrahepatic ducts syndrome, allograft rejection, graft versus host disease (GVHD), sickle cell syndrome, mastocytosis, hypereosinophilic syndrome, Hyperthyroidism
Space occupying lesions
Blood-hematoma, peliosis; pus-bacterial, amebic; cyst-hydatid, polycystic Cancer-primary, secondary

**Table 3 Common drugs known to cause cholestatic jaundice**

Antimicrobial agents
Augmentin (amoxicillin-clavulanic acid), cloxacillin, erythromycin, ethambutol, dapsone, fluconazole, nitrofurantoin, griseofulvin, ketoconazole, terbinafine
Cardiovascular agents
Disopyramide beta-blockers, ACE inhibitors, propafenone, ticlopidine, warfarin, methyl dopa
Endocrine agents
Sulfonylureas, clofibrate, estrogens, tamoxifen, androgens, niacin, oral contraceptives
Gastrointestinal agents
H2 blockers (e.g., ranitidine), penicillamine
Immunosuppressive agents
Azathioprine, cyclosporine, gold salts, NSAIDs (e.g. diclofenac, nimesulide, piroxicam)
Psychopharmacologic agents
Tricyclic antidepressants, benzodiazepines, phenothiazines, phenytoin, halothane

ACE: angiotensin-converting enzyme; NSAIDs: non-steroidal anti-inflammatory drugs.

**Alcoholic hepatitis.** Alcoholic hepatitis with severe cholestasis must always be considered. Marked hepatomegaly with hepatic tenderness and evidence of hepatocellular failure (aminotransferases <500U/L), along with a compatible history of alcohol intake and fever, suggests the diagnosis. Alkaline phosphatase can vary from normal to values in the thousands U/L. Bilirubin levels range from normal to 340 µmol/L • 510 µmol/L<sup>[58]</sup>.

**Viral hepatitis.** Infrequently, a severe cholestatic syndrome may follow the acute phase of viral hepatitis; this is most commonly seen with hepatitis A<sup>[59]</sup>, Hepatitis C<sup>[60]</sup>, and hepatitis E<sup>[61]</sup>. Despite the fact that jaundice may be profound for up to 6 months, complete recovery is the rule. Recently, we described a case of severe cholestatic jaundice in the elderly due to Epstein-Barr virus infection, which led to a diagnostic delay since the clinical presentation mimicked biliary obstruction<sup>[62]</sup>.

**AIDS.** In AIDS-related cholangiopathy, *Cryptosporidium* is the most frequent cause, but *Microsporidia*, CMV, *Mycobacterium avium*-complex, and *Cyclospora* have also been reported. Papillary stenosis may be present in patients with CD4 lymphocyte counts of <100/mm<sup>[3]</sup> and alkaline phosphatase >500IU/L. Jaundice is an unusual manifestation of AIDS-related cholangiopathy. If present, it suggests other disorders, including drug or alcohol abuse or neoplasm<sup>[63]</sup>.

**Primary biliary cirrhosis.** PBC could account for cholestatic jaundice. Classic PBC is described as a chronic non-suppurative cholangitis associated with AMA positivity in 95% of cases (anti-M2). Thirty percent will have positive ANA<sup>[64]</sup>. Histologically, bile duct injury along with portal inflammation are the usual findings, which are most often associated with elevation in alkaline phosphatase, IgM, and cholesterol. A female predominance is characteristic. Patients may, most commonly, be asymptomatic at presentation or may describe fatigue, pruritus, or right upper quadrant pain. Less than 20% of patients will have jaundice at time of presentation, and less than 5% will exhibit complications of portal hypertension<sup>[64]</sup>. The majority of patients will have associated autoimmune disorders (Sjögren's syndrome, scleroderma, and arthritis). Ursodeoxycholic acid (UDCA) is the only drug shown to prolong survival and to improve biochemical abnormalities. However, there is no evidence that it improves liver histology<sup>[65]</sup>. Presentation of HLA-II antigens as well as the expression of ICAM-1 and LFA3 induced by proinflammatory cytokines like TNF-α and interferon-γ appear to

contribute to the biliary cell lysis observed in PBC<sup>[66]</sup>.

*Autoimmune cholangitis.* AIC is a recent entity in which liver biopsy findings are indistinguishable from classic PBC, but AMA positivity is lacking. Clinical and biochemical parameters are similar to PBC, except that in AIC other autoantibodies such as ANA and ASMA are often found in varying titers. The IgM titers are typically lower as well. These patients are treated as if they have PBC<sup>[67]</sup>.

*Primary sclerosing cholangitis.* PSC patients are more likely to be young men. PSC is associated with inflammatory bowel disease in 40% of cases<sup>[68]</sup>. Current information suggests immune-mediated damage of the biliary epithelium, although a precise mechanism has not been defined. Patients typically present with cholestasis, although occasionally jaundice and less commonly portal hypertension are present. Serum ANCA is positive in up to 80% of patients<sup>[69]</sup>. Both intra and extrahepatic bile ducts are involved, although a small percentage of patients have their disease confined to the hilar extrahepatic duct. Liver histology is not particularly useful in making the diagnosis, but does aid in the diagnosis of small-duct PSC (pericholangitis). Recurrent bacterial cholangitis as well as the development of cholangiocarcinoma and (in 15%-30% of cases) carcinoma of the colon constitute the morbid complications<sup>[70]</sup>. UDCA has no benefit in these patients regarding survival and quality of life. Whether other therapies such as FK-506 and colchicine offer significant benefit has not been established<sup>[71]</sup>.

*Idiopathic adulthood ductopenia.* This entity is rare and is defined by the presence of ductopenia (decrease of bile ducts in >50% of the portal triads) and cholestasis in the absence of known cholestatic liver disease. It is a diagnosis of exclusion<sup>[72]</sup>. In addition to ductopenia, the biopsy may show lymphocytic cholangitis and features of chronic cholestasis. In some patients the process progresses to biliary cirrhosis. A recent report suggests that UDCA may result in biochemical improvement<sup>[72]</sup>.

*Autoimmune hepatitis.* AIH can present as a primary cholestatic disorder<sup>[73]</sup>. By the criteria proposed by the International Autoimmune Hepatitis Group, a score can be calculated that defines the probability of a diagnosis of AIH. Patients are usually females (70% of cases) ANA and ASMA are present in the serum of the majority of patients. Furthermore hypergammaglobulinemia is present in 80% of cases. Associated autoimmune disorders include arthritis, rash, thyroiditis, Sjögren's syndrome, and ulcerative colitis<sup>[74]</sup>.

*Decompensated chronic liver disease.* Jaundice

may occur during the course of chronic hepatitis or cirrhosis. In cirrhosis, jaundice often is accompanied by other evidence of severe hepatocellular dysfunction and is a prognostically grave sign. Cirrhosis induced by extrahepatic obstruction is associated with increased levels of circulating endotoxins<sup>[75]</sup>, and elevated levels of proinflammatory cytokines can be documented in patients with cirrhosis of biliary or viral origin<sup>[76]</sup>.

## INFILTRATIVE DISEASES

*Granulomatous hepatitis.* GH is a common cause of cholestatic liver disease. Most often the liver manifestations are secondary to a more disseminated process, but isolated GH has been described<sup>[77]</sup>. GH is a well-described entity associated with a long list of causes, including sarcoidosis, infection (tubercular and fungal, especially histoplasmosis), hypersensitivity reaction, foreign-body reaction, malignant conditions, inflammatory bowel disease, drug reaction, and as a manifestation of other chronic liver disease<sup>[77]</sup>. In one series, approximately 20% of cases of patients with granulomas were attributed to associated liver conditions. On the other hand, idiopathic GH accounts for 5%-36% of cases in which hepatic granulomas are found<sup>[78]</sup>. Pathologically, hepatic granulomas are usually multiple nodular infiltrates consisting of aggregates of epithelioid cells or macrophages surrounded by a rim of mononuclear cells. Multinucleated giant cells are sometimes present. The normal architecture of the liver is usually not disturbed. In some cases, granuloma may be confined to the liver with no evidence of extrahepatic granulomatosis. Clinically, patients are often asymptomatic, and granulomas are found as part of a work-up for abnormal liver function tests or in the evaluation of fever of unknown origin (FUO). In studies of FUO, GH accounts for up to 13% of cases<sup>[79]</sup>. In GH, nonspecific symptoms are the rule, usually including malaise, anorexia, and fever. Manifestations of profound cholestasis or hepatic failure are rare<sup>[77]</sup>. In such cases, routine bacterial and fungal blood culture as well as special culture and stains of involved tissue would be required. GH tends to follow a benign course, with spontaneous recovery in most cases.

*Sarcoidosis.* Sarcoidosis is a systemic disease characterized by non-caseating granuloma of multiple organs. Seventy percent of patients have hepatic granuloma. Localization of portal granuloma may result in cholestasis with destruction of interlobular bile ducts<sup>[80]</sup>. A non-caseating granuloma indicates a combined role of activated CD4 T cells and macrophages. Elevated alkaline

phosphatase is the most characteristic abnormality found on liver testing and may be reduced by treatment with corticosteroids used to treat other manifestations of the disease. Concomitant intrathoracic disease, pulmonary symptoms, and significant anemia/leukopenia make this diagnosis very likely<sup>[81]</sup>.

**Lymphoma.** Between 3% and 10% of patients with lymphoma develop jaundice during the course of their disease and its treatment<sup>[82]</sup>. The causes of jaundice include hepatic infiltration, portal tract destruction, obstruction of the extrahepatic biliary tree, and jaundice associated with chemotherapy<sup>[82]</sup>. Histiocytic lymphoma may produce a rapidly progressive syndrome characterized by fever, hepatosplenomegaly, deep jaundice, lymphadenopathy, and pancytopenia. A rare syndrome of lymphoma<sup>a2</sup> associated idiopathic cholestasis has been reported most commonly with Hodgkin's disease, but may also occur with non-Hodgkin's lymphoma<sup>[84]</sup>.

**Fatty liver.** Fatty liver, or non-alcoholic steatohepatitis, most commonly occurs in middle-aged women with obesity, diabetes, and hyperlipidemia and a variety of other medical problems. Cholestasis can be seen in about 5% of patients with fatty liver<sup>[85]</sup>.

## SYSTEMIC DISEASES

**Bacterial infection (sepsis).** Mild hyperbilirubinemia develops in 1%-6% of patients with bacterial infections. The bilirubin is usually <170  $\mu\text{mol/L}$ . Serum alkaline phosphatase levels range from 1.5 to 3-fold above normal, whereas serum aminotransferases usually show less than a 2-fold increase<sup>[86]</sup>. The organisms most commonly associated with infections producing cholestatic jaundice are the gram-negative bacteria. Gram-positive infection from *Staphylococcus aureus*, in particular toxic shock syndrome and streptococcal pneumonia, may also be associated with jaundice<sup>[86]</sup>. The pathogenesis of cholestasis in sepsis is unclear, but direct hepatotoxicity from gram-negative bacterial endotoxins, gram-positive bacterial lipoteichoic acid, hepatic hypoxia, destruction of transfused red cells, and hematomas may all play a role. Endotoxins and inflammation-induced cytokines such as TNF are potent cholestatic agents<sup>[87-90]</sup>. Bile may also precipitate within larger intrahepatic bile ducts in conditions in which sepsis is playing a role, producing massive ductular dilatation with retained bile at the interface of the hepatic parenchyma and portal tracts, so-called "cholangitis lenta"<sup>[91]</sup>. Other uncommon infections may produce cholestatic jaundice include

leptospira, clostridium, and borrelia.

**Total parental nutrition.** TPN-associated cholestatic jaundice in adults usually follows infusions containing in excess of 60% of calories as lipids for a period longer than 3-4 weeks. Gallbladder stasis is almost universal in patients on TPN, with a marked increase in the incidence of gallstones<sup>[92]</sup>. If the TPN cannot be discontinued, it should be cycled around 10 hours per day. Excess caloric infusion can be avoided by keeping glucose <6 g/kg per day and lipid <2 g/kg per day. Recent reports have demonstrated improvement in cholestatic parameters by administration of UDCA<sup>[93]</sup>. Patients receiving hyperalimentation are susceptible to developing cholestasis because of the diminished stimulus to bile flow associated with the absence of oral feeding and release of hormones that stimulate bile flow<sup>[94]</sup>, as well as the direct oxidant stress to the liver. Whether there are toxic effects of the hyperalimentation solutions has never been clearly established<sup>[95]</sup>. However, hyperalimentation fluids are hypertonic and may aggravate a cholestatic state by further desiccating bile through osmotic effects<sup>[95]</sup>.

**Benign recurrent intrahepatic cholestasis.** BRIC is characterized by recurrent episodes of jaundice with pruritus, biochemical signs of cholestasis, and histological hepatocanicular bilirubinostasis, with normal intra- and extrahepatic bile ducts and absence of inflammation and fibrosis, absence of factors known to produce intrahepatic cholestasis such as drugs or pregnancy, and symptom-free intervals<sup>[96]</sup>. Cholestatic episodes may last for many months. BRIC may occur in sporadic or familial form; the latter has recently been attributed to genetic abnormalities on chromosome 18<sup>[97]</sup>. As in Byler disease, GGT is normal in the presence of high alkaline phosphatase. The episodes eventually resolve without morphological sequelae.

**Cholestasis of pregnancy.** This entity occurs recurrently in the third trimester of pregnancy in susceptible individuals and resolves after parturition. It is characterized by biochemical cholestasis with pruritus, usually accompanied by jaundice. Contraceptive drugs are a risk factor. Histology of the liver is similar to BRIC. It is associated with increased risk of premature delivery or stillborn births<sup>[98]</sup>. UDCA has been used with success<sup>[99]</sup>.

**Cystic fibrosis.** In the liver, mutation and deletion in cystic fibrosis transmembrane conductance regulator impair biliary secretion and result in cholestasis in 15% of cystic fibrosis patients<sup>[100]</sup>. UDCA also may be useful in these cases<sup>[101]</sup>. Biliary cirrhosis occurs in approximately

5% of patients and affects more males than females<sup>[100]</sup>.

**Disappearing intrahepatic bile ducts.** Disappearance of intrahepatic bile ducts occurs in a variety of congenital and disease conditions (Table 4). The pathogenic mechanism responsible for bile duct destruction remains poorly defined. Moreover, it is likely that multiple mechanisms are operative in individual diseases. The primary mechanism includes direct or indirect cytotoxicity of biliary epithelial cells, ischemic injury and necrosis, and progressive obliterative peribiliary fibrosis<sup>[102]</sup>.

**Table 4 Causes and syndromes of ductopenia in the adult patient**

Syndromatic ductopenia (Alagille syndrome)
Non-syndromatic adult ductopenia
Ductal plate malformation (congenital hepatic fibrosis, biliary atresia)
Primary biliary cirrhosis, autoimmune cholangitis
Primary sclerosing cholangitis
Chronic rejection
Graft-versus-host disease
Sarcoidosis
Cystic fibrosis
Byler disease (progressive familial intrahepatic cholestasis)
Histiocytosis X and
Different drugs (amoxicillin-clavulanic acid, carbamazepine)
Duct destruction after regional chemotherapy (e.g. floxuridine)
Idiopathic adulthood ductopenia

**Allograft rejection.** Causes of cholestasis after liver transplantation are multifactorial, including postoperative dysfunction of the biliary tree (ductular or vascular), infection, recurrence of the primary disease, drugs, and rejection. In both acute and chronic rejection, small bile ducts are destroyed, resulting in cholestatic changes. Alkaline phosphatase, bilirubin, and GGT, along with aminotransferases, are elevated. Because of their lack of specificity, histological evaluation is needed to make the diagnosis<sup>[103]</sup>.

**Graft-versus-host disease.** GVHD is the major complication of allogeneic bone marrow transplantation. Donor T cells recognize foreign host antigens in an immunocompromised host, resulting in injury to skin, intestine, and liver. In liver, the small bile duct cells are the primary targets of injury. The diagnosis is based on the development of rash, diarrhea, and elevated alkaline phosphatase. Acute GVHD usually begins in the third week, whereas chronic GVHD develops at around the sixth month after transplant. The extreme hyperbilirubinemia seems out of proportion to the degree of bile duct or hepatocellular damage<sup>[104]</sup>. Although liver biopsy can be

performed, skin or rectal biopsy is preferred.

**Sickle cell anemia.** In patients with sickle cell anemia, jaundice may occur from a variety of factors, including viral hepatitis, choledocholithiasis, hepatic sickle cell crisis, and a syndrome of severe intrahepatic cholestasis. Hepatic sickle cell crisis is characterized by severe right upper quadrant pain, fever, leukocytosis, jaundice, tender hepatomegaly, and moderate elevation of alkaline phosphatase. Resolution of acute symptoms with hydration and analgesia may be followed by persistent cholestatic jaundice for several weeks<sup>[105]</sup>.

**Postoperative jaundice.** The prevalence of jaundice following major surgery has been estimated at 17% for bilirubin levels of 2 mg/dl-4 mg/dl, with 4% of patients developing more pronounced elevations. The etiology of cholestatic jaundice in the postoperative period may be discrete or multifactorial. Responsible factors include sepsis, drug- or anesthetic-induced hepatitis, and obstruction of the biliary tree resulting from pancreatitis, choledocholithiasis, or direct injury to the biliary tree<sup>[106]</sup>. The entity termed "benign postoperative cholestatic jaundice" occurs between 1 and 10 days following major surgery. The jaundice may be profound, with a 2 to 4-fold elevation of alkaline phosphatase levels and only mild increases in serum aminotransferases. Liver biopsy reveals cholestasis without inflammation. The condition is self-limited and requires differentiation from obstructive jaundice<sup>[106]</sup>.

**Sweet's syndrome.** This is an idiopathic condition, but approximately 20% of patients have an associated malignancy<sup>[107]</sup>. The disease is thought to be a hypersensitivity reaction, either as a parainflammatory (e.g., infections, autoimmune disorders, vaccination) or paraneoplastic event. The most frequently observed neoplasm is acute myelogenous leukemia; lymphomas, chronic leukemia, myelomas, myelodysplastic syndromes, and a variety of solid tumors also are represented. The onset of Sweet's syndrome is widely distributed around the time of development of malignancy, appearing most often within 2 months before or after the clinical diagnosis of overt malignancy. A definitive derangement in neutrophil function in Sweet's syndrome has not been identified. Rather, elevated levels of circulating granulocyte colony-stimulating factor and IL-6 or of local cytokines have been implicated<sup>[108-110]</sup>.

## OTHER INTRAHEPATIC CAUSES OF CHRONIC CHOLESTASIS

Nodular regenerative hyperplasia (NRH), bone marrow transplant (BMT), connective tissue diseases (CTD), Felty's syndrome, mastocytosis,

hypereosinophilic syndrome, hyperthyroidism, and space occupying lesions that can lead to chronic intrahepatic cholestasis are listed in Table 1. The pathology of these entities is not discussed further here.

## CONCLUSIONS

The causes of cholestatic jaundice can usually be identified if one keeps in mind the important steps of transport of bilirubin and secretion of bile flow through the intra and extrahepatic biliary tree.

Most causes of cholestatic jaundice are a result of diseases of the liver or biliary tract, including intrahepatic forms caused by drugs, alcohol, infection, and destruction of the interlobular ducts. In postoperative jaundice, multiple mechanisms, such as a combination of pigment load with hypoxic injury to the liver, can result in jaundice. It is easy to visualize how mechanical obstruction of the biliary tree will give rise to jaundice, as in a patient with carcinoma of the bile duct or PSC. There is no substitute for a good history, physical examination, and review of the standard chemistries. With the initial information, the correct diagnosis can be made 85% of the time. In the remaining cases, non-invasive scanning procedures will help in confirming suspicions, but the final diagnosis will usually be made only with direct forms of cholangiography and/or liver biopsy. Occasionally we encounter a case of cholestatic jaundice where we cannot readily establish the diagnosis. Tincture of time generally will lead to the appearance of further signs and symptoms that eventually will clarify the disease.

In every case, the responsibility rests on the physician to adopt a thoughtful approach to minimize risk, expense, and time involved in obtaining sufficient information for a definitive diagnosis and treatment.

## REFERENCES

- 1 Stazi F, Fareello P, Stazi C. Intrahepatic cholestasis. *Clin Ter*, 1996; 147:575-583
- 2 Scharschmidt BF, Goldberg HI, Schmid R. Current concepts in diagnosis. Approach to the patient with cholestatic jaundice. *N Engl J Med*, 1983;308:1515-1519
- 3 Frank BB. Clinical evaluation of jaundice. A guideline of the Patient Care Committee of the American Gastroenterological Association. *JAMA*, 89;262:3031-3034
- 4 Moseley RH. A molecular basis for jaundice in intrahepatic and extrahepatic cholestasis. *Hepatology*, 1997;6:1682-1684
- 5 Crawford JM. Cellular and molecular biology of the inflamed liver. *Curr Opin Gastroenterol*, 1997;13:175-185
- 6 Uhl B, Speth V, Wolf B, Jung G, Bessler WG, Hauschildt S. Rapid alterations in the plasma membrane structure of macrophages stimulated with bacterial lipopeptides. *Eur J Cell Biol*, 1992;58: 90-98
- 7 Spitzer JA, Zhang P. Hepatic cellular interactions in endotoxaemia and sepsis. *Biochem Soc Trans*, 1995;23:993-998
- 8 Roelofsen H, Schoemaker B, Bakker C, Ottenhoff R, Jansen PLM, Elferink RPJO. Impaired hepatocanicular organic anion transport in endotoxemic rats. *Am J Physiol*, 1995;269:G427-G434
- 9 Moseley RH, Wang W, Takeda H, Lown K, Shick L, Ananthanarayanan M, Suchy FJ. Effect of endotoxin on bile acid transport in rat liver: a potential model for sepsis-associated cholestasis. *Am J Physiol*, 1996;271: G137-G146
- 10 Ayres RCS, Neuberger JM, Shaw J, Joplin R, Adams DH. Intercellular adhesion molecule-1 and MHC antigens on human intrahepatic bile duct cells: effect of pro-inflammatory cytokines. *Gut*, 1993;34:1245-1249
- 11 Edoute Y, Lachter J, Furman E, Assy N. Severe cholestatic jaundice induced by EBV infection in the elderly. *J Gastroenterol Hepatol*, 1998;13:821-824
- 12 McKnight JT, Jones JE. Jaundice. *Am Fam Physician*, 1992;45: 1139-1148
- 13 Fisher DA, Wright TL. Pruritus as a symptom of hepatitis C. *J Am Acad Dermatol*, 1994;30:629-632
- 14 Mainenti PP, Petrelli G, Lamanda R, Amalfi G, Castiglione F. Primary systemic amyloidosis with giant hepatomegaly and a swiftly progressive course. *J Clin Gastroenterol*, 1997; 24:173-175
- 15 Chang HC, Nguyen B, Regan F. Hepatomegaly and multiple liver lesions. *Post grad Med J*, 1998;74:439-440
- 16 Shah SH, Hayes PC, Allan PL, Nicoll J, Finlayson ND. Measurement of spleen size and its relation to hypersplenism and portal hemodynamics in portal hypertension due to hepatic cirrhosis. *Am J Gastroenterol*, 1996;91:2580-2583
- 17 O'Reilly RA. Splenomegaly in 2505 patients at a large university medical center from 1913 to 1995. 1963 to 1995: 449 patients. *West J Med*, 1998;169:88-97
- 18 Bass NM. An integrated approach to the diagnosis of jaundice. In: Neil Kaplowitz, eds. Liver and biliary disease. Baltimore: Williams & Wilkins, 1996:651-672
- 19 Pasanen PA, Pikkarainen P, Alhava E, Partanen K, Janatuinen E. Evaluation of a computer-based diagnostic score system in the diagnosis of jaundice and cholestasis. *Scand J Gastroenterol*, 1993; 28:732-736
- 20 Brice P. Staging of Hodgkin's disease. *Rev Prat*, 1998;48:1070-1074 (in French with English Abstract)
- 21 Khan MA, Khan AA, Shafqat F. Comparison of ultrasonography and cholangiography (ERCP/PTC) in the differential diagnosis of obstructive jaundice. *JPMA J Pak Med Assoc*, 1996; 46:188-190
- 22 Liu CL, Lo CM, Lai EC, Fan ST. Endoscopic retrograde cholangiopancreatography and endoscopic endoprosthesis insertion in patients with Klatskin tumors. *Arch Surg*, 1998;133: 293-296
- 23 de Ledinghen V, Lecesne R, Raymond JM, Gense V, Amouretti M, Drouillard J, Couzigou P, Silvain C. Diagnosis of choledocholithiasis. EUS or magnetic resonance cholangiography. A prospective controlled study. *Gastrointest Endosc*, 1999;49:26-31
- 24 Dixit VK, Jain AK, Agrawal AK, Gupta JP. Obstructive jaundice-a diagnostic appraisal. *J Assoc Physicians India*, 1993;41:200-202
- 25 Roca I, Ciofetta G. Hepatobiliary scintigraphy in current pediatric practice. *Q J Nucl Med*, 1998;42:113-118
- 26 Mendler MH, Bouillet P, Sautereau D, Chaumerliac P, Cessot F, Le Sidaner A, Pillegand B. Value of MR cholangiography in the diagnosis of obstructive diseases of the biliary tree: a study of 58 cases. *Am J Gastroenterol*, 1998;93:2482-2490
- 27 Meduri B, Aubert A, Chiche R, Fritsch J. Laparoscopic cholecystectomy and lithiasis of the common bile duct: prospective study on the importance of preoperative endoscopic ultrasonography and endoscopic retrograde cholangiography. *Gastroenterol Clin Biol*, 1998;22: 759-765
- 28 Froehlich F, Lamy O, Fried M, Gonvers JJ. Practice and complications of liver biopsy: results of a nationwide survey in Switzerland. *Dig Dis Sci*, 1993;38:1480-1484
- 29 Garcia-Tsao G, Boyer JL. Outpatient liver biopsy: how safe is it. *Ann Intern Med*, 1993;118:150-153
- 30 Tobkes AI, Nord HJ. Liver biopsy: review of methodology and complications. *Dig Dis*, 1995;13:267-274
- 31 Sawyerr AM, McCormick PA, Tennyson GS, Chin J, Dick R, Scheuer PJ, Burroughs AK, McIntyre N. A comparison of transjugular and plugged-percutaneous liver biopsy in patients with impaired coagulation. *J Hepatol*, 1993;17:81-85
- 32 Desmet VJ. Cholestasis: extrahepatic obstruction and secondary biliary cirrhosis. In: MacSween RNM, Anthony PP, Scheuer PJ, Burt AD, Portmann BC, eds. Pathology of the liver. Edinburgh: Churchill Livingstone, 1994;425-476
- 33 Van Ness MM, Diehl AM. Is liver biopsy useful in the evaluation of patients with chronically elevated liver enzymes. *Ann Intern Med*, 1989;111:473-478



- 34 Jenkins D, Gilmore IT, Doel C, Gallivan S. Liver biopsy in the diagnosis of malignancy. *Q J Med*, 1995;88:819-825
- 35 Snover DC. Biopsy diagnosis of liver disease. *Baltimore: Williams & Wilkins*, 1992:28
- 36 Jensen K, Gluud C. The Mallory body: morphological, clinical and experimental studies (Part I of a literature survey). *Hepatology*, 1994;20:1061-1077
- 37 Mergener K, Enns R, Eubanks WS, Baillie J, Branch MS. Pseudo-Mirizzi syndrome in acute cholecystitis. *Am J Gastroenterol*, 1998;93:2605-2606
- 38 Seitz U, Bapaye A, Bohnacker S, Navarrete C, Maydeo A, Soehendra N. Advances in therapeutic endoscopic treatment of common bile duct stones. *World J Surg*, 1998;22:1133-1144
- 39 Csendes A, Diaz JC, Burdiles P, Maluenda F, Morales E. Risk factors and clas40 Teehey SA, Baron RL, Rohrmann CA, Shuman WP, Freeny PC. Sclerosing cholangitis: CT findings. *Radiology*, 1988;169:635-639
- 41 Smits ME, Rauws EA, van Gulik TM, Gouma DJ, Tytgat GN, Huibregtse K. Long-term results of endoscopic stenting and surgical drainage for biliary stricture due to chronic pancreatitis. *Br J Surg*, 1996;83:764-768
- 42 Cello JP. Acquired immunodeficiency syndrome cholangiopathy: spectrum of disease. *Am J Med*, 1989;86:539-546
- 43 Pasanen PA, Partanen KP, Pikkarainen PH, Alhava EM, Janatuinen EK, Pirinen A E. A comparison of ultrasound, computed tomography and endoscopic retrograde cholangiopancreatography in the differential diagnosis of benign and malignant jaundice and cholestasis. *Eur J Surg*, 1993;159:23-29
- 44 Iwatsuki S, Todo S, Marsh JW, Madariaga JR, Lee RG, Dvorchik I, Fung JJ, Starzl TE. Treatment of hilar cholangiocarcinoma (Klatskin tumors) with hepatic resection or transplantation. *J Am Coll Surg*, 1998;187:358-364
- 45 Wetter LA, Ring EJ, Pellegrini CA, Way LW. Differential diagnosis of sclerosing cholangiocarcinomas of the common hepatic duct (Klatskin tumors). *Am J Surg*, 1991;161:57-62
- 46 Fidias P, Carey RW, Grossbard ML. Non-Hodgkin's lymphoma presenting with biliary tract obstruction. A discussion of seven patients and a review of the literature. *Cancer*, 1995;75:1669-1677
- 47 Buckmaster MJ, Schwartz RW, Carnahan GE, Strodel WE. Hepatocellular carcinoma embolus to the common hepatic duct with no detectable primary hepatic tumor. *Am Surg*, 1994;60:699-702
- 48 Maes M, Depardieu C, Dargent JL, Hermans M, Verhaeghe JL, Delabie J, Pittaluga S, Troufleau P, Verhest A, De Wolf-Peeters C. Primary low-grade B-cell lymphoma of MALT-type occurring in the liver: a study of two cases. *J Hepatol*, 1997;27:922-927
- 49 Jesudason SR, Govil S, Mathai V, Kuruvilla R, Muthusami JC. Choledochal cysts in adults. *Ann R Coll Surg Engl*, 1997;79:410-413
- 50 Mosenkis BN, Brandt LJ. Bleeding causing biliary obstruction after endoscopic sphincterotomy. *Am J Gastroenterol*, 1997;92:708-709
- 51 Liu LX, Harinasuta KT. Liver and intestinal flukes. *Gastroenterol Clin North Am*, 1996;25:627-636
- 52 Forbes A, Blanshard C, Gazzard B. Natural history of AIDS related sclerosing cholangitis: a study of 20 cases. *Gut*, 1993;34:116-121
- 53 Farrell GC. Drug-induced hepatic injury. *J Gastroenterol Hepatol*, 1997;12:S242-S250
- 54 Erlinger S. Drug-induced cholestasis. *J Hepatol*, 1997;26(suppl 1):1-4
- 55 Feuer G, Di Fonzo CJ. Intrahepatic cholestasis: a review of biochemical-pathological mechanisms. *Drug Metabol Drug Interact*, 1992;10:1-161
- 56 Ludwig J, Kim CH, Wiesner RH, Krom RA. Floxuridine-induced sclerosing cholangitis: an ischemic cholangiopathy. *Hepatology*, 1989;9:215-218
- 57 Sherlock S. The syndrome of disappearing intrahepatic bile ducts. *Lancet*, 1987;2:493-496
- 58 Nissenbaum M, Chedid A, Mendenhall C, Gartside P. Prognostic significance of cholestatic alcoholic hepatitis. *Dig Dis Sci*, 1990;35:891-896
- 59 Schiff ER. Atypical clinical manifestations of hepatitis A. *Vaccine*, 1992;10(Suppl 1):S18-S20
- 60 Chia SC, Bergasa NV, Kleiner DE, Goodman Z, Hoofnagle JH, Di Bisceglie AM. Pruritus as a presenting symptom of chronic hepatitis C. *Dig Dis Sci*, 1998;43:2177-2183
- 61 Khuroo MS, Rustgi VK, Dawson GJ, Mushahwar IK, Yattoo GN, Kamili S, Khan BA. Spectrum of hepatitis E virus infection in India. *J Med Virol*, 1994;43:281-286
- 62 Edoute Y, Baruch Y, Lachter J, Furman E, Bassan L, Assy N. Severe cholestatic jaundice induced by Epstein Barr virus infection in the elderly. *J Gastroenterol Hepatol*, 1998;13:821-824
- 63 Lefkowitz JH. The liver in AIDS. *Semin Liver Dis*, 1997;17:335-344
- 64 Leung PS, Coppel RL, Ansari A, Munoz S, Gershwin ME. Antimitochondrial antibodies in primary biliary cirrhosis. *Semin Liver Dis*, 1997;17:61-69
- 65 Heathcote J. Treatment of primary biliary cirrhosis. *J Gastroenterol Hepatol*, 1996;11:605-609
- 66 Bloom S, Fleming K, Chapman R. Adhesion molecule expression in primary sclerosing cholangitis and primary biliary cirrhosis. *Gut*, 1995;36:604-609
- 67 Sherlock S. Ludwig Symposium on biliary disorders. Autoimmune cholangitis: a unique entity. *Mayo Clin Proc*, 1998;73:184-190
- 68 Ponsioen CI, Tytgat GN. Primary sclerosing cholangitis: a clinical review. *Am J Gastroenterol*, 1998;93:515-523
- 69 Bansil DS, Fleming KA, Chapman RW. Importance of antineutrophil cytoplasmic antibodies in primary sclerosing cholangitis and ulcerative colitis: prevalence, titre, and IgG subclass. *Gut*, 1996;38:384-389
- 70 Chapman RW. The colon and PSC: new liver, new danger? *Gut*, 1998;43:595-596
- 71 Stiehl A. Ursodeoxycholic acid therapy in treatment of primary sclerosing cholangitis. *Scand J Gastroenterol Suppl*, 1994;204:59-61
- 72 Ludwig J. Idiopathic adulthood ductopenia: an update. *Mayo Clin Proc*, 1998;73:285-291
- 73 Motoo Y, Sawabu N, Watanabe H, Okai T, Nakanuma Y. Prolonged intrahepatic cholestasis in acute-onset, severe autoimmune hepatitis. *J Gastroenterol*, 1997;32:410-413
- 74 Czaja A, Carpenter HA. Validation of scoring system for diagnosis of autoimmune hepatitis. *Dig Dis Sci*, 1996;41:305-314
- 75 Grinko I, Geerts A, Wisse E. Experimental biliary fibrosis correlates with increased numbers of fat-storing and Kupffer cells, and portal endotoxemia. *J Hepatol*, 1995;23:449-458
- 76 Shindo M, Mullin GE, Braun-Elwert L, Bergasa NV, Jones EA, James SP. Cytokine mRNA expression in the liver of patients with primary biliary cirrhosis (PBC) and chronic hepatitis B (CHB). *Clin Exp Immunol*, 1996;105:254-259
- 77 Sartin JS, Walker RC. Granulomatous hepatitis: a retrospective review of 88 cases at the Mayo Clinic. *Mayo Clin Proc*, 1991;66:914-918
- 78 McCluggage WG, Sloan JM. Hepatic granulomas in Northern Ireland: a thirteen year review. *Histopathology*, 1994;25:219-228
- 79 Zoutman DE, Ralph ED, Frei JV. Granulomatous hepatitis and fever of unknown origin. An 11-year experience of 23 cases with three years' follow-up. *J Clin Gastroenterol*, 1991;13:69-75
- 80 Moreno-Merlo F, Wanless IR, Shimamatsu K, Sherman M, Greig P, Chiasson D. The role of granulomatous phlebitis and thrombosis in the pathogenesis of cirrhosis and portal hypertension in sarcoidosis. *Hepatology*, 1997;26:554-560
- 81 Albu E, Saraiya RJ, Carvajal SJ, Sehonanda A, Balar N, Gerst PH. Sarcoidosis presenting as obstructive jaundice. *Am Surg*, 1995;61:516-517
- 82 Abe H, Kubota K, Makuuchi M. Obstructive jaundice secondary to Hodgkin's disease. *Am J Gastroenterol*, 1997;92:526-527
- 83 Young IF, Roberts Thomson IC, Sullivan JR. Histiocytic lymphoma presenting with extrahepatic biliary obstruction: a report of three cases. *Aust N Z J Surg*, 1981;51:181-183
- 84 Hubscher SG, Lumley MA, Elias E. Vanishing bile duct syndrome: a possible mechanism for intrahepatic cholestasis in Hodgkin's lymphoma. *Hepatology*, 1993;17:70-77
- 85 French SW, Nash J, Shitabata P, Kachi K, Hara C, Chedid A, Mendenhall CL. Pathology of alcoholic liver disease. VA Cooperative Study Group 119. *Semin Liver Dis*, 1993;13:154-169
- 86 Navasa M, Rimola A, Rodes J. Bacterial infections in liver disease. *Semin Liver Dis*, 1997;17:323-333
- 87 Green RM, Whiting JF, Rosenbluth AB, Beier D, Gollan JL. Interleukin-6 inhibits hepatocyte taurocholate uptake and sodium potassium adenosinetriphosphatase activity. *Am J Physiol*, 1994;267:G1094-G1100
- 88 Green RM, Crawford JM. Hepatocellular cholestasis: pathobiology and histological outcome. *Semin Liver Dis*, 1995;15:372-389
- 89 Moseley RH. Sepsis-associated cholestasis. *Gastroenterology*, 1997;112:302-306
- 90 Shiomi M, Wakabayashi Y, Sano T, Shinoda Y, Nimura Y,

- Ishimura Y, Suematsu M. Nitric oxide suppression reversibly attenuates mitochondrial dysfunction and cholestasis in endotoxemic rat liver. *Hepatology*, 1998;27:108-115
- 91 Lefkowitz JH. Bile ductular cholestasis. an ominous histopathologic sign related to sepsis and "cholangitis lenta". *Hum Pathol*, 1982;13:19-24
  - 92 Klein S, Nealon WH. Hepatobiliary abnormalities associated with total parenteral nutrition. *Semin Liver Dis*, 1988;8:237-246
  - 93 Spagnuolo MI, Iorio R, Vegnente A, Guarino A. Ursodeoxycholic acid for treatment of cholestasis in children on long-term total parenteral nutrition: a pilot study. *Gastroenterology*, 1996;111:716-719
  - 94 Wiechmann DA, Heubi JH. Pediatric hepatobiliary disease. *Curr Opin Gastroenterol*, 1997;13:427-431
  - 95 Bhatia J, Moslen MT, Haque AK, McCleery R, Rassin DK. Total parenteral nutrition associated alterations in hepatobiliary function and histology in rats: is light exposure a clue. *Pediatr Res*, 1993;33:487-492
  - 96 Nakamuta M, Sakamoto S, Miyata Y, Sato M, Nawata H. Benign recurrent intrahepatic cholestasis: a long-term follow-up. *Hepatogastroenterology*, 1994;41:287-289
  - 97 Bull LN, van Eijk MJ, Pawlikowska L, De Young JA, Juijn JA, Liao M, Klomp LW, Lomri N, Berger R, Scharschmidt BF, Knisely AS, Houwen RH, Freimer NB. A gene encoding a P-type ATP ase mutated in two forms of hereditary cholestasis. *Nat Genet*, 1998;18:219-224
  - 98 Assy N, Minuk GY. Liver disease in pregnancy. *J Am Coll Surg*, 1996;183:643-653
  - 99 Diaferia A, Nicastrì PL, Tartagni M, Loizzi P, Iacovizzi C, Di Leo A. Ursodeoxycholic acid therapy in pregnant women with cholestasis. *Int J Gynaecol Obstet*, 1996;52:133-140
  - 100 Strazzabosco M. Transport systems in cholangiocytes: their role in bile formation and cholestasis. *Yale J Biol Med*, 1997;70:427-434
  - 101 Lindblad A, Glaumann H, Strandvik B. A two-year prospective study of the effect of ursodeoxycholic acid on urinary bile acid excretion and liver morphology in cystic fibrosis associated liver disease. *Hepatology*, 1998;27:166-174
  - 102 Woolf GM, Vierling JM. Disappearing intrahepatic bile ducts: the syndromes and their mechanisms. *Semin Liver Dis*, 1993;13:261-275
  - 103 Mor E, Solomon H, Gibbs JF, Holman MJ, Goldstein RM, Husberg BS, Gonwa TA, Klintmalm GB. Acute cellular rejection following liver transplantation: clinical pathologic features and effect on outcome. *Semin Liver Dis*, 1992;12:28-40
  - 104 Crawford JM. Graft-versus-host disease of the liver. In: Ferrara JLM, Deeg J, Burakoff S, eds. Graft-versus-host disease. *New York: Marcel Dekker*, 1996:315-336
  - 105 Krauss JS, Freant LJ, Lee JR. Gastrointestinal pathology in sickle cell disease. *Ann Clin Lab Sci*, 1998;28:19-23
  - 106 Becker SD, Lamont JT. Postoperative jaundice. *Semin Liver Dis*, 1988;8:183-190
  - 107 Cohen PR, Talpaz M, Kurzrock R. Malignancy associated Sweet's syndrome: review of the world literature. *J Clin Oncol*, 1988;6:1887-1897
  - 108 Reuss-Borst MA, Pawelec G, Saal JG, Horny HP, Muller CA, Waller HD. Sweet's syndrome associated with myelodysplasia: possible role of cytokines in the pathogenesis of the disease. *Br J Haematol*, 1993;84:356-358
  - 109 Park JW, Mehrotra B, Barnett BO, Baron AD, Venook AP. The Sweet syndrome during therapy with granulocyte colon-stimulating factor. *Ann Intern Med*, 1992;116:996-998
  - 110 Paydas S, Sahin B, Seyrek E, Soylu M, Gonlusen G, Acar A, Tuncer I. Sweet's syndrome associated with G-CSF. *Br J Haematol*, 1993;85:191-192

Edited by MA Jing-Yun

# Clarithromycin resistance in *Helicobacter pylori* and its clinical relevance

Xia<sup>1</sup> Harry Hua-Xiang, FAN Xue-Gong and Talley<sup>1</sup> Nicholas J.

**Subject headings** *Helicobacter pylori*; *Helicobacter* infections; clarithromycin resistance

## INTRODUCTION

The macrolide clarithromycin has emerged as the most important antibiotic in combined therapy for eradication of *H. pylori* infection<sup>[1,2]</sup>. However, concerns about increasing clarithromycin resistance in *H. pylori* and its impact on the efficacy of eradication therapy have been raised since its widespread acceptance in *H. pylori* therapy<sup>[3,4]</sup>. Here, we sought to review the geographic prevalence of clarithromycin resistance in *H. pylori* and its molecular mechanisms, and assess the clinical relevance of clarithromycin resistance.

## Geographic prevalence of clarithromycin resistant *H. pylori*

The worldwide, prevalence of primary (pre-treatment) clarithromycin resistance to *H. pylori* ranges from 0.8% to 18% (Figure 1)<sup>[5-29]</sup>. The reported prevalence in China is between 4.8% and 7.5%, while the rate in Australia ranges from 6.1% to 7.8%<sup>[5,6,11,12]</sup>.

## Molecular mechanisms of clarithromycin resistance

Versalovic *et al* were the first to identify an A→G transition mutation within a conserved loop of 23S rRNA of *H. pylori*, and its association with clarithromycin-resistance<sup>[30]</sup>. The mutation occurs commonly at two gene positions cognate with positions 2058 and 2059 of *Escherichia coli*-23S rRNA, which were re-named 2143 and 2144, and now revised as 2142 and 2143, respectively<sup>[4,31]</sup>. Point mutations may occasionally occur at other positions, and can be a transition (A→G) or a transversion (A→C), but the transition is far more frequent<sup>[4,32-35]</sup>. Moreover, Versalovic *et al*<sup>[32]</sup> also observed that the A2142G mutation was associated with a high level of resistance (MIC>64 mg/L)

than the A2143G mutation<sup>[32]</sup>. These observations are supported by others studies<sup>[33,36]</sup>.

It has been reported that macrolide-resistance was not stable in some strains of *H. pylori in vitro*<sup>[17]</sup>. This phenomenon was also observed *in vivo*; i.e., strains developed resistance post-treatment and then reverted to being susceptible after a period of follow-up<sup>[17,30]</sup>. Versalovic *et al* cultured five genotypically identical isolates subsequently from one patient before and after treatment with clarithromycin alone<sup>[30]</sup>. They observed that the first two post-treatment isolates with a low-level clarithromycin resistance had an A2143G mutation, which was not present in the susceptible pretreatment isolate or in the last two post-treatment isolates with reverted susceptibility<sup>[30]</sup>. This suggests that the mutation may be unstable<sup>[35]</sup>. However, Hulten *et al* reported that clarithromycin resistance was stable after 50 subcultures *in vitro*<sup>[35]</sup>, which is consistent with other studies<sup>[37]</sup>.

Cross-resistance between macrolides in *H. pylori* has been observed<sup>[12,17,30]</sup>. Generally, *H. pylori* strains resistant to clarithromycin are also resistant to erythromycin, azithromycin and roxithromycin or vice versa. These observations have been confirmed at the molecular level<sup>[36]</sup>.

## Detection of clarithromycin resistance in *H. pylori*

The methods currently used for susceptibility testing of *H. pylori* to clarithromycin include agar dilution method, broth dilution method, disc diffusion test and the Epsilometer test (E-test)<sup>[17,38]</sup>. The agar dilution method determines the minimal inhibitory concentrations (MICs) of antibiotics against bacteria. This method is time consuming and not feasible for routine use. However, it is a reliable technique which is usually carried out as a reference method for other techniques<sup>[17,38,39]</sup>. Broth dilution method is rarely used because of the difficulty in growing *H. pylori* in broth. The disc diffusion test is the easiest and cheapest way of testing susceptibility. However, this test requires strict standardization before it can be used<sup>[39]</sup>. The E-test, developed in 1988, provides the MIC of a strain directly by using a diffusion-like method<sup>[40]</sup>. A plastic-coated strip contains a preformed antimicrobial gradient on one side and a scale on the other. The reading is taken at the point where the

<sup>1</sup>Department of Medicine, University of Sydney, Nepean Hospital, Sydney, Australia

<sup>2</sup>Department of Infectious Diseases, Xiang-Ya Hospital, Hunan Medical University, The People's Republic of China

**Correspondence to:** Harry Hua-Xiang Xia, Clinical Sciences Building, Department of Medicine, The University of Sydney, Nepean Hospital, P.O. Box 63, Penrith NSW 2751, Australia  
Tel. +61 • 2 • 47 • 242682, Fax. +61 • 2 • 47 • 242614  
Email. xia@med.usyd.edu.au

Received 1999-04-08

ellipse of growth inhibition intersects the strip. Standardization and correlation with the agar dilution method are also required prior to application. This method is now widely used by many investigators<sup>[12,13,15,16,18,22-28]</sup>. At present, no "gold standard" method has been proposed for testing *H. pylori* susceptibility to antibiotics including clarithromycin and metronidazole, as there is still a need for standardization regarding the appropriate medium, the supplementation, the size of the inoculum, the incubation atmosphere, the appropriate time to read the plates and the breakpoint differentiating resistance and susceptibility<sup>[38]</sup>. Since cross-resistance exists between macrolides, erythromycin susceptibility testing may be useful in predicting (determining) clarithromycin resistant *H. pylori* strains<sup>[12,17]</sup>. Erythromycin susceptibility testing is well established in many microbiological laboratories, and it is much cheaper than clarithromycin susceptibility testing at present.

The association between point mutations on the 23S rRNA gene and macrolide resistance in *H. pylori* potentially provides a new approach for diagnosing macrolide resistant *H. pylori* strains. Although cycle DNA sequencing of the 23S rRNA gene amplicons is regarded as the reference method, simpler techniques have been developed<sup>[38]</sup>. These include polymerase chain reaction based restriction fragment length polymorphism (PCR-RFLP), an oligonucleotide ligation assay (PCR-OLA), a DNA enzyme immunoassay (PCR-DEIA), a reverse hybridisation line probe assay (PCR-LiPA), and a preferential homoduplex formation assay (PCR-PHFA)<sup>[30,31,33,41-43]</sup>. The PCR-based molecular techniques are quicker than microbiological susceptibility testing, and more importantly, they can be performed directly on gastric biopsies and gastric juice<sup>[10,44,45]</sup>.

### **Clinical relevance of clarithromycin resistance in *H. pylori***

Studies have shown that clarithromycin resistance in *H. pylori* substantially affects the success rate of eradication regimens containing clarithromycin (Table 1). Generally, dual therapy with an antisecretory agent (e.g., H<sub>2</sub> antagonist or proton pump inhibitor) and clarithromycin achieves eradication rates of 60% to 80% for susceptible strains, but less than 40% for resistance strains (Table 1). Triple therapy with an antisecretory agent, clarithromycin and another antibiotic (i.e., amoxycillin or metronidazole) increases the eradication rates to 80%-95% for susceptible strains, but the rates remain under 40% for resistant ones (Table 1). A preliminary study reported that a combination of ranitidine bismuth citrate and

clarithromycin eradicated *H. pylori* at a rate of 98% and 92%, respectively, for both susceptible and resistant strains, but remains to be confirmed<sup>[13]</sup>.

Current anti *H. pylori* treatment regimens consisting of clarithromycin do not achieve an eradication rate of 100%. Emergence of clarithromycin-resistant strains during ineffective treatment has also been observed; the prevalence of clarithromycin-resistant strains cultured after treatment ranges between 40% and 100% (Table 1). This implies a likelihood of potential spread of clarithromycin-resistant strains in the population. Thus, the prevalence of clarithromycin resistance in *H. pylori* may exhibit a similar trend to the prevalence of metronidazole resistance in *H. pylori*. In Ireland, the prevalence of metronidazole resistant strains was 7% in 1989, 34% in 1992 and 38% in 1996<sup>[17]</sup>. In Australia, the prevalence of metronidazole resistance was 17% in 1988, but increased to 40% in 1995 and over 60% in 1998<sup>[11,47]</sup>. It is most likely that this increase is due to the use of metronidazole as a key agent in classic triple therapy (consisting of bismuth, metronidazole and tetracycline or amoxycillin), or increased use of this drug for other infections. Similarly, the current prevalence of clarithromycin-resistant strains of 6%-8% in Australia is much higher than the rate of 1.9% reported four years ago in this country<sup>[11,12,48]</sup>. This increase in the prevalence of clarithromycin resistance has been also reported in Europe and the United States<sup>[14,20,27,49]</sup>. It is assumed that prescriptions of macrolides, especially the new members such as spiramycin, roxithromycin, azithromycin and clarithromycin have been increased over the past years for the treatment of respiratory infection, sexually transmitted diseases and other infectious diseases. Thus, patients treated with any member of macrolides alone may select macrolide resistant *H. pylori* organisms (if infected), as cross-resistance exists between macrolides.

Overall, *H. pylori* resistance to clarithromycin is of less clinical relevance as compared with resistance to metronidazole, mainly because of the low prevalence and the possible reversibility of resistance in some strains. Susceptibility testing is not routinely required before treatment because of the low prevalence of clarithromycin resistance (Figure 1). However, *H. pylori* should be cultured and tested for clarithromycin susceptibility in patients who have failed the therapy containing clarithromycin (Table 1). Moreover, any previous use of macrolides not aimed at anti-*H. pylori* infection should be also taken into account when clarithromycin is chosen for eradication of *H. pylori*.

**Table 1** Effect of primary clarithromycin resistance on the efficacy of eradication therapy for *Helicobacter pylori* infection

Authors	Treatment regimens	Eradication rate (%)		Prevalence of resistant strains post-treatment (%)*
		Susceptible strains	Resistant strains	
Liu <i>et al.</i> , 1996 <sup>[5]</sup>	LFC or BFC	98(45/46)	0(0/4)	100(5/5)
Suzuki <i>et al.</i> , 1998 <sup>[8]</sup>	LAC	94(66/70)	0(0/1)	40(2/5)
Miyaji <i>et al.</i> , 1997 <sup>[9]</sup>	OC or LC	64(9/14)	0(0/5)	80(20/25)
	OAC or LAC	85(57/67)	28(2/7)	(Overall)
	OCM or LCM	86(68/79)	38(3/8)	
Maeda <i>et al.</i> , 1998 <sup>[10]</sup>	LAC	85(29/34)	40(2/5)	63(5/8)
Megraud <i>et al.</i> , 1997 <sup>[13]</sup>	OC	70(33/47)	38(3/8)	81(17/21)
	RbCC	98(42/43)	92(11/12)	(Overall)
Debets-Ossenkopp <i>et al.</i> , 1996 <sup>[16]</sup>	RC	81(58/72)	0(0/1)	73(11/15)
Tompkins <i>et al.</i> , 1997 <sup>[18]</sup>	OC	80(101/127)	0(0/4)	74(14/19)
Moayyedi <i>et al.</i> , 1998 <sup>[19]</sup>	OCT	91(104/114)	40(2/5)	Nor reported
Schutze <i>et al.</i> , 1996 <sup>[24]</sup>	RC	75(21/28)	20(1/5)	91(10/11)
Laine <i>et al.</i> , 1998 <sup>[25]</sup>	AC	35(73/208)	7.7(2/2.6)	53(70/131)
	OAC	81(153/190)	27(4/15)	(Overall)
Yousfi <i>et al.</i> , 1996 <sup>[26]</sup>	RanMC	87(20/23)	25(1/4)	67(4/6)
Buckley <i>et al.</i> , 1997 <sup>[46]</sup>	OMC	85(71/84)	0(0/3)	58(7/12)

O, omeprazole; C, clarithromycin; A, amoxycillin; Ran, ranitidine; M, metronidazole; Rbc, ranitidine bismuth citrate; L, lansoprazole; Rox, Roxithromycin; B, colloidal bismuth subcitrate (CBS).

\*The number of resistant strains post treatment was greater than the number of resistant strains before treatment in all the studies, suggesting acquisition of clarithromycin resistance during the unsuccessful treatment.

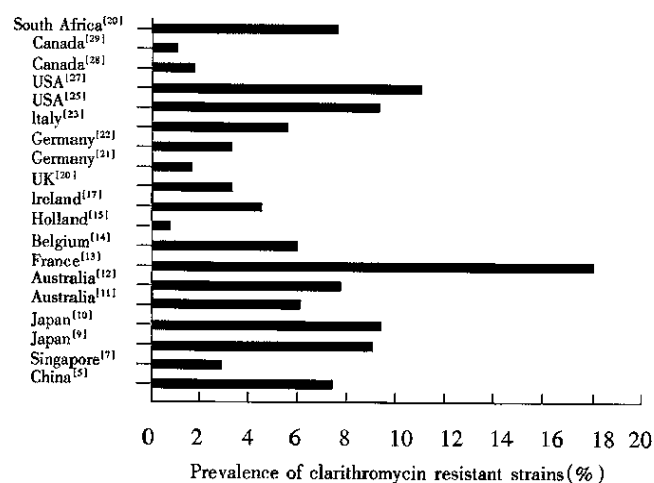


**Figure 1** Worldwide prevalence of clarithromycin resistant *H. pylori* strains. Each of these studies included at least 50 strains. The number after each country is the reference number.

### Conclusions

The prevalence of clarithromycin resistant *H. pylori* is low, but appears to be increasing. Point mutations in the 23S rRNA gene, mainly at the positions 2142 and 2143 with a transition of A→G, are responsible for the resistance. Although current triple therapies containing clarithromycin are able to eradicate up to 90% of susceptible strains, the eradication rates may be significantly reduced for resistant strains. Moreover, unsuccessful treatment with regimens containing clarithromycin can be associated with acquisition of resistance to the drug, which may explain the increasing rate of clarithromycin resistance.

### REFERENCES

- Graham DY. Clarithromycin for treatment of *Helicobacter pylori* infections. *Eur J Gastroenterol Hepatol*, 1995;7 (Suppl 1): S55-S58
- Xia H H-X, Talley NJ. Prospects for improved therapy for *Helicobacter pylori* infection. *Exp Opin Invest Drugs*, 1996;5: 959-976
- Xia HX, Buckley M, Hyde D, Keane CT, O' Morain CA. Effects of antibiotic-resistance on clarithromycin-combined triple therapy for *Helicobacter pylori*. *Gut*, 1995;37(Suppl.1):A55
- Megraud F. Epidemiology and mechanism of antibiotic resistance in *Helicobacter pylori*. *Gastroenterology*, 1998;115:1278-1282
- Liu W, Lu B, Xiao S, Xu W, Shi L, Zhang D. Clarithromycin combined short-term triple therapies for eradication of *Helicobacter pylori* infection. *Chin J Intern Med*, 1996;35: 803-806
- Hu P, Li Y, Chen M, Wu H, Cui J, Li Q. Clinical study of one week clarithromycin combination therapy for the treatment of *H. pylori* infection. *Chin J Dig*, 1997;17:204-206
- Hua J, Ng HC, Yeoh KG, Ho KY, Ho B. Characterization of clinical isolates of *Helicobacter pylori* in Singapore. *Microbios*, 1998;94:71-81
- Suzuki J, Mine T, Kobayashi I, Fujita T. Assessment of a new triple agent regimen for the eradication of *Helicobacter pylori* and the nature of *H. pylori* resistance to this therapy in Japan. *Helicobacter*, 1998;3:59-63
- Miyaji H, Azuma T, Ito S, Suto H, Ito Y, Yamazaki Y. Susceptibility of *Helicobacter pylori* isolates to metronidazole, clarithromycin and amoxycillin in vitro and in clinical treatment in Japan. *Aliment Pharmacol Ther*, 1997;11:1131-1136
- Maeda S, Yoshida H, Ogura K, Kanra F, Shiratori Y, Omata M. *Helicobacter pylori* specific nested PCR assay for the detection of 23S rRNA mutation associated with clarithromycin resistance. *Gut*, 1998;43:317-321
- Xia H H-X, Kalantar J, Talley NJ. Metronidazole- and clarithromycin-resistant *Helicobacter pylori* in dyspeptic patients in Western Sydney as determined by testing multiple isolates from different gastric sites. *J Gastroenterol Hepatol*, 1998;13:1027-1032
- Midolo PD, Bell JM, Lambert R, Turnidge JD. Antimicrobial resistance testing of *Helicobacter pylori*: a comparison of E test and disk diffusion methods. *Pathology*, 1997;29:411-414
- Megraud F, Pichavant R, Palegry D, French PC, Roberts PM, Williamson R. Ranitidine bismuth citrate (RBC) co-prescribed with clarithromycin is more effective in the eradication of *Helicobacter pylori*

- than omeprazole with clarithromycin. *Gut*, 1997;41(Suppl 1): A92
- 14 De Koster E, Cozzoli A, Jonas C, Ntounda R, Butzler JP, Deltenre M. Six years resistance of *Helicobacter pylori* to macrolides and imidazoles. *Gut*, 1996;39(Suppl 2):A5
  - 15 Van Zwet AA, de Boer WA, Schneeberger PM, Weel J, Jansz AR, Thijs JC. Prevalence of primary *Helicobacter pylori* resistance to metronidazole and clarithromycin in the Netherlands. *Eur J Clin Microbiol Infect Dis*, 1996;15:861-864
  - 16 Debets Ossenkopp YJ, Sparrius M, Kusters JG, Kolkman JJ, Vandenbroucke-Grauls CMJE. Mechanism of clarithromycin resistance in clinical isolates of *Helicobacter pylori*. *FEMS Microbiol Lett*, 1996;142:37-42
  - 17 Xia H X, Buckley M, Keane CT, O' Morain CA. Clarithromycin resistance in *Helicobacter pylori*: prevalence in untreated dyspeptic patients and stability *in vitro*. *J Antimicrobial Chemother*, 1996;37:473-481
  - 18 Tompkins DS, Perkin J, Smith C. Failed treatment of *Helicobacter pylori* infection associated with resistance to clarithromycin. *Helicobacter*, 1997;2:185-187
  - 19 Moayyedi P, Ragunathan PL, Mapstone N, Axon ATR, Tompkins DS. Relevance of antibiotic sensitivities in predicting failure of omeprazole, clarithromycin, and tinidazole to eradicate *Helicobacter pylori*. *J Gastroenterol*, 1998;33(Suppl X):62-65
  - 20 Morton D, Bardhan D. A six-year assessment of tinidazole, metronidazole, clarithromycin, tetracycline and amoxicillin resistance in *Helicobacter pylori*- clinical isolates: a rising tide of antibiotic resistance. *Gastroenterology*, 1998;114:A907
  - 21 Adamek RJ, Suerbaum S, Pfaffenbach B, Opferkuch W. Primary and acquired *Helicobacter pylori* resistance to clarithromycin, metronidazole, and amoxicillin influence on treatment outcome. *Am J Gastroenterol*, 1998;93:386-389
  - 22 Wolle K, Nilius M, Leodolter A, Muller WA, Malfertthneiner P, Konig W. Prevalence of *Helicobacter pylori* resistance to several antimicrobial agents in a region of Germany. *Eur J Clin Microbiol Infect Dis*, 1998;17:519-521
  - 23 Piccolomini R, Di Bonaventura G, Catamo G, Carbone F, Neri M. Comparative evaluation of the E test, agar dilution, and broth microdilution for testing susceptibilities of *Helicobacter pylori* strains to 20 antimicrobial agents. *J Clin Microbiol*, 1997;35: 1842-1846
  - 24 Schutze K, Hentschel E, Hirschl AM. Clarithromycin or amoxycillin plus high dose ranitidine in the treatment of *Helicobacter pylori*-positive functional dyspepsia. *Eur J Gastroenterol Hepatol*, 1996; 8:41-46
  - 25 Laine L, Suchower L, Frantz J, Connors A, Neil G. Low rate of emergence of clarithromycin resistant *Helicobacter pylori* with amoxycillin co therapy. *Aliment Pharmacol Ther*, 1998;12:887-892
  - 26 Yousfi MM, El Zimaity HMT, Cole RA, Genta RM, Graham DY. Metronidazole, ranitidine and clarithromycin combination for treatment of *Helicobacter pylori* infection (modified Bazzoli's triple therapy). *Aliment Pharmacol Ther*, 1996;10:119-122
  - 27 Vakil N, Hahn B, McSorley D. Clarithromycin-resistant *Helicobacter pylori* in patients with duodenal ulcer in the United States. *Am J Gastroenterol*, 1998;93:1432-1435
  - 28 Best LM, Haldane DJM, Bezanson GS, Veldhuyzen van Zanten SJO. *Helicobacter pylori*: primary susceptibility to clarithromycin *in vitro* in Nova Scotia. *Can J Gastroenterol*, 1997;11:298-300
  - 29 Loo VG, Fallone CA, De Souza E, Lavallee J, Barkun AN. *In vitro* susceptibility of *Helicobacter pylori* to ampicillin, clarithromycin, metronidazole and omeprazole. *J Antimicrob Chemother*, 1997; 40:881-883
  - 30 Versalovic J, Shortridge D, Kibler K, Griffy MV, Beyer J, Flamm RK. Mutation in 23S rRNA are associated with clarithromycin resistance in *Helicobacter pylori*. *Antimicrobial Agents Chemother*, 1996;40:477-480
  - 31 Taylor DE, Ge Z, Purych D, Lo T, Hiratsuka K. Cloning and sequence analysis of two copies of a 23S rRNA gene from *Helicobacter pylori* and association of clarithromycin resistance with 23S rRNA mutations. *Antimicrob Agents Chemother*, 1997;41:2621-2628
  - 32 Versalovic J, Osato MS, Spakovsky K, Dore MP, Reddy R, Stone GG. Point mutation in the 23S rRNA gene of *Helicobacter pylori* associated with different levels of clarithromycin resistance. *J Antimicrob Chemother*, 1997;40:283-286
  - 33 Stone GG, Shortridge D, Versalovic J, Beyer J, Flamm RK, Graham DY. A PCR-oligonucleotide ligation assay to determine the prevalence of 23S rRNA gene mutations in clarithromycin-resistant *Helicobacter pylori*. *Antimicrob Agents Chemother*, 1997;41:712-714
  - 34 Occhialini A, Urdaci M, Doucet Populaire F, Bebear CM, Lamouliatte H, Megraud F. Macrolide resistance in *Helicobacter pylori*: rapid detection of point mutations and assays of macrolide binding to ribosomes. *Antimicrob Agents Chemother*, 1997;41: 2724-2728
  - 35 Hulten K, Gibreel A, Skold O, Engstrand L. Macrolide resistance in *Helicobacter pylori*: mechanism and stability in strains from clarithromycin treated patients. *Antimicrob Agents Chemother*, 1997;41:2550-2553
  - 36 Wang G, Taylor DE. Site specific mutations in the 23S rRNA gene of *Helicobacter pylori* confer two types of resistance to macrolide-lincosamide streptogramin B antibiotics. *Antimicrob Agents Chemother*, 1998;42:1952-1958
  - 37 Debets Ossenkopp YJ, Brikman AB, Kuipers EJ, Vandenbroucke Grauls CMJE, Kusters JG. Explaining the bias in the 23S rRNA gene mutations associated with clarithromycin resistance in clinical isolates of *Helicobacter pylori*. *Antimicrob Agents Chemother*, 1998;42:2749-2751
  - 38 Megraud F. Resistance of *Helicobacter pylori* to antibiotics. *Aliment Pharmacol Ther*, 1997;11(Suppl 1):43-53
  - 39 Xia HX, Keane CT, Beattie S, O' Morain CA. Standardization of disc diffusion test and its clinical significance for susceptibility testing of metronidazole against *Helicobacter pylori*. *Antimicrob Agents Chemother*, 1994;38:2357-2361
  - 40 Xia HX, Daw MA, Keane CT, O' Morain CA. Prevalence of metronidazole resistant *Helicobacter pylori* in dyspeptic patients. *Irish J Med Sci*, 1993;162:91-94
  - 41 Pina M, Occhialini A, Monteiro L, Doermann HP, Megraud F. Detection of point mutation associated with resistance of *Helicobacter pylori* to clarithromycin by hybridization in liquid phase. *J Clin Microbiol*, 1998;36:3285-3290
  - 42 Van Doorn L J, Debets Ossenkopp YJ, Marais A, van Hoek K, Sanna R, Megraud F. Detection of 23S rRNA mutation associated to macrolide-resistance of *Helicobacter pylori* by PCR and a reverse hybridization line probe assay. *Gut*, 1998;43(Suppl 2):A7-8
  - 43 Maeda S, Yoshida H, Ogura K, Maysunaga H, Kawamata O, Shiratori Y. Detection of *Helicobacter pylori* 23S rRNA gene mutation associated with clarithromycin resistance using preferential homoduplex formation assay (PCR-PHFA). *Gut*, 1998;43(Suppl 2):A7
  - 44 Bjorkholm B, Befrils R, Jaup B, Engstrand L. Rapid PCR detection of *Helicobacter pylori* associated virulence and resistance genes directly from gastric biopsy material. *J Clin Microbiol*, 1998;36: 3689-3690
  - 45 Sevin E, Lamarque D, Delchier JC, Soussy CJ, Tankovic J. Co-detection of *Helicobacter pylori* and its resistance to clarithromycin by PCR. *FEMS Microbiol Lett*, 1998;165:369-372
  - 46 Buckley MJM, Xia HX, Hyde DK, Keane CT, O' Morain CA. Metronidazole resistance reduces efficacy of triple therapy and leads to clarithromycin resistance. *Dig Dis Sci*, 1997;42:2111-2115
  - 47 Katelaris PH, Nguyen TV, Robertson GJ, Bradbury R, Ngu MC. Prevalence and determinants of metronidazole resistance by *Helicobacter pylori* in a large cosmopolitan cohort of Australian dyspeptic patients. *Aust NZ J Med*, 1998;28:633-638
  - 48 Lian JX, Carrick J, Lee A, Daskalopoulos G. Metronidazole resistance significantly affects eradication of *H. pylori* infection. *Gastroenterology*, 1993;104:A133
  - 49 Xia HX, Keane CT, O' Morain CA. A 5-year survey of metronidazole and clarithromycin resistance in clinical isolates of *Helicobacter pylori*. *Gut*, 1996;39(Suppl 2):A6-7



# Clinical study on the treatment of liver fibrosis due to hepatitis B by IFN- $\alpha_1$ and traditional medicine preparation \*

CHENG Ming-Liang<sup>1</sup>, WU Ya-Yun<sup>1</sup>, HUANG Ke-Fu<sup>2</sup>, LUO Tian-Yong<sup>1</sup>, DING Yi-Shen<sup>1</sup>, LU Yin-Yin<sup>1</sup>, LIU Ren-Cai<sup>3</sup> and WU Jun<sup>1</sup>

**Subject headings** hepatitis B; liver cirrhosis/therapy; interferon- $\alpha$ ; drugs, Chinese herbal

## INTRODUCTION

In China, liver fibrosis in most patients resulted from the viruses of hepatitis B. Both anti-virus and anti-fibrosis should be considered in designing a program for the treatment of liver fibrosis. Therefore, 40 cases of liver fibrosis due to hepatitis B were treated by using IFN- $\alpha_1$  and traditional medicinal preparations from February 1994 to April 1996. Good curative effect was achieved.

## MATERIALS AND METHODS

### *Clinical materials*

A group of 40 patients (33 men and 7 women) was investigated. Their age ranged from 28 years to 45 years with a mean of 36. Their course of disease was from 4 years to 12 years, averaging 7 years. All patients had the typical history of hepatitis B. The diagnosis of liver fibrosis was confirmed by experimental serology and liver biopsy (the criteria of diagnosis referred to the criteria amended during the 5th National Academic Conference on Infectious Diseases and Parasitic Diseases). Patients whose clinical manifestations were not consistent with the findings in serological and pathohistological tests were not included in the study.

<sup>1</sup>Department of Infectious Diseases, Affiliated Hospital, Guiyang Medical College, Guiyang 550004, Guizhou Province, China

<sup>2</sup>Central Hospital of the Fifth Engineering Bureau of Railway Ministry

<sup>3</sup>Hospital of Bijie County, Guizhou Province, China

Dr. CHENG Ming-Liang, male, born on January 17, 1959 in Guiyang, Guizhou Province, graduated from Guiyang Medical College as B.S. in 1982. Professor of Infectious Diseases, specialized in hepatitis and hepatofibrosis, having 38 papers and books published.

\*Supported by the key project of the "8th Five Year Plan" of Scientific Committee of Guizhou Province (1993 No. 2037) and the key project of the "9th Five Year Plan" of Scientific Committee of Guizhou Province. (1996 No.1028)

**Correspondence to:** Professor CHENG Ming-Liang, Department of Infectious Diseases, Affiliated Hospital, Guiyang Medical College, Guiyang 550004, China.

Tel. +86 • 851 • 6829499 (H), 6855119 Ext. 3263 (O)

Received 1997-12-02 Revised 1999-01-18

### *Therapeutic*

All the patients received intramuscular injection of 3 000 000U IFN- $\alpha_1$  (Produced by Shengzhen Kexing Company, batch number 94010), once a day for the first month, and once two days after a month. Traditional medicinal preparation (composed mainly of Tetrandrae, Salvia miltiorrhiza Bge, Semen Ginkgo, Radix paeoniae rubrae, each gram has 0.8 g herb, produced by Duyun Pharmaceutical Factory, Guizhou Province, batch number 940102) was taken, three times a day for 3 months (45 g/d). Besides vitamin E and C, none of other medicines had been used in this group.

### *Observation index and methods*

Detection of serum liver fibrosis indexes and hepatitis B virus marker: 6 mL serum was taken from the patients before treatment, by the end of treatment and 6 months after treatment respectively. Laminin (LN), hyaluronic acid (HA) and procollagen type III (PC III) were measured by radioimmunoassay (the reagents were purchased from Shanghai Naval Medical Research Institute and Chongqing Tumor Research Institute). Radioimmunoassay was also used to detect the markers of hepatitis B virus such as HBsAg, anti-HBs, HBcAg, anti-HBc, HBeAg and anti-HBe. HBV-DNA was measured by PCR (the reagent was bought from 3V Company, Shandong Province).

### *Ultrasonography and fibergastroscopy*

Each patient was detected once by HPSONOS-1000 Colour Doppler (HP Company of USA) before and after the treatment and by direct vision fibergastroscopy (Olympus-XQ20, Japan).

### *Liver biopsy*

The liver tissue was quickly taken by fine needle under local anesthesia. The liver tissue was about 3 cm long. It was fixed by 10% formalin, then imbedded in paraffin, sliced and routinely stained. These slices taken from 12 biopsied patients before and after the treatment were read by single blind method. After a pathologist read these slices according to the criteria, another pathologist reported the results after reread them.

**Table 1 Comparison of the 5 serum indexes of the 40 patients before and after treatment and after 6 months of follow-up ( $\bar{x} \pm s$ )**

Time	n	LN	PCIII	HA	Albumin	Globulin
		(ng/L)	(ng/L)	(ng/L)	(g/L)	(g/L)
Before treatment	40	420.0 $\pm$ 68.0	146.2 $\pm$ 44.8	182.40 $\pm$ 42.20	30.51 $\pm$ 2.42	26.25 $\pm$ 6.84
After treatment	40	290.3 $\pm$ 36.4 <sup>b</sup>	112.4 $\pm$ 30.6 <sup>b</sup>	136.32 $\pm$ 39.20 <sup>b</sup>	35.25 $\pm$ 4.46 <sup>b</sup>	31.32 $\pm$ 6.74 <sup>b</sup>
Effective type after 6 months follow-up	22	142.6 $\pm$ 32.8 <sup>c</sup>	80.0 $\pm$ 31.8 <sup>c</sup>	84.54 $\pm$ 36.33 <sup>c</sup>	39.13 $\pm$ 3.24 <sup>c</sup>	25.98 $\pm$ 3.22 <sup>c</sup>
Non-effective type after 6 months follow-up	18	403.5 $\pm$ 41.5 <sup>a</sup>	156.3 $\pm$ 43.9 <sup>a</sup>	178.20 $\pm$ 38.60 <sup>a</sup>	29.35 $\pm$ 2.71 <sup>a</sup>	37.00 $\pm$ 4.54 <sup>a</sup>

<sup>a</sup> $P < 0.05$ ; <sup>b</sup> $P < 0.001$ , compared with those before treatment; <sup>c</sup> $P < 0.001$  the effective type compared with the non-effective type.

## RESULTS

The serum LN, HA, PC III and globulin of the 40 cases after treatment were noticeably lower than those before treatment ( $P < 0.001$ ). The albumin was obviously increased compared with that before treatment ( $P < 0.001$ ). After 6 months of follow-up, LN, HA and globulin in the effective type (HBsAg, HBeAg and HBV-D NA turned negative after using IFN $\alpha_1$ , suggesting that the viruses of hepatitis B were temporarily suppressed. Otherwise, it was considered to be non-effective type) were obviously lower than those in the non-effective type ( $P < 0.001$ ), while the albumin was obviously higher than that in the non-effective type ( $P < 0.001$ , Table 1).

Before treatment, 32 patients were found with HBsAg, anti-HBc and HBeAg; 8 patients with HBsAg and anti-HBc; and 21 patients with HBV-DNA. After 3 months of treatment, HBsAg, HBeAg and HBV-DNA became negative in 6 (15%), 16 (50%), and 16 (76.2%) patients, respectively. Among the 12 patients who received liver puncture biopsy, dekris-type necrosis disappeared in 3 patients, no obvious proliferation of fiber with more new-born liver cells in one patient, improvement of bridge-joint necrosis with elimination of the ramus septi-fibrosis in 3 patients, improvement of bridge-joint with new-born liver cells and unclear ramus septi-fibrosis in 2 patients, complete foliole with a great number of liver cells in 3 patients. Before treatment, the portal vein of 34 patients was  $\geq 14$  mm in width among the 40 patients, while after treatment, the portal vein of 28 patients was  $\leq 12$  mm. After 6 months of follow-up, among the 28 patients, the portal vein of 23 patients was  $\leq 11$  mm, the others remained 12 mm. Before treatment, the blood flow rate of portal vein in 36 patients was  $\geq 16$  mm/s, while after treatment, it was  $\leq 12$  mm/s in 32 patients. No change was found in the rest. By using fibergastroscopy the line or snake-shaped grey-white or grey-blue changes could be seen at the lower segment of esophageal mycoderma in 32 patients before treatment, while the changes disappeared in 28 patients after treatment. No obvious changes were found in 4 patients.

## DISCUSSION

Up to now, there has been no good way to cure liver fibrosis resulting from chronic hepatitis B. A number of researches have been made by domestic scientists who had made great progress by using traditional medicines such as *Salvia miltiorrhiza* Bge, *Tetrandrae*, *Radix paeoniae rubrae* and *Prunus persicae* (L), batsch *et al*<sup>[1-3]</sup>. However these methods have not been considered to suppress the virus of hepatitis B. For this reason, some tests were made by using IFN $\alpha_1$  and traditional medicinal preparations to treat 16 patients with early-stage hepatic cirrhosis, and have achieved rather good curative effect which was confirmed by liver biopsy before and after treatment<sup>[4]</sup>. On the other hand, short-term curative effect was significant in 20 patients treated simply by the traditional medicinal preparations<sup>[5]</sup>, but there was recurrence in some patients. Therefore, IFN $\alpha_1$  and traditional medicinal preparation were used to treat hepatitis and liver fibrosis at the same time. At present IFN $\alpha_1$  is regarded as one of the most effective agents to treat hepatitis B because it is a biologically regulatory and active material with antiviral and immunoregulatory function<sup>[6,7]</sup>. *Tetrandrine* is an effective ingredient of *Tetrandrae*. In modern medicine the research has proved that it can block the channel of calcium on the cytomembrane of liver, obstruct the depletion of ATP in the cytomembrane, protect the liver cells, and inhibit the proliferation of internal lipocyte of liver and synthesis of collagen. The effective ingredients of dansheng are *Tanshinone* and *tanshine* which may suppress the reaction of inflammation and promote the regeneration of liver cells by reducing the degeneration and necrosis of liver cells. The effective ingredient of chichao is *paeoniflorin* which may improve the microcirculation of liver, decrease the portal pressure and promote the histologic change of liver fiber. Flavonoid substance in ginkgo leaves can strengthen the immunologic function of body, decrease the free radical of oxygen, increase the activity of NK cells and intensify the anti virus capacity of body<sup>[8,9]</sup>. After 3 months of treatment with the herbal medicinal preparations, the changes of LN, HA, PC III, albumin and globulin were

obviously different from those before treatment, which were confirmed by liver biopsy, ultrasonography and fibergast roscopy. It is suggested that this preparation can improve the function of liver and suppress the fibrosis of liver in a short time. Follow-up was made for 6 months after withdrawing the medicine. The result proved that the difference between IFN $\alpha_1$  effective type and ineffective type was very obvious. It indicated that the virus of hepatitis B was suppressed in the patients cured by IFN $\alpha_1$ , and the liver fibrosis due to clinical hepatitis B was continuously improved or reversed by using the traditional herbal preparations which can cure liver fibrosis. The patients in this group are being followed up continuously.

## REFERENCES

- 1 Ma XH, Zhao YC, Yi L. The action of dansheng to reabsorption of hepatofibrosis. *Chin J Integrated Traditional West Medi*, 1988;8: 161-163
- 2 Liu P, Liu C, Hu Ying. The clinical observation of supporting the healthy energy and eliminate the evil to cure hepatic cirrhosis after hepatitis. *Chin J Integrated Traditional West Medi*, 1996;16: 459-462
- 3 Yang DG, Wang LJ, Song WY. The comparison of histology in liver puncture by re-using chichao to treat chronic hepatitis before and after treatment. *Chin J Integrated Traditional West Medi*, 1994;14:207-208
- 4 Cheng ML, LT, Wu YY. The histological study on IFN $\alpha_1$  and traditional medicine preparation to treat early stage hepatic cirrhosis. *Chin J Integrated Traditional West Medi*, 1995;15: 300-301
- 5 Cheng ML, Ding YS, Luo YF. The clinical study on handanbituo to treat chronic hepatitis hepatofibrosis. *Chin J Integrated Traditional West Medi*, 1996;1:431-432
- 6 Billiau A. The model of action of interferons in viral infections and their possible role in the control of hepatitis B. *J Hepatol*, 1986; 3(suppl):S171
- 7 Yao GB, Fei GH, Wu XH. The study on IFN to treat chronic hepatitis B. *Chin J Digest*, 1991;11:133-136
- 8 Cheng ML, Liu SD. The basic study and clinics of hepatofibrosis. First edition. *Beijing: People's Health Publishing House*, 1996: 228-248
- 9 Li W, Dai QT, Liu ZE. The first-step observation of early-stage fibrosis after the dissolvable of the complex prescription sinkgo to treat chronic hepatitis B. *Chin J Integrated Traditional West Medi*, 1995; 15:593-595

Edited by WANG Xian-Lin

# Antibody detection and sequence analysis of sporadic HEV in Xiamen region \*

HUANG Ru-Tong, LI Xiao-Yu, XIA Xiao-Bing, YUAN Xin-Tong, LIU Min-Xia and LI De-Rong

**Subject headings** hepatitis E virus; antibodies; viral analysis; nucleotide sequences; sequence analysis

## INTRODUCTION

Hepatitis E virus (HEV) is transmitted through a fecal-oral route<sup>[1]</sup>. HEV induces acute hepatitis and is responsible for a significant portion of the fulminant hepatitis in epidemic and sporadic cases, especially in the mixed infection patients and women in their third trimester of pregnancy<sup>[1]</sup>. It has been reported that HEV infection is more prevalent in underdeveloped and developing countries in Asia, Africa, and Central America, but is rare in developed countries<sup>[1]</sup>. In China, a large outbreak occurred between 1986 and 1988 in Xinjiang, and sporadic spread was often found in other regions.

HEV is a non-enveloped virus, approximately 27 nm-34 nm in diameter and has a positive-sense, single-stranded RNA genome of approximately 7.2 kb. The viral genome consists of three discontinuous open reading frames (ORFs). Since the molecular cloning and sequencing of HEV were described<sup>[2]</sup>, several genomic analyses of HEV strains obtained from different geographic areas have been reported<sup>[3]</sup>. The existing variations on the gene structure of HEV strains from some regions of China was reported by us<sup>[4]</sup>. In this study, after the collection of the serum samples of patients with acute hepatitis in Xiamen, anti-HEV antibody and HEV RNA in serum were detected, further HEV RNA was cloned and sequenced. The results are described and discussed.

## PATIENTS AND METHODS

### Patients

From September 1996 to March 1997, 81 samples of serum of patients (71 male and 10 female, aged 13

Institute of Microbiology and Epidemiology, Academy of Military Medical Sciences, Beijing 100850, China

Dr. HUANG Ru-Tong, male, born on 1942-11-11 in Zhejiang Province, graduated from Shanghai Fudan University as a postgraduate in 1966, now associate professor of microbiology, majoring aetiology of medical virology, having 60 papers published.

\*Supported by the Foundation of General Logistics Department of Chinese PLA, No.9608037.

**Correspondence to:** Dr. HUANG Ru-Tong, Institute of Microbiology and Epidemiology, Academy of Military Medical Sciences, Beijing 100850, China

Tel. +86 • 10 • 66931535, Fax. +86 • 10 • 68213044

**Received** 1999-01-20

-69 years) with acute hepatitis at clinic and admitted to the Infections Disease Hospital in Xiamen were collected. These serum samples were provided by professor LIAO Mian-Chu and were stored at -25 °C before test. The sera showed elevated ALT levels. The serum of patients with acute hepatitis was tested for detection of serum IgM anti-HAV, HBsAg, IgM anti-HBc, anti-HCV and anti-HEV antibodies. According to above detections, all samples suspected of hepatitis E were taken to our laboratory and were further studied. One case (sample No.3, Zhou, male aged 52 years) used in the determination of sequence was diagnosed as fulminant hepatitis. He had complained of tiredness, anorexia, urine-yellow, jaundice in skin and sclera and spider nevus, with ALT 20420 nmol • s<sup>-1</sup>/L and SB-205.2 μmol/L, and virus markers of anti-HAV IgM and anti-HEV IgM positive.

### Detection of anti-HEV antibody

Anti-HEV IgG and IgM antibodies were further detected by ELISA with recombinant antigens (Institute of Virology, Chinese Academy of Preventive Medicine) according to the manufacturer's instructions.

### Cloning and sequencing of HEV RNA

Two sets of pair primers were synthesized at Institute of Microbiology of Chinese Science Academy according to the Burmese HEV sequence<sup>[3]</sup>. The sequence of each oligonucleotide primer was: outer primers (F1) 5'-GCT ATT ATG GAG GAG TGT GG 3' and (R1) 5'-CAG GGC CCC AAT TCT TCT 3', inner primers (F2) 5'-GCG TGG ATC TTG CAG GCC 3' and (R2) 5'-TTC AAC TTC AAG CCA CAG CC 3'. HEV RNA was extracted from 200 μL serum by proteinase K (10 g/L) guanidine thiocyanate buffer (4.2M guanidine thiocyanate and 5 g/L N-lauroyl sarcosine and 0.025 mol/L Tris-HCl, pH 8.0) phenol/chloroform<sup>[5]</sup>. All viral RNA were used to be transcribed and nested-PCR<sup>[4]</sup>. The amplified PCR products were ligated into pGEM-T vector (Promega products) according to the manufacturer's instructions. The ligation mixture was transformed to *E. coli* strain JM 109. The positive clones were picked up and cultured in LB medium. The positive

recombinant clones were identified and sequenced. The nucleotide sequence (location 4522-4761) of X-S1 isolate of HEV was compared with those of other known HEV strains. Percentage of similarity and divergence were calculated as described previously<sup>[4]</sup>.

## RESULTS

### Detection of anti-HEV and HEV RNA in serum samples of patients with acute hepatitis

Twelve of 81 serum samples of acute hepatitis in Xiamen were positive for anti-HEV IgG, of them, 11 were also positive for anti-HEV IgM. Eight of 12 serum samples of positive anti-HEV IgG were used to detect HEV RNA, 2 samples were found positive for HEV RNA. The results are shown in Table 1.

### Cloning and sequencing of HEV

The amplified PCR positive products obtained from X-S1 and X-S6 samples were purified and ligated into pGEM-T vector, then transformed to *E. coli* JM 109. One of two white specks obtained from X-S1 had a band of about 239 bp in gel electrophoresis. Two white specks of the X-S6 were positive and a band of 239 bp was found after digested by *EcoR* I and *Hind* III. One positive clone of X-S1 was sequenced. HEV sequence of the X-S1 isolate could be recognized, this HEV X-S1 strain was neither lost nor inserted in length 239 bp compared with Burma strain of HEV. Aberrance occurred in 48 bases, 5 of them took place at the first codon position, 4 at the second position and 39 at the third codon position. The nucleotide sequence of X-S1 isolate is shown in Figure 1.

**Table 1** Results of anti-HEV antibody and HEV RNA detection in serum of patients from Xiamen

Patients	Name	Sex	Age	Collection time	Anti-HEV <sup>a</sup>		Results of HEV RNA detection
					IgG	IgM	
1	Ling JD	M	31	97-03-05	+	+	ND <sup>b</sup>
2	Du YM	M	24	97-02-05	+	+	-
3	Zhou SL	M	52	97-02-15	+	+	+
4	Huang JC	M	50	97-02-19	+	-	ND
5	Qiu SS	M	53	97-02-19	+	+	-
6	Huang JZ	M	45	97-01-28	+	+	-
7	Mei SP	F	31	96-02-17	+	+	ND
8	Zhen MC	M	68	96-12-09	+	+	-
9	Zhang MS	M	60	97-12-09	+	+	-
10	Zhong M	M	29	96-11-13	+	+	+
11	Kang CR	M	24	96-10-10	+	+	N
12	Jiang XW	M	29	97-02-19	+	+	-

<sup>a</sup>A>0.30 +  $\bar{x}$  of negative samples; positive. <sup>b</sup>Not done.

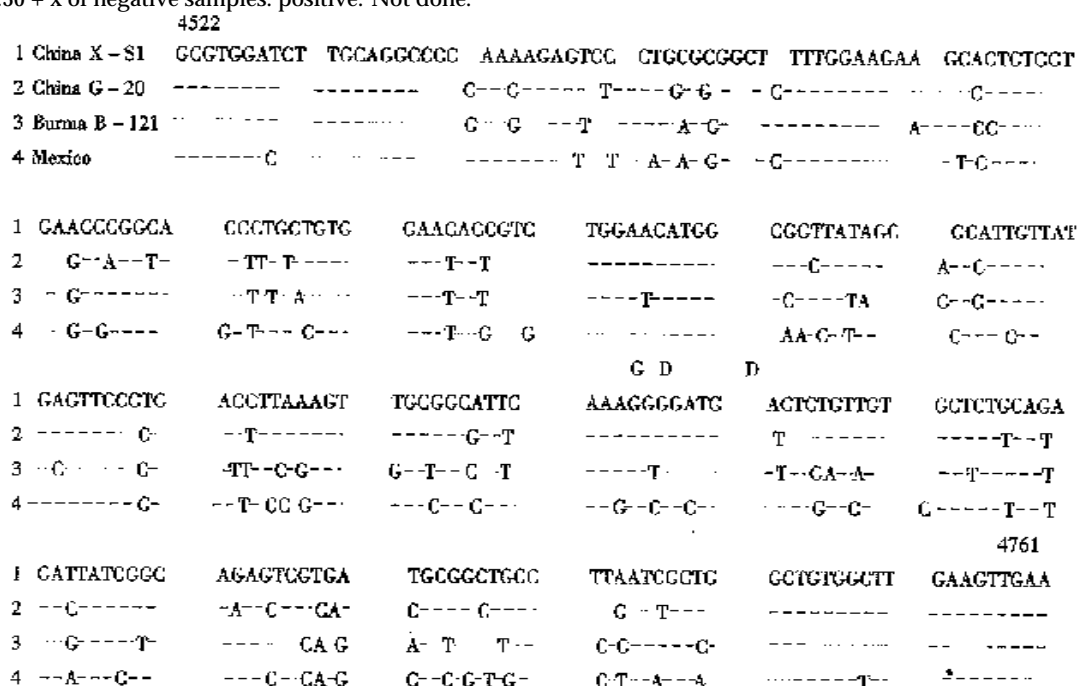


**Figure 1** Comparison of the nucleotide sequences among four strains of HEV.

### Comparison of the nucleotide sequence of HEV

The sequence of HEV X-S1 strain was compared with the Chinese (G-20), Burmese (B-121) and Mexican strains of HEV. The similarity of nucleotide sequences was 85.4%, 79.2% and 76.4% respectively. The divergence of nucleotide sequences was 14.2%, 19.9% and 22.3% respectively.

### DISCUSSION

This paper reports the results of serological survey on hepatitis E virus infection in Xiamen population. The serum samples from 81 patients with acute hepatitis were tested for anti-HEV IgG and IgM antibodies with HEV recombination antigen by ELISA. Twelve (14.8%) of 81 patients with acute hepatitis had antibody to HEV, 11 were positive for IgM anti-HEV and 2 positive for HEV RNA. The results show that there is hepatitis E virus infection in Xiamen again, but there has been no documented report of detection of HEV RNA in anti-HEV positive patients from this area.

The mixed infection of HEV and HBV were described previously<sup>[4]</sup>. This paper reports the co-infection of HEV and HAV. This case is positive for both antibodies of HAV and HEV. The patient presented as severe hepatitis in the clinical characteristics, with very high ALT ( $20420 \text{ nmol} \cdot \text{s}^{-1}/\text{L}$ ). This shows that both the HEV and HAV are transmitted primarily through a fecal-oral route. In this study, the partial nucleotide sequence of Xiamen X-S1 isolate of sporadic HEV was described and compared. It is shown that Xiamen (X-S1) strain and Guangzhou (G-20) strain<sup>[4]</sup> are most

identical to each other (85.4%), with a lower range of identities to the Burmese strain<sup>[2]</sup> and Mexican strain<sup>[3]</sup> (80.1%-77.3%). The nucleotide sequences of the X-S1 strain and the G-20 strain may belong to a novel and unique branch. Similar results have been reported by other investigators<sup>[6,7]</sup>. Recently the HEV-US-1 strain was discovered by George G. Schlauder<sup>[8]</sup>, it is significantly divergent from other human HEV isolates, which may be the fourth genotype. The discovery of these HEV variants may be important in understanding the worldwide distribution of HEV infection.

### REFERENCES

- 1 Gust ID, Purcell RH. Report of a workshop: waterborne non-A, non-B hepatitis. *J Infect Dis*, 1987;156:630-635
- 2 Tam AW, Smith MM, Guerra ME, Huang CC, Bradley DW, Fry KE, Reyes GR. Hepatitis E virus (HEV): molecular cloning and sequencing of the full-length viral genome. *Virology*, 1991;185:120-131
- 3 Huang CC, Nguyen D, Fernandez J, Yun KY, Fry KE, Bradley DW, Tam AW, Reyes GR. Molecular cloning and sequencing of the Mexico isolate of hepatitis E virus. *Virology*, 1992;191:550-558
- 4 Huang RT, Nakazono N, Ishii K, Kawamata O, Kawaguchi R, Tsukada Y. Existing variations on the gene structure of hepatitis E virus strains from some regions of China. *J Med Virol*, 1995;47:303-308
- 5 Tsarev SA, Emerson SU, Reyes GR, Tsareva TS, Legters LJ, Malik IA, Iqbal M, Purcell RH. Characterization of a prototype strain of hepatitis E virus. *Proc Natl Acad Sci USA*, 1992;89:559-563
- 6 Wei SJ, Walsh P, Tong YB, Dong HQ, Cai XL. Nucleic acid sequence analysis of the sporadic hepatitis E virus strains in Guangzhou. *Chin J Microbiol Immunol*, 1998;18:92-95
- 7 Wu JC, Sheen IJ, Chiang TY, Sheng WY, Wang YJ, Chan CY, Lee SD. The impact of traveling to endemic areas on the spread of hepatitis E virus infection: epidemiological and molecular analyses. *Hepatology*, 1998;27:1415-1420
- 8 Schlauder GG, Dawson GJ, Erker JC, Kwo PY, Kningge F, Smalley L, Rosenblatt JE, Desai SM, Mushahwar IK. The sequence and phylogenetic analysis of a novel hepatitis E virus isolated from a patient with acute hepatitis reported in the United States. *J Gen Virol*, 1998;79:447-456

Edited by MA Jing-Yun

# Primary malignant tumor of the small intestine

ZHOU Zhi-Wei, WAN De-Sen, CHEN Gong, CHEN Ying-Bo and PAN Zhi-Zhong

**Subject headings** intestinal neoplasms/diagnosis; intestinal neoplasms/therapy; small intestine; survival analysis

## INTRODUCTION

Primary malignant tumors of the small intestine are easy to be misdiagnosed because of its low morbidity, nonspecific clinical manifestations and the limited examination methods. Most cases are already in advanced stage at the time of diagnosis, so therapeutic result is very poor. In order to have a better understanding of the clinical characteristics of malignant tumor of the small intestine, an analysis was made for the diagnosis, treatment and prognosis-influencing factors of 75 cases with their diagnoses confirmed by pathological examination from 1964 to August, 1995 in our hospital, so as to improve their early diagnosis, timely treatment and therapeutic effect.

## MATERIALS AND METHODS

### General data

This group consisted of 75 cases, 42 males and 33 females. The onset age ranged from 4 to 75 years with an average of 47 years. The course of disease was 1 to 99 months, averaging 47 months.

### Pathological type and tumor site

The diagnoses of the 75 cases were confirmed by pathological examination, 26 were cases of leiomyosarcoma, 25 adenocarcinomas, 20 malignant lymphomas, and 4 other malignant neoplasms. The tumors were located at duodenum, jejunum and ileum in 18, 28 and 29 cases respectively (Table 1).

### Clinical manifestations

Clinical manifestations of these malignant tumors are shown in Table 2.

Cancer Centre, Sun Yat-Sen University of Medical Sciences, Guangzhou 510060, Guangdong Province, China

ZHOU Zhi-Wei, male, born on 1964-01-28 in Pengze County, Jiangxi Province, Han nationality, graduated from Sun Yat-Sen University of Medical Sciences in 1984, associate professor, majoring in gastroenteric oncology, having 10 papers published.

**Correspondence to:** Dr. ZHOU Zhi-Wei, Department of Abdominal Surgery, Cancer Centre, Sun Yat-Sen University of Medical Sciences, Guangzhou 510060, Guangdong Province, China

Tel. +86 • 20 • 87765368 Ext.5214

Received 1998-11-09

**Table 1 Pathological types and distributions**

Type of neoplasms	Number by region			
	Duodenum	Jejunum	Ileum	Total
Leiomyosarcoma	5	14	7	26
Adenocarcinoma	10	9	6	25
Malignant lymphoma	2	4	14	20
Malignant fibrous histiocytoma		1	1	2
Malignancy of neurofibroma			1	1
Malignancy of fibroma	1			1
Total	18	28	29	75

### Preoperative diagnosis

Before the exploratory laparotomy, 33 cases were diagnosed as intestinal carcinoma, 25 cases as abdominal mass, and 17 cases were misdiagnosed as other diseases, such as intestinal perforation, acute peritonitis, ovary tumor, colon carcinoma, and intussusception of ileum to cecum, and so on.

### Accessory examinations

No abnormal CEA (carcinoembryonic antigen) was detected in 10 cases. Twenty-three out of 26 cases were found to have abdominal mass by B-type ultrasonography. CT (computed tomography) scans showed a clear demonstration of tumor on the diseased region and the structures around it in 20 cases. Of the 13 cases accepted barium meal roentgenography, 11 were diagnosed as intestinal tumor, with an accuracy of 84.6%. Of the 7 cases of duodenal tumors, 6 were diagnosed as duodenal tumor by fibroscopy which were confirmed by pathological examination. Barium enema was performed in 18 cases and 8 of them were found to have tumor in their ileum.

### Methods of treatment

Surgical treatment was the main therapeutic method for this group of cases. Thirty-seven cases received radical resection, 21 palliative resection, and 10 bypass operation, 3 exploratory laparotomy and 3 direct biopsy. The operation mortality was 1.4%. Four cases did not receive surgical operation. 27 cases received adjuvant chemotherapy. 5-fluorouracil (5-FU), mitomycin (MMC), cyclophosphamide (CTX) and adriamycin (ADM) were commonly used.

## RESULTS

Survival rates were calculated with Life Table, and computer's COX multivariate analysis model was used for survival analysis.



**Table 2 Clinical manifestations**

Symptom	Abdominal pain	Abdominal mass	Emaciation	Intestinal obstruction	Melena	Acute peritonitis	Jaundice	Fever	Anemia
Number	45	43	18	11	6	5	5	4	3
%	60	57.3	24	14.7	8	6.7	6.7	5.3	5

**Follow-up data**

Duration of follow-up ranged from 1 to 30 years, the follow-up rate was 94.2%. One-, 3- and 5-year survival rates of the 71 operated cases were 70.7%, 49.9% and 35.1% respectively (Tables 3-5).

**Table 3 Survival rate by operation type**

Operation type	n	Survival rate (%)		
		1 year	3 years	5 years
Radical resection	37	87.5	68.7	48.1
Palliative resection	21	57.9	33.8	24.1
Symptom- relieving and exploratory operation	13	42.9	21.4	0.0

**Table 4 Survival rate by pathological type**

Pathological type	n	Survival rate (%)		
		1 year	3 years	5 years
Adenocarcinoma	25	53.9	27.9	14.0
Leiomyosarcoma	26	95.8	82.1	57.5
Malignant lymphoma	20	48.6	39.7	23.8

**Table 5 Survival rate by location of tumor**

Location of tumor	n	Survival rate (%)		
		1 year	3 years	5 years
Duodenum	17	69.2	38.5	0.0
Jejunum	27	81.8	59.6	50.4
Ileum	27	51.1	29.2	17.5

**Prognostic factors analysis by computer's COX multivariate analysis model**

An analysis was made by COX multivariate analysis model, for the following factors which may influence prognosis such as patient sex, age, clinical course, histological type, tumor site, tumor size, gross type, lymph node metastasis, liver metastasis, invasion to adjacent organs, operation type, and chemotherapy. The critical value of alpha was 0.05. Statistical results showed that patient age, histological type, tumor site and operation type had significant influence on survival rate. But chemotherapy had no significant effect on prognosis.

**DISCUSSION****General consideration**

The incidence of primary malignant tumor of the small intestine is very low, accounting for 1%-3.6% of all gastrointestinal malignant neoplasms and 0.2%-0.3% of that of the whole body<sup>[1,2]</sup>.

From 1964 to 1995, 75 cases of primary malignant tumor of the small intestine were admitted to our hospital, constituting about 1.4% of 4427 cases of malignancy of all GI tract in the same period. In China, the leiomyosarcoma, adenocarcinoma, and malignant lymphoma account for the most of the small intestine malignancies, but carcinoid is rare. However, in other countries the most frequently encountered malignancies of small intestine are in order of adenocarcinoma and carcinoid, malignant lymphoma and leiomyocarcinoma<sup>[3]</sup>.

Relationship between pathology and tumor site. The predilection site of leiomyosarcoma is jejunum, ileum and duodenum. The predilection site of adenocarcinoma is in order of duodenum, jejunum and ileum, while the predilection site of malignant lymphoma is ileum and jejunum, and is lower in duodenum<sup>[3]</sup>. The tumor distribution rates in this group cases are consistent with those reported in the literature (Table 1).

Tumor distribution in small intestine. Adenocarcinoma accounts for about 50%-66% of tumors in the duodenum (55.6% in this group), and followed by malignant lymphoma and leiomyosarcoma. In the jejunum, leiomyosarcoma is the most encountered (accounting for 50% in this group), the next is adenocarcinoma and malignant lymphoma. But in the ileum, malignant lymphoma constitutes about half of all malignancies (48.3% in this group), and followed by adenocarcinoma and leiomyosarcoma.

Many scholars hold that the low incidence of malignant tumors in small intestine is associated with the following factors: ① Alkalinity in the small intestinal lumen is unfit for the growth of tumor. ② Rapid peristalsis of small intestine is suggested to minimize the time of mucosal exposure to potential carcinogens from food, and liquid content in lumen may dilute carcinogens, which will lead to the reduction of carcinogenicity. ③ The lack of intraluminal bacterial flora obviously reduces carcinogenic agents, and these bacteria are necessary in the process of metabolism. ④ A large concentration of IgA produced mainly in the lymphoid tissue of small intestine, is protective against tumorigenesis by neutralizing virus and potential carcinogenic agents. ⑤ The T-lymphocyte with strong immunity, accounting for the majority

of lymphocytes in collecting lymphadens of small intestines, has a strong ability and specific characteristics to protect against tumor growing. ⑥ Benzopyrene hydroxylase is present in large amounts in the mucosa of small intestine and may detoxify carcinogens<sup>[1]</sup>.

### Diagnosis

Primary malignant tumor of small intestine is easy to be misdiagnosed because of its low incidence, its vague and nonspecific clinical presentations, and the limited diagnostic methods. Misdiagnosis rate in literature reports is 40%-80%<sup>[4]</sup>, and 56% in our group. We hold that following are the key points to increase its diagnostic accuracy and to decrease its misdiagnostic rate.

A better understanding should be acquired in primary malignant tumor of small intestine. In clinics the following should be highly suspicious of the disease: unknown abdominal pain, abdominal mass, melena, and obstruction, especially when an abdominal mass is palpable.

Barium meal roentgenography is the routine method for detecting primary malignant tumor of small intestine, its diagnostic accuracy can be as high as 50%<sup>[2,5]</sup>. We think that for the patients who are suspicious of tumor in small intestine, barium meal roentgenography should be performed if possible. In our studied group, diagnoses were established by barium meal X-rays in 11 out of 13 cases with an accuracy of 84.6%. Air-barium contrast roentgenography, in which a large amounts of barium and air are injected into the duodenum lumen through a gastric tube, is suggested to be performed to visualize small intestine segment by segment, so as to increase its diagnostic accuracy rate. The distal ileum usually is poorly visualized in upper GI series studies, but it may be demonstrated through barium enema in which contrast material from colon is refluxed into the distal small intestine through the ileocecal valve. Combination of barium meal roentgenography and barium enema can achieve a positive rate of 50%-80%.

Flexible endoscopic examination and direct biopsy are the most reliable methods to establish the diagnosis, especially in early stage of the disease. It is also helpful and reliable for diagnosis of tumors in the duodenum. In our studied group, the diagnosis was established in 6 of 7 cases by flexible endoscopic examination and were confirmed by pathological examination. In foreign countries, the flexible endoscopy for small intestine was used in clinic in 1969. But it developed very slowly because of its technical difficulties in inserting and the great suffering of patients<sup>[5]</sup>.

Computed Tomography (CT) scans can show a good demonstration of the tumor-involved region and the structures around it. Furthermore, CT scan can define whether there is local or distant metastasis. Especially for those whose diagnosis can not be confirmed by GI barium roentgenography, CT scan is an effective method<sup>[6]</sup>.

### Treatment

Surgical resection is so far the most effective therapeutic method for malignant tumor of small intestine. If diagnosis is established, radical resection should be performed as early as possible, which requires at least segmental resection of 10cm of the involved region, including removal of the corresponding mesentery and its lymph nodes<sup>[7]</sup>. It was reported the 5-year survival rate of radical resection is 25%-54%<sup>[1,8]</sup>, which is consistent with that (48.1%) in our study. For carcinoma in the duodenum, Whipples operation should be performed if possible. Tumor in the distal ileum should be treated by right hemicolectomy. Palliative resection of tumor is somewhat valuable and should not be given up easily. Its 5-year survival rate is 0%-25% reported in literature<sup>[1]</sup>, and is 24.1% in our study. Bypass operation can temporarily relieve symptoms but could not prolong the patient's life. Reexploratory resection should be performed for recurrence if possible<sup>[9,10]</sup>.

Adjuvant postoperative chemotherapy for malignant lymphoma is necessary. The unresectable malignant lymphoma of small intestine should be treated mainly by chemotherapy in order to relieve symptoms and prolong life. The usual chemotherapy regimen is CHOP (CTX+VCR+ADM+Prednisone). Leiomyosarcoma of small intestine is partly sensitive to chemotherapeutic agents. For huge leiomyosarcoma, preoperative combination chemotherapy of ADM and CTX can minimize the size of tumor and improve resection rate. Chemotherapy has no effect on adenocarcinoma of small intestine due to its nonsensitivity to chemotherapeutic agents. In our study, 27 cases had accepted chemotherapy, but neither postoperative adjuvant nor palliative chemotherapy is effective in prolonging the survival, which is possibly associated with the late stage of the disease.

### Prognostic factors

It was reported that prognostic factors of primary malignant tumor of the small intestine are chiefly the operation type, histological type, tumor site and tumor size<sup>[1,7]</sup>, and each of them was analyzed by monovariate analysis. Up to now there have been no reports in the world about the prognostic factors

studied by multivariate analysis model. In our study, 12 factors were analyzed by computer's COX multivariate analysis model, including patient sex, age, clinical course, histological type, tumor site, tumor size, gross type, lymph node metastasis, liver metastasis, invasion to adjacent organs, operation type, and chemotherapy. The results showed that significant prognostic factors were histological type, operation type, patient age and tumor site in order, neither tumor size nor chemotherapy had significant effect on prognosis.

## REFERENCES

- 1 Han YF, Zhang QZ. An analysis of 36 cases of primary tumor of the small bowel. *Tumor*, 1995;15:406-407
- 2 Wang WD, Chen XY. A report of 77 cases of Primary malignant tumors of the small bowel. *Tumor*, 1990;10:44-45
- 3 Wang D, Xu JX, Wang ZX. CT diagnosis of Primary malignant tumors of the small bowel. *J Clin Radiol*, 1995;15:220-222
- 4 Wei JZ, Zhu YF, Wang JH. A diagnostic analysis of 27 cases of Primary malignant tumors of the small bowel. *Prac J Cancer*, 1993;8:175-176
- 5 Ciccirelli O, Welch JP, Kent GG. Primary malignant tumors of the small bowel. *Am J Surg*, 1987;153:350-354
- 6 He SW. A clinical analysis of 41 cases of Primary malignant tumors of the small bowel. *J Prac Oncol*, 1992;6:54-55
- 7 Chen YR, Wang L. Tumor of the small bowel in China. *J Prac Surg*, 1991;11:437-439
- 8 Zheng YL, Zhao QY. A synthetic analysis of malignant tumor of the small bowel in China. *Prac J Cancer*, 1989;4:138-139
- 9 Sellner F. Investigation on the significance of the adenocarcinoma sequence in the small bowel. *Cancer*, 1990;66:702-711
- 10 Zhou HG, Chen ZP, Kuang YL. Diagnosis and treatment of Primary malignant tumors of the small bowel. *Shanghai Dier Yike Daxue Xuebao*, 1995;15:138-141

Edited by WANG Xian-Lin